INFORME	**Identificación: H-2**
	Fecha 18 de febrero de 2012

TÍTULO: Caracterización del acuífero Cuaternario del Campo de Cartagena y modelización matemática en el contacto con el Mar Menor.

PROYECTO: Caracterización del acuífero Cuaternario del Campo de Cartagena y modelización matemática en el contacto con el Mar Menor.

RESUMEN:

El proyecto pretende la mejora del conocimiento de los aspectos hidrológicos e hidrogeológicos, en la evaluación experimental de la calidad hídrica del acuífero en el entorno costero, y la estimación local de los aportes de flujo y cargas contaminantes al mar con ayuda de técnicas de simulación. Durante el desarrollo del proyecto, y a la vez que se mejoraba el conocimiento de la zona, algunas de las actividades del proyecto han sido más ambiciosas. De esta manera, se ha confirmado que este Proyecto ha supuesto el inicio de una línea de actualización y mejora del conocimiento de las aguas subterráneas de la zona, con una fuerte componente de colaboración e implicación de grupos de investigación nacionales e internacionales del el ámbito mediterráneo, que incluyen como aspectos relevantes la aplicación de técnicas hidroquímicas e isotópicas y su modelización a nivel global. Asimismo, se pretende que en un futuro próximo las aguas subterráneas puedan ser integradas con el resto de los recursos disponibles (trasvase, desalación y aguas regeneradas), y que ello suponga un uso óptimo de los recursos, que se podría ver beneficiado por un factor de escala.

Revisión **Nombre**: **Unidad**: **Fecha**:	**Autores**: José Luis García Aróstegui, Ramón Aragón Rueda, Jorge Hornero Díaz, Clemente Trujillo Toro, Carolina Guardiola Albert, Juan María Fornés Azcoiti, Lucila Candela Lledó Joaquín Jiménez Martínez, Francisco Javier Elorza Tenreiro, Manuel Soler Manuel, Víctor del Castillo Sánchez, Gonzalo González Barberá, Javier García García, Manuel Erena Arrabal **Responsable**: José Luis García Aróstegui

CORREO
igme@igme.es

RÍOS ROSAS, 23
28003-MADRID
TEL. : 91 349 5700
FAX : 91 442 6216

MINISTERIO
DE ECONOMÍA
Y COMPETITIVIDAD

Instituto Geológico y Minero de España

REFERENCIA / CANOA: 554 / 73 3 00 24 00

CIRCULAR 1/2005. ANEXO V

INFORME FINAL DE RESULTADOS DEL PROYECTO

FECHA INICIO (mes/año)	FECHA FINALIZACIÓN (mes/año)		RESPONSABLE DEL PROYECTO
Mayo / 2009	Prevista: Enero/2011	Real: Mayo/2011	JOSE LUIS GARCIA ARÓSTEGUI

TÍTULO DEL PROYECTO
CARACTERIZACIÓN DEL ACUÍFERO CUATERNARIO DEL CAMPO DE CARTAGENA Y MODELIZACIÓN MATEMÁTICA EN EL CONTACTO CON EL MAR MENOR.

TÍTULO ABREVIADO	LÍNEA DE ACCIÓN
MAR MENOR	Hidrogeología y Calidad ambiental

PROYECTO			
Propio ☐	Subvencionado ☒	En Convenio ☐	Op. Comercial ☐
INFORME FINAL ENTREGADO EN EL CENTRO DE DOCUMENTACIÓN:	Si ☐	No ☒	FECHA DE ENTREGA:_____

EQUIPO DE TRABAJO			
Nombre	Categoría	Organismo	Actividad realizada
José Luis García Aróstegui	26	IGME	Investigador Principal. Todas las tareas
Ramón Aragón Rueda	26	IGME	Actividades 1, 2, 3 y 8
Jorge Hornero Díaz	24	IGME	Actividades 3, 4, 5, 6 y 7
Clemente Trujillo Toro	16	IGME	Actividades 2, 3, 4, 5, 6 y 10
Carolina Guardiola Albert	26	IGME	Actividades 8 y 10
Juan María Fornés Azcoiti	26	IGME	Actividad 8 y 9
Otros Organismos Participantes en el Proyecto			
Organismo	Responsable		Actividad realizada
UPC: Grupo de Hidrología Subterránea	Lucila Candela Lledó Joaquín Jiménez Martínez		Incluidos en el Subgrupo 1: IGME-UPC-UPM:
UPM: Dpto. de Matemática Aplicada y Métodos Informáticos. ETSI Minas	Francisco Javier Elorza Tenreiro		Interpretación de trabajos en Zona No Saturada y testigos de sondeos. Cambio climático y recarga. Modelización
UPC: ETS Ingenieros Industriales-Tarrasa	Manuel Soler Manuel		
Centro de Edafología y Biología Aplicada del Segura-CEBAS/CSIC: Grupo de Erosión y Conservación de Suelos	Víctor del Castillo Sánchez Gonzalo González Javier García		Subgrupo 2: CEBAS/CSIC-IMIDA: Ensayos de laboratorio de testigos de sondeos, análisis de global de datos de aguas subterráneas. Apoyo a la elaboración de modelo de flujo y transporte. Incorporación de datos a SIG y difusión web de resultados
Instituto Murciano de Investigación y Desarrollo Agrario y Alimentario IMIDA. Grupo de SIG y Teledetección	Manuel Erena Arrabal		

RÍOS ROSAS, 23
28003-MADRID
TELÉFONO: 91 349 5700
FAX: 91 442 6216

BREVE DESCRIPCIÓN DEL PROYECTO (máximo 10 líneas)

El proyecto pretende la mejora del conocimiento de los aspectos hidrológicos e hidrogeológicos, en la evaluación experimental de la calidad hídrica del acuífero en el entorno costero, y la estimación local de los aportes de flujo y cargas contaminantes al mar con ayuda de técnicas de simulación. Durante el desarrollo del proyecto, y a la vez que se mejoraba el conocimiento de la zona, algunas de las actividades del proyecto han sido más ambiciosas. De esta manera, se ha confirmado que este Proyecto ha supuesto el inicio de una línea de actualización y mejora del conocimiento de las aguas subterráneas de la zona, con una fuerte componente de colaboración e implicación de grupos de investigación nacionales e internacionales del el ámbito mediterráneo, que incluyen como aspectos relevantes la aplicación de técnicas hidroquímicas e isotópicas y su modelización a nivel global. Asimismo, se pretende que en un futuro próximo las aguas subterráneas puedan ser integradas con el resto de los recursos disponibles (trasvase, desalación y aguas regeneradas), y que ello suponga un uso óptimo de los recursos, que se podría ver beneficiado por un factor de escala.

OBJETIVOS DEL PROYECTO

OBJETIVOS GENERALES (máximo 5 líneas)

Caracterizar el acuífero cuaternario, en contacto directo con el Mar Menor, evaluar de forma experimental la calidad hídrica del acuífero en el entorno costero, y estimar los aportes de flujo y cargas contaminantes al mar con ayuda de técnicas de simulación. El desarrollo de modelos hidrogeológicos de flujo subterráneo y de transporte, servirá como instrumento de apoyo al desarrollo de códigos de buenas prácticas agrarias, como los actualmente establecidos, y a las posibles modificaciones de los mismos para la mejor conservación y regeneración del valor ambiental de la laguna.

OBJETIVOS ESPECÍFICOS (máximo 5 líneas)

1) Analizar las características hidroquímicas en la zona litoral y evaluar el grado de contaminación por nitratos de origen agrario; 2) Evolución temporal de niveles piezométricos en el acuífero en áreas circundantes al Mar Menor, para la determinación de líneas de flujo verticales y horizontales; 3) Establecer los parámetros hidráulicos mediante técnicas directas e indirectas; 4) Estudio del impacto del cambio climático respecto a la modificación de la recarga al acuífero e implicaciones en el Mar Menor; 5) Desarrollar modelos de flujo subterráneo y transporte para la simulación y evaluación de migración de contaminantes al Mar Menor; 6) Evaluar la contaminación difusa bajo distintos escenarios de sistema de producción agrícola.

SÍNTESIS DE LOS LOGROS DEL PROYECTO (en relación con los objetivos)

El proyecto de investigación “Caracterización del acuífero Cuaternario del Campo de Cartagena y modelización matemática en el contacto con el Mar Menor” ha centrado sus objetivos generales, además de la mejora del conocimiento de los aspectos hidrológicos e hidrogeológicos, en la evaluación experimental de la calidad hídrica del acuífero en el entorno costero, y la estimación local de los aportes de flujo y cargas contaminantes al mar con ayuda de técnicas de simulación. Durante el desarrollo del proyecto, y a la vez que se mejoraba el conocimiento de la zona, algunas de las actividades del proyecto han sido más ambiciosas, y de hecho se ha continuado a través de otros proyectos en que participan incluso organismos internacionales. A finales de 2012 se tiene prevista la finalización de una Tesis Doctoral codirigida por el IP de este proyecto.

De esta manera, se ha confirmado que este Proyecto ha supuesto el inicio de una línea de actualización y mejora del conocimiento de las aguas subterráneas de la zona, con una fuerte componente de colaboración e implicación de grupos de investigación nacionales e internacionales del el ámbito mediterráneo. Asimismo, se pretende que en un futuro próximo las aguas subterráneas puedan ser integradas con el resto de los recursos disponibles (trasvase, desalación y aguas regeneradas), y que ello suponga un uso óptimo de los recursos, que se podría ver beneficiado por un factor de escala.

PRODUCTOS DEL PROYECTO (GENERALES Y DE INTERÉS PARA EL IGME)

PUBLICACIONES (autores, título, libro o revista, lugar publicación, volumen, páginas, ISBN o ISSN)

De acuerdo con la Memoria inicial del Proyecto y los resultados preliminares obtenidos, las contribuciones científico-técnicas se han centrado fundamentalmente en 1) los aspectos relativos a la mejora de las técnicas de evaluación de la recarga y el impacto del cambio climático en ésta, 2) resultados de la modelización matemática, y 3) multicaracterización de un área experimental mediante combinación de sondeos ejecutados, ensayos de laboratorio y campo y técnicas geofísicas de tomografía eléctrica. En revistas SCI se han publicado las siguientes:

- Jiménez-Martínez, J., Candela, L., García-Aróstegui, J. L., Aragón, R. L. 2012. A 3D geological model of Campo de Cartagena, SE Spain:
- Hydrogeological implications. Geologica Acta (in press).
- Jiménez-Martínez, J., Candela, L., Molinero, J., Tamoh, K. 2010. Groundwater recharge in irrigated semi-arid areas: quantitative hydrological modelling and sensitivity analysis. Hydrogeology Journal, 18: 1811–1824.
- J. Jiménez-Martínez & R. Aravena & L. Candela. 2001. The Role of Leaky Boreholes in the Contamination of a Regional Confined Aquifer. A Case Study: The Campo de Cartagena Region, Spain. Water Air Soil Pollution, 215: 311–327.
- Rey, J., Martínez, J., Barberá, G.C., García-Aróstegui, J.L., García-Pintado, J. 2011. Identification of freshwater/saltwater interface via Electrical resistivity tomography: Campo de Cartagena aquifer (SE Spain) (En elaboración).

INFORMES INÉDITOS (autores, título, extensión, serie, lugar de depósito)

Se dispone de la Memoria del proyecto entregada a la Agencia Regional de Ciencia de Murcia (Fundación Séneca)

DATOS (tipo y características, base de datos que los contiene)

Se ha obtenido información hidrogeológica sustancial (piezometría, bases de datos hidroquímicas, litologías, etc.) que continúan siendo interpretadas con nuevos datos obtenidos en el marco de otros proyectos (CARTAG-EAU), y en colaboración con el Proyecto de Modelización Hidrológica en Zonas Semiáridas (Instituto Euromediterráneo del Agua).

OBRAS (tipo y características)

Tres piezómetros en Playa de la Hita (uno doble) y un nuevo sondeo a unos 500 m al norte (Los Alcázares).

INSTALACIONES (tipo y características)

Varios piezómetros han sido acondicionados con sensores de medida del nivel y conductividad del agua.

FORMACIÓN CONSEGUIDA

Tesis Doctoral en desarrollo (Paul Baudron) prevista para finales de 2012.

ACTIVIDADES EXTERIORES RELACIONADAS CON EL PROYECTO (Participación en reuniones científicas y congresos, de seguimiento de convenios, etc.)

Comunicaciones a Congresos

- Jiménez-Martínez, J., Tamoh, K., Candela, L. 2009. Tritium tracer test to estimate aquifer recharge under irrigated conditions, Eos Trans. AGU, 90(52), Fall Meet. Suppl., Abstract H31A-0757.
- Jiménez-Martínez, J., Molinero-Huguet, J., Candela, L. Drainage estimation to aquifer and water use irrigation efficiency in semi-arid zone for a long period of time. Geophysical Research Abstracts, Vol. 11, EGU2009-11131, 2009 EGU General Assembly 2009.
- Jiménez-Martínez, J., Aravena, R., Candela, L. 2010. Contamination of a regional confined aquifer by leaky boreholes. Campo de Cartagena case study (SE Spain). XXXVIII IAH Congress 2010 (Krakow.Poland).
- Jiménez-Martínez, J., Tamoh, K., Candela, L.Multiphase transport of tritium in unsaturated porous media bare and vegetated soils.
- Jiménez-Martínez, J., Jiménez, A., Candela, L. 2010. Use of TDR to estimate aquifer recharge in intensively irrigated areas. The Third International Symposium on Soil Water Measurement Using Capacitance, Impedance and TDT (2010, Murcia, Spain), New Developments, Paper 3.3.
- Jiménez-Martínez, J., Molinero, J., Candela, L. 2009. Estimación de la recarga por retorno de riego a través de la ZNS en áreas de agricultura intensiva bajo clima semiárido. Análisis de sensibilidad. Estudios en la Zona no Saturada del Suelo. Volumen IX, O. Silva et al. Barcelona, Noviembre-2009.
- García Aróstegui, J.L. (2011). Current status of hydrogeological research in the experimental watershed of Campo de Cartagena (Murcia, SE Spain). Presentado en: Increasing the regional competitiveness and economic growth through the RTD&I on Sustainable Water Management (SWAM); Regional Seminar on Competitiveness. Galilee (Israel), 17-19 January 2011.

EXPLICACIÓN DE LAS DESVIACIONES EN LA EJECUCIÓN DEL PROYECTO (si las hubo)

COMENTARIOS

La complejidad de la investigación hidrogeológica ha impedido el desarrollo completo en el marco del presente proyecto de un modelo de flujo subterráneo., si bien se ha desarrollado una importante labor de trabajos del modelo hidrogeológico conceptual y modelo geométrico 3D no sólo para el acuífero Cuaternario sino también para el resto de los acuíferos.

En este Proyecto se ha impulsado la colaboración con otros organismos regionales, nacionales e internacionales, entre los que cabe destacar el Instituto Euromediterráneo del Agua, el Instituto del Agua y del Medio Ambiente de la Universidad de Murcia, el Instituto del Agua de la Universidad de Granada, el Institut de Recherche pour le Développement (IRD-Montpellier, Francia), la Universidad de Montpellier (Francia), el Centre de Recherche pour le Géosciences, la Universidad Paris 11, y el Zuckerberg Institute for Water Research (Universidad Ben-Gurion de Israel).

El proyecto tiene parte de continuidad en la línea de investigación con el Proyecto CARTAG-EAU (CANOA MU-3-00-01-00) 2011-2012.

El Responsable del Proyecto	Enterado, El Jefe de la Unidad	Enterado, El Director Adjunto	Recibido, El Gestor de Proyectos
			
Nombre: José Luis García Aróstegui Fecha: 18/2/2012	Nombre: Ramón Aragón Rueda Fecha:	Nombre: Fecha:	Nombre: Fecha:

MINISTERIO
DE ECONOMÍA
Y COMPETIVIDAD

INSTITUTO GEOLÓGICO
Y MINERO DE ESPAÑA

Financiado por:

Proyecto Fundación Séneca
Nº Expediente 08825/PI/08

"CARACTERIZACIÓN DEL ACUÍFERO CUATERNARIO DEL CAMPO DE CARTAGENA Y MODELIZACIÓN MATEMÁTICA EN EL CONTACTO CON EL MAR MENOR"

Murcia, 20de abril de 2011.

Proyecto coordinado.

Participantes:

Subgrupo 1: IGME-Murcia: José Luis García-Aróstegui (IP), Ramón Aragón Rueda, Jorge Hornero Díaz, Clemente Trujillo Toro
UPC: Lucila Candela, Joaquín Jiménez, Manuel Soler
UPM: Francisco Javier Elorza
Subgrupo 2: CEBAS-CSIC: Víctor Castillo (IP), Gonzalo González, Javier García
IMIDA: Manuel Erena

Asunto: Memoria final del Proyecto (años 2009 y 2010)

Estructura

1. Memoria final del Proyecto
   a. Estado de avance de las actividades previstas
   b. Actividades complementarias y sinergias
   c. Otras consideraciones
2. Resultados
3. Abstract

1. MEMORIA FINAL DEL PROYECTO

El proyecto de investigación "Caracterización del acuífero Cuaternario del Campo de Cartagena y modelización matemática en el contacto con el Mar Menor" ha centrado sus objetivos generales, además de la mejora del conocimiento de los aspectos hidrológicos e hidrogeológicos, en la evaluación experimental de la calidad hídrica del acuífero en el entorno costero, y la estimación local de los aportes de flujo y cargas contaminantes al mar con ayuda de técnicas de simulación. Durante el desarrollo del proyecto, y a la vez que se mejoraba el conocimiento de la zona, algunas de las actividades del proyecto han sido más ambiciosas, como ya se destacaba en informes previos. De esta manera, se ha confirmado que este Proyecto ha supuesto el inicio de una línea de actualización y mejora del conocimiento de las aguas subterráneas de la zona, con una fuerte componente de colaboración e implicación de grupos de investigación nacionales e internacionales del el ámbito mediterráneo. Asimismo, se pretende que en un futuro próximo las aguas subterráneas puedan ser integradas con el resto de los recursos disponibles (trasvase, desalación y aguas regeneradas), y que ello suponga un uso óptimo de los recursos, que se podría ver beneficiado por un factor de escala.

La región mediterránea concentra el 60% de la población mundial pobre en agua (< 1000 m3/habitante/año), y constituye un medio árido o semiárido en el que las aguas subterráneas son la principal fuente de agua dulce o

CORREO ELECTRÓNICO
IP-1: j.arostegui@igme.es
IP-2: victor@cebas.csic.es

IGME-Murcia
Avda. Miguel de Cervantes, 45, 5ºA
30009-Murcia
TELÉFONO: 968 24 50 00/12
FAX: 968 24 50 00

un complemento fundamental y estratégico de los limitados recursos superficiales. La escasez de agua en estas zonas se traduce en frecuentes casos de explotación intensiva de acuíferos, e incluso minera, que podrían ser soluciones transitorias o definitivas aceptables siempre que las consecuencias sean conocidas, consensuadas y hayan sido planificadas sobre la base de un análisis coste/beneficio que debe incluir al menos los aspectos socioeconómicos y ambientales. Sin embargo, en la mayoría de los países, el uso de las aguas subterráneas se ha desarrollado sin el suficiente conocimiento, a partir de la iniciativa privada y con escaso control y planificación por parte de la administración, lo que ha conllevado a una explotación de reservas que supera los 9000 hm^3 en casos como los de la cuenca del Segura, cifra que puede suponer la mitad del total español.

El acuífero multicapa del Campo de Cartagena (SE de España) constituye, a nivel internacional, uno de los principales acuíferos de la cuenca mediterránea, en términos de extensión, aprovechamiento y productividad del agua subterránea. Las interrelaciones con la laguna costera del Mar Menor y las implicaciones ambientales proporcionan un interés científico adicional y una trascendencia socioeconómica evidente. Asimismo es un caso paradigmático particularmente interesante por los diversos tipos de cambios ambientales e hidrológicos ocasionados por la explotación intensiva del agua subterránea que se inició en el siglo XIX a través de la perforación de pozos artesianos (los primeros de España), se incrementó en la segunda mitad del siglo XX, se redujo tras la llegada en 1979 de importantes recursos externos (Trasvase Tajo-Segura), y, en las últimas décadas, las aguas subterráneas han adquirido un papel estabilizador en el balance oferta/demanda de tal manera que satisfacen entre el 30% y el 75% de las necesidades hídricas. En todo este contexto, el desarrollo y aplicación de nuevas metodologías de investigación hidrogeológica que resuelvan las incertidumbres en el complejo funcionamiento del sistema, y su encuadre en el ámbito mediterráneo y los principios de gestión integrada de recursos hídricos, deben permitir la obtención de las claves para un uso racional y planificado del sistema en términos cuantitativo y cualitativo.

El interés en este Proyecto por el acuífero Cuaternario no se deriva de la relativamente escasa productividad hidrogeológica, sino del papel que juega como receptor de los flujos y cargas contaminantes y su transmisión a los acuíferos inferiores y al Mar Menor. Sin embargo, a pesar de que los objetivos del proyecto centraban su atención al acuífero Cuaternario, poco a poco se ha ido confirmando que el sistema debe ser investigado en su totalidad dada las relaciones hidráulicas con los acuíferos inferiores, ya que de no ser así, los resultados se verían sustancialmente mermados.

Conviene señalar, que el acuífero multicapa del Campo de Cartagena además de ser considerado uno de los principales acuíferos de Europa, presenta similitudes con otros acuíferos estratégicos de indudable valor, como es el caso de los acuíferos del Poniente Almeriense, en los que también se bombea en los acuíferos inferiores y los problemas se evidencian con especial intensidad en los acuíferos superficiales, con deterioros significativos de la calidad de las aguas. La puesta en valor de las aguas subterráneas como elemento clave del desarrollo de la zona sólo puede basarse en la mejora de su conocimiento, sobre el cual aun queda mucho camino por recorrer. Desde el punto de vista socioeconómico, el impacto de los resultados del Proyecto incide directamente en uno de los pilares de la zona, la agricultura. Conviene señalar que la reducción de las aportaciones de agua para riego en el Campo de Cartagena procedentes del Trasvase Tajo-Segura, conlleva un incremento notable del bombeo de aguas subterráneas, que desde el año 2005 son las que están sustentando la agricultura de la zona, y a nivel general representan, según los periodos de sequía, entre el 30 y el 75% del agua para riego. Respecto al Mar Menor, resulta evidente que una mejora del conocimiento de las aportaciones procedentes del acuífero Cuaternario puede ayudar a en la toma de decisiones para minimizar el impacto sobre esta laguna de indudable valor.

En el presente documento se sintetizan las actividades desarrolladas a lo largo de los dos años de Proyecto y los resultados obtenidos. Los primeros meses del Proyecto se destinaron fundamentalmente a aspectos administrativos, logísticos y de coordinación entre los grupos involucrados. En una primera reunión de coordinación de equipos y lanzamiento del proyecto celebrada el 25 de mayo de 2009, en la sede del IGME en Murcia con asistencia de 10 de los 12 miembros del equipo, se comentaron todas estas circunstancias y las cuestiones relacionadas con una redistribución de la financiación entre los dos subgrupos, que hubo que

efectuar una vez ya iniciado el Proyecto. Asimismo en dicha reunión fue comentada la propia exigencia interna del IGME, que requiere la elaboración de una ficha interna de Proyecto y su aprobación por el Comité de Dirección en Madrid; la resolución correcta de estas circunstancias incide en los trámites administrativos necesarios para realizar el contrato menor con la Universidad Politécnica de Cataluña y la contratación de las asistencias técnicas incluidas en el Proyecto. Por parte, del subgrupo 2 gestionado por CEBAS-CSIC, los trámites fueron algo más rápidos y permitieron al Investigador Principal una mayor capacidad para el manejo de los fondos. El día 9/11/2009 fue celebrado un encuentro informal de Proyecto con la participación de 8 de los 12 miembros del equipo y representación de todos los organismos involucrados.

Durante, el año 2010, los contactos entre los miembros del equipo se han establecido principalmente a través de reuniones más reducidas que han permitido centrarse en aspectos concretos. De esta manera, como ejemplo, el IP ha asistido a varias reuniones en Barcelona y Madrid para reunirse con sendos investigadores participantes de las universidades politécnicas de Cataluña y de Madrid.

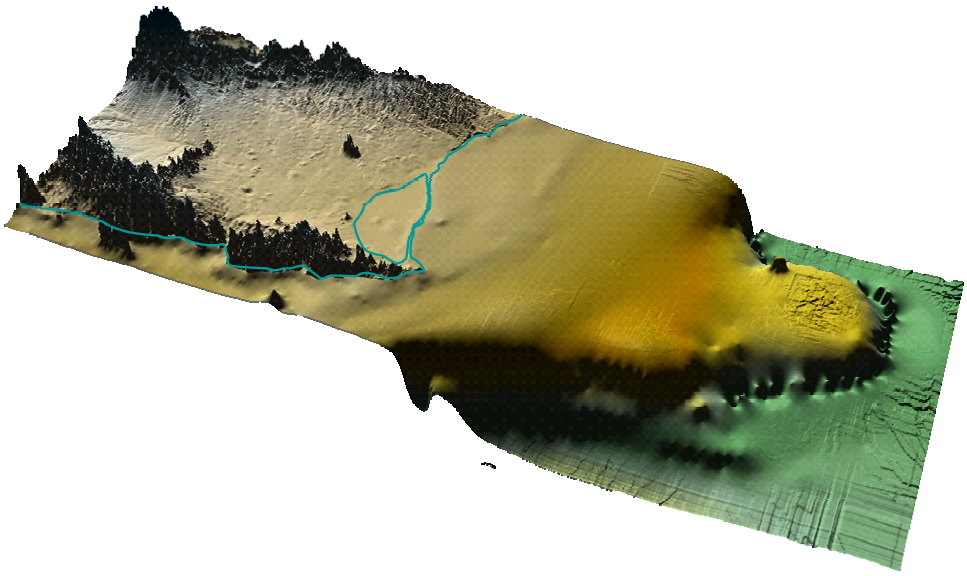

a. Estado de desarrollo de las actividades previstas

A continuación se repasa brevemente el estado final de desarrollo de las actividades y los resultados obtenidos, para lo cual se sigue el cuadro de distribución presentado en la solicitud. Conviene señalar que se han producido algunas modificaciones en las personas adscritas a cada actividad. Se adjunta una presentación de los resultados obtenidos e investigaciones en marcha, que fue mostrada en una reciente reunión en el marco del proyecto europeo SWAM, dentro de la colaboración entre IGME e IEA, que está facilitando la continuidad de este Proyecto.

Actividad 1 (Recopilación de datos procedentes de estudios previos).

Esta actividad ha consistido en la recopilación en interpretación de las bases de datos históricas del IGME y CHS. Asimismo se han analizado, fundamentalmente, los siguientes documentos:

- Albacete, M.; Solís, L.; Quintana, J.L.; Gil, F.; Gómez, A.; Gómez, A., Sánchez, M., 2001. Bases para una gestión sostenible de las aguas subterráneas del Campo de Cartagena. En: VII Simposio de Hidrogeología-AEH. Murcia. España. Vol. XXIII, 13-24.

- CARM, 2008. Consejería de Agricultura y Agua de la Región de Murcia. Datos estadísticos Agrarios. Disponible: <http://www.carm.es>.

- CHEVRON, 1982. Campaña Sísmica S-82. Fondo Documental del Archivo de Hidrocarburos del Ministerio de Industria, Turismo y Comercio.

- CHEVRON, 1984. Campaña Sísmica S-84. Fondo Documental del Archivo de Hidrocarburos del Ministerio de Industria, Turismo y Comercio.

- CHEVRON, 1985. Campaña Sísmica S-85. Fondo Documental del Archivo de Hidrocarburos del Ministerio de Industria, Turismo y Comercio.

- CHEVRON, 1986. Campaña Sísmica S-86. Fondo Documental del Archivo de Hidrocarburos del Ministerio de Industria, Turismo y Comercio.

- CHS, 1997. Plan Hidrológico de la cuenca del Segura. Aprobado por RD 1664/1998, de 24 de julio (BOE de 11 de agosto de 1997).

- García, C., 2004. Impacto y riesgo ambiental de los residuos minero-metalúrgicos de la Sierra de Cartagena-La Unión (Murcia-España). Tesis Doctoral. Universidad Politécnica de Cartagena, 424 pp.

- García-Pintado, J., Martínez-Mena, M; Barberá, G.G.; Albaladejo, J., Castillo, V., 2007. Anthropogenic nutrient sources and loads from a Mediterranean catchment into a coastal lagoon: Mar Menor, Spain. Science of the Total Environment, 373, 220-239.

- García-Tortosa, F.J., López-Garrido, A., Sanz de Galdeano, C., 2000b. Las unidades alpujárrides y maláguides entre Cabo Cope y Cabo de Palos (Murcia, España). Geogaceta, 28, 67-70.

- García-Tortosa, F.J., López-Garrido, A., Sanz de Galdeano, C., 2000c. Présence du complexe tectonique Malaguide à l'est de Carthagène (zone interne Bétique, Espagne). C.R. Acad. Sci. Paris, Sciences de la Terre et des Planètes. Earth and Planetary Sciences, 330, 139-146.

- IGME, 1983. Campaña de prospección geofísica en el Campo de Cartagena (Murcia). Sondeos Eléctricos Verticales. Informe Técnico (Inédito).

- IGME, 2005. Estudio de la información geológica y geofísica del subsuelo (sísmica de reflexión y sondeos) en el sector SE de la Provincia de Murcia. Consejería de Industria y Medio Ambiente de la Región de Murcia. 37 pp. Anexos 1-37. Informe Técnico (Inédito).

- IGME-IRYDA, 1978. Plan Nacional de Investigación de aguas subterráneas. Investigación hidrogeológica de la cuenca baja del Segura. Tomos 8 y 9: Campo de Cartagena. Informe Técnico (Inédito).

- INI-COPAREX, 1967. Sondeo San Miguel de Salinas 1. Fondo Documental del Archivo de Hidrocarburos del Ministerio de Industria, Turismo y Comercio.

- INI-COPAREX, 1970. Sondeo San Miguel de Salinas 2. Fondo Documental del Archivo de Hidrocarburos del Ministerio de Industria, Turismo y Comercio.

- ITGE, 1989. Geometría de los acuíferos del Campo de Cartagena (Murcia) Volumen 1/3 Memoria. Volumen 2/3 Mapas. Volumen 3/3 Anexos: inventario de puntos de agua. Informe Técnico (Inédito).

- ITGE, 1991. Estudio Hidrogeológico del Campo de Cartagena (2ª Fase). Volumen 1/2 Memoria. Volumen 2/2 Anexos 1, 2, 3 y 4. Informe Técnico (Inédito).

- ITGE, 1994. Las aguas subterráneas del Campo de Cartagena (Murcia). ITGE, 62 pp.

- Jiménez García, J., 1998. Quantificació de les deformacions verticals recents a l´Est de la Península Ibérica a partir d´anivellaments topogràfics de precisió. Tesis Doctoral. Institut Cartogràfic de Catalunya. Monografies tècniques, 5, 363 pp.

- Jiménez-Martínez, J., Himi, M., Robles-Arenas, V.M., Díaz, Y., Casas, A., Candela, L., 2008. Identificación mediante tomografía eléctrica del límite geológico entre el Campo de Cartagena y la Sierra de Cartagena-La Unión. En: Pérez Torrado, F. y Cabrera Santana M.C. (eds.) VII Congreso Geológico de España, Las Palmas de Gran Canaria. Geotemas, 10, 295-298.

- Lambán, J.L., Aragón, R., 2003. Estado de la intrusión marina en el Campo de Cartagena: evaluación preliminar a partir de la composición química del agua subterránea. En: Tecnología de la Intrusión Marina en Acuíferos Costeros, Países Mediterráneos (TIAC'03). Publicación Series IGME, Madrid, 345-355.

- López-Bermúdez, F., Conesa-García, C., 1990. Características granulométricas de los depósitos aluviales en el Campo de Cartagena. Cuadernos de Investigación Geográfica, 16, 31-54.

- López-Garrido, A. C., Pérez López, A., Sanz de Galdeano, C., 1997. Présence de Facies Muschelkalk dans des unités Alpujarrides de la région de Murcie (Cordillere Bétique, SE de I'Espagne) et implications paléogéographiques. C. R. Acad. Sc. Paris. Sér. l1a., 324, 647-654.

- Manteca, J.I., García, C., 2001. La falla de Cartagena-La Unión. Aportación visual de su existencia gracias a una obra pública. En: F. Guillen y A. Del Ramo (eds.). Patrimonio Geológico, Cultura y Medio Ambiente. Murcia, 239-246.

- Manteca, J.I., Ovejero, G., 1992. Los yacimientos Zn, Pb, Ag-Fe del distrito minero de La Unión-Cartagena, Bética Oriental (Zn, Pb, Ag-Fe ore deposits of La Unión-Cartagena mining district, eastern Betic Cordillera). En: J. García y J. Martínez (eds.). Recursos Minerales de España, CSIC, 1085-1101.

- Manteca Martínez, J.I., Rodríguez Martínez-Conde, J.A., Puga, E., Díaz de Federico, A., 2004. Deducción de la existencia de un relieve Nevado-Filábride durante el Mioceno Medio-Superior, actualmente bajo el mar, al sur de las sierras costeras alpujárrides de El Roldán y La Muela (oeste de Cartagena, Cordillera Bética Oriental). Rev. Soc. Geol. España, 17(1-2), 27-37.

- Mora Cuenca, V., Rodríguez Estrella, T., Aragón Rueda, R., 1988. Intrusión marina fósil en el Campo de Cartagena (Murcia). En: Tecnología de la Intrusión Marina en Acuíferos Costeros, Países Mediterráneos (TIAC'88). Publicación Series IGME, Madrid, 221-236.

- Ovejero, G., Jacquin, J.P., Servajean, G., 1976. Les minéralisations et leur contexte géologique dans la Sierra de Cartagena (Sud-Est de L'Espagne) (Mineralizations and their geologic context in the Sierra de Cartagena (SE Spain)). Bulletin Société Géologique de France (7), XVIII (3), 613-633.

- Pérez Ruzafa, A., Aragón, R. 2003. Implicaciones de la gestión y el uso de las aguas subterráneas en el funcionamiento de la red trófica de una laguna costera. En: Fornés, J. M. y Llamas, M. R (eds.). Conflictos entre el desarrollo de las aguas subterráneas y la conservación de los humedales: litoral mediterráneo. Fundación Marcelino Botín. Ediciones Mundi-Prensa. Madrid, 215-245.

- Ramos, G., Sánchez, J., 2003. Estructura geológica profunda "Murcia Sur-I". Definición geológica, geométrica y confinamiento. En: Tecnología de la Intrusión Marina en Acuíferos Costeros, Países Mediterráneos (TIAC'03). IGME Book series, Madrid, 691-700.

- Robles-Arenas, V.M., Rodríguez, R., García, C., Manteca, J.I., Candela, L., 2006. Sulphide-mining impacts in the physical environment: Sierra de Cartagena-La Unión (SE Spain) case study. Environmental Geology, 51, 47-64.

- Rodríguez Estrella, T., 1983. Criterios hidrogeológicos aplicables al estudio de la neotectónica en el Sureste Español. Mediterránea Ser. Geol., 2, 53-66.

- Rodríguez Estrella, T., 1986. La Neotectónica en la Región de Murcia y su incidencia en la ordenación del territorio. En: 1ª Jornadas de estudio del fenómeno sísmico y su incidencia en la ordenación del territorio. Murcia, 281-303.

- Rodríguez Estrella, T., 2000. Modifications physiques, chimiques et biologiques porvoquées par les eaux du canal Tage-Segua dans l'unité hydrogéologique du Campo de Carthagéne et dans la lagune de Mar Menor (Province de Murcie, Espagne). Hydrogéologie, 3, 23-37.

- Rodriguez Estrella, T., 2004. Decisive influence of neotectonics on the water connection between the Mediterranean Sea, Mar Menor and the Campo de Cartagena aquifers. (South-East of Spain): Consequences on extracting sea water by means of borings for desalination. En: L. Araguás, E. Custodio y M. Manzano (eds.). Proceedings 18th SWIM Groundwater and Saline Intrusion. Publicaciones Series IGME, Madrid, 745-758.

- Rodríguez Estrella, T., Jiménez-Martínez, J., López Chicano, M., 2004. Ensayo de correlación entre transmisividades y espesores de los acuíferos del Plioceno y Messiniense del Campo de Cartagena (Murcia y Alicante). En: VIII Simposio de Hidrogeología-AEH. Zaragoza, España. Vol. XXVI, 239-249.

- Rodríguez Estrella, T., Lillo, M., 1992. Geomorfología del Mar Menor y sectores litorales contiguos (Murcia-Alicante). Estudios de geomorfología en España. En: II Reunión Nacional de Geomorfología, 787-807.

- Rolandi Sánchez-Solís, M., Yugin, V., Herrero Pacheco, J. L. 2008. Aportación al conocimiento de la caracterización y el funcionamiento hidrogeológico de la U.H. del Campo de Cartagena (Cuenca del Segura), mediante utilización de técnicas de Tomografía Remota Térmica. En: IX Simposio de Hidrogeología. Elche, España. Vol. XXVIII, 691-700.

- Sanz de Galdeano, C., López-Garrido, A. C., García-Tortosa, F.J., Delgado, F., 1997. Nuevas observaciones en el Alpujárride del sector centro-occidental de la Sierra de Carrascoy (Murcia). Consecuencias paleogeográficas. Estudios Geológicos, 53, 229-236.

- SEPESA, 1968. Campaña Sísmica MM. Fondo Documental del Archivo de Hidrocarburos del Ministerio de Industria, Turismo y Comercio.

Actividad 2 (Inventario del área de estudio. Emplazamiento de sondeos).

Se ha avanzado en el conocimiento de la zona de estudio a partir sobre todo del análisis de los datos obtenidos. Con esta nueva información se ha tratado de mejorar aquellos aspectos de carácter estructural a nivel espacial, tanto en las dimensiones X-Y como en la disposición de los materiales en profundidad (Z).Mejorar el nivel de información geológica así como ampliar la base de conocimiento sobre las características litológicas de las distintas formaciones es fundamental, ya que convergen con la necesidad de dotar al modelo de un volumen de datos de suficiente calidad para que minimicen las incertidumbres asociadas en el desarrollo del modelo. Asimismo la toma de datos está dentro de las prioridades establecidas en la propia investigación, sobre todo teniendo en cuenta las evidentes lagunas de información que existen actualmente en aquellos aspectos relacionados con las posibles aportaciones subterráneas en el borde NW del Mar Menor. Inicialmente fue elegido como dominio del modelo el sector comprendido entre el borde NW de la laguna y el límite hidrogeológico de la MAS, sin excluir cualquier otra zona de este entorno que fuese necesario investigar parcialmente por sus implicaciones con la zona designada. El desarrollo de la investigación durante este último año aconseja realizar la modelación para el dominio hidrogeológico completo, es decir, la totalidad de la masa de agua subterránea. Los procesos que se han observado y la predicción en el funcionamiento requiere considerar todos los sectores hidrogeológicos implicados, ya que la complejidad hidrogeológica (acuífero multicapa) y la repercusión de la explotación de agua subterránea que dota de recursos a la actividad agrícola, afecta, por un lado a los procesos relacionados con la hidrodinámica del sistema, y por otro a los que tienen relación con el transporte de masa, en definitiva, al cómputo de descarga de solutos por escorrentía subterránea desde el acuífero hacia el Mar Menor.

Dentro de los trabajos específicos y singulares encaminados a mejorar la información hidrogeológica ha estado la construcción de 3 sondeos de investigación, uno de ello doble, en las inmediaciones de la Playa de la Hita, cercana al Aeropuerto de San Javier. La situación de los emplazamientos se ha elegido una vez se ha analizado la información y resultados de la prospección geofísica efectuada con anterioridad, lo cual supuso un cambio en el cronograma de actividades inicialmente previsto.

Actividad 3 (Realización de sondeos y ensayos de testigos recuperados)

La ejecución de los sondeos ha requerido los correspondientes permisos por parte del Excmo. Ayuntamiento de San Javier y la Consejería de Medio Ambiente dada su incidencia en el espacio protegido comprendido dentro de éste término municipal. Una vez efectuada la contratación de la empresa perforadora y gestionados administrativamente los permisos correspondientes, han sido ejecutados los sondeos. Los resultados obtenidos han sido parcialmente interpretados, ya que para obtener conclusiones más relevantes de carácter hidrogeológico se ha optado por instrumentar los sondeos dotándolos de sensores de registro continuo que en principio estarán operativos al menos durante dos años, independientemente de las medidas puntuales que se vayan realizando. Han sido muy positivas las discusiones científicas mantenidas entre los miembros del equipo para obtener la mayor cantidad posible de información, con posibles sinergias para llevar a cabo futuras investigaciones. Respecto a los testigos recuperados, han sido almacenados para su posterior ensayo en laboratorio.

Actividad 4 (Adquisición e instalación de instrumentación).

Como se ha expuesto en la actividad 3, una vez ejecutados los sondeos se han mantenido diferentes discusiones entre los responsables del Proyecto para decidir las características de las sondas y equipos de control e instrumentación. Tanto los equipos como las infraestructuras necesarias se han dimensionando no sólo para su uso durante el presente proyecto sino también para permitir la continuidad temporal del registro y

toma de datos en el tiempo, ya que las variables climatológicas, principalmente aquellos relacionados con fenómenos extremos pluviométricos, y los efectos antrópicos derivados del usos más o menos intensivo que se realiza en el acuífero del agua subterránea implican cambios en el funcionamiento hidrogeológico que requieren ser observados y analizados con una mayor amplitud temporal.

Actividad 5 Ejecución e interpretación de ensayos de bombeo.

Se ha realizado un ensayo de trazadores mediante la inyección controlada de un trazador ambiental (Tritio). Los resultados están siendo interpretados y la información que se obtenga es fundamental para relacionar determinadas características hidrogeológicas con la capacidad de recarga y el papel que juegan determinados parámetros hidráulicos en el funcionamiento del flujo subterráneo. Esta información ha sido incorporada como datos de entrada al modelo matemático a nivel global.

Actividad 6 Campañas de muestreos de campo.

Se han realizado dos campañas de toma de muestras distribuidas espacialmente sobre el acuífero y los cauces superficiales. Los puntos de agua muestreados han sido seleccionados siguiendo criterios hidrogeológicos y de acuerdo a las posibles interacciones agua subterránea-agua superficial. Las muestras fueron sido enviadas a los laboratorios del IGME en Madrid para la determinación de elementos mayoritarios, minoritarios y algunos componentes trazas. Los resultados aún son parciales ya que se han introducido algunos cambios en el Proyecto relacionados con la necesidad de evaluar mejor los cambios temporales en las características hidroquímicas del agua. Por tanto se han efectuado dos campañas extensivas con mayor número de muestras y mayores determinaciones en cada una de ellas. El análisis previo indicaba que para observar cambios significativos se necesitaría mayor duración de la especificada en el proyecto inicial (un año). En definitiva, las campañas de muestreo hidroquímico han correspondido a mayo-junio de 2009 y febrero-marzo de 2010.

Por otro lado, las campañas de medidas piezométricas en sondeos e hidrométricas en el cauce del Albujón y drenajes significativos no han experimentado ningún cambio y se han realizado de acuerdo a lo especificado en el Proyecto. Una novedad importante que ha surgido en le transcurso del Proyecto ha sido la colaboración con otros equipos de trabajo de la Universidad de Murcia e Instituto Euromediterráneo del Agua, en determinados temas en los que convergen intereses comunes y que tienen que ver con el hecho de optimizar esfuerzos y mejorar el conocimiento conjunto en la zona de estudio.

Actividad 7 Estudios geofísicos e interpretación.

Previamente a la implantación y ejecución de los sondeos en el área de la playa de la Hita, se ha realizado una campaña de prospección geofísica mediante Tomografía Eléctrica. Los resultados obtenidos han mejorado sustancialmente la información geométrica de las formaciones geológicas en contacto con el Mar Menor. Estos trabajos específicos han sido efectuados por el equipo de investigación geofísica de la Escuela de Minas (Universidad Politécnica de Linares).

Actividad 8 Análisis global de datos de aguas subterráneas.

Esta actividad ha sido realizada en cada una de las fases del proyecto y queda integrado dentro de los trabajos desarrollados de forma continua por cada subgrupo. Con los resultados obtenidos se ha podido realizar un primer balance que ha permitido avanzar y mejorar la calidad de la información, de cara a su futura integración en los trabajos de modelación de flujo e interpretación hidrogeoquímica.

Actividad 9 “Escenarios climáticos y modificación de la recarga” y Actividad 10 “Modelización y calibración de aportes subterráneos al Mar Menor”.

Estas actividades están relacionadas con el planteamiento de un modelo extenso que comprenda toda la masa de agua subterránea. Las actividades de modelización han sido objeto de debate continuo por el equipo del Proyecto. Se ha constatado la complejidad del caso de estudio, se requiere una elevada cantidad de datos, circunstancia que excede los objetivos del proyecto. De todas formas es fundamental desarrollar un modelo preliminar que proporcione información fiable sobre el funcionamiento del acuífero y su interacción con el Mar Menor. Esta labor de cierta complejidad se ha dimensionado a nivel espacial (superficie del área de estudio a modelizar y perfil vertical de los acuíferos que deben integrarse en la modelación), asimismo se ha recopilado un importante volumen de información principalmente relacionada con datos de carácter espacial y temporal vinculados con la infraestructura hidrogeológica. Se ha avanzado también en el conocimiento y evaluación cualitativa y cuantitativa de los aportes subterráneos al Mar Menor. Toda esta información se ha considerado indispensable para llevar a cabo un modelo de flujo y transporte, en principio limitado al área experimental de la Playa de la Hita.

Actividades adicionales especificadas en Proyecto de creación de página web: Ha sido efectuada por el IMIDA que ha incorporado información cartográfica de interés y soporte para el intercambio de datos.

b. Actividades complementarias y sinergias

Hay que destacar como actividades complementarias al Proyecto que han permitido un mayor desarrollo del mismo las siguientes:

- Jornada científica sobre el estado de conocimiento en el Mar Menor (San Pedro del Pinatar, 1 abril de 2009), promovida Fundación Cluster y organizada por la Fundación Instituto Euromediterráneo del Agua (IEA). En esta reunión fue presentado el Proyecto con representación de IGME, CEBAS e IMIDA.
- Reunión científica sobre "Investigación hidrogeológica en zonas semiáridas", 22-26 de junio de 2009, organizado por IGME e IEA. Presentación del Proyecto Séneca y sinergias en el respecto al convenio específico IGME-IEA "Cuantificación de los componentes del flujo subterráneo y recarga en acuíferos en zonas semiáridas, y análisis integrado de recursos hídricos subterráneos: cuenca del Segura".
- Posibilidades de cooperación en los estudios preliminares para la cuantificación de fuentes de recarga y establecimiento de flujos entre acuíferos del Campo de Cartagena. Investigación UGR (José Benavente) para el IEA. Objetivo: muestreo hidroquímico (analítica en IGME) e isotópico (analítica UGR) en captaciones representativas. Aplicación de códigos hidroquímicos y Mixing Cell Model. El IGME apoya el muestreo de campo.
- Actividades paralelas relacionadas con la Encomienda de Gestión Ministerio de Medio Ambiente Rural y Marino con el IGME para el "Establecimiento de indicadores de intrusión marina y cálculo de volúmenes ambientales al mar" (2008-2009). Empresa consultora: Eptisa.
- Presentación de la investigación en Galilea (Israel) en el marco del Proyecto del SWAM (Sustainable Water Management; 7 PM de la UE).
- Presentación de comunicaciones a varios Congresos.

c. Otras consideraciones

El equipo de investigación de este Proyecto ha debatido y analizado en varias reuniones la problemática que gira en torno al Mar Menor, incidiendo sobre el nivel de conocimiento y los retos futuros en materia de investigación. Con este proyecto se han acortado en gran medida una importante laguna de información en lo relacionado con la toma de datos que apoya y permite determinar con menos incertidumbre los aspectos cuantitativos y cualitativos de las relaciones hídricas subterráneas Mar Menor-acuífero Cuaternario del Campo de Cartagena. En este sentido se ha diseñado una metodología específica para el cálculo de la descarga subterránea hacia el Mar Menor. Es evidente el papel que debe jugar en la comprensión del funcionamiento de la masa de agua subterránea el desarrollo del modelo de flujo. También la selección en la localización del emplazamiento de los sondeos de investigación, así como su definición y diseño constructivo en el entorno del borde de la laguna costera ha formado parte del trabajo conjunto entre las partes involucradas en el proyecto.

2. RESULTADOS

Publicaciones:

De acuerdo con la Memoria inicial del Proyecto y los resultados preliminares obtenidos, las contribuciones científico-técnicas se han centrado fundamentalmente en 1) los aspectos relativos a la mejora de las técnicas de evaluación de la recarga y el impacto del cambio climático en ésta, 2) resultados de la modelización matemática, y 3) multicaracterización de un área experimental mediante combinación de sondeos ejecutados, ensayos de laboratorio y campo y técnicas geofísicas de tomografía eléctrica.

- Jiménez-Martínez, J., García-Aróstegui, J. L., Aragón, R., Candela, L. 2010. A quasi 3D geological model of the Campo de Cartagena, SE Spain: Hydrogeological implications. Geologica Acta (in press).
- Jiménez-Martínez, J., Candela, L., Molinero, J., Tamoh, K. 2010. Groundwater recharge in irrigated semi-arid areas: quantitative hydrological modelling and sensitivity analysis. Hydrogeology Journal, 18: 1811–1824.
- J. Jiménez-Martínez & R. Aravena & L. Candela. 2001. The Role of Leaky Boreholes in the Contamination of a Regional Confined Aquifer. A Case Study: The Campo de Cartagena Region, Spain. Water Air Soil Pollution, 215: 311–327.
- Rey, J., Martínez, J., Barberá, G.C., García-Aróstegui, J.L., García-Pintado, J. 2011. Identification of freshwater/saltwater interface via Electrical resistivity tomography: Campo de Cartagena aquifer (SE Spain) (En elaboración).

Comunicaciones a Congresos

- Jiménez-Martínez, J., Tamoh, K., Candela, L. 2009. Tritium tracer test to estimate aquifer recharge under irrigated conditions, Eos Trans. AGU, 90(52), Fall Meet. Suppl., Abstract H31A-0757.
- Jiménez-Martínez, J., Molinero-Huguet, J., Candela, L. Drainage estimation to aquifer and water use irrigation efficiency in semi-arid zone for a long period of time. Geophysical Research Abstracts, Vol. 11, EGU2009-11131, 2009 EGU General Assembly 2009.
- Jiménez-Martínez, J., Aravena, R., Candela, L. 2010. Contamination of a regional confined aquifer by leaky boreholes. Campo de Cartagena case study (SE Spain). XXXVIII IAH Congress 2010 (Krakow.Poland).
- Jiménez-Martínez, J., Tamoh, K., Candela, L.Multiphase transport of tritium in unsaturated porous media bare and vegetated soils.
- Jiménez-Martínez, J., Jiménez, A., Candela, L. 2010. Use of TDR to estimate aquifer recharge in intensively irrigated areas. The Third International Symposium on Soil Water Measurement Using Capacitance, Impedance and TDT (2010, Murcia, Spain), New Developments, Paper 3.3.
- Jiménez-Martínez, J., Molinero, J., Candela, L. 2009. Estimación de la recarga por retorno de riego a través de la ZNS en áreas de agricultura intensiva bajo clima semiárido. Análisis de sensibilidad. Estudios en la Zona no Saturada del Suelo. Volumen IX, O. Silva et al. Barcelona, Noviembre-2009.
- García Aróstegui, J.L. (2011). Current status of hydrogeological research in the experimental watershed of Campo de Cartagena (Murcia, SE Spain). Presentado en: Increasing the regional competitiveness and economic growth through the RTD&I on Sustainable Water Management (SWAM); Regional Seminar on Competitiveness. Galilee (Israel), 17-19 January 2011.

Patentes

No está previsto

Contratos I+D

No está previsto

Tesis Doctorales y Tesinas de Licenciatura

En la Convocatoria Séneca-2009 fue solicitada una Beca-contrato predoctoral FPI "Estimación de la recarga y de los flujos inter-acuíferos mediante métodos hidroquímicos e isotópicos y realización de un modelo hidrogeológico de flujo y transporte en el acuífero multicapa del Campo de Cartagena, Murcia" (Doctorando: Paul Baudron; Director: José Luis García Aróstegui). A pesar de que esta beca NO fue adjudicada, el doctorando ha iniciado la investigación citada gracias a la financiación con cargo a proyecto del Instituto Universitario del Agua y Medio Ambiente de la Universidad de Murcia.

La continuidad de la investigación y de la infraestructura desarrollada en este Proyecto está asegurada ya que IP (García Aróstegui) es actualmente codirector de la Tesis Doctoral antes citada, junto con los doctores Christian Leduc (IRD-Francia) y Melchor Senent (UM-España). Está previsto que esta Tesis se finalice en el año 2012.

Otros:

En este Proyecto se ha impulsado la colaboración con otros organismos regionales, nacionales e internacionales, entre los que cabe destacar el Instituto Euromediterráneo del Agua, el Instituto del Agua y del Medio Ambiente de la Universidad de Murcia, el Instituto del Agua de la Universidad de Granada, el Institut de Recherche pour le Développement (IRD-Montpellier, Francia), la Universidad de Montpellier (Francia), la Universidad Paris 11, y el Zuckerberg Institute for Water Research (Universidad Ben-Gurion de Israel).

Objetivos año siguiente (si procede)

No procede

Material inventariable y viajes (indicar fecha y concepto)

El subgrupo 1 ha realizado las siguientes compras de material inventariable con un importe total de 3397,63 euros, tal y como se detallan a continuación:

- Nº Factura 2019/10. Concepto: Factura M/2677 de fecha 13/09/2010 de la Empresa Foxen Murcia por 1000,05 euros, para Ordenador portátil. Autorizado con fecha 28 de mayo de 2010.
- Nº Factura 2020/10. Concepto: Factura de Geonatura nº 34075 de 11/08/2010 de compra de GPS y conductivímetro por importe de 897,98 euros. Autorizado con fecha 28 de mayo de 2010.
- Nº Factura: 01001994. Concepto: Factura 095/2010 de Miliarium de fecha 24/05/2010 por importe de 1499,60 euros para software hidrogeología previsto inicialmente en Proyecto.

Los gastos de viaje del subgrupo 1 (IGME) ascienden a un total de 2985,16 euros. Al inicio del Proyecto se solicitó una redistribución de la financiación concedida entre los dos subgrupos; en el subgrupo 1 quedaron incluidos los componentes de UPC y UPM y sus gastos de viaje han sido incorporados en el correspondiente contrato menor necesario para permitir su participación en el Proyecto.

En la tabla siguiente se indican las fechas de viaje y concepto de los participantes del subgrupo 1 (IGME).

Año	Investigador	Código	Fecha viaje	Fecha justificación	Objeto	Lugar
2009	CTT	1496/09	18/05/2009	01/06/2009	Toma muestras Mar Menor	Campo de Cartagena
	CTT	1504/09	14-15/05/2009	01/06/2009	Toma muestras Mar Menor	Campo de Cartagena
	CTT	1616/09	25-28/05/2009	01/06/2009	Toma muestras Mar Menor	Campo de Cartagena
	JHD	1653/09	27/05/2009	01/06/2009	Reconocimiento hidrogeológico Campo de Cartagena	San Pedro del Pinatar-Cartagena
	JLGA	1615/09	01-04/06/2009	05/06/2009	Reconocimiento hidrogeológico Campo de Cartagena	Cartagena
	RAR	1660/09	02/06/2009	04/06/2009	Reconocimiento hidrogeológico Campo de Cartagena	San Pedro del Pinatar-Cartagena
	CTT	1680/09	02-03/06/2009	04/06/2009	Toma de muestras Mar Menor	Campo de Cartagena
	CTT	1813/09	08-11/06/2009	16/06/2009	Toma de muestras Mar Menor	Campo de Cartagena
	CTT	1939/09	22/06/2009	24/06/2009	Reconocimiento hidrogeológico Campo de Cartagena	San Pedro del Pinatar-Cartagena
	RAR	1999/09	22/06/2009	24/06/2009	Reconocimiento hidrogeológico Campo de Cartagena	San Pedro del Pinatar-Cartagena
	CTT	2055/09	30/06/2009	01/07/2009	Puesta en marcha de sensores Campo de Cartagena	Campo de Cartagena
	CTT	2147/09	14/07/2009	16/07/2009	Reconocimiento hidrogeológico Campo de Cartagena	Campo de Cartagena
	CTT	2321/09	28/07-12/08/2009	13/08/2009	Reconocimiento hidrogeológico Campo de Cartagena	Campo de Cartagena
	CTT	2529/09	08-9-10-18 y 22/09/2009	28/09/2009	Reconocimiento hidrogeológico Campo de Cartagena	Campo de Cartagena
	JHD	3018/09	14-15/10/2009	16/10/2009	Reconocimiento hidrogeológico Campo de Cartagena	Murcia-Cartagena-Murcia
	JHD	3047/09	22-23/10/2009	26/10/2009	Reconocimiento hidrogeológico Campo de Cartagena	Murcia-Cartagena-Murcia
	CTT	3073/09	22-23/10/2009	26/10/2009	Reconocimiento hidrogeológico Campo de Cartagena	Murcia-Cartagena-Murcia
	JLGA	3048/09	22-23/10/2009	26/10/2009	Reconocimiento hidrogeológico Campo de Cartagena	Murcia-Cartagena-Murcia
	JHD	3202/09	27/10/2009	30/10/2009	Descarga de datos y visita a los futuros sondeos en el Campo de Cartagena	Murcia-Campo de Cartagena-Murcia
	CTT	3203/09	27/10/2009	30/10/2009	Descarga de datos y visita a los futuros sondeos en el Campo de Cartagena	Murcia-Campo de Cartagena-Murcia
2010	CTT	32/10	19,21,22/01/2010	01/02/2010	Reconocimiento hidrogeológico Campo de Cartagena	Murcia-Campo de Cartagena-Murcia
	RAR	33/10	13,15,18, 20-22/01/2010	01/02/2010	Seguimiento Sondeos Campo de Cartagena	Murcia-Campo de Cartagena-Murcia
	CTT	56/10	14/01/2010	01/02/2010	Reconocimiento hidrogeológico y seguimiento de sondeos Campo de Cartagena	Murcia-Campo de Cartagena-Murcia
	JLGA	57/10	13,15,19,21/01/2010	01/02/2010	Seguimiento de sondeos Campo de Cartagena	Murcia-Campo de Cartagena-Murcia
	CTT	165/10	4,5,8,9,10,11,12/02/2010	15/02/2010	Muestreo Campo de Cartagena	Murcia-Campo de Cartagena-Murcia
	JLGA	260/10	18-19/02/2010	25/02/2010	Reunión desarrollo modelo Campo Cartagena	Murcia-Madrid-Murcia
	CTT	261/10	18-19/02/2010	22/02/2010	Toma de muestras Mar Menor	Murcia-Campo de Cartagena-Murcia
	JHD	355/10	1,3,4/03/2010	05/03/2010	Encuestas de explotación	Murcia-Campo de Cartagena-Murcia
	CTT	356/10	1,2,3,4/03/2010	05/03/2010	Encuestas de explotación	Murcia-Campo de Cartagena-Murcia
	JLGA	398/10	04/03/2010	08/03/2010	Reunión de Proyecto	Murcia-Valencia-Murcia
	CTT	433/10	8,10,11/03/2010	15/03/2010	Encuestas de explotación Campo Cartagena	Murcia-Campo de Cartagena-Murcia
	JHD	434/10	8,10,11/03/2010	15/03/2010	Encuestas de explotación Campo Cartagena	Murcia-Campo de Cartagena-Murcia
	CTT	540/10	23/03/2010	26/03/2010	Encuestas de explotación Campo Cartagena	Murcia-Campo de Cartagena-Murcia
	CTT	866/10	26/04/2010	05/05/2010	Encuestas de explotación Campo Cartagena	Murcia-Campo de Cartagena-Murcia
	JLGA	884/10	3-4-5/05/2010	06/05/2010	Reconocimiento hidrogeológico Campo de Cartagena	Murcia-Campo de Cartagena-Murcia
	CTT	1072/10	21/05/2010	26/05/2010	Red piezométrica del Campo Cartagena	Murcia-Campo de Cartagena-Murcia
	CTT	1295/10	14,15,22,23,24/06/2010	25/06/2010	Encuestas de explotación	Murcia-Campo de Cartagena-Murcia
	JHD	1357/10	24/06/2010	25/06/2010	Encuestas de explotación	Murcia-Campo de Cartagena-Murcia
	RAR	1340/10	05-06/07/2010	05/08/2010	Reunión del Proyecto Campo Cartagena	Murcia-Aeropuerto Alicante-Barcelona
	RAR	1486/10	13,14/07/2010	05/08/2010	Reconocimiento hidrogeológico y ensayos	Murcia-Campo de Cartagena-Murcia
	JLGA	1616/10	28,29,30/07/2010	04/08/2010	Trabajos de campo del Proyecto: redes de control	Campo de Cartagena
	JLGA	2040/10	13-14-15/10/2010	18/10/2010	Trabajos de campo del Proyecto	Campo de Cartagena
	JHD	2166/10	22/10/2010	02/11/2010	Estudio hidrogeológico Campo de Cartagena. Proyecto Séneca	Campo de Cartagena
	JLGA	2189/10	8-9-10/11/2010	11/11/2010	Seguimiento Tesis Doctoral Campo de Cartagena	Montpellier (Francia)
	JLGA	2339/10	15-16-17/11/2010	19/11/2010	Estudio hidrogeológico Campo de Cartagena. Proyecto Séneca	Campo de Cartagena
	JLGA	2407/10	22-23-24-25-26/11/2010	29/11/2010	Trabajos de campo estudio hidrogeológico Campo de Cartagena	Campo de Cartagena
	JHD	2448/10	29-30/11-01/12/2010	09/12/2010	Trabajos proyecto Séneca. Reunión UPC sobre modelo de flujo	Barcelona
	JLGA	2449/10	29-30/11-01/12/2010	09/12/2010	Trabajos proyecto Séneca. Reunión UPC sobre modelo de flujo	Barcelona

AÑO 2009	AÑO 2010	TOTAL	
112.20	1091.22	1203.42	José Luis García Aróstegui
37.40	463.20	500.60	Ramón Aragón Rueda
112.20	350.56	462.76	Jorge Hornero Díaz
423.30	395.08	818.38	Clemente Trujillo Toro
685.10	2300.06	2985.16	

Observaciones al estado de ejecución presupuestaria

El gasto total del Proyecto efectuado por el Subgrupo 1 en los años 2009 y 2010 ha sido de 37.646,82 euros, lo que supone una ligera diferencia respecto al total concedido (37.535,00). La justificación económica del IGME fue enviada a la Fundación Séneca con fecha 25/2/2011 (y fecha de entrada Séneca 1/3/2011). Respecto al subgrupo 2, la justificación económica ha sido realizada directamente por el correspondiente órgano económico (CEBAS-CSIC).

En la tabla siguiente se sintetiza la información justificativa de los gastos realizados.

Año	Tipo	Expediente	Importe	Detalle
2009	Factura contrato de servicios	´01001877	8800.00	Factura A.864 de fecha 30/12/2009 de la Empresa Sycro
	Comisiones de servicio		685.10	Comisiones de servicio (cuatro personas)
	Órdenes de trabajo Laboratorio del IGME	DTT 09/0413	420.00	Orden de trabajo DTT 09/0413: 15 análisis de cloruros a 28 euros/muestra = 420 euros
	Gastos generales		500.00	Gastos generales
2010	Factura Centro de Coste	1363/10	109.30	Factura M/2048 de fecha 07/04/2010 de la Empresa Foxen Murcia por 109.30 euros
	Factura Centro de Coste	1363/10	307.76	Factura de Papelería La Técnica por importe de 307.76 euros
	Factura Centro de Coste	1363/10	165.20	Factura M/2678 de fecha 13/09/2010 de la Empresa Foxen Murcia por 165.20 euros
	Factura Centro de Coste	1363/10	1121.00	Factura de SYCRO 2010.A.877 de 18/11/2010 para el acondicionamiento hidrogeológico de piezómetro 1121 euros
	Factura compra material	2019/10	1000.05	Factura M/2677 de fecha 13/09/2010 de la Empresa Foxen Murcia por 1000,05 euros. Ordenador portatil
	Factura compra material	2020/10	897.98	Factura de Geonatura nº 34075 de 11/08/2010 de compra de GPS y conductivímetro por importe de 897,98 euros
	Factura compra material	´01001994	1499.60	Factura 095/2010 de Miliarium de fecha 24/05/2010 por importe de 1499,60 euros. Software hidrogeologia
	Factura contrato de servicios	1901/09	5800.00	Primera factura (PY10050 de 10/3/2010) por importe de 5800.00 euros. Contrato Menor CIMNE
	Factura contrato de servicios	1901/09	5945.77	Segunda factura (PY10209 de 20/9/2010) por importe de 5945.77 euros. Contrato Menor CIMNE
	Comisiones de servicio		2300.06	Comisiones de servicio (cuatro personas)
	Órdenes de trabajo Laboratorio del IGME	DTT 10/0093	5270.00	Orden de trabajo DTT 10/0093: Feb-2010 con 34 muestras de análisis mínimo con 16 determinaciones a 155 euros/muestra.
	Órdenes de trabajo Laboratorio del IGME	DTT 10/0306	2325.00	Orden de trabajo DTT 10/0306: Jun-2010 15 muestras de análisis mínimo con 16 determinaciones a 155 euros/muestra.
	Gastos generales		500.00	Gastos generales

Gasto total en 2009	10,405.10 €
Gasto total en 2010	27,241.72 €
Gasto total del Proyecto	**37,646.82 €**

Importe concedido por F. Séneca: **37,535.00 €**
Diferencia **111.82 €**

3. RESUMEN DEL PROYECTO

Palabras clave: aguas subterráneas, acuíferos, modelos de flujo, modelos de transporte de masas, Campo de Cartagena.

Abstract:
El proyecto de investigación "Caracterización del acuífero Cuaternario del Campo de Cartagena y modelización matemática en el contacto con el Mar Menor" ha centrado sus objetivos generales, además de la mejora del conocimiento de los aspectos hidrológicos e hidrogeológicos, en la evaluación experimental de la calidad hídrica del acuífero en el entorno costero, y la estimación local de los aportes de flujo y cargas contaminantes al mar con ayuda de técnicas de simulación. Durante el desarrollo del proyecto, y a la vez que se mejoraba el conocimiento de la zona, algunas de las actividades del proyecto han sido más ambiciosas. De esta manera, se ha confirmado que este Proyecto ha supuesto el inicio de una línea de actualización y mejora del conocimiento de las aguas subterráneas de la zona, con una fuerte componente de colaboración e implicación de grupos de investigación nacionales e internacionales del el ámbito mediterráneo, que incluyen como aspectos relevantes la aplicación de técnicas hidroquímicas e isotópicas y su modelización a nivel global. Asimismo, se pretende que en un futuro próximo las aguas subterráneas puedan ser integradas con el resto de los recursos disponibles (trasvase, desalación y aguas regeneradas), y que ello suponga un uso óptimo de los recursos, que se podría ver beneficiado por un factor de escala.

PRESENTACION DE LA INVESTIGACIÓN HIDROGEOLOGICA EN EL CAMPO DE CARTAGENA

MINISTERIO
DE EDUCACIÓN
Y CIENCIA

INSTITUTO
GEOLÓGICO
Y MINERO DE ESPAÑA

Current status of hydrogeological research in the experimental watershed of Campo de Cartagena (Murcia, SE Spain)

José Luis García Aróstegui

Geological Survey of Spain (www.igme.es)

Increasing the regional competitiveness and economic growth through the RTD&I on Sustainable Water Management
Regional Seminar on Competitiveness. Galilee (Israel), 17-19 January 2011

Introduction

In the framework of the creation of the new

Research Platform of Water Resources in Scarcity Areas (PIRHZE),

this study is a part of:
Project "Hydrological modeling in Semi-arid zones“,

coordinated by

Euro-Mediterranean Water Institute Foundation (IEA)

financed by:

Regional Ministry of Universities, Business and Research
(Government of Murcia)

executed by:

Institute for Water and Environment (INUAMA, University of Murcia)

with the active collaboration of:

Geological Survey of Spain (IGME)
Institut de Recherche pour le Développement (IRD, France)

Other collaborations:
CEBAS/CSIC, IMIDA, UPC,
UGR, UPCT, Segura River Basin Authority, ZIWR (BGU, Israel),

Other funds of: 08225/PI/08 research project financed by “Programa de Generación del Conocimiento Científico de Excelencia” of Fundación Seneca, Región de Murcia (II PCTRM 2007-10).

Main Groundwater Bodies in Mediterranean Basin

(Margat and Vallée, 2000, in Blue Plan)

Country & Entities		Name	Type of reservoir	Area (km²)	Average Discharge (hm³/yr)
ES	Spain	Mancha Oriental	multi-layered sediments	3300	330
		Valencia plain	"	760	430
		Campo de Cartagena	"	1390	32
		Valle del Ebro	alluvial	1000	336
FR	France	Jura, bassins du Doubs et de La Loue	karstic	6350	4200
		Bas-Dauphiné	multi-layered sediments (mollasse)	3300	1245
		Vaucluse	karstic	1230	600
		Vercors	"	846	950
		Plan de Canjuers / Verdon	"	911	450
		Larzac	"	950	400
		Comtat / Miocène du Vaucluse	alluvial	668	165
		Crau	"	545	200
		Roussillon	multi-layered sediments	860	60
IT	Italy	Po Bassin	alluvial, multi-layered sediments	30000	15145
		Italie centrale	egroup of karstic aquifers	15000	10000
HR, SI	Croatia-Slovenia	Dinarik region	group of karstic aquifers	80000	15000
LB	Lebanon	Mont Liban	group of karstic aquifers	2085	930
IL-WE	Israel-West Bank	Mountain Aquifer	karstic	~ 5000	660
IL-GZ	Israel-Gaza Strip	Coastal plain	multi-layered sediments	2165	325
EG	Egypt	Nil Delta	alluvial, multi-layered sediments	30000	2300
		Vailée du Nil	alluvial	11000	
		Moghra Aquifer	sedimentary, carbonate	~ 200000	100 à 200
LY	Libya	Kikla Aquifer (Hamada Basin)	multi-layered sediments (c)	215000	100 à 300
		Jebal Al-Akhdar	karstic	~ 20000	~ 500
LY-TN	Libya-Tunisia	Jeffara plain	multi-layered sediments	35000	~ 400
TN	Tunisia	Nord-Ouest de Tunisie	group of karstic aquifers	8100	55

Campo de Cartagena represents one of the main aquifer system in Mediterranean Basin

Campo de Cartagena aquifer: "An excellent Natural Laboratory"

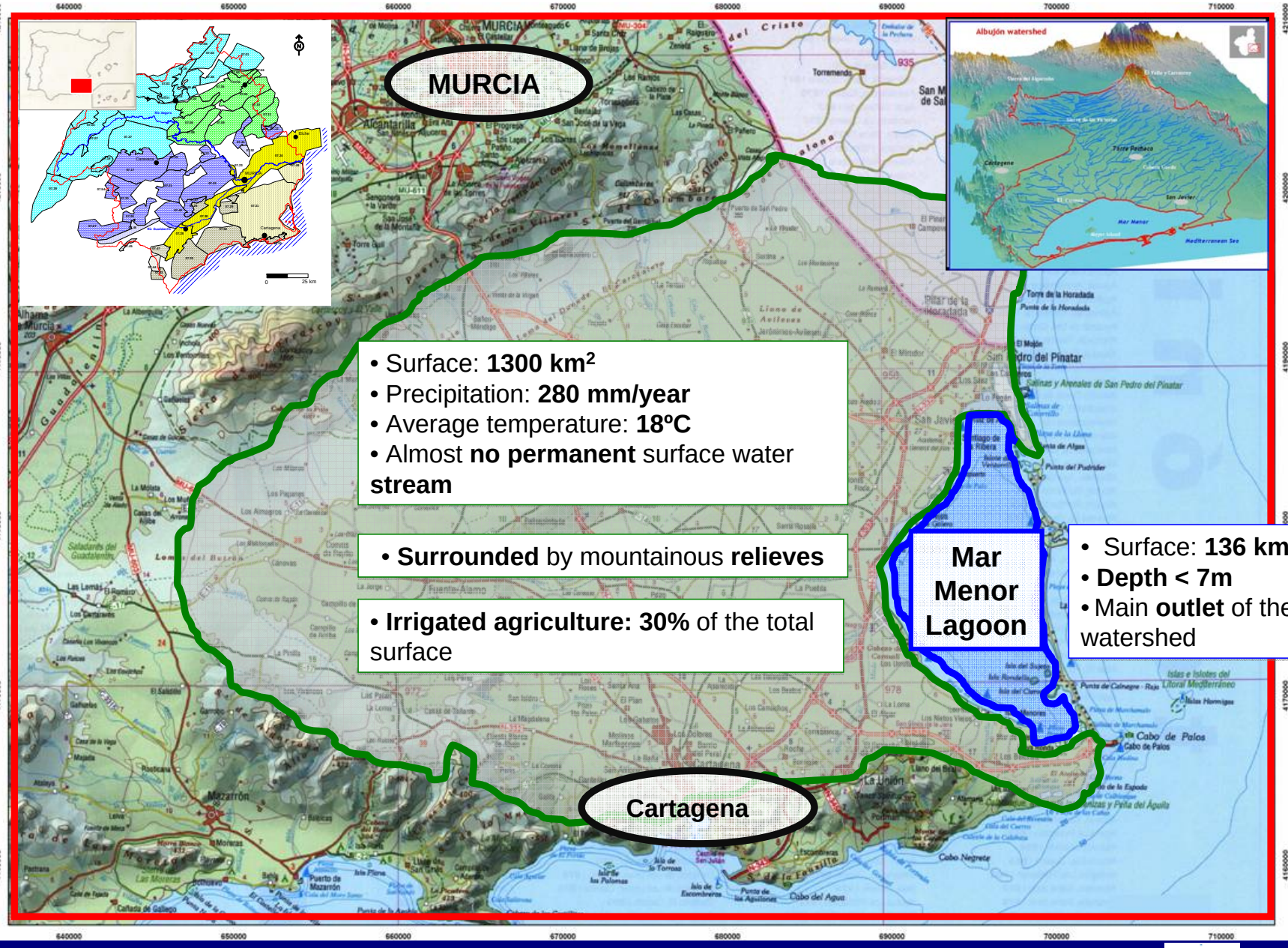

WATER FOR AGRICULTURE=WATER FOR FOOD

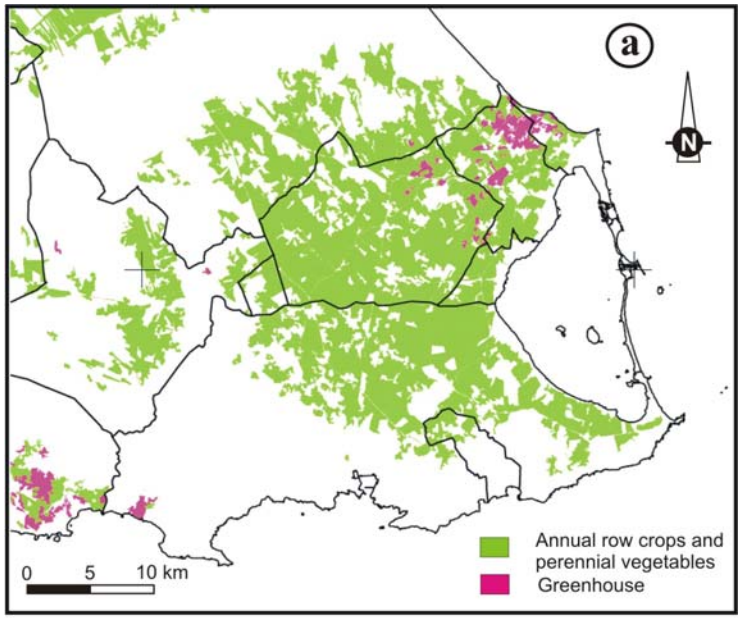

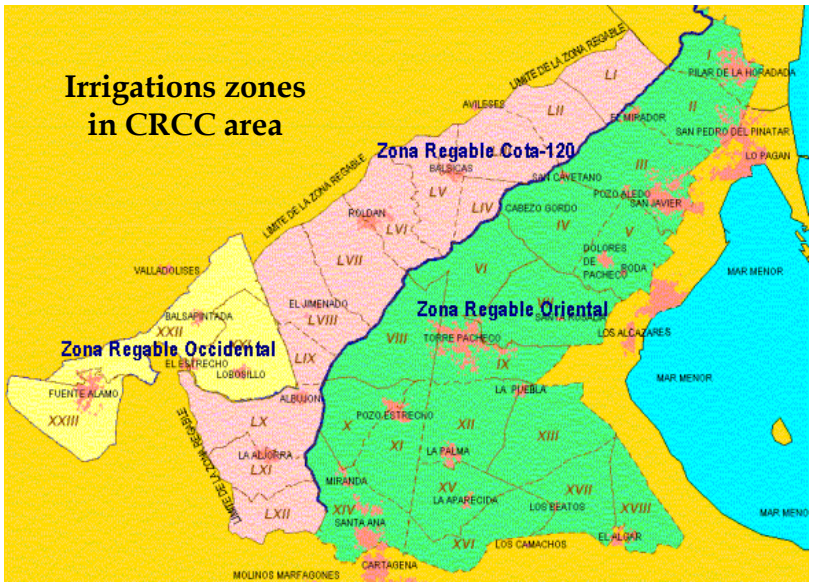

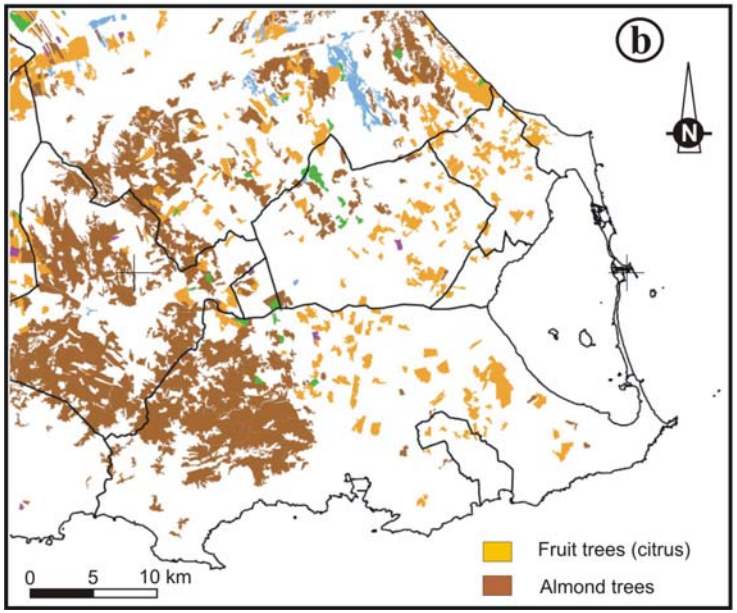

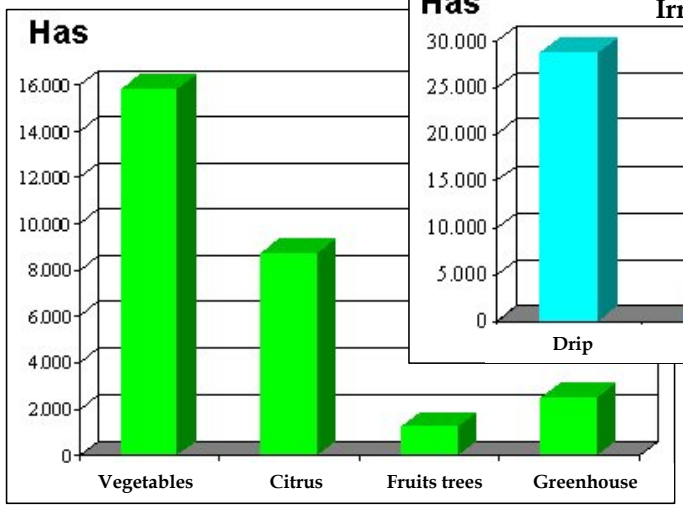

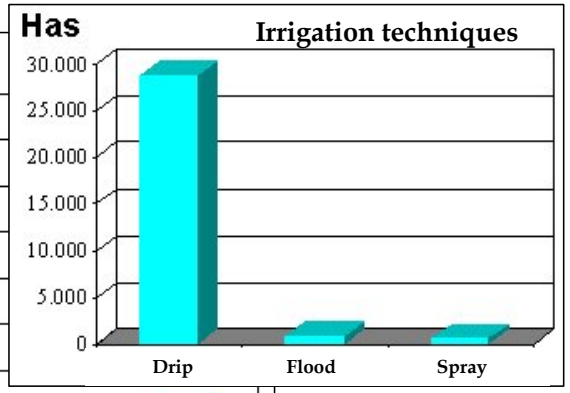

(*) in CRCC area

Total demand of water and sources of supply

TOTAL DEMAND OF WATER (AGRICULTURE):

→ Close to 200 MCM/year

SOURCES OF WATER:

- **Tagus-Segura water transfer canal (TTS)**
- **Groundwater (GW):** More than 1200 privates wells.
  Associated desalination plants of brackish GW
- **Desalinated Water** (seawater: large plants under construction)
- **Treated Sewage Water**
- **Precipitation and natural surface water:** limited availability

Simplified hydrogeological map

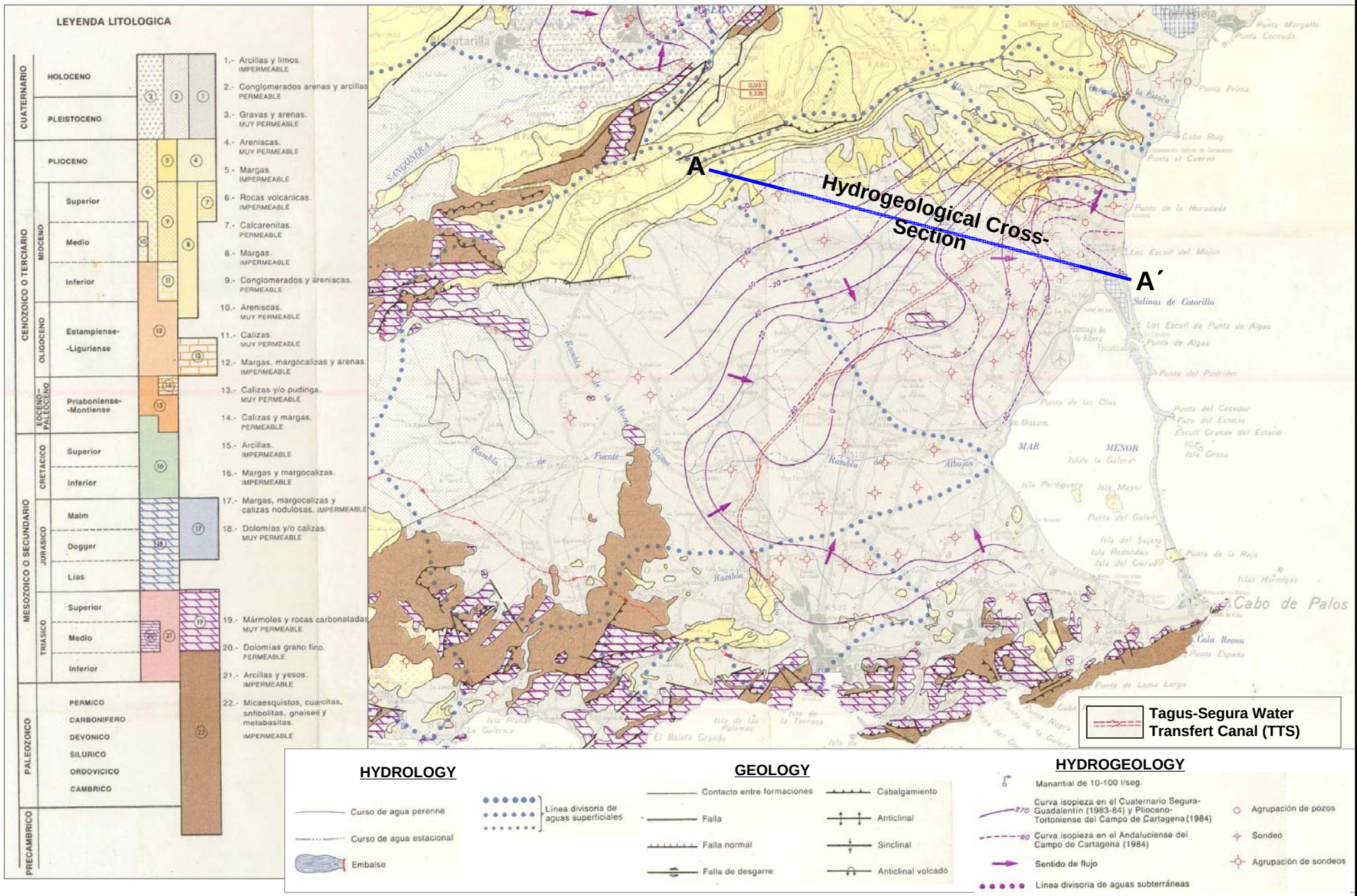

(IGME, 1985)

HYDROGEOLOGICAL CROSS-SECTION

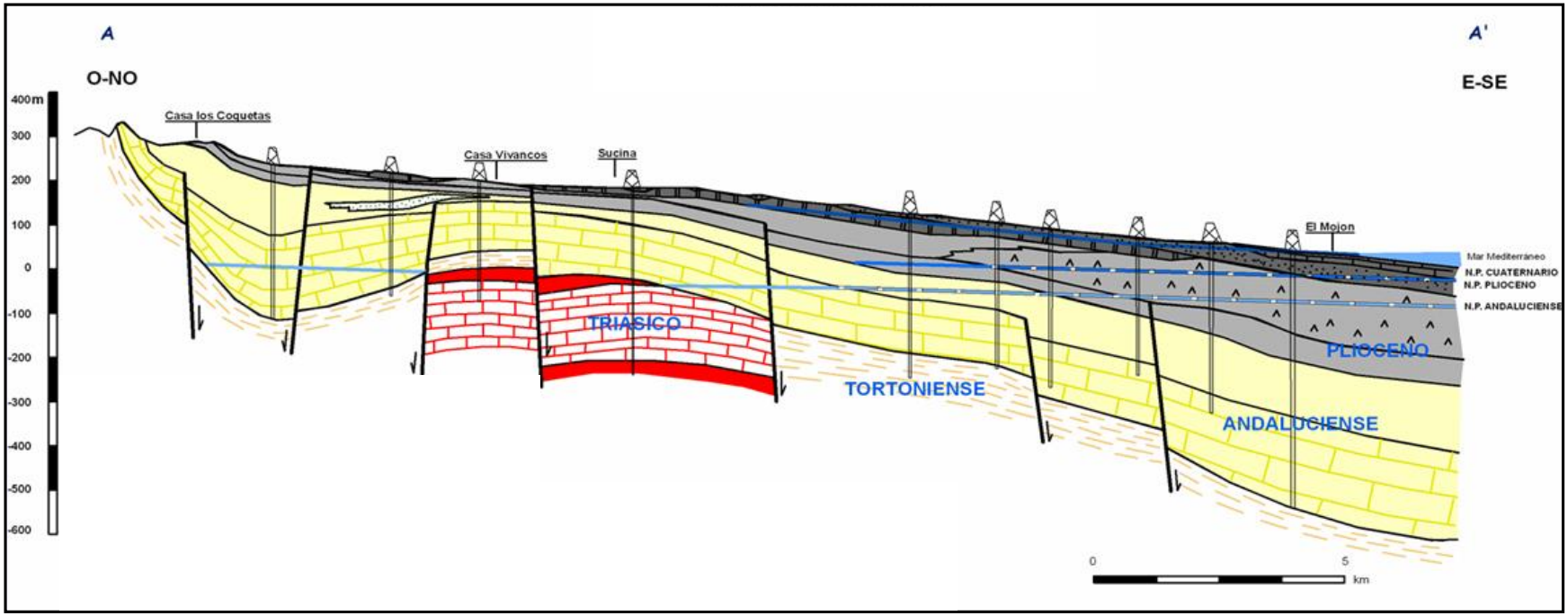

Aquifer/layer	Geological material	Total surface	Outcroping surface
Quaternary	Alluvium	1135 km^2	1135 km^2
Pliocene	Sandstone	817 km^2	22 km^2
Messinian (=Andalucian)	Sandstone, Sand, Clays (North) Bioclastic limestone (South)	570 km^2	28 km^2
Tortonian	Conglomerates and Sandstone	43 km^2 (?)	25 km^2
Triassic	Marble	101 km^2	1 km^2

CONCEPTUAL MODEL OF THE MULTI AQUIFER SYSTEM (values under review)

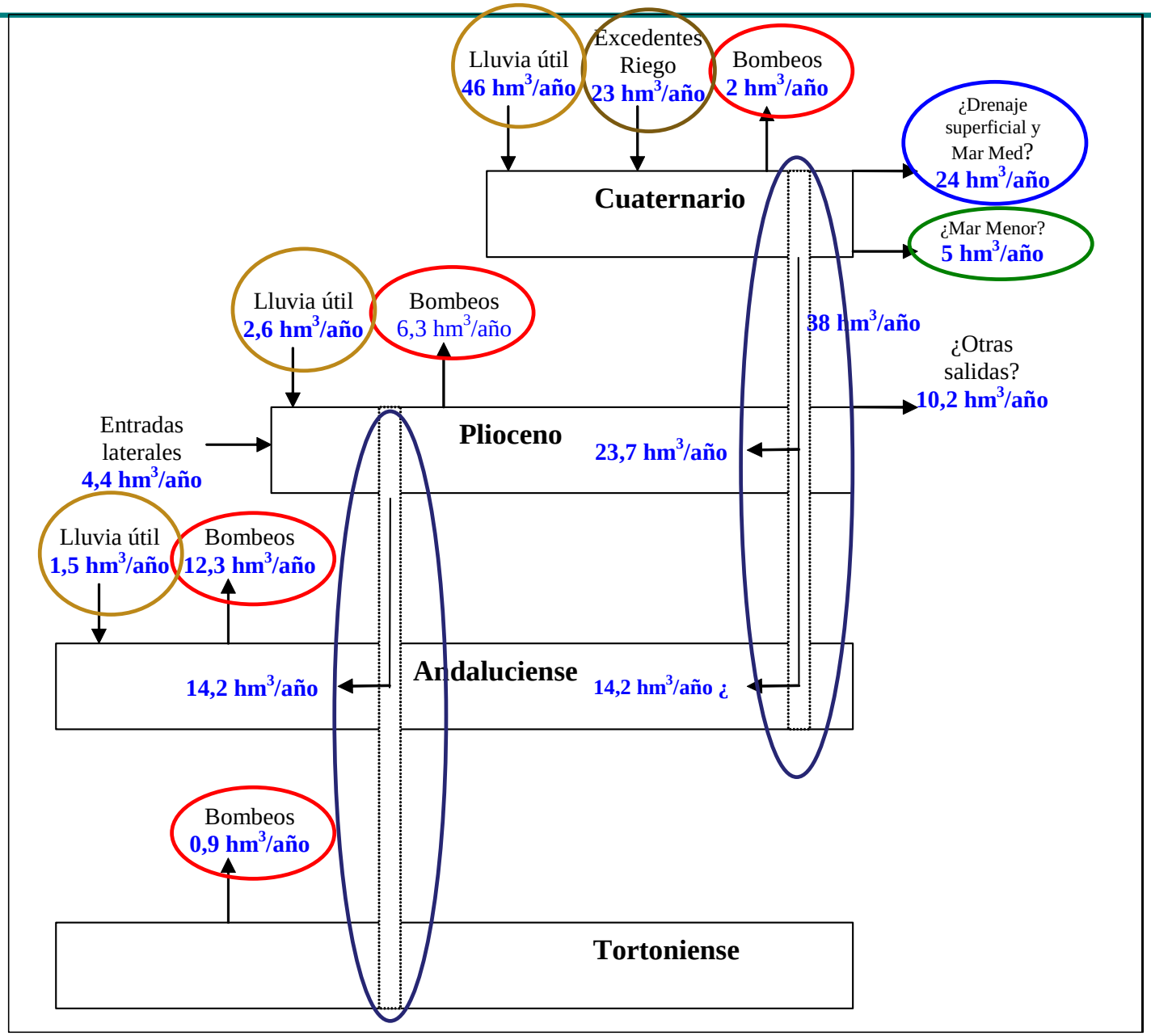

A) Rain water infiltration

B) Irrigation return-flow

C) Pumping well

D) Surface water / groundwater interaction

E) Submarine Groundwater discharge

F) Inter-aquifer exchanges through wells

(Based on IGME, 1991)

THE STRATEGIC ROLE OF GROUNDWATER

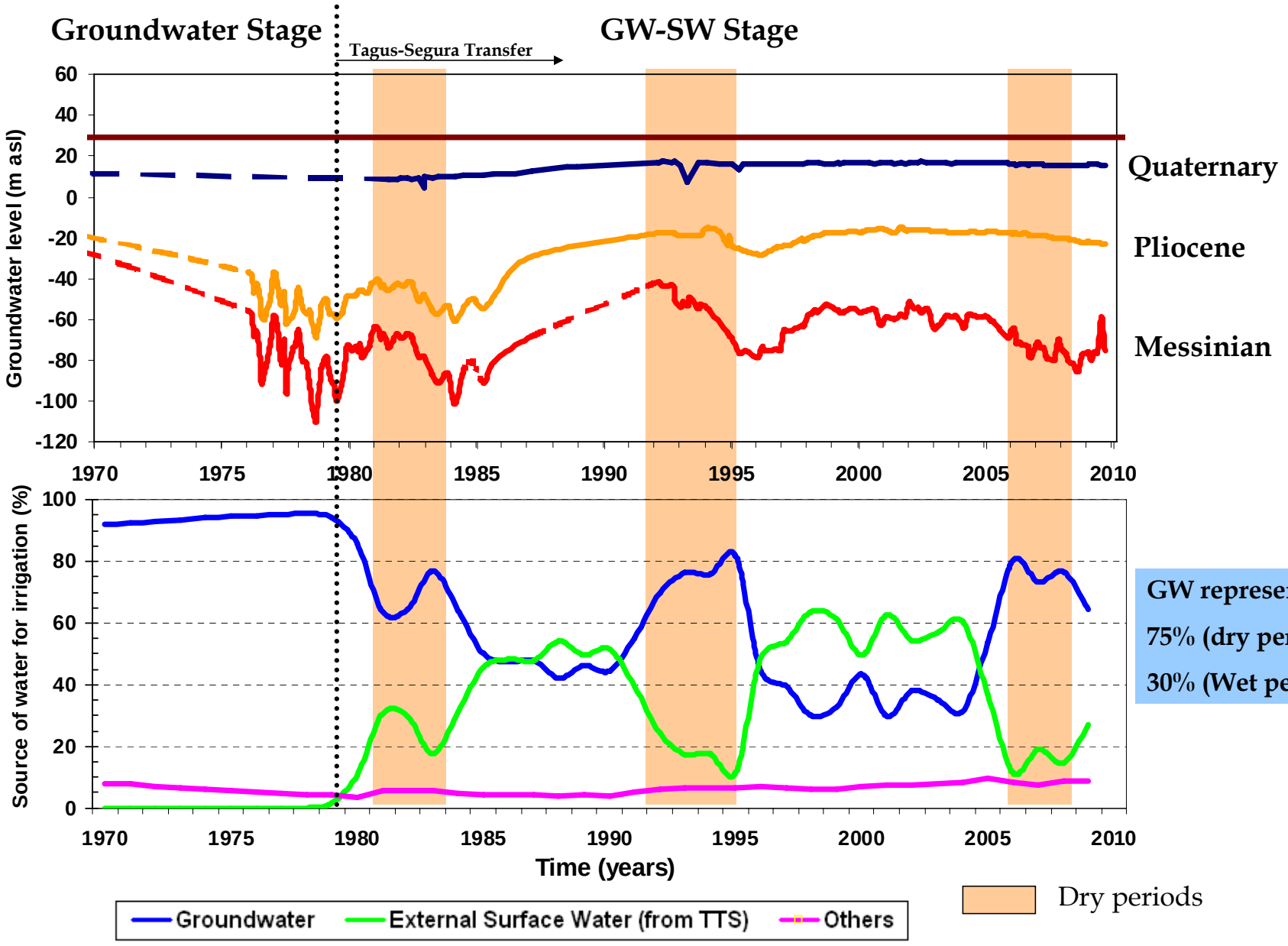

Major hydrogeological uncertainties

1. Hydrogeological geometry
2. Natural aquifer system conditions
3. Similar Hydrochemical characteristics of the main aquifer layers
4. Multiple recharge sources
5. Interconnectivity between the superficial aquifer and the deep confined aquifers (role of wells)
6. Submarine Groundwater Discharge (SGD): to Mar Menor and Mediterranean Sea

These uncertainties turn into Research Opportunities and Challenges

Updating geometry: Re-interpretation of Geology from a hydrogeological point of view

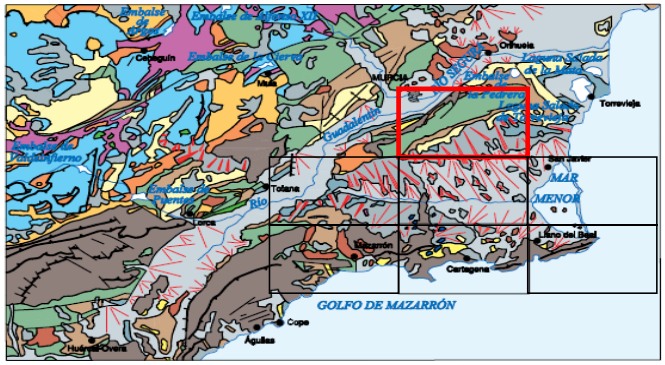

Since late 2010, updated geological maps (1:50.000) in the area are available (made by IGME and Government of Murcia)

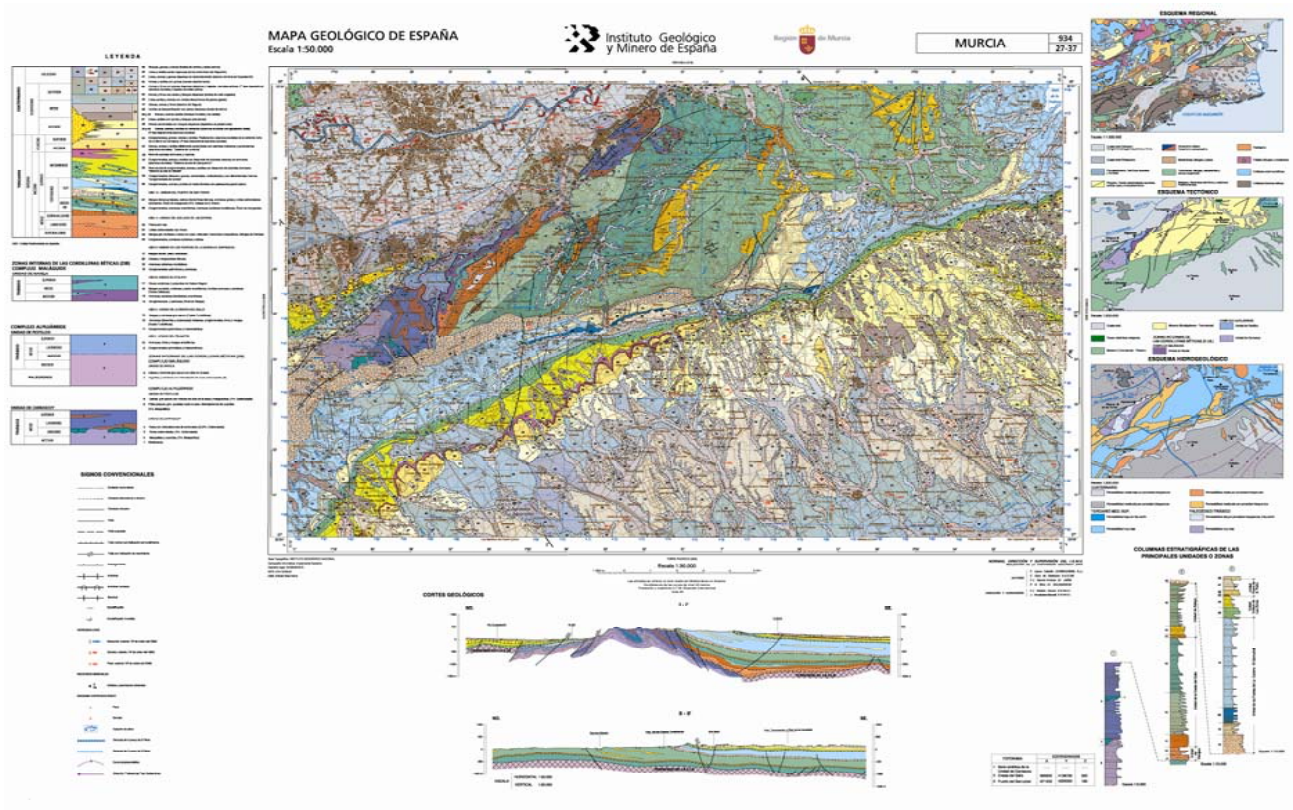

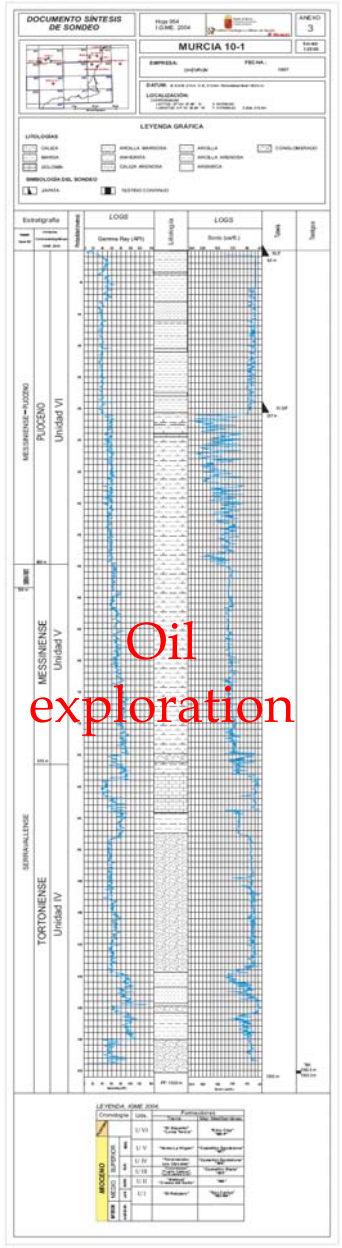

Updating geometry: boundaries

Surface of the aquifer below sea level

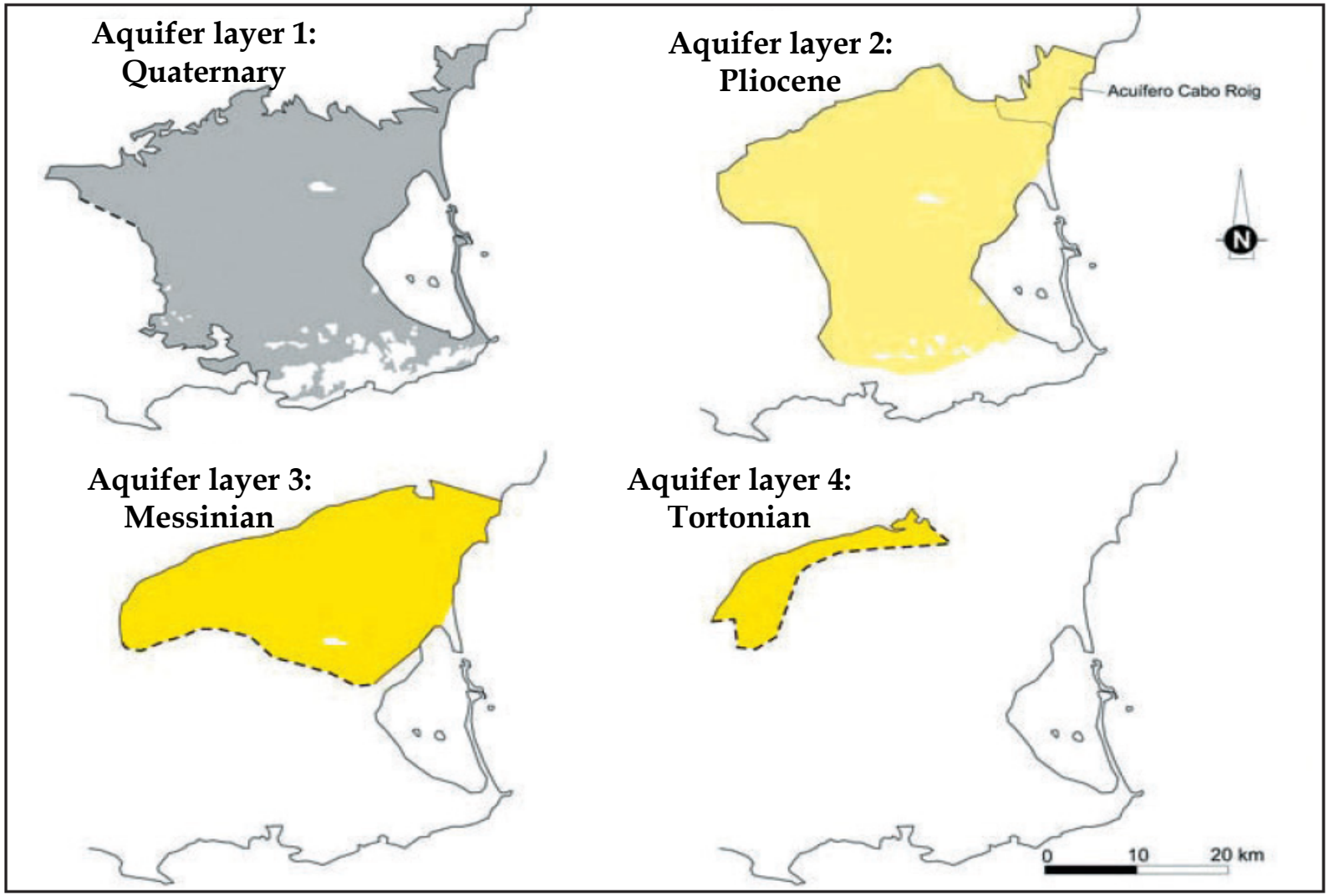

Updating geometry: Determination of aquifer boundaries extending under the sea

Digital topography and bathymetry of the area of the Campo de Cartagena-Mar Menor-Continental Platform

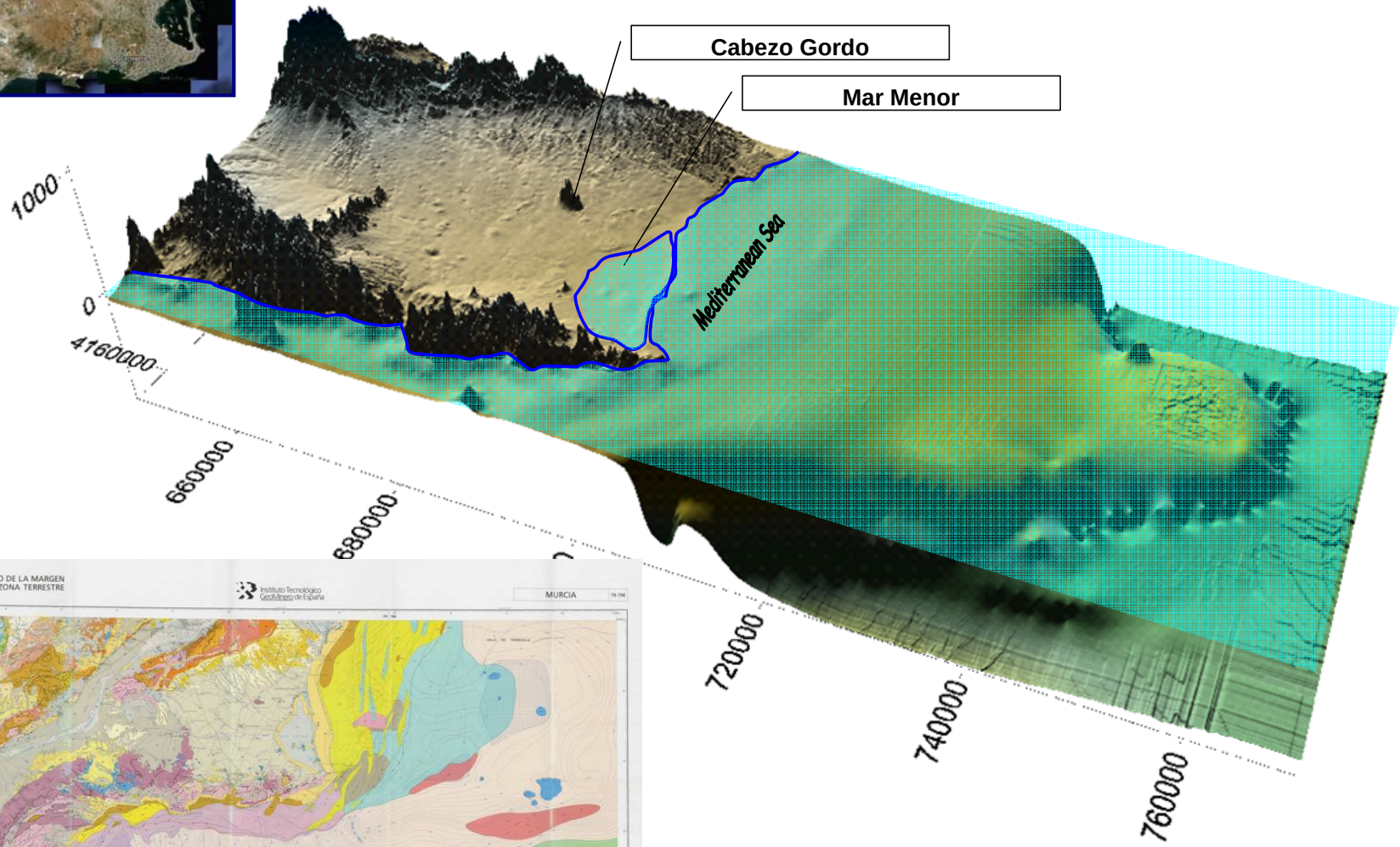

Geological map to the continental platform in front of Murcia's coast

GEOMETRY: building a 3D hydrogeological model

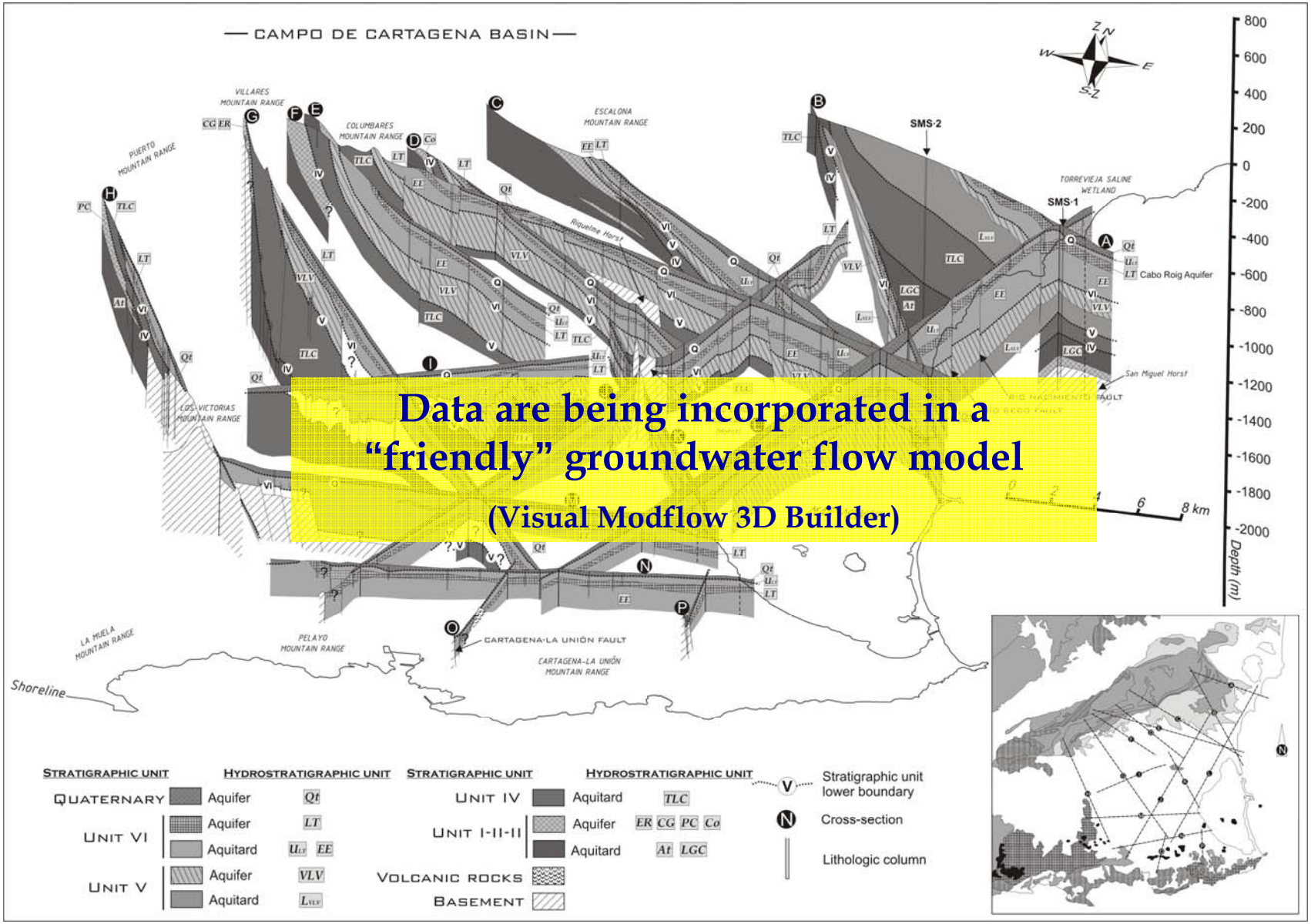

Jiménez-Martínez, J., Candela, L., García-Aróstegui, J.L. and Aragón, R. (in press). Geologica Acta

Natural aquifer conditions

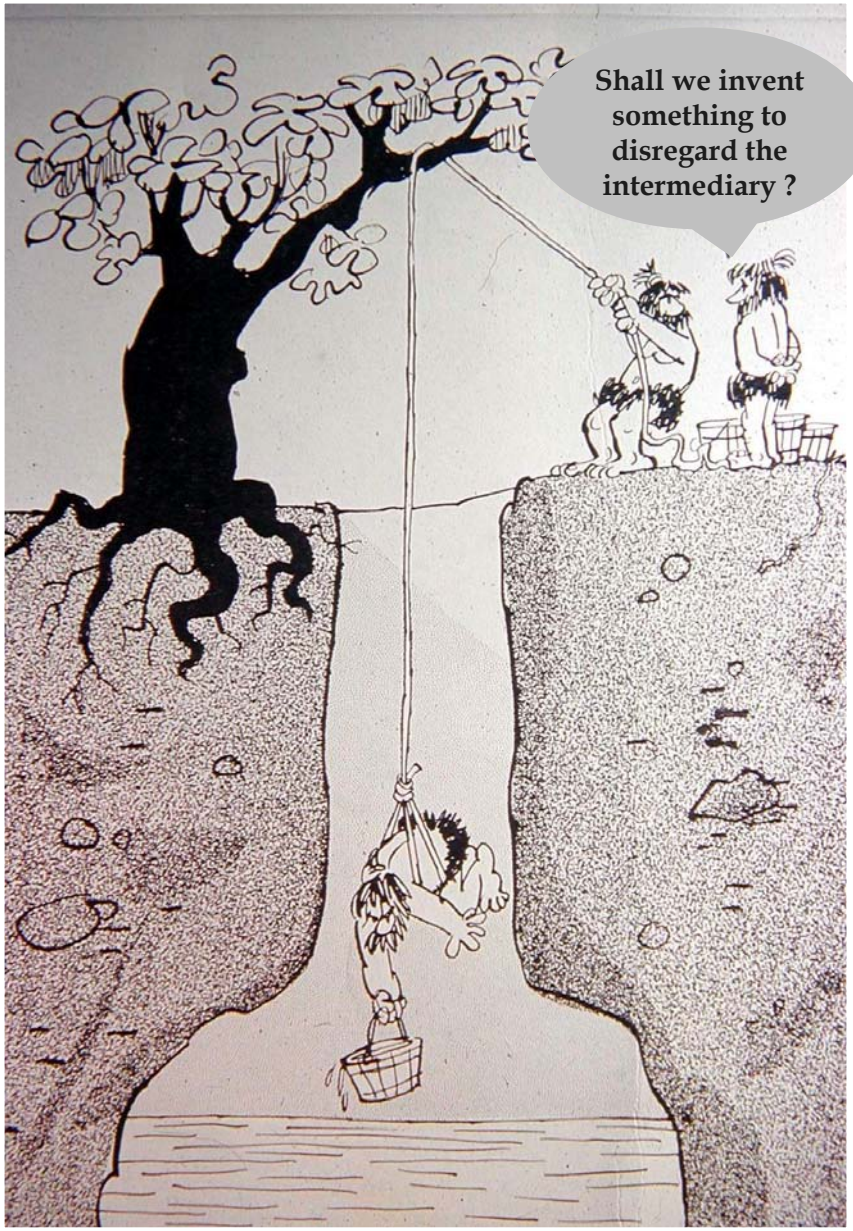

- Highly anthropized system
  - Doubts about the pre-development groundwater flow (before 1920)

✓ Searching older data

✓ Cross-checking with hydrochemical, isotopes and hydrogeological conceptual model

Looking for natural aquifer conditions

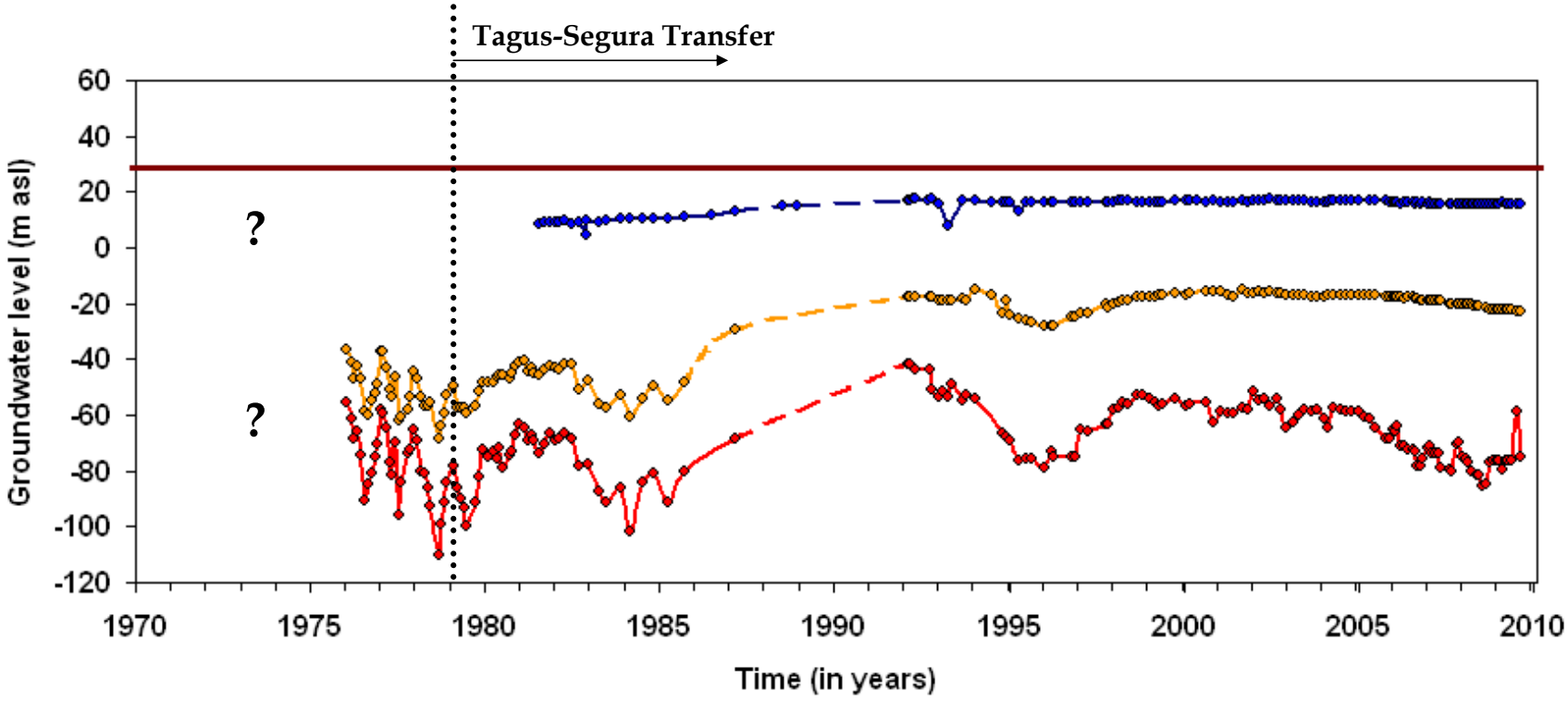

- Systematic data recording since 1975

From natural conditions to the current situation

Representative trend of water levels in San Javier area, since 1920

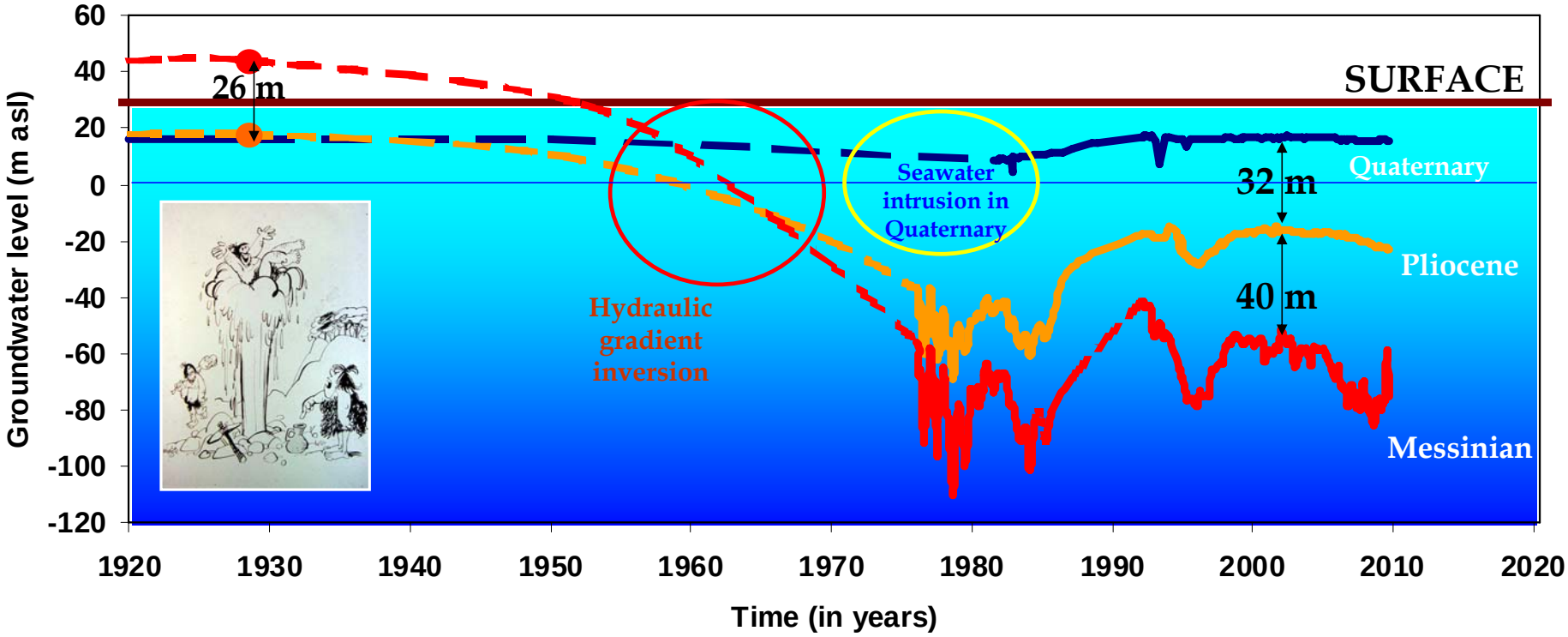

IGME´s reports encouraged the construction of artesian wells in Campo de Cartagena, in 1851, 1918 and 1928. 1925-1928: First artesian wells

Rubio, J.M. (1928). Revista Minera

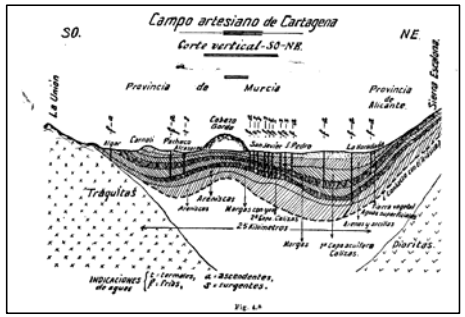

Sondeo Casa Grande (San Javier. Año 1928)

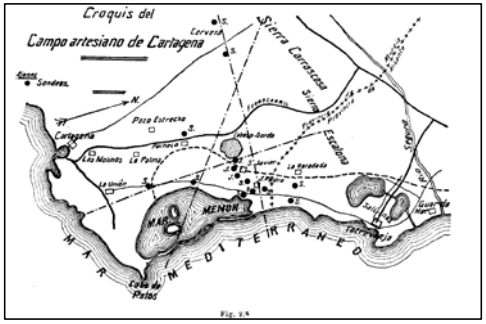

Similar Hydrochemical characteristics

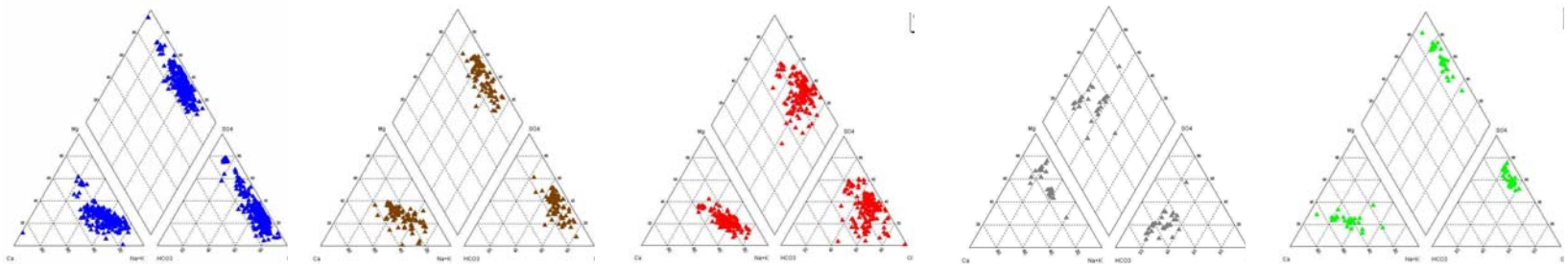

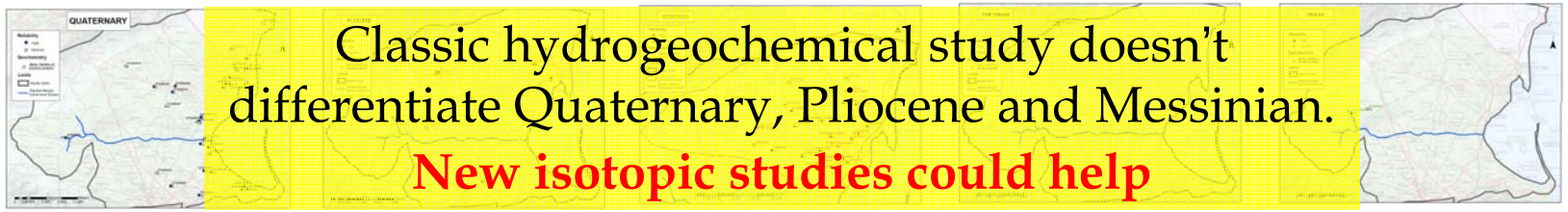

Classic hydrogeochemical study doesn't differentiate Quaternary, Pliocene and Messinian.

New isotopic studies could help

Many attemps with different techniques and sets of hydrochemical data (aquifers, time periods, spatial areas…)
--> No interesting results

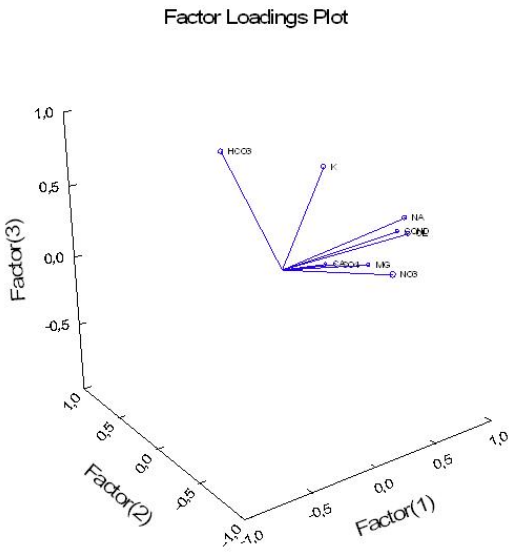

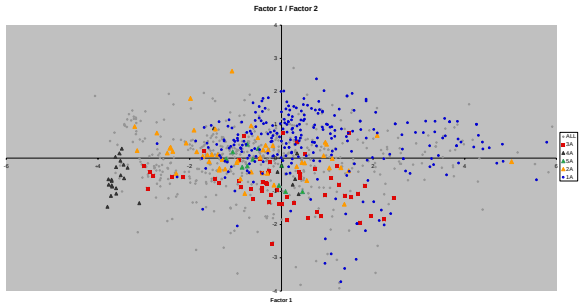

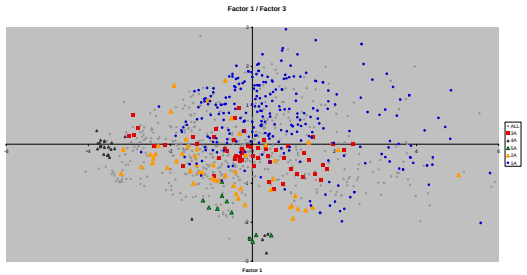

% of total variance explained:
Factor 1: 51%
Factor 2: 13%
Factor 3: 12%

Quantification of multiple recharge sources

Collaboration with Zuckerberg Institute for Water Research, Ben-Gurion University of the Negev (IL): Mixing Cell Model developed by Prof. Eilon Adar

In a complex hydrogeological basin like Campo de Cartagena, common hydrological models cannot be used due to lack of hydrogeological information and scarce hydrological data. Therefore, a firm regional groundwater flow pattern, groundwater balance and the groundwater quality distribution cannot be achieved.

Using Hydrochemical & Environmental Isotopes in a flow model may provide a quantitative evaluation of groundwater fluxes in complex basins with scarce hydrological data.

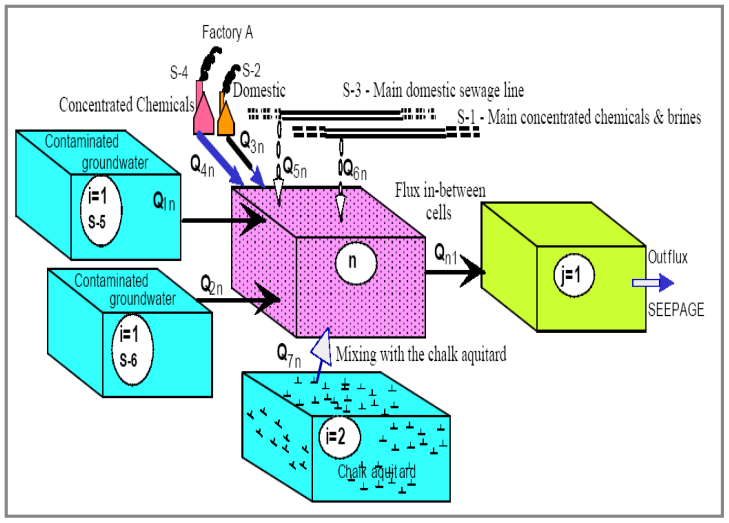

Recharge by contaminated effluents

The Mixing Cells Modeling (MCM) concept

Objectives: Demonstrating that a simple, yet reliable hydro-chemical and environmental isotopes model can be adopted for assessing the hydrological system in complex basins:

Elaborating on:

Sources of groundwater recharge

Sub-surface flow pattern

Developing a numerical model that can identify and provide a quantitative assessment of recharge components, groundwater fluxes, and physical properties of the aquifer.

Quantification of multiple recharge sources

First results:

- → **MCM is a useful tool to distinguish the signature of each aquifer hydrochemistry.**
- → **However, the calibration needs better information on the groundwater abstraction**

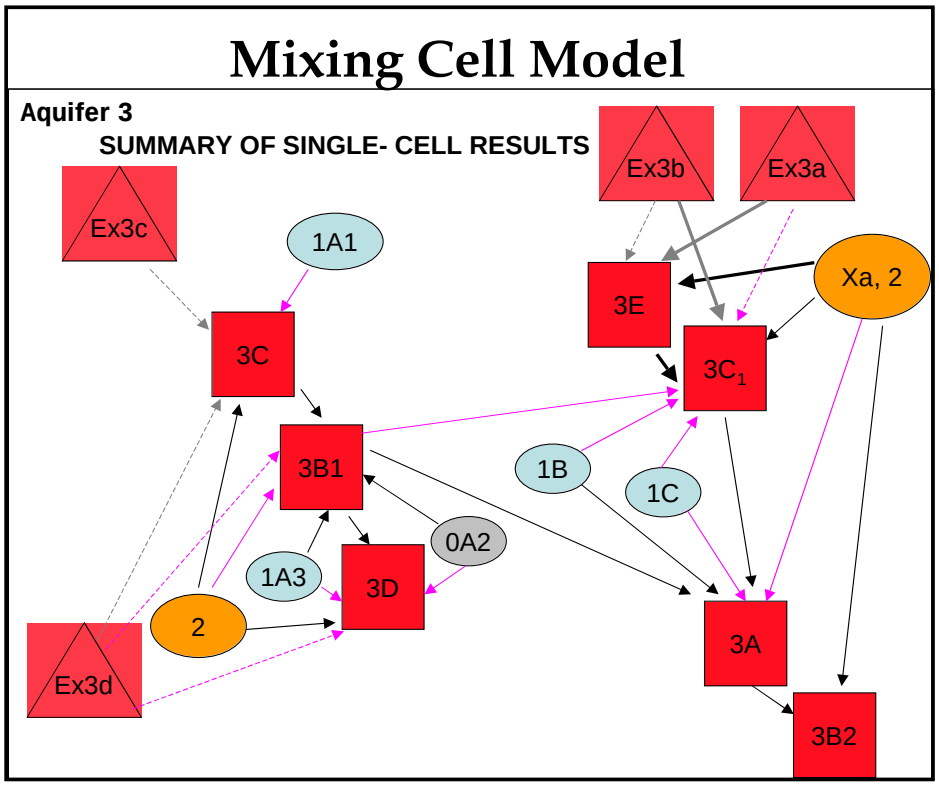

Next step:

- → Improve the groundwater abstraction data.
- → To introduce new isotopic data.

Hydrochemical and Isotopic research

- Promote national and international (active) cooperation
- In a first step, the idea is to combine the use of geochemical tracers including noble gases (Ne, Ar, Kr, Xe and Rn), and isotopes (^{18}O, ^{2}H, ^{13}C, ^{14}C, ^{34}S), in order to estimate the groundwater recharge, groundwater flow and mineralization processes, in the last 50.000 years.

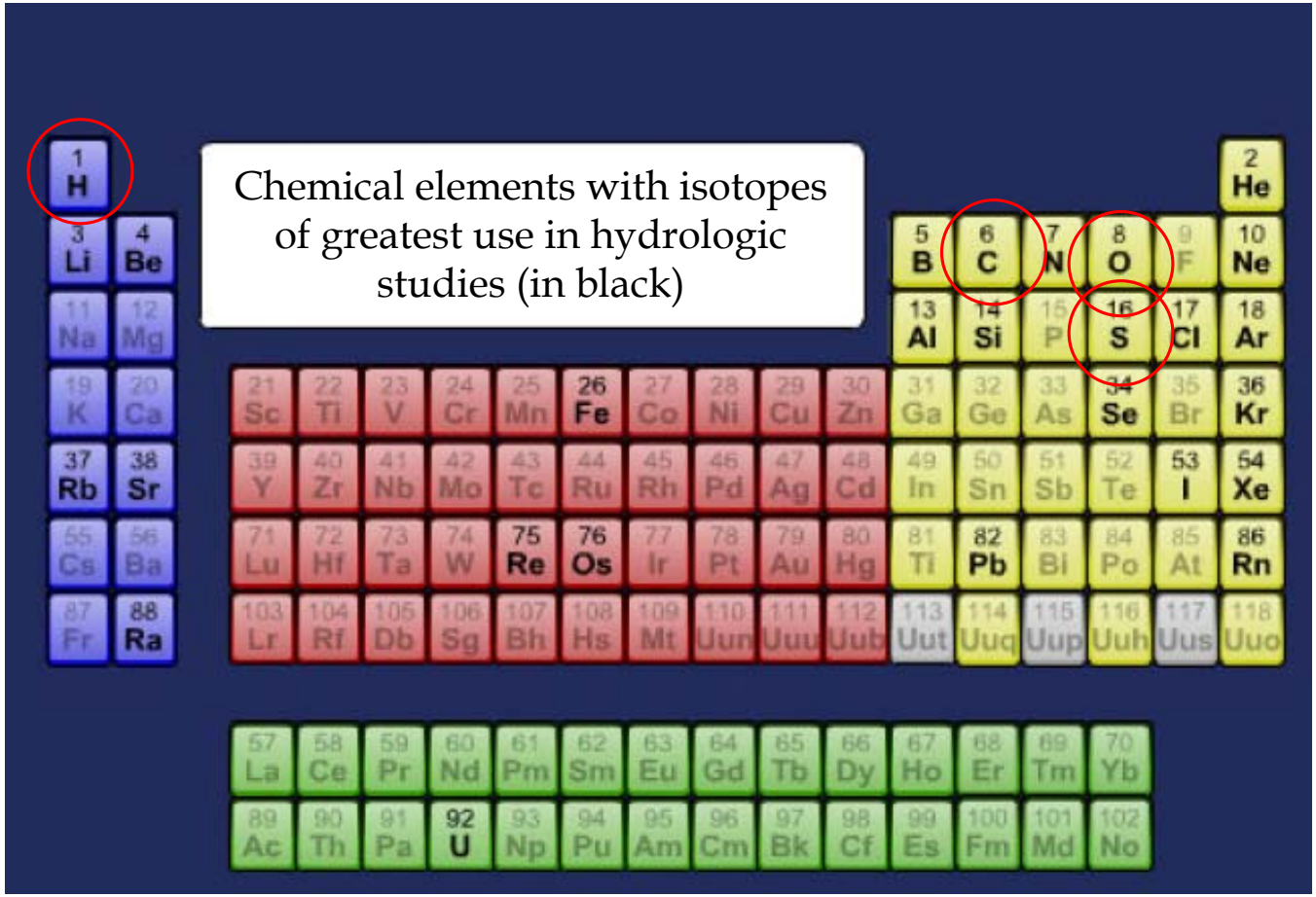

From: Sustainable of semi-Arid Hydrology and Riparian Areas SAHRA (www.sahra.arizona.com)

Isotopic research collaborations

ENVIRONMENTAL ISOTOPE	MAIN APPLICATIONS	COLLABORATION	STATE OF DEVELOPMENT
Oxygen-18 (^{18}O) and Deuterium (^{2}H) (in H_2O)	Origin of groundwater (identification of recharge areas and palaeowaters); interconnection with surface water; salinisation mechanisms	**LaMA,** Laboratoire Mutualisé d'Analyse des isotopes stables de l'Eau. University of Montpellier II, France.	Routine application
Carbon-13 (^{13}C in HCO_3)	Correction for C-14 dating and identification of paleowaters	**IDES,** University of Paris Sud-Orsay, and **CEA,** French Atomic Energy Commission	
Sulphur-34 (^{34}S) and Oxygen-18 (^{18}O) (in SO_4)	Identification of pollution sources	Considered in a second step	Research deployment
Nitrogen-15 (^{15}N) and Oxygen-18 (^{18}O) (in NO_3 and N species)	Identification of pollution sources and microbial denitrification processes		
Boron-11 (^{11}B) (in $B(OH)_4$ and $B(OH)_3$)	Identification of pollution sources and origin of salinity		
Krypton-85 (^{85}Kr)	Groundwater transport mechanisms and delineation of protection zones		Development stage
Tritium (^{3}H)	Identification of recent aquifer recharge and vadose zone tracer	Laboratoire d´Hydrogéologie. University of Avignon. France	Routine application
Helium-3 (^{3}He)	Dating of young groundwater		Research deployment
Carbon-14 (^{14}C)	Dating of old groundwater	**IDES,** University of Paris Sud-Orsay, and **CEA,** French Atomic Energy Commission	
Argon-39 (^{39}Ar)	Dating of very old groundwater		Development stage
Krypton-81 (^{81}Kr)			
Uranium-234 (^{234}U)			
Chlorine-36 (^{36}Cl)			

Noble gases: recharge temperature, i.e. paleoclimatic information: GEOTOP, Québec, Montreal, Canada

Interconnectivity between the superficial aquifer and the deep confined aquifers (role of wells)

1.18 wells per km^2!!!! and most of them connecting several aquifers

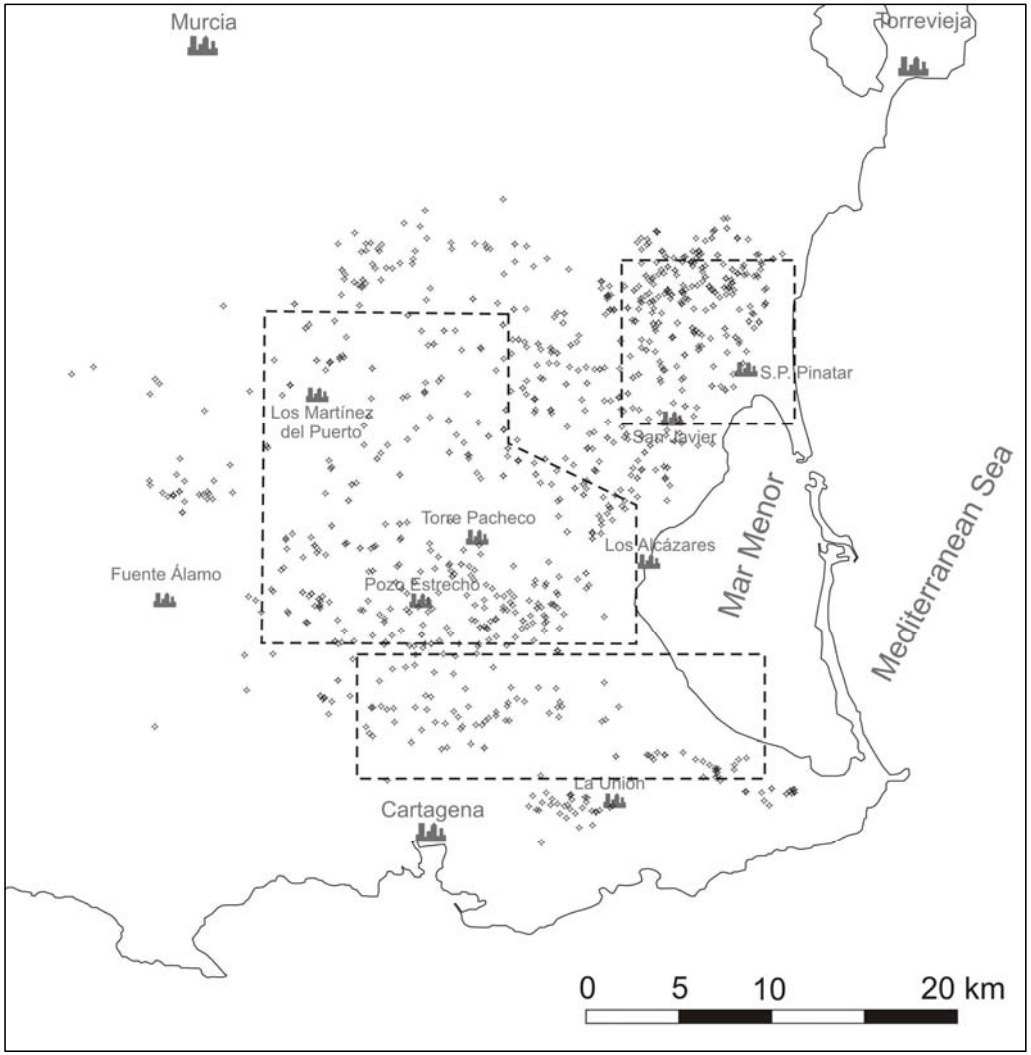

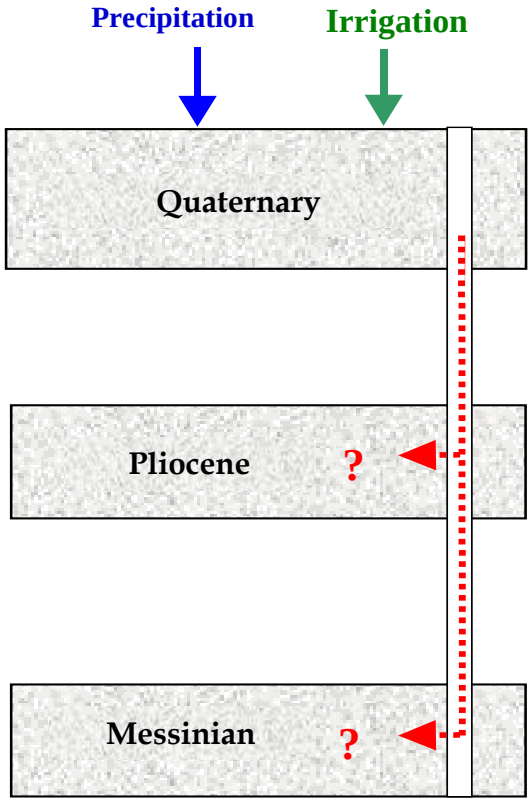

Interconnectivity between the superficial aquifer and the deep confined aquifers. Tracing and dating Young Groundwater

Methodology: Sulfur hexafluoride (SF_6) and **Tritium (^3H)**

Can be used to:

- Trace the flow of young water (water recharged within the past 50 years)
- Determine the time elapsed since recharge.

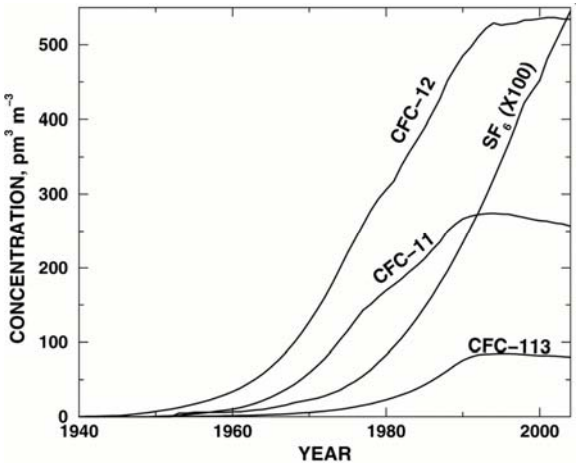

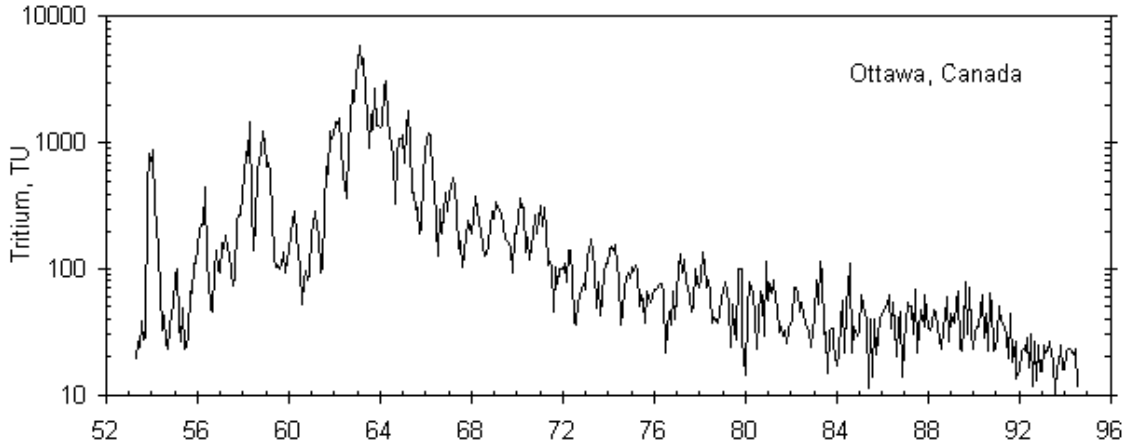

Clark y Fritz, 1997, datos: Brown, AECL, Canadá)

Collaboration:
IDES, University of Paris Sud-Orsay, France
Laboratoire d´Hydrogéologie, University of Avignon, France
Institut de Recherche pour le Développement, Montpellier, France

Submarine Groundwater Discharge (SGD):
to Mar Menor and Mediterranean Sea

Identification of freshwater/saltwater interface via Electrical resistivity tomography: Mar Menor area

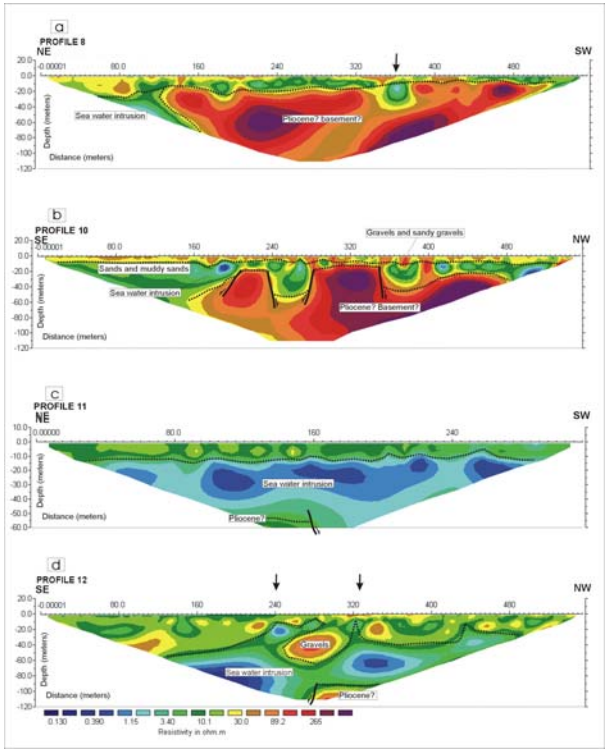

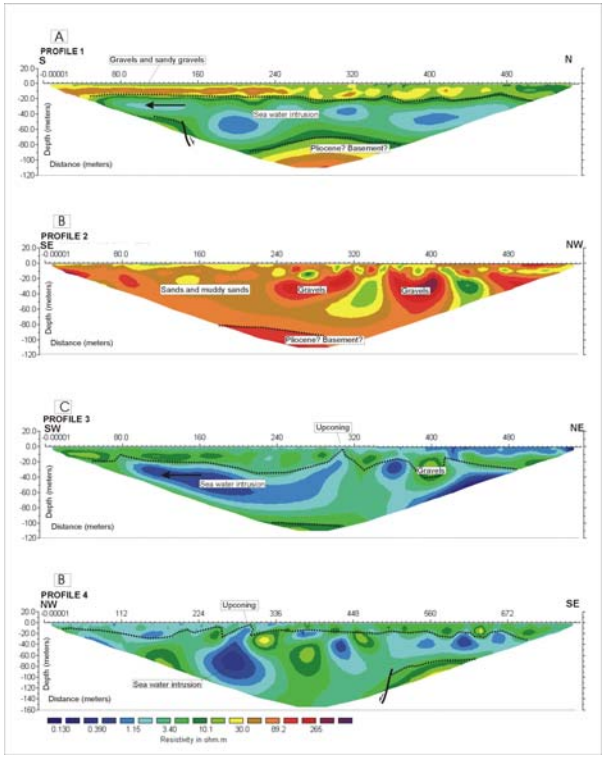

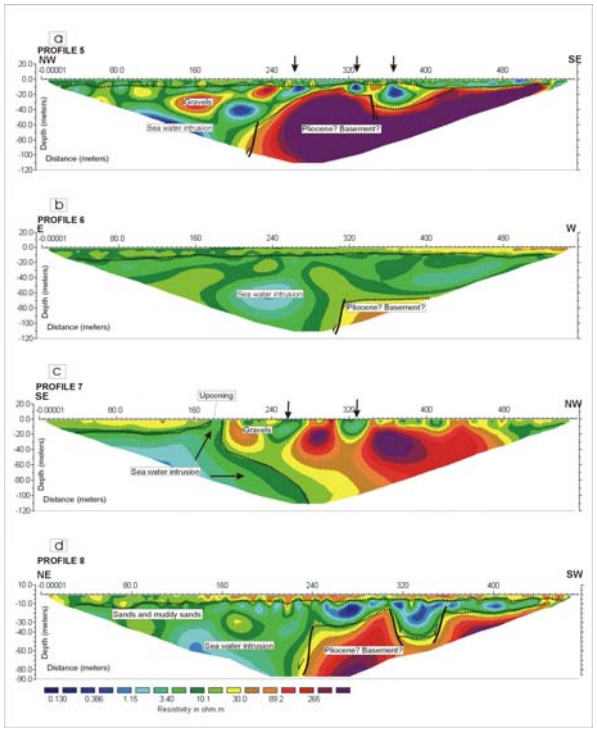

Submarine Groundwater Discharge (SGD):
to Mar Menor and Mediterranean Sea

Applying isotopes of Radon to Mar Menor

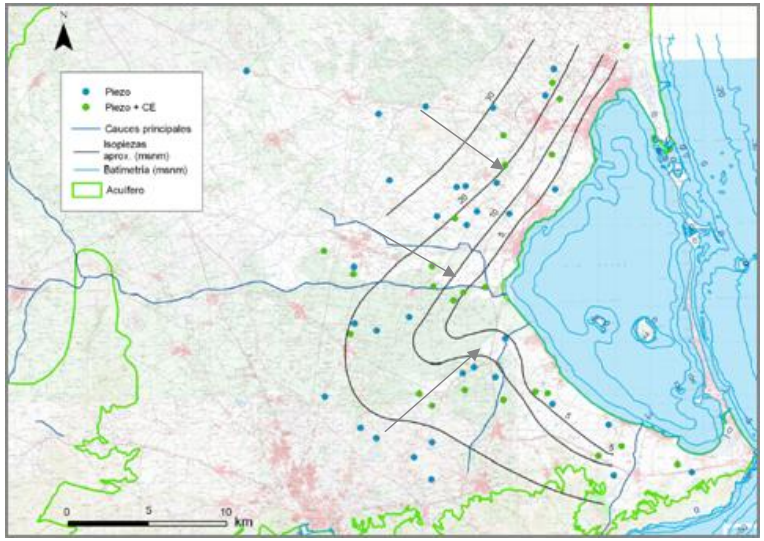

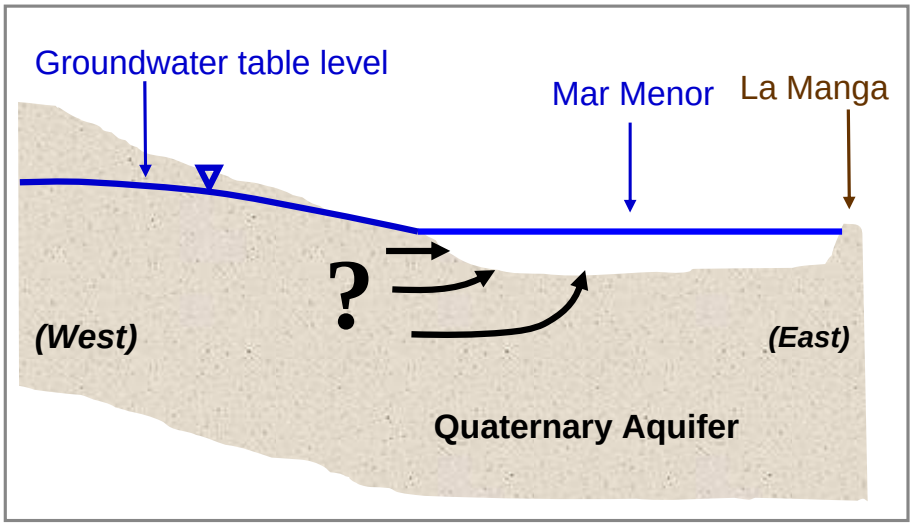

Submarine Groundwater Discharge (SGD):

to Mar Menor and Mediterranean Sea

Ejecuted by Aformhidro Company (www.aformhidro.com)

Groundwater tracer test near Mar Menor

(Los Alcazares area)

CROSS-CHECKING

Using geochemical, isotopic and hydrogeological information. These data could be interpreted in relation to past climatic and environmental conditions

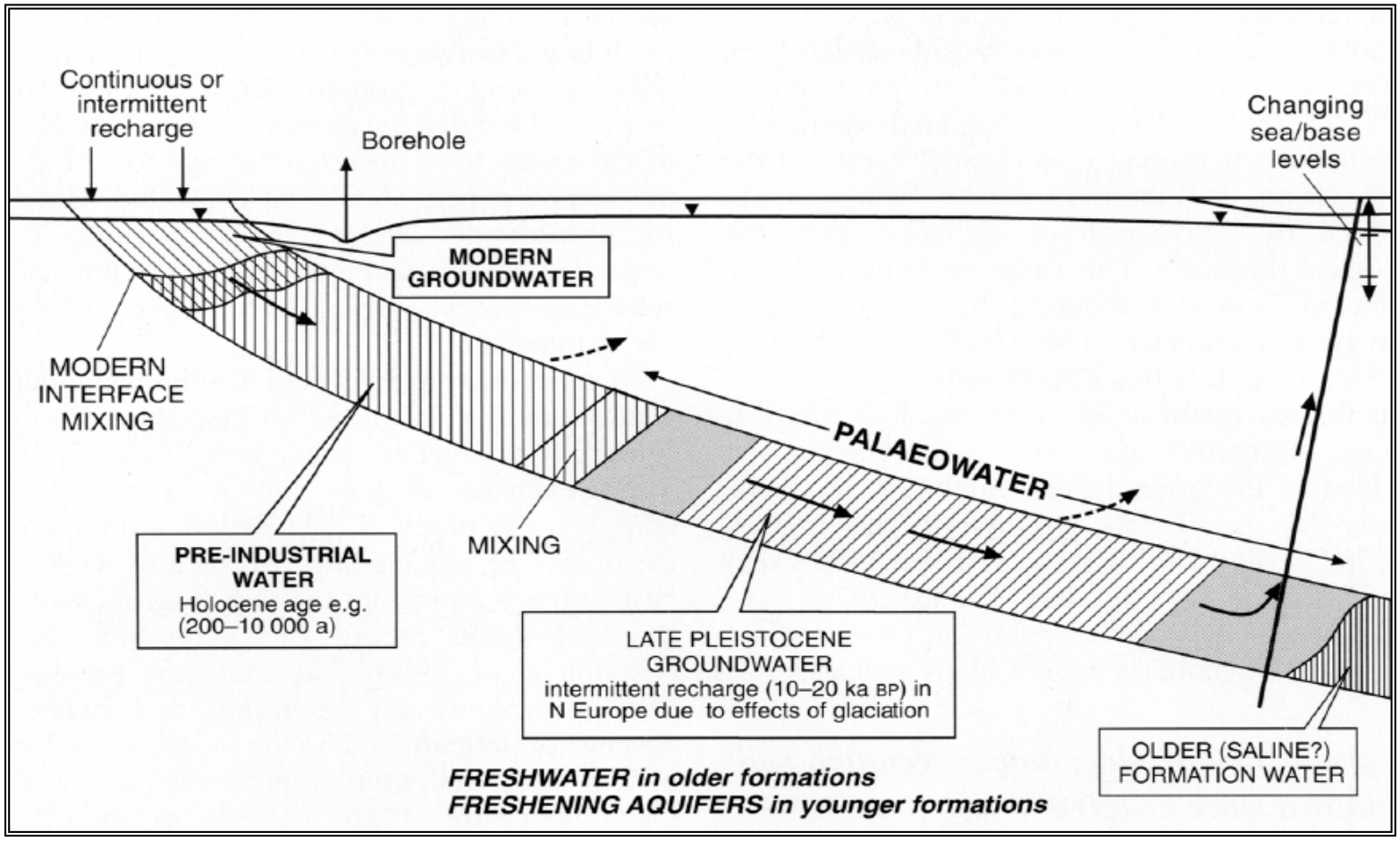

Conceptual model of a confined groundwater system to show definitions used in a PALAEOWATER study.

Edmunds, W. M. (2001). Palaeowaters in European coastal aquifers — the goals and main conclusions of the PALAEAUX project. *Geological Society, London, Special Publications* 2001; v. 189; p. 1-16. doi:10.1144/GSL.SP.2001.189.01.02

Knowledge to decide

Time for deciding:

Additional water from the system optimization

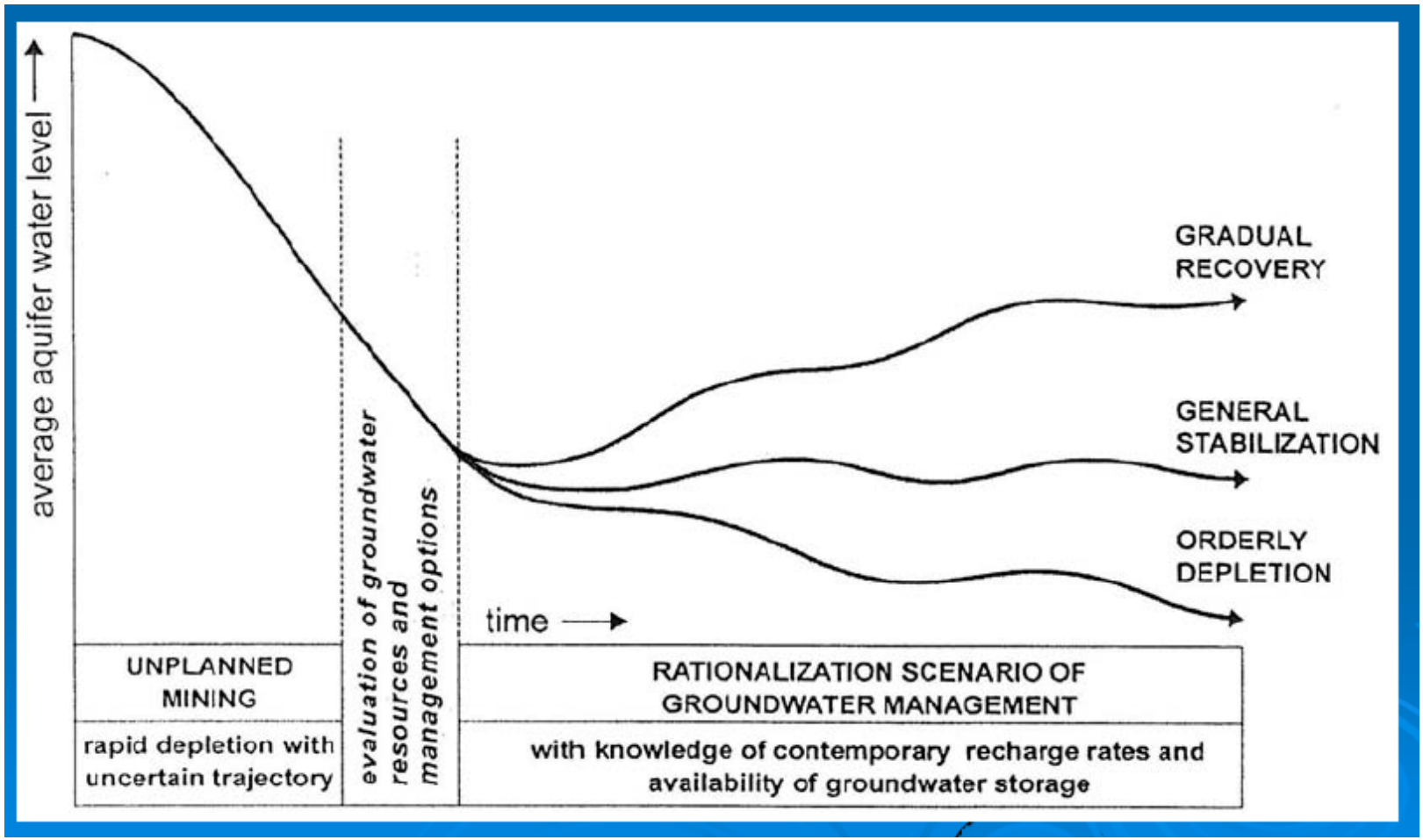

Water, a only resource

The Campo de Cartagena Aquifer is an excellent natural laboratory but it´s a substantial water resource as well!!!!!!

Clear message for the future:

Integrated Water Resources Management

-the holistic approach to development should include groundwater and ecology

Sustainable Water Management

SWAM

Increasing the regional competitiveness and economic growth through the RTD&I on Sustainable Water Management
Regional Seminar on Competitiveness. Galilee (Israel), 17-19 January 2011

Next: Additional slices for other meetings

Geometry of the Geological Basin: Isobaths of the Mesozoic basement

The three sub-basins (Fuente Alamo, Torre Pacheco and San Javier) where the existing depocentres (> 2000 m thick) are clearly observed

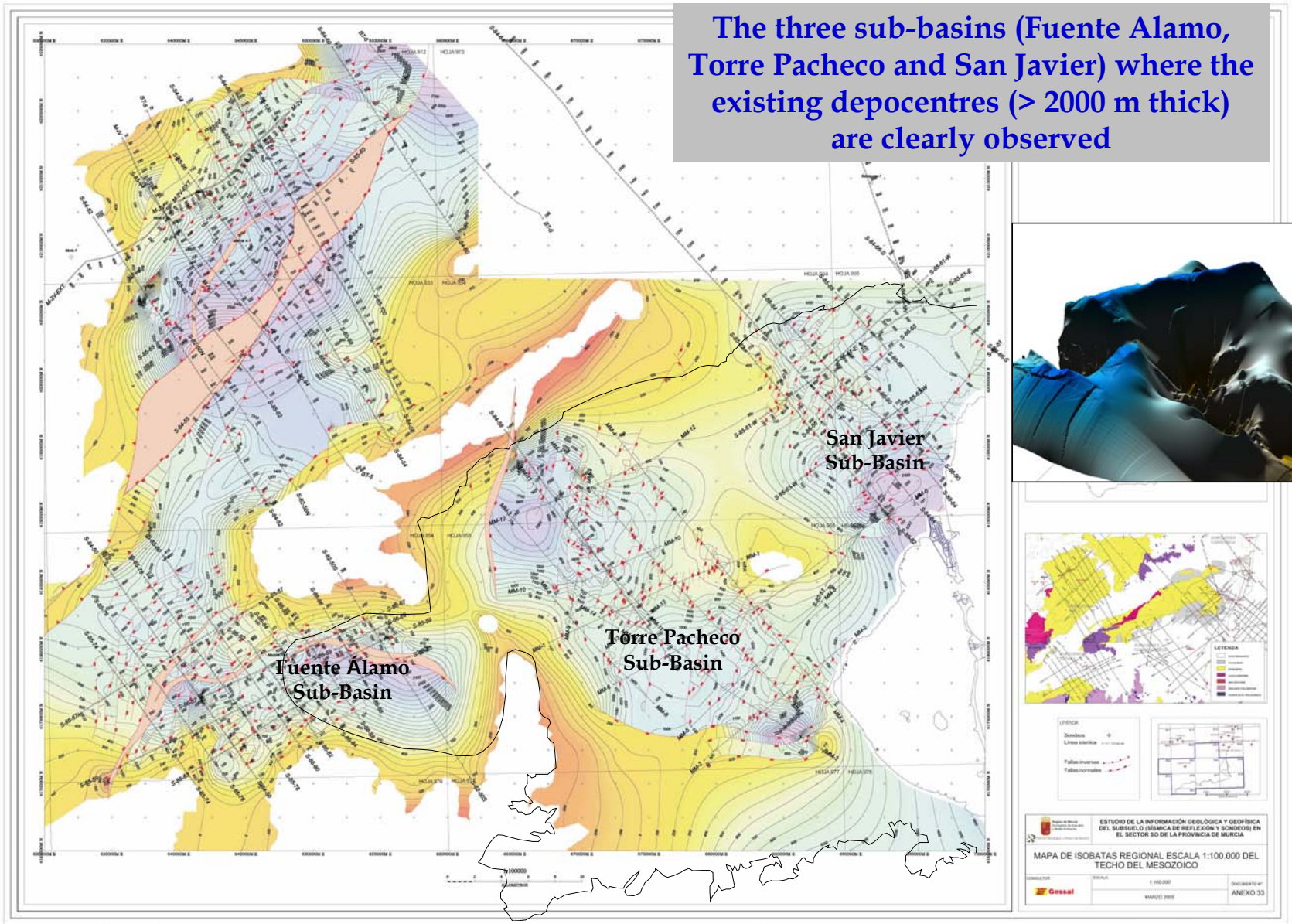

Updating geometry: Determination of aquifer boundaries extending under the sea

Digital topography and bathymetry of the area of the Campo de Cartagena-Mar Menor-Continental Platform

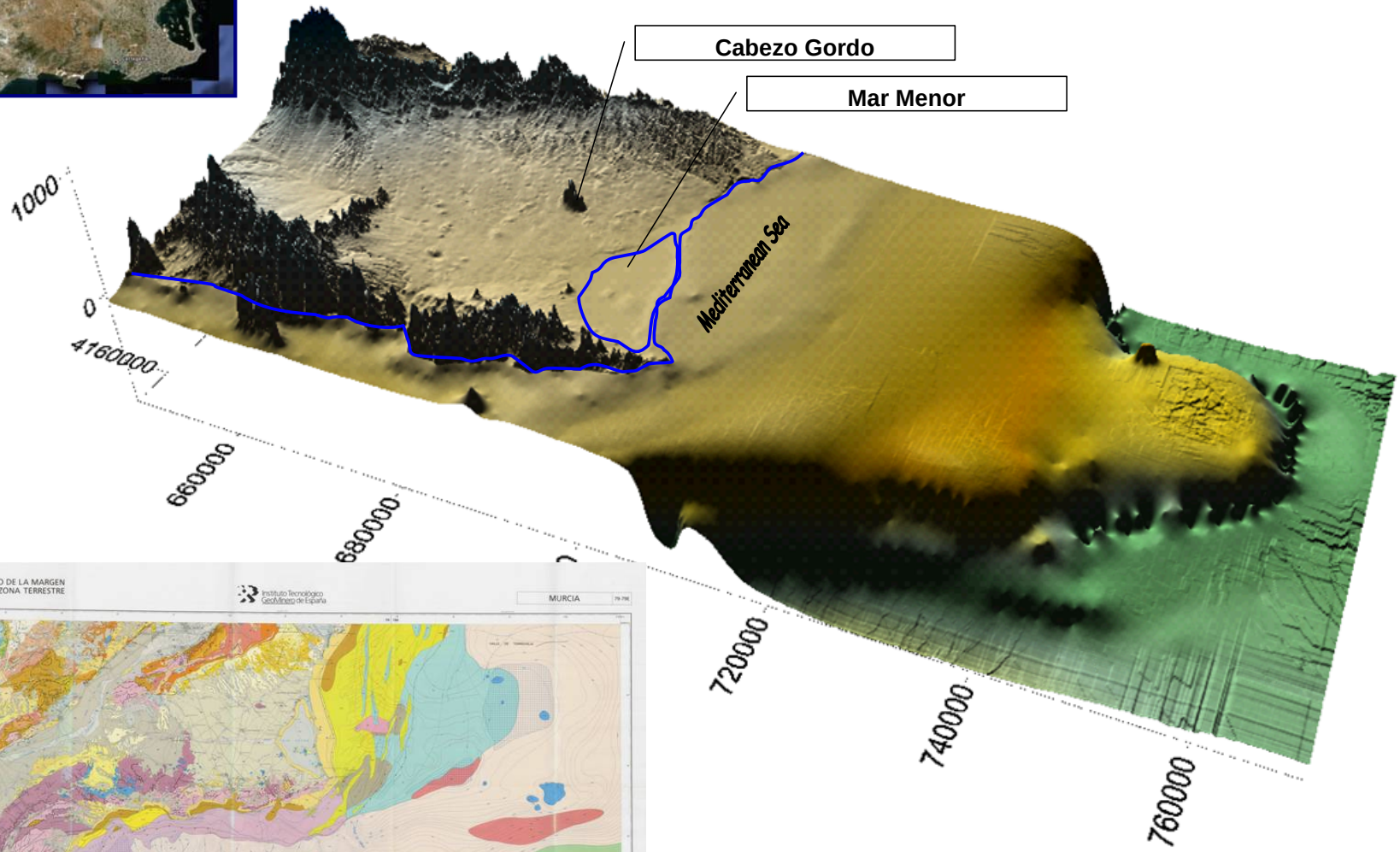

Geological map to the continental platform in front of Murcia's coast

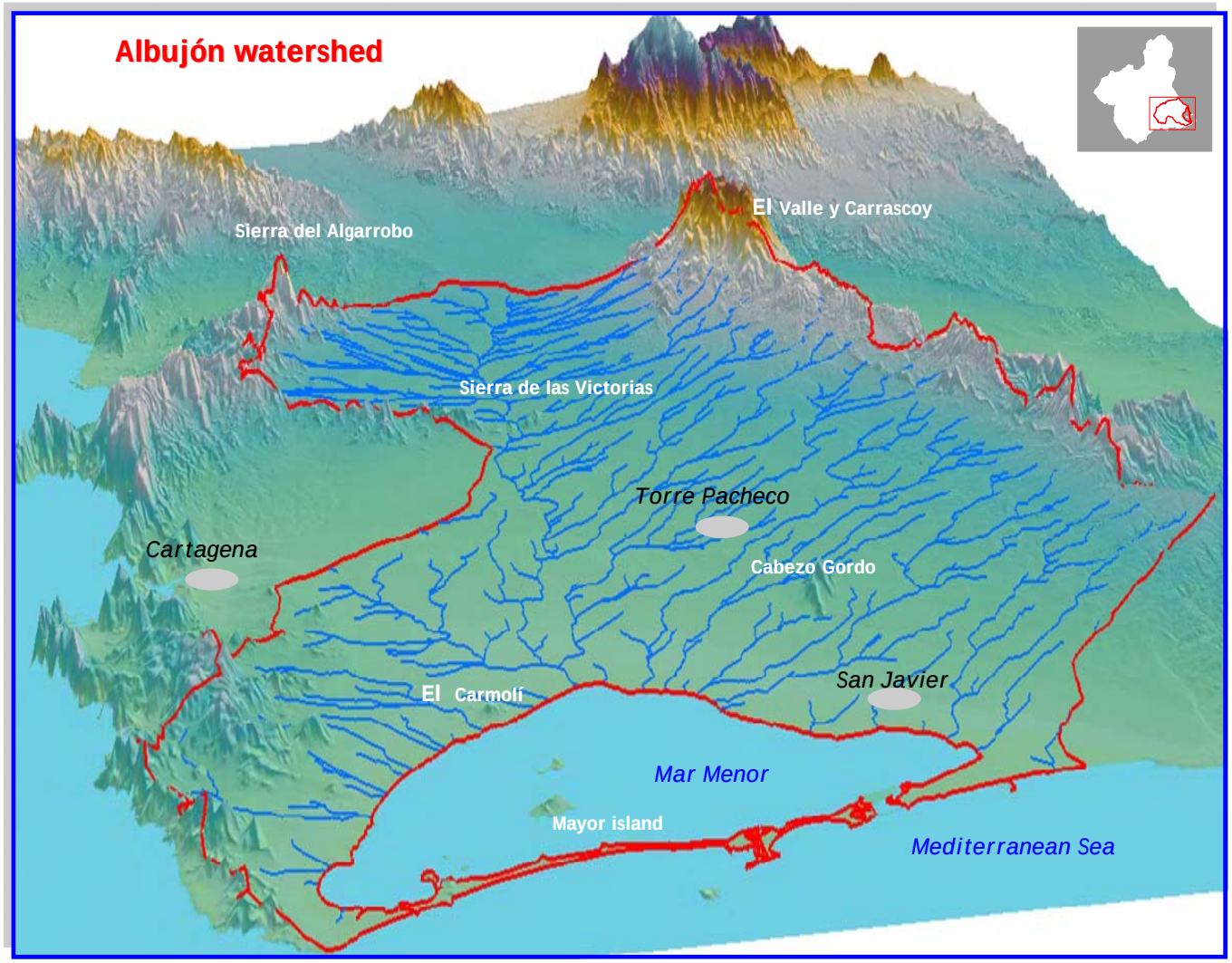
Albujón watershed
El Valle y Carrascoy
Sierra del Algarrobo
Sierra de las Victorias
Torre Pacheco
Cartagena
Cabezo Gordo
El Carmolí
San Javier
Mar Menor
Mayor island
Mediterranean Sea

Aquifer interconnection-leaky boreholes

- HYDROCHEMISTRY APPROACH (INDICATORS, SPECIATION and MIXING)

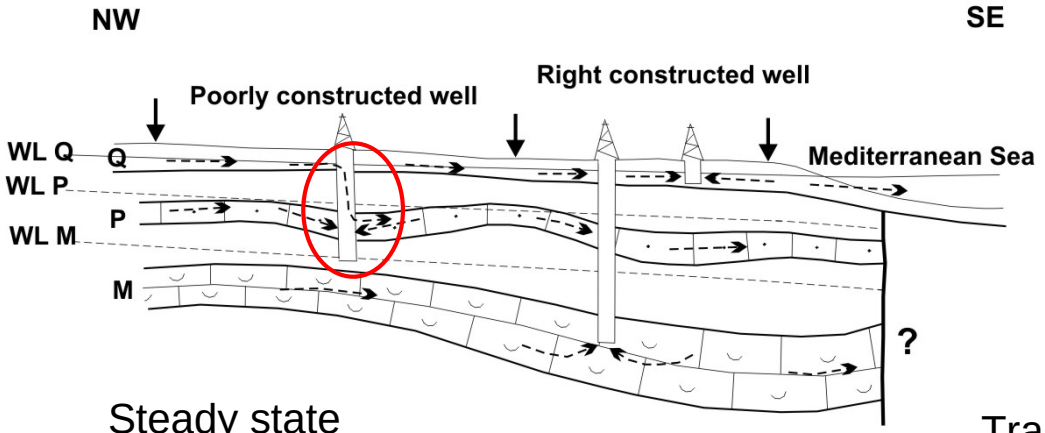

Steady state

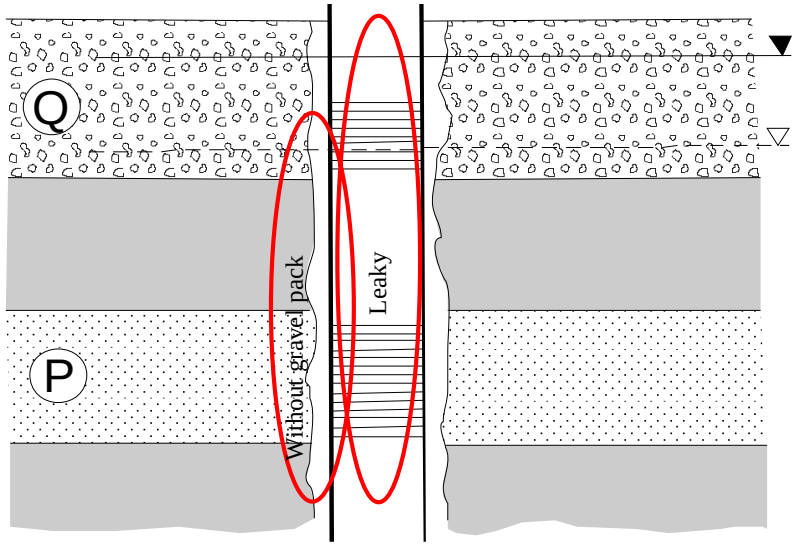

Flow rate more dependent on the borehole radius than vertical hydraulic gradient

Lacombe et al. (1995)

Transient state

Pumping in the deep aquifer (Pliocene aquifer)

Increase the connection degree and mixing

Filter
Packing

Jiménez-Martínez et al. (2010) Water Air and Soil Pollution

CROSS-CHECKING

Interpretation of the results in the context of Palaeogeographic Evolution & Sea level variations

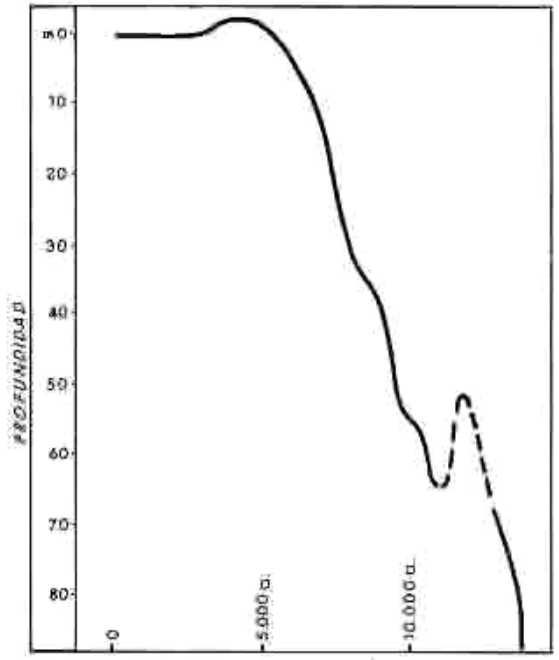

Sea level variations since Holocece in eastern Mediterranean

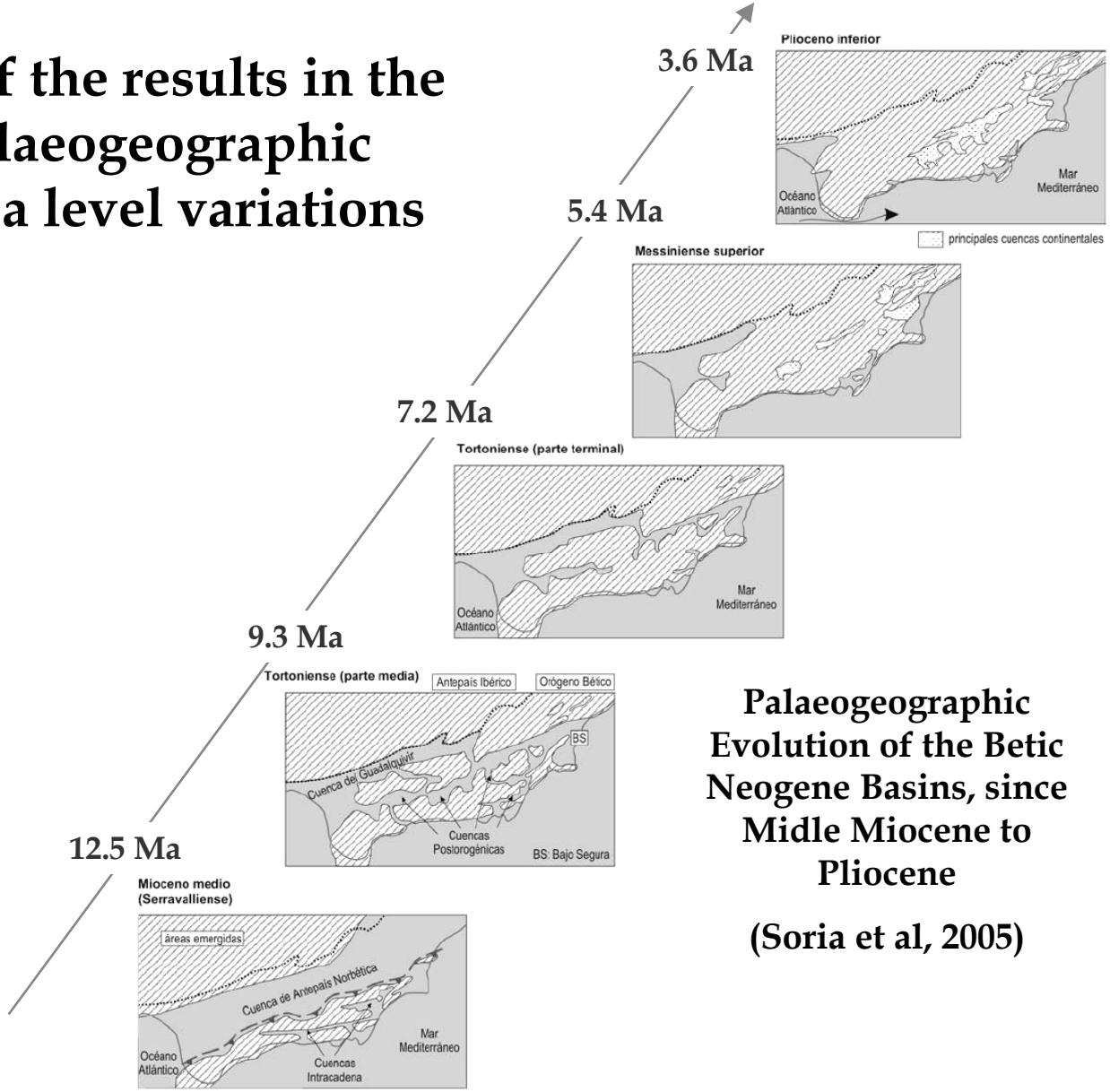

Palaeogeographic Evolution of the Betic Neogene Basins, since Midle Miocene to Pliocene

(Soria et al, 2005)

Hydrogeological geometry

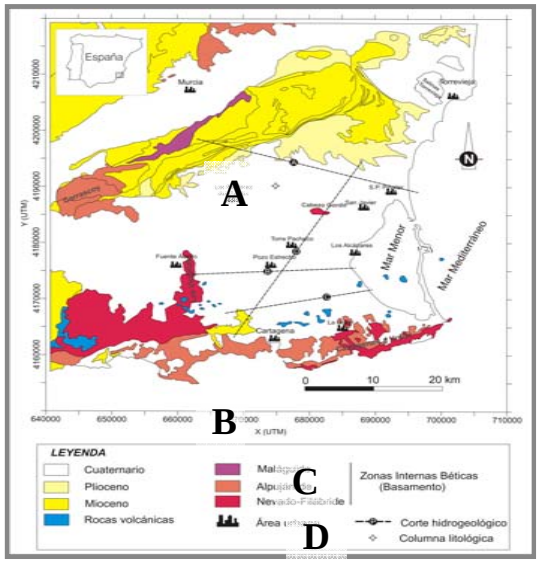

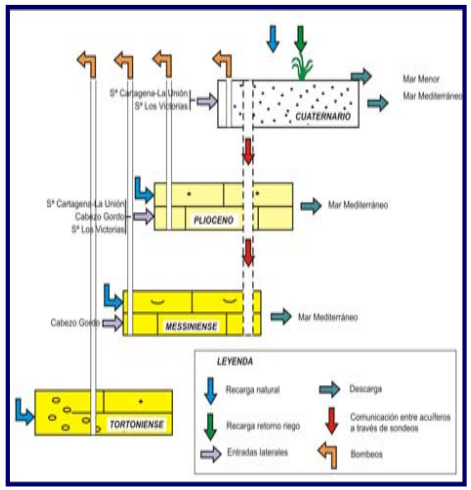

HYDROGEOLOGICAL CROSS-SECTION

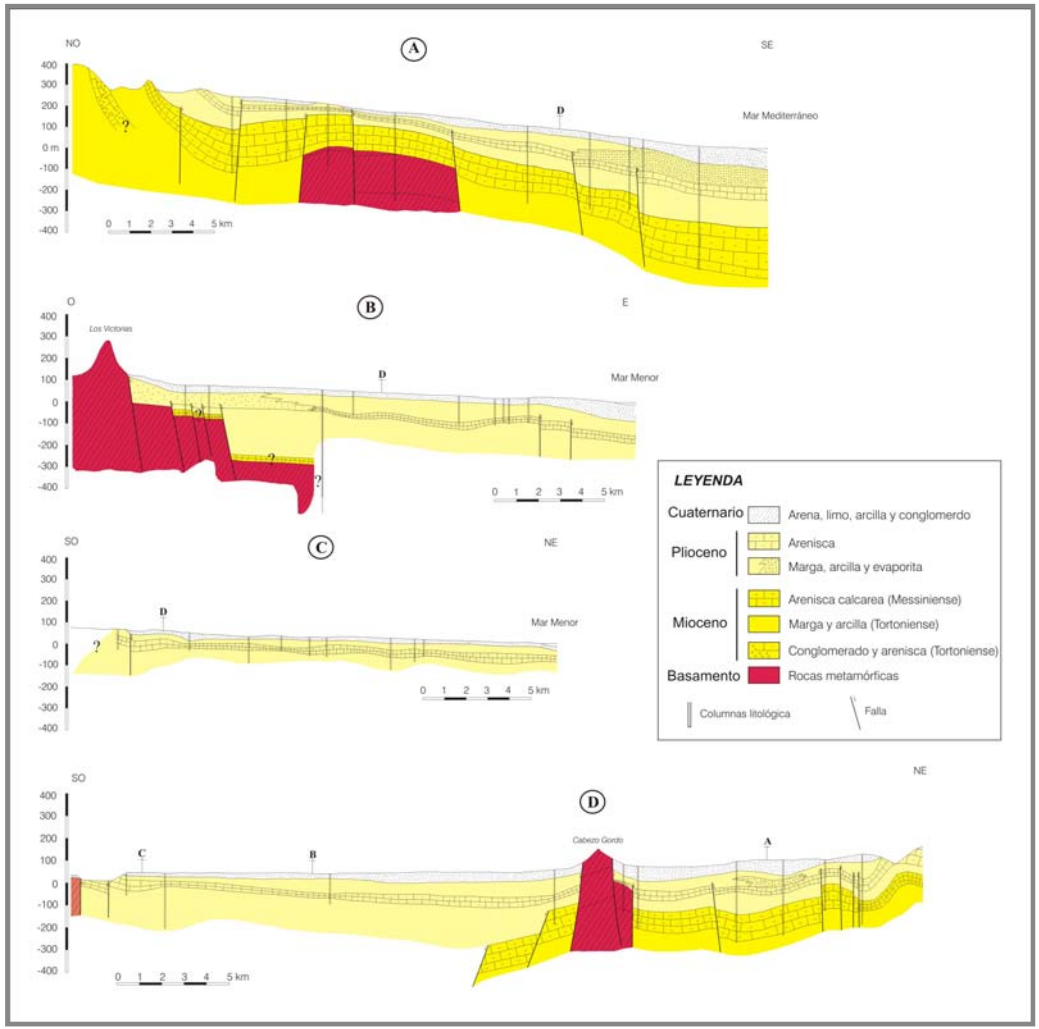

PUBLICACIONES

MINISTERIO
DE EDUCACIÓN
Y CIENCIA

INSTITUTO
GEOLÓGICO
Y MINERO DE ESPAÑA

Groundwater recharge in irrigated semi-arid areas: quantitative hydrological modelling and sensitivity analysis

Joaquín Jiménez-Martínez · Lucila Candela · Jorge Molinero · Karim Tamoh

Abstract For semi-arid regions, methods of assessing aquifer recharge usually consider the potential evapotranspiration. Actual evapotranspiration rates can be below potential rates for long periods of time, even in irrigated systems. Accurate estimations of aquifer recharge in semi-arid areas under irrigated agriculture are essential for sustainable water-resources management. A method to estimate aquifer recharge from irrigated farmland has been tested. The water-balance-modelling approach was based on VisualBALAN v. 2.0, a computer code that simulates water balance in the soil, vadose zone and aquifer. The study was carried out in the Campo de Cartagena (SE Spain) in the period 1999–2008 for three different groups of crops: annual row crops (lettuce and melon), perennial vegetables (artichoke) and fruit trees (citrus). Computed mean-annual-recharge values (from irrigation +precipitation) during the study period were 397mm for annual row crops, 201mm for perennial vegetables and 194mm for fruit trees: 31.4, 20.7 and 20.5% of the total applied water, respectively. The effects of rainfall events on the final recharge were clearly observed, due to the continuously high water content in soil which facilitated the infiltration process. A sensitivity analysis to assess the reliability and uncertainty of recharge estimations was carried out.

Keywords Arid regions · Groundwater recharge/water budget · Agriculture · Irrigation · Spain

Received: 26 February 2010 / Accepted: 21 September 2010
Published online: 20 October 2010

J. Jiménez-Martínez (✉) · L. Candela · J. Molinero · K. Tamoh
Department of Geotechnical Engineering and Geo-Sciences,
Technical University of Catalonia-UPC,
Campus Nord, Building D-2, Jordi Girona, 1–3, 08034, Barcelona, Spain
e-mail: joaquin.jimenez@upc.edu
Tel.: +34-93-401733
Fax: +34-93-4017251

J. Molinero
Amphos XXI Consulting S.L.,
Passeig de Garcia i Faria, 49–51, 08019, Barcelona, Spain

Introduction

In arid and semi-arid areas in which irrigated agriculture prevails, the accurate calculation of aquifer recharge, evaporation and transpiration is crucial for assessing scarce water resources and their sustainable management (e.g. Garatuza-Payán et al. 1998). Reliable natural recharge estimation can be difficult. Recharge is limited by water availability, which is temporally and spatially controlled by climatic factors such as precipitation and evapotranspiration (Scanlon et al. 2002) and is predominately concentrated during short periods of time. In some areas, recharge estimation is even more complex due to irrigation, which may simultaneously abstract water from recharge sources while creating new diffuse recharge. One of the most critical elements for recharge estimation (and also modelling) is the determination of *actual* evapotranspiration rates (Droogers 2000; Haque 2003; Lascano and van Bavel 2007), which can be below *potential* evapotranspiration rates for long periods of time. Recent analyses of recharge evaluation taking into account land cover and irrigated cropland include the works of Ghulam and Bhutta 1996; Dawes et al. 1997; Zhang et al. 1999; Kendy et al. 2003; Brunner et al. 2004; Wang et al. 2008.

The methods that are currently used to estimate groundwater recharge can be loosely grouped into three categories, depending on whether the focus is on surface water, the vadose zone or the saturated zone. The best choice for a particular situation depends upon the spatial and temporal scales that are considered, data availability, and the intended application of the recharge estimate (Scanlon et al. 2002). Several methods have been used to estimate groundwater recharge with varying degrees of success (reviews include e.g. Simmers 1988; Sharma 1989; Lerner et al. 1990; de Vries and Simmers 2002; Scanlon et al. 2002). Experimental and tracer techniques and numerical modelling approaches can be used in all of these methods.

Modelling aquifer water balance is not a new undertaking and several numerical codes are applied, generally. For codes describing balance processes, the reader is referred to SAHYSMOD (ILRI 2005), VisualBALAN v. 2.0 (Samper et al. 2005), TOPOG (CSIRO 2008), and INFIL (USGS 2008), among others.

In this study, recharge in the Campo de Cartagena area of southeast Spain, a semi-arid region in which irrigated

 DOI 10.1007/s10040-010-0658-1

agriculture is prevalent, is assessed. The objective was to test a method and water-balance-modelling approach, based on water table fluctuations (Healy and Cook 2002), to estimate aquifer recharge from irrigated farmland for different types of crops. The current work concerns the application of a computer code, VisualBALAN v. 2.0 (Samper et al. 2005), to simulate water balance in the soil, vadose zone and aquifer. The boundary conditions were detailed for each crop and according to the agricultural practices.

This paper starts with the study area description, Campo de Cartagena, and the corresponding hydrogeological context. Next, the experimental method and the numerical modelling approach are described. Finally, a critical discussion of the recharge results from irrigation return flow obtained for each crop is undertaken. A comprehensive sensitivity analysis is performed to evaluate the reliability and uncertainty of the estimated recharge values.

Study area

The Campo de Cartagena plain extends over an area of 1,440 km^2 in the region of Murcia (SE Spain; Fig. 1a). The climate is Mediterranean, with a mean annual temperature of 18°C and an average annual rainfall of 300 mm. Precipitation, which mainly occurs during spring and autumn, is unevenly distributed in a few intensive events of high variability in space and time. Estimates of annual *potential* evapotranspiration (ET_P) range from 800 to 1,200 mm/year, depending on the applied method (Sánchez et al. 1989).

The primary land use is irrigated and rain-fed agriculture. Irrigated farmland covers 299 km^2. Vegetables, fruits, and citrus trees are the main cultivated crops. The agricultural land distribution is as follows: 128 km^2 of annual row crops (mainly lettuce and melon), 34 km^2 of perennial vegetables (mainly artichoke), and 137 km^2 of fruit trees (mainly citrus) (CARM 2008). Drip irrigation is widely used, due to water scarcity and the need for water conservation. During the last decade, tourism has developed rapidly in the area, as a result of the region's mild climate and coastal and golf resorts. The high water demand for domestic supply is an additional constraint to water resource availability.

From a geological point of view, the Campo de Cartagena plain consists of sedimentary Neogene and Quaternary materials overlying the bedrock, which corresponds to the Internal Betic Zone tectonic complex (metamorphic materials). Limestone, sand and conglomerate of Tortonian age, organic limestone of Messinian age, and sandstone of Pliocene age are the main aquifers in the area. The top unconfined aquifer of detrital origin (mainly Quaternary silt) extends over 1,135 km^2 with an average thickness of 50 m (Fig. 1b). The average depth of the water table is 15 m, and the hydraulic gradient of the aquifer ranges from 10^{-4} to 10^{-3} m/m, and they hardly ever change over time. This aquifer is barely exploited, due to the high pollution by agrochemicals, and the water-table fluctuations are mainly caused by the recharge based on the combined water input from irrigation and precipitation. The hydraulic conductivity ranges between 10^{-1} and 10^{1} m/day, whereas the transmissivity values vary from 10^{1} to 10^{2} m^2/day, depending on the spatial location.

A preliminary study by the Spanish Geological Survey (IGME 1994) estimated that total recharge to the top unconfined aquifer, Quaternary age, was about 69 10^6 m^3/year, ranging between 46 10^6 m^3/year (due to natural recharge) and 23 10^6 m^3/year (due to irrigation return flow). The IGME (1994) study to estimate natural recharge was based on the Thornthwaite method (Thornthwaite 1948); to estimate irrigation return flows a combination of methods were applied according to existing data: (1) for areas where crop and irrigation data were available, irrigation return flows were calculated as the difference between the applied water and the potential crop water use; (2) for other areas, where only irrigation data were available, irrigation efficiency coefficients for different irrigation methods (e.g. drip, furrow, flooding) were used to determine the fraction of water contributing to recharge. Thus, return flow estimate was only based on irrigation water application and did not consider water input from precipitation. Instead, precipitation-based recharge from irrigated farmland was implicitly included in the estimate of natural recharge, which was a single value uniformly distributed in the entire region.

Field site and experiment

Three experimental plots with different types of crops (*LM*, *A* and *C* in Fig. 1a) were selected to assess the water balance: *LM*, with annual row crops (rotation of lettuce and melon); *A*, with perennial vegetables (artichoke); and *C*, with fruit trees (citrus). The main criteria for selecting the sites were prior long-term cultivation of the crops in the experimental area (1999–2008), the existence of piezometric records (piezometers 1, 2 and 3) and nearby meteorological stations (TB and SJ), as shown in Fig. 1a.

Each experimental plot had an area of 10,000 m^2. The soil is a silty loam (US Department of Agriculture soil textural classification) with 16% sand, 79% silt and 5% clay, and it is relatively uniform throughout the Campo de Cartagena region (Ramírez et al. 1999). Daily meteorological data for the study period were provided by SIAM (Servicio de Información Agrária de Murcia) and the groundwater level data, manually recorded at bimonthly basis, were obtained from the CHS (Confederación Hidrográfica del Segura) database.

The plots (*LM*, *A* and *C*) were managed according to agricultural practices that are common in the Campo de Cartagena region (Table 1), including crop rotation for annual row crops (lettuce and melon), drip irrigation and water requirements (Fig. 2). For summer row crops (melon), cultivation is carried out under plastic to increase irrigation efficiency. For simulation purposes and to avoid boundary effects, the same agricultural management practices were conducted in the neighbouring areas of experimental plots.

 DOI 10.1007/s10040-010-0658-1

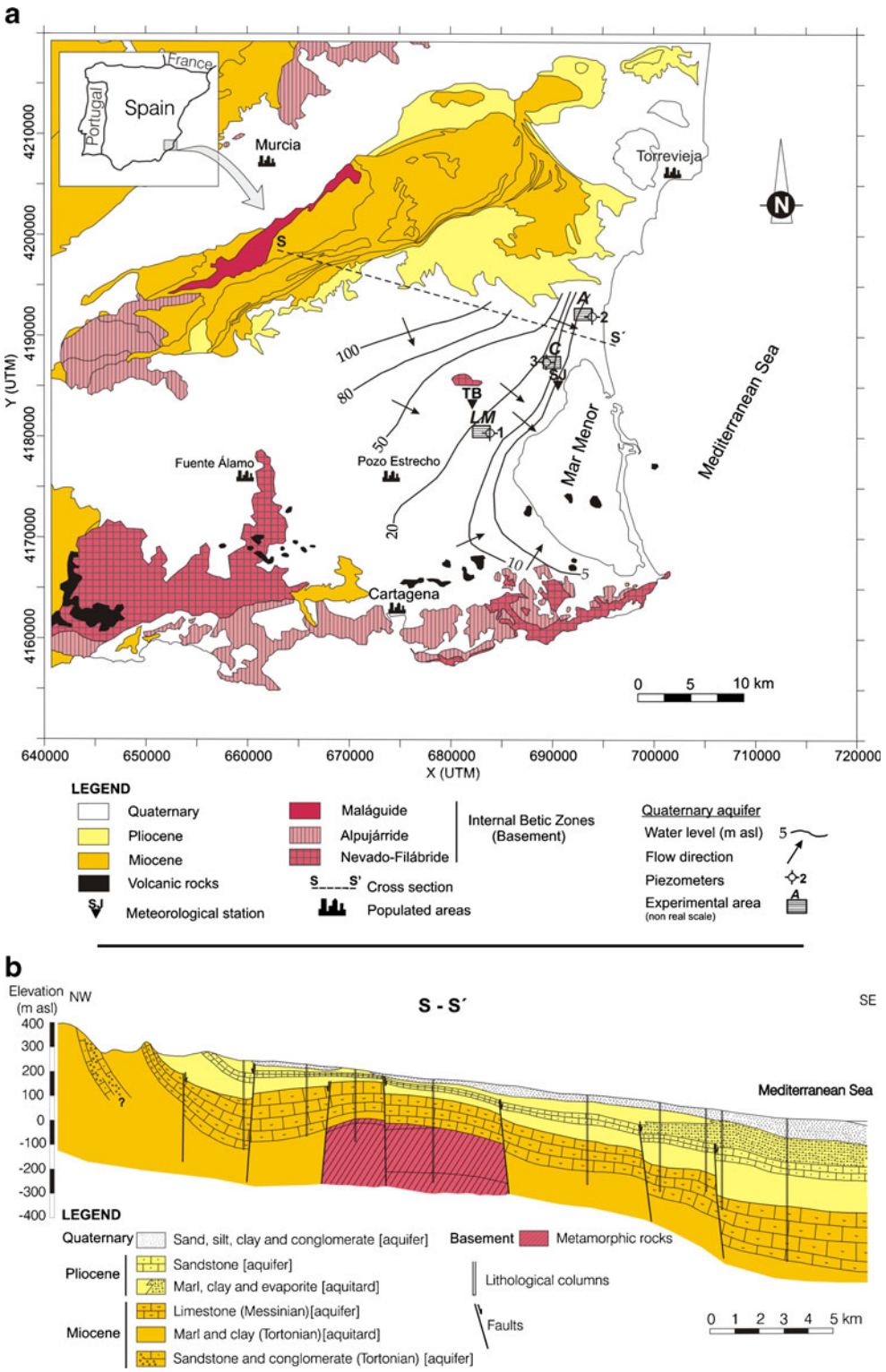

Fig. 1 **a** Location and geological sketch of the Campo de Cartagena area, southeastern Spain. *LM*, *A* and *C* are experimental plots. **b** Geological cross-section with the principal aquifer and aquitard rocks and sediments of the Campo de Cartagena. Modified from IGME (1994)

Estimation of recharge using water balance modelling

The water-table-fluctuation method (WTF) to estimate aquifer recharge is a groundwater-based approach founded on groundwater level data. Its application requires knowledge of specific yield and changes in water level over time. Although simplicity is one of the advantages, uncertainties associated with the limited accuracy in determination of some parameters (e.g. specific yield)

 DOI 10.1007/s10040-010-0658-1

Table 1 Main characteristics of the experimental plots (source: Allen et al. 1998 and CARM 2007)

Experimental plot	Meteorological station	Piezometer	Crop	Mean height crop (cm)	Maximum root depth (cm)	Furrow spacing (m)	Drip irrigation			Crop water requirements (m^3/ha/year)
							Inside diameter tubing (mm)	Emitter spacing (cm)	Discharge (L/h)	
LM	TB	1	lettuce/melon	30/30	30–50/80–150	1	16	30	4	3287.8/6169.2
A	SJ	2	artichoke	70	60–90	1.7	16	40	4	6622.8
C	SJ	3	citrus	300	80–150	6	16	25–125	4	6407.1

may restrict its applicability. Techniques based on groundwater level are among the most widely applied methods for estimating recharge rates. This is likely due to the availability of groundwater level records and the simplicity of estimating recharge rates from temporal fluctuations or spatial patterns of groundwater levels (Healy and Cook 2002).

The WTF approach can only be applied to unconfined aquifers. It is based on the premise that rise in groundwater level is due to recharge water arriving at the water table. The time lag between the water application (from irrigation or precipitation) and the water arriving at the water table during a recharge event is critical for this approach. It is valid over short periods of time (hours or a few days). If the rate of water abstraction from the aquifer is not significantly lower than the rate of recharge water arrival at the water table, then the method is of limited value.

Water-balance-modelling description: equations and parameters used

Water recharge was calculated with VisualBALAN v. 2.0 (Samper et al. 2005), a computer code suitable for long-term simulation of water balance in the soil, vadose zone and aquifer. VisualBALAN has been applied successfully at many Spanish and South American case studies—for example Carrica and Lexow 2004; Gracía-Santos et al. 2005; Samper et al. 2007; Castañeda and García-Vera 2008; Candela et al. 2009; Sena and Molinero 2009, among many others. The experiment was performed for the period October 1999 to September 2008, over nine hydrological years. The calibration and prediction were accomplished for annual row crops (lettuce and melon), perennial vegetables (artichoke) and fruit trees (citrus).

In comparison to other existing codes (INFIL, SAHYSMOD, TOPOG), VisualBALAN aims at using generally available input data, that can be estimated with reasonable accuracy, or easily measured. For example, INFIL (USGS 2008) focuses in the root zone, whereas SAHYSMOD (ILRI 2005) was designed for long-term management applications and output results are based on weighted seasonal averages. Moreover, the latter requires runoff as input data.

The code used in this investigation comprises three sub-models that take into account processes in (1) the upper part of the soil (root zone), (2) the vadose or unsaturated zone (lower soil) and (3) the saturated zone (aquifer). A schematic representation of the balance components is represented in Fig. 3.

The state variable in each of the three zones is water volume, expressed as volume per surface unit (e.g. L/m^2) or equivalent height of water (e.g. mm). The water volume in soil (V_s) is the product of water content (θ) and soil thickness (b_s), $V_s = \theta b_s$. The amount of water in the vadose zone is $V_h = \Phi_e y_h$, where Φ_e is the drainable porosity and y_h the thickness of the waterfront. In the saturated zone, the relationship between water volume (V_a) and height of the groundwater level (h) are related to specific yield S_y by $V_a = S_y h$ (for unconfined aquifer

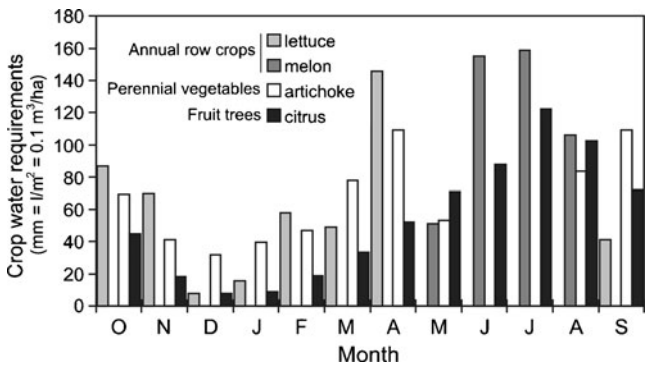

Fig. 2 Monthly water requirements for the three types of crop studied

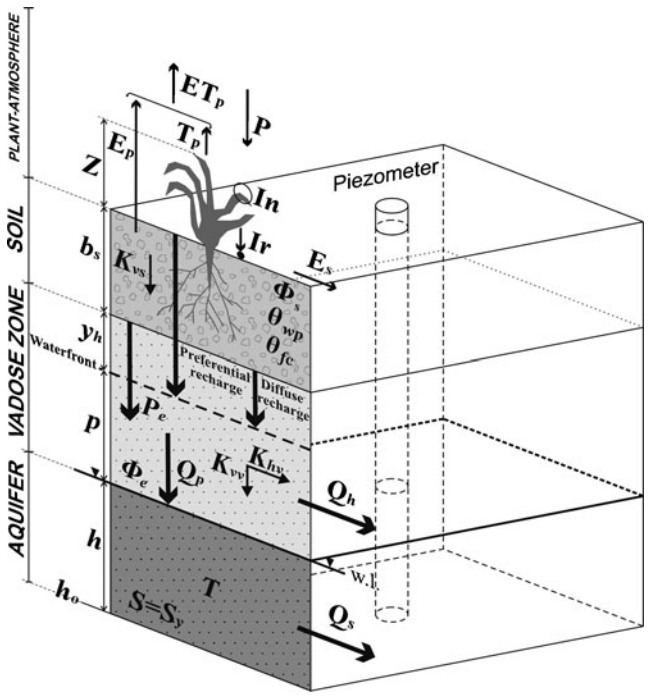

Fig. 3 Scheme of the water balance components in soil, vadose zone and aquifer as defined in the VisualBALAN computer code (Samper et al. 2005). *w.l.* is water level; other notation can be found in the text

DOI 10.1007/s10040-010-0658-1

assume $S=S_y$, where S is storage coefficient, also know as storativity). Model parameters are automatically calibrated by means of the comparison between measured and estimated water levels, and are optimized by minimizing the objective function through the Powell method or multidimensional minimization (Press et al. 1989).

The water balance for *vegetated soil* is represented by:

$$P + \mathrm{Ir} - \mathrm{In} - E_s - \mathrm{ET_a} - P_e = \Delta\theta \quad (1)$$

where P is precipitation, Ir is irrigation, In is canopy interception, E_s runoff, $\mathrm{ET_a}$ represents the *actual* evapotranspiration, P_e is the potential recharge to the vadose zone and $\Delta\theta$ is the variation of soil water storage. The approach assumes a cascade model for precipitation, interception, runoff, evapotranspiration and the recharge process. In the aforementioned model, water balance in soil is attained by using rainfall and daily irrigation data. The model simulates temporal differences (between t_i and t_f, $\Delta t=t_f-t_i$) of *actual* evapotranspiration and groundwater recharge.

As infiltrated water is the residual water after evapotranspiration, the infiltration term, I, can be introduced in the water-balance equation as:

$$I - (\mathrm{ET_a} + P_e) = \Delta\theta \quad (2)$$

$$P + \mathrm{Ir} - \mathrm{In} - E_s = I \quad (3)$$

Equation. 1 is the sum of Eqs. 2 and 3.

Canopy interception (In) is the fraction of precipitation intercepted by the vegetation (leaves, branches and trunk), which involves loss of water by evaporation and runoff decrease. Canopy interception was derived from the empirical model of Horton (1919), which describes a linear relationship between intercepted volume In and total precipitation on vegetation P_d in a rainfall event:

$$\mathrm{In} = S_d + \gamma P_d \quad (4)$$

S_d and γ being empirical parameters related to the type of vegetation and plant height (Table 2). As In is a fraction of precipitation, it cannot exceed the P_d value; therefore, Eq. 4 is valid only when P_d exceeds a threshold defined by:

$$P_d > \frac{S_d}{1-\gamma} \quad (5)$$

For values lower than threshold, $\mathrm{In}=P_d$.

The surface-runoff estimation, E_s, is derived from the curve-number method (Soil Conservation Service 1975), which is based on the relations between losses by canopy interception and precipitation. Before runoff occurs, there is a precipitation threshold, P_o, due to interception and infiltration. If this is taken into account, precipitation is $P-P_o$. For dry conditions and intensive rainfall events, as in the specific study area reported here, E_s can be empirically calculated according to:

$$E_s = \frac{(P-P_o)^2}{P+4P_o} \quad (6)$$

A critical element for recharge estimation is to determine *actual* evapotranspiration $\mathrm{ET_a}(t)$ rates, which can be below *potential* rates $\mathrm{ET_p}(t)$ for long periods of time in arid and semi-arid regions, even for irrigated systems. To relate $\mathrm{ET_a}(t)$ with $\mathrm{ET_p}(t)$, an exponential method was used (e.g. Poulavassilis et al. 2001). The method works with hydric deficits θ_{hd} at time t:

$$\mathrm{ET_a}(t) = \begin{cases} 1.9\mathrm{ET_p}(t)\mathrm{e}^{\{-0.6523[\theta_{hd}(t)-W(t)]/\theta_{ceme}\}} & \theta_{hd}(t) - W(t) > \theta_{ceme} \\ \mathrm{ET_p}(t) & \theta_{hd}(t) - W(t) < \theta_{ceme} \end{cases} \quad (7)$$

where $W(t)$ represents the input water over time (available water), being $\theta_{hd}(t) = \theta_{fc} - \theta(t)$, θ_{fc} is field capacity and $\theta(t)$ soil-water content. θ_{ceme} constitutes the hydric deficit limit value and ranges between field capacity (θ_{fc}) and wilting point (θ_{wp}). All parameters are expressed as equivalent height of water.

The potential diffuse recharge to the vadose zone P_e was estimated assuming that the soil is homogeneous and isotropic. To solve this aspect a linear function was applied (e.g. Castañeda and García-Vera 2008), defined as:

$$P_e(t) = \begin{cases} 0 & \theta(t) < \theta_{fc} \\ \theta(t) - \theta_{fc} & \theta_{fc} \le \theta(t) < \theta_{fc} + K_{vs}\Delta t \\ K_{vs}\Delta t & \theta(t) \ge \theta_{fc} + K_{vs}\Delta t \end{cases} \quad (8)$$

where K_{vs} is the soil vertical-hydraulic conductivity and θ_{fc} and $\theta(t)$ are expressed as equivalent height of water.

In the *vadose zone*, potential recharge P_e, constitutes the entry of water, which can be divided into hypodermic Q_h and vertical flow or percolation to the aquifer Q_p, defined by the following expressions:

$$Q_h(t) = \alpha_h V_h(t) \quad (9)$$

$$Q_p(t) = K_{vv} + \alpha_p V_h(t) \quad (10)$$

Table 2 Applied S_d and γ parameters (Horton method) and crop height (from López-Rodríguez and Giráldez-Cervera 1997)

Crop	S_d	γ	Mean height crop Z (m)
Annual row crops (lettuce and melon)	$1.67 \times Z$	$0.49 \times Z$	0.3
Perennial vegetables (artichoke)	$1.67 \times Z$	$0.49 \times Z$	0.7
Fruit trees (citrus)	1.02	0.18	3

 DOI 10.1007/s10040-010-0658-1

where V_h is the water volume stored in the vadose zone, α_h and α_p are depletion coefficients for hypodermic flow and vertical flow or percolation, respectively, and K_{vv} the vertical hydraulic conductivity in the vadose zone. The α_h parameter is proportional to the horizontal hydraulic conductivity K_{hv}, drainable porosity Φ_e, mean slope i and length in the hypodermic flow direction L, according to:

$$\alpha_h = \frac{2K_{hv}i}{L\Phi_e} \tag{11}$$

As in Eq. 10, α_p is obtained by considering that V_h and y_h are related by means of $V_h = \Phi_e y_h$, where y_h is the thickness of the waterfront, taking into account the distance between the waterfront and the regional groundwater level p:

$$\alpha_p = \frac{K_{vv}}{p\Phi_e} \tag{12}$$

In this study, an explicit scheme was applied for solving water balance in the vadose zone.

Water balance in the *aquifer*, using VisualBALAN (Samper et al. 2005), was obtained by estimating the groundwater level in the aquifer at each Δt. The code enables solving of the water balance by treating the region as a mono-cell or multi-cell pattern. For this exercise, the experimental plot (10,000 m^2) was considered as only one cell. The water volume in the aquifer, V_a, and the groundwater level, h, are related to a reference value, h_o (base value), which corresponds to a volume V_{ao}. The water volume stored over the reference value, $\Delta V_a=(V_a-V_{ao})$, is related to the change of level $\Delta h=(h-h_o)$ through the specific yield S_y by means of $\Delta V_a=S_y\Delta h$. Balance in the aquifer is carried out considering the entry of water by vertical flow or percolation Q_p and the groundwater discharge Q_s:

$$Q_s(t) = \alpha_s \Delta V_a \tag{13}$$

where α_s is the discharge depletion coefficient,

$$\alpha_s = a\frac{T}{S\lambda^2} \tag{14}$$

which is related to hydraulic diffusivity (T/S) by means of the transmissivity, T, and storage coefficient, S ($S=S_y$ for unconfined aquifer), a characteristic length λ and a dimensionless constant α (common range between 1/3 and 1/1.5). The stored volume in the aquifer at time t, $V_a(t)$, is obtained from:

$$V_a(t) = V_a(t-1) + (Q_p - Q_s)\Delta t \tag{15}$$

Once the final volume is known, the water level is calculated, $h(t)$:

$$h(t) = h_o + \frac{V_a(t) - V_{ao}}{S} \tag{16}$$

which allows an estimation of the water level in the aquifer. Goodness of fit between measured and simulated water levels was assessed by the root mean square error (*RMSE*) and mean absolute error (*MAE*).

Atmospheric boundary conditions

Daily irrigation (Ir) and precipitation (P) rates are the only input to the system. In order to determine evaporation and transpiration rates, reference evapotranspiration, $ET_0(t)$, was calculated according to Penman-Monteith method. The *potential* evapotranspiration, $ET_p(t)$, was derived from (Allen et al. 1998):

$$ET_p(t) = K_c(t) \cdot ET_0(t) \tag{17}$$

where $K_c(t)$ is a crop-specific coefficient that characterizes plant water uptake and evaporation relative to the reference crop. $ET_0(t)$ was obtained at daily time steps. Values for $K_c(t)$ are shown in Table 3 for annual row crops, along with growth stages and length (days). An annual mean value of K_c=0.95 (Allen et al. 1998) for perennial vegetables (artichoke) and a monthly mean value (Castel 2001) for fruit trees (citrus) respectively was applied, although for the last case the annual mean value is K_c=0.68 for a ground cover ≥ 64%.

Potential evaporation $E_p(t)$ was calculated according to (e.g. Kroes and Van Damm 2003; Pachepsky et al. 2004):

$$E_p(t) = ET_p(t) \cdot \exp^{-\beta \cdot LAI(t)} \tag{18}$$

Table 3 Planting date, growth stage and crop coefficient for different row crops (source: Allen et al. 1998 and CARM 2007)

Crop	Planting date	Growth stage (number of days)				Crop coefficient (K_c)			Mean height crop (cm)	Maximum root depth (cm)	Crop water requirements (m^3/ha/year)
		Initial	Development	Mid-season	Late-season	Initial	Mid	End			
Lettuce	Jan/Sept	35/30	50/40	45/25	10/10	0.7	1	0.95	30	30–50	3287.8
Broccoli	Jan/Sept	35	45	40	15	0.7	1.05	0.95	30	45–60	1595.7
Cauliflower	Jan/Sept	35	50	40	15	0.7	1.05	0.95	40	45–60	1595.7
Celery	Jan/Sept	25	40	45	15	0.7	1.05	1	60	45–60	2466
Endive	Jan/Sept	[a]	[a]	[a]	[a]	0.7	0.95	0.90	[a]	30–45	3474.4
Melon	May	25	35	40	20	0.5	1.05	0.75	30	80–150	6169.2
Watermelon	May	20	30	30	30	0.4	1	0.75	40	80–200	5435.1

[a] No data available, but field observations suggest growth stages similar to lettuce crop

 DOI 10.1007/s10040-010-0658-1

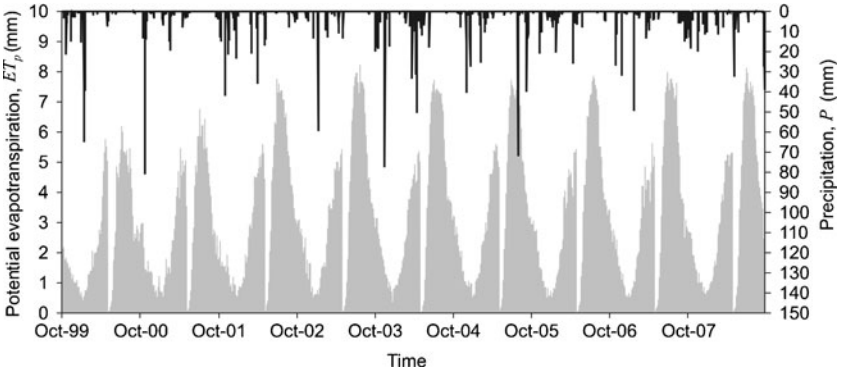

Fig. 4 Estimated daily potential evapotranspiration ET_p (*grey colour*) as a soil input boundary condition (Eqs. 17–20) for annual row crops (lettuce and melon). $ET_p \sim 0$ is recognized at the beginning of each summer crop due to the plastic cover. *Black bars* represent daily precipitation data

where β (≈ 0.4) is the radiation extinction coefficient and LAI(t) is the leaf area index. Data on LAI(t) were not available and it was estimated as:

$$E_p(t) = \mathrm{ET_p} f(t) \tag{19}$$

The $f(t)$ function was defined on the basis of the following reasoning: when a crop is planted for the first time, ground cover is nonexistent, potential evaporation is maximal, transpiration is zero, and thus $f(t)=1$. Conversely, when the crop reaches the mid-season growth stage, ground cover is complete, evaporation is effectively zero, and thereafter $f(t)=0$. The transition from $f(t)=1$ at planting to $f(t)=0$ at the beginning of the mid-season growth stage was modelled using a sigmoid curve (Jiménez-Martínez et al. 2009).

Therefore, potential transpiration $T_p(t)$ was determined as:

$$T_p(t) = \mathrm{ET_p}(t) - E_p(t) \tag{20}$$

According to agricultural practices in the area, the $\mathrm{ET_p}(t)$ for winter crops (lettuce) is given by Eq. 17, while for summer crops (melon) only $T_p(t)$ from Eq. 20 was taken into consideration. Selection was based on the fact that the plastic cover reduces $E_p(t)$ to zero (Fig. 4). For perennial vegetables and fruit trees, the $\mathrm{ET_p}(t)$ given by Eq. 17 was applied considering that a complete growth development occurs.

Uncertainty and sensitivity analysis

The modelling approach contains several potential sources of uncertainty, which are either related to model param-

Table 4 Initial value and final fitted parameter estimates. Prescribed values when not fitted parameters. Calibration period is shown between brackets

Parameter	Annual row crops (lettuce and melon)		Perennial vegetables (artichoke)		Fruit trees (citrus)	
	Initial value (1999–2002)	Fitted value	Initial value (1999–2005)	Fitted value	Initial value (1999–2003)	Fitted value
Fitted						
Rainfall threshold to downpour, P_o (mm)	2	2	2	2	2	2
Hypodermic flow depletion coefficient, α_h (1/day)	0.01	0.01	0.01	0.01	0.01	0.01
Groundwater discharge depletion coefficient, α_s (1/day)	0.0173	0.0050050	0.0173	0.0009812	0.0173	0.0009812
Storage coefficient, S	0.2	0.2098	0.2	0.2065	0.2	0.2
Discharge single-cell aquifer water level, h_d (m)	15.80	15.78	1.50	1.50	13.55	13.57
Vadose zone vertical hydraulic conductivity, K_{vv} (mm/day)	432	432	432	432	432	432
Vertical flow depletion coefficient, α_p (1/day)	0.6931	0.6931	0.6931	0.6931	0.6931	0.6931
θ_{ceme} (mm) [hydric deficit limit value, between θ_{wp} and θ_{fc}]	20	1.549	20	0.965	20	1.006
Prescribed[a]						
Soil thickness, b_s (m)	0.5		1		1.50	
Soil total porosity, Φ_s (m^3/m^3)	0.4		0.4		0.4	
Wilting point, θ_{wp} (m^3/m^3)	0.1		0.1		0.1	
Field capacity, θ_{fc} (m^3/m^3)	0.2		0.2		0.2	
Curve number[b]	58		58		25	
Soil vertical hydraulic conductivity, K_{vs} (mm/day)	382		382		382	

[a] Source: Jiménez et al. (2007); Jiménez-Martínez et al. (2009)

[b] Source: Soil Conservation Service (1975)

 DOI 10.1007/s10040-010-0658-1

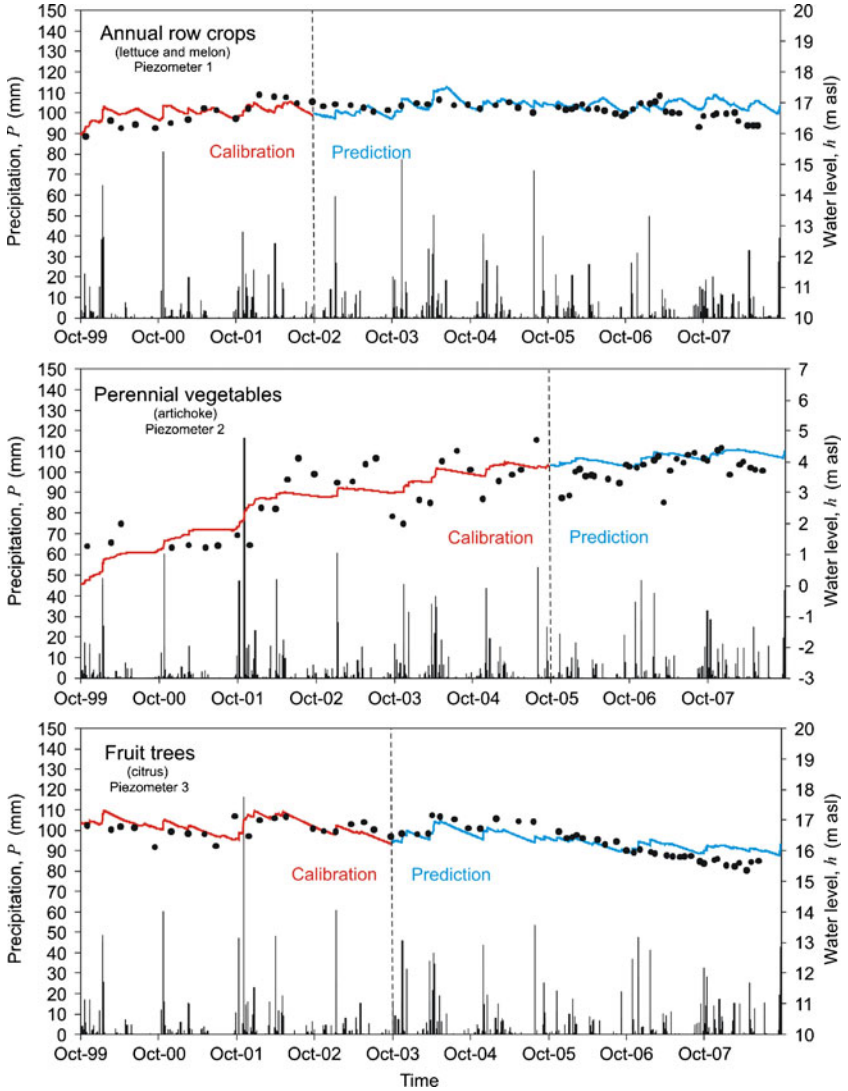

Fig. 5 Simulated (calibration: *red line*; prediction: *blue line*) and observed (*dots*) water level for the piezometers 1, 2 and 3 located in each experimental plot (see Fig. 1a). Daily precipitation is shown as *black bars*.

eters (P_o; α_h; α_s; S; h_d; K_{vv}; α_p; θ_{ceme}; b_s; Φ_s; θ_{wp}; θ_{fc}; curve number; K_{vs}), initial conditions (initial water content in the soil and vadose zone; initial water level in the single-cell aquifer) or the boundary conditions (precipitation; crop coefficient; reference evapotranspiration; irrigation; height of the crop). Quantifying the effect of uncertainties on the recharge calculation requires knowledge of the aforementioned model parameters and of their statistical variability and correlation structure. To the authors' knowledge, the literature provides little or no information on quantifying uncertainty for some of the parameters. However, it is possible to evaluate the importance of the parameter uncertainties on recharge as the objective function by means of sensitivity analysis.

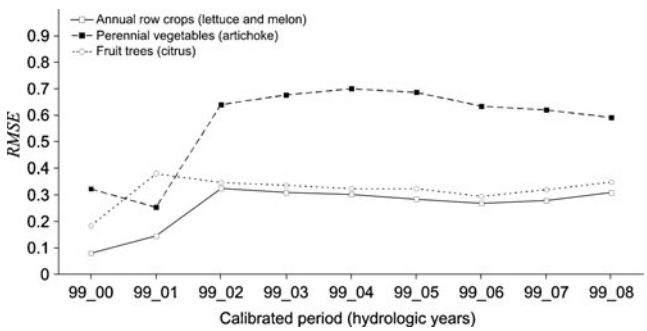

Fig. 6 Root mean square error (*RMSE*) for the calibrated periods and the three crop types (e.g. 99_00 means 1999–2000)

As this is a cascade model, the parameters and initial conditions that potentially concern recharge are those characterizing the soil and vadose zone (P_o; α_h; K_{vv}; α_p; θ_{ceme}; b_s; Φ_s; θ_{wp}; θ_{fc}; curve number; K_{vs}; initial water content in soil and vadose zone), whereas for the parameters and initial conditions of the aquifer (α_s; S; h_d), their impact is on water level, not on the objective function, recharge. A series of simulations were performed on individual parameters by a given amount of perturbation and by estimating water balance.

The uncertainties associated with the boundary conditions were evaluated by computing a defined relative

 DOI 10.1007/s10040-010-0658-1

Table 5 Model performance assessment by fitting experimental data (water level, *h*) for calibrated and predicted periods shown in Fig. 6

Simulation	Calibration period		Prediction period	
	RMSE[a]	*MAE*[b]	*RMSE*[a]	*MAE*[b]
Annual row crops (lettuce and melon)	0.324	0.276	0.312	0.246
Perennial vegetables (artichoke)	0.686	0.607	0.529	0.397
Fruit trees (citrus)	0.337	0.260	0.352	0.306

[a] Root mean square error, $RMSE = \sqrt{\frac{1}{n}\sum_{i=1}^{n}(x_i - y_i)^2}$

[b] Mean absolute error, $MAE = \frac{1}{n}\sum_{i=1}^{n}|x_i - y_i|$

sensitivity as *AS/CP*. Parameter *CP* is the relative change of a given variable or parameter, defined as $|P_s - P_b|/P_b \cdot 100$, and *AS* is the relative change in the output (recharge) value, defined as $|C_s - C_b|/C_b \cdot 100$. P_s and P_b are variable values used for sensitivity and calibrated base runs, respectively, and C_s and C_b are output data (recharge) computed in sensitivity and calibrated base runs, respectively. The magnitude of the perturbation (*CP*) was ±10% with respect to the original data. However, for the height crop, this figure stood at ±30%.

Results and discussion

Model calibration and predictions

As could be expected, initial simulations using guessed parameters were in poor agreement with measured data. Therefore, an attempt was made to calibrate model parameters in the three zones (soil, vadose zone and aquifer) by parameter optimization routines and field data (water level data). Several possible parameterizations were considered, according to the number and type of parameters that were fitted. The best overall parameterization was determined on the basis of diagnostic information from the computer program, a visual inspection of the model fit to the data and the principle of parsimony (i.e., if two parameterizations produce equal fit, the simplest was taken, namely, fewer fitted parameters). Subsequently, the fitting was repeated using different initial estimates to ensure that the same fitted parameters were obtained. The best parameterization was found for eight of a total of fourteen parameters. Table 4 shows the initial value of the parameters, the prescribed value when not fitted, and the fitted parameter estimates. The final fitted parameter values were very similar for the three experimental plots, which confirmed the homogeneity of soil type in the study area (Ramírez et al. 1999). Field observations suggest that hypodermic flow is negligible, confirmed by the fitted

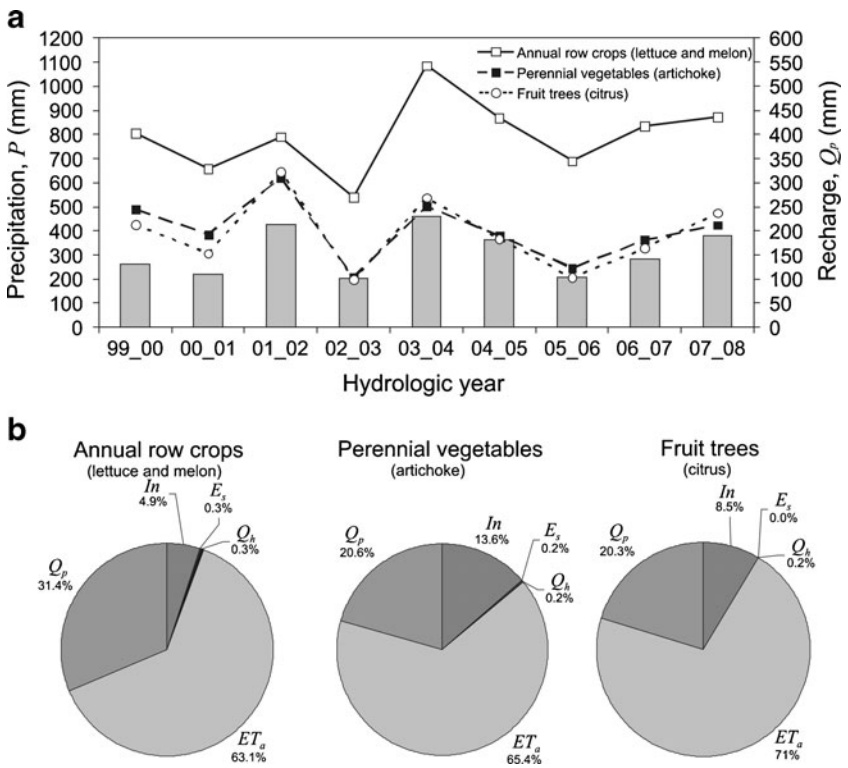

Fig. 7 **a** Annual recharge evolution (annual row crops: *solid line*; perennial vegetables: *dashed line*; fruit trees: *dotted line*) and annual precipitation (*grey bars*) for each crop and studied period (Oct 1999–Sept 2008). **b** Pie diagrams present average value (%) of the different water balance components for each crop. *In* canopy interception; E_s runoff; Q_h hypodermic flow; ET_a *actual* evapotranspiration; Q_p aquifer recharge

 DOI 10.1007/s10040-010-0658-1

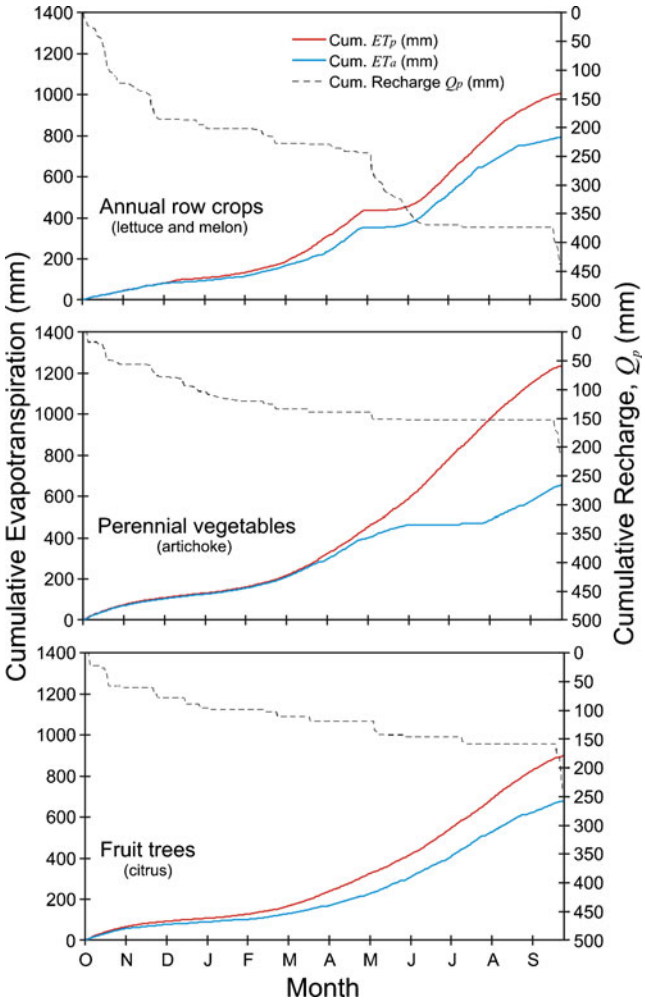

Fig. 8 Cumulative *potential* evapotranspiration ET_p (*red line*), *actual* evapotranspiration ET_a (*blue line*) and aquifer recharge Q_p (*dashed line*) for the different crops, Oct 2007–Sept 2008 hydrological year

hypodermic flow depletion coefficient (α_h) and estimated values for this water balance component. Higher values of vertical flow depletion coefficient (α_p) than groundwater discharge depletion coefficient (α_s) confirm that: (1) the time lag span between the water application and the water arriving at the aquifer is short; and (2) the water transport rate away from the water table is significantly slow.

Calibration for each crop type was carried out for a given number of years (annual row crops 3 years; perennial vegetables 6 years; fruit trees 4 years). Once fitted parameterization was attained, it was used to predict at the site (Fig. 5) the water level for the rest of the period (annual row crops 6 year; perennial vegetables 3 year; fruit trees 5 year), in order to evaluate the model's reliability. Figure 6 shows for each crop type the root mean square error (*RMSE*) for a selected calibration period. As can be observed, the *RMSE* reaches a plateau and remains more or less constant after a certain number of years. Obtained results were used to assess the optimum number of years for model calibration in the area. In the annual row crops (lettuce and melon) and perennial vegetables (artichoke) the *RMSE* value was stabilized in 3 years (≈ 0.3 and ≈ 0.65, respectively), while for the fruit trees (citrus) it stabilized after 2 years of calibration (≈ 0.3). Figure 5 shows observed and simulated water level measurements, while Table 5 presents the goodness-of-fit for the calibrated and predicted periods shown in Fig. 5. Good agreement was obtained for annual row crops and fruit trees. However, this was not the case for perennial vegetables, which has been related to pumping nearby this experimental plot.

Water balance and recharge estimation

Figure 7 shows the recharge evolution for each crop during the October 1999–September 2008 period. Considering that irrigation has remained more or less constant throughout the study period, the annual recharge has to be related to changes in precipitation. For the study period, mean annual recharge was 397±70 mm for annual row crops (lettuce and melon), 201±64 mm for perennial vegetables (artichoke) and 194±75 mm for fruit trees (citrus). Values were consistent with data for these types of crops provided by different authors (e.g. Castel et al. 1987; Hanson et al. 1997; Lidón et al. 1999). Table 3 shows the agricultural parameters for some crops currently cultivated in the Campo de Cartagena, presenting similar planting date, growth stages, crop coefficients, height, root depth and water requirements as the crops of the *LM* field plot (lettuce and melon). Obtained results from the present experiment could be also applied to assess recharge derived from other types of crops.

Due to the high irrigation dose and frequency of application, recharge dramatically increases when intensive precipitation events occur. As shown in Fig. 5, the groundwater level increase correlates with the heaviest precipitation events. This rapid water level response is due to the relative narrowness of the vadose zone in the study area, and was accounted for as 3, 11 and 8 m in plots *LM*, *A* and *C*, respectively. Moreover, continuous and relatively high water content in the soil facilitates the infiltration process during intensive precipitation events. The pie diagrams in Fig. 7 present the average value (%) of the different water balance components for each crop and study period (October 1999–September 2008). A higher value of interception for perennial vegetables and fruit trees than for the annual row crops is observed. The amount of hypodermic flow and runoff is very low.

Figure 8 shows ET_p, ET_a and recharge cumulative values for the last simulated hydrological year (October 2007–September 2008) and the three crop types. The ET_a rate was frequently lower than the ET_p, as soil moisture at various times failed to sustain the potential transpiration T_p. This is particularly important for perennial vegetables, due to the lack of irrigation during June and July. Regarding the recharge process, it could be divided into three stages for each experimental plot. Groundwater recharge mainly occurred between October and December, the rate decreased between January and May, and there was no recharge between June and September. Note that

 DOI 10.1007/s10040-010-0658-1

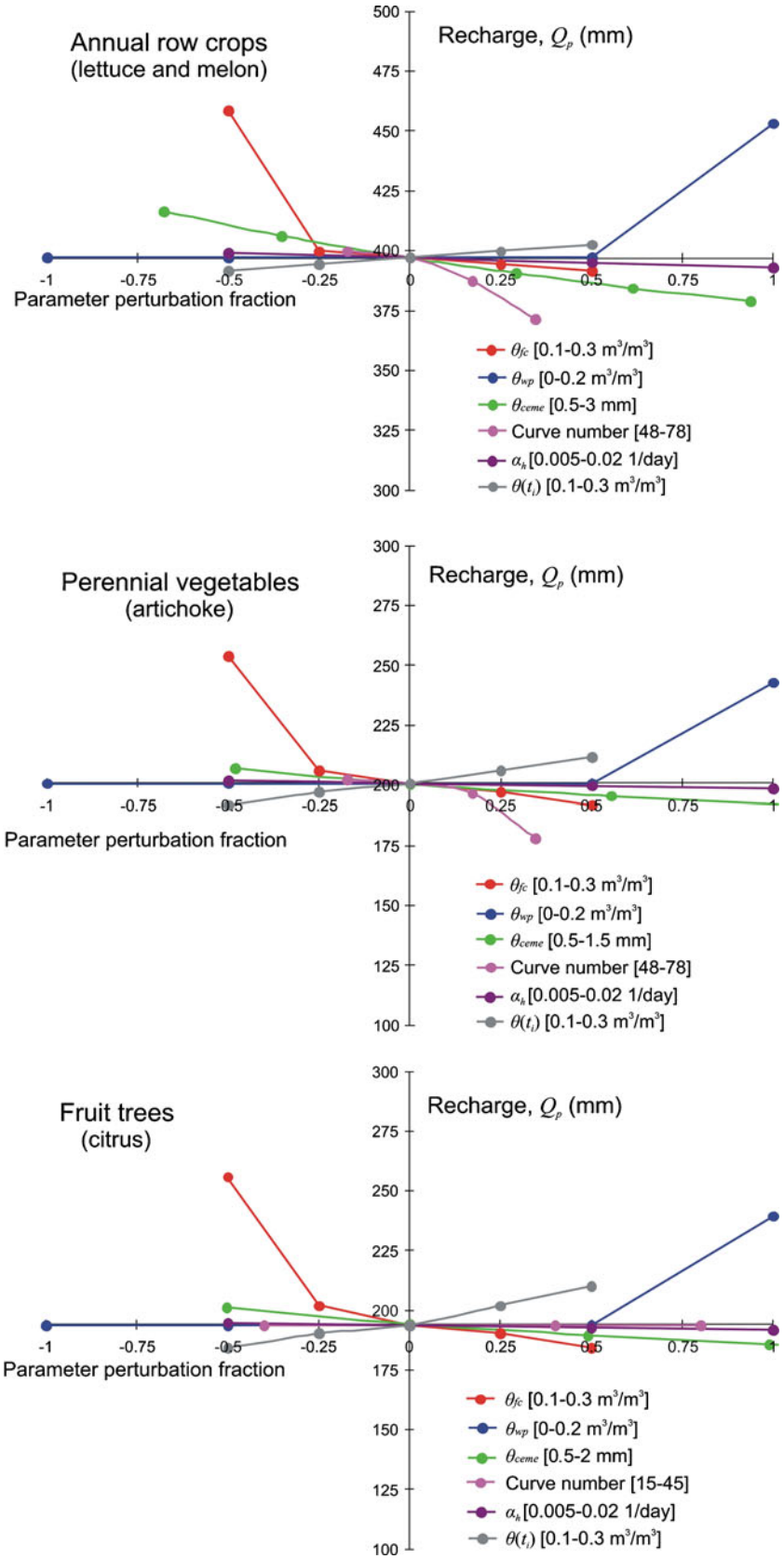

Fig. 9 Effect of parameters and initial conditions (horizontal axes, expressed as a fraction of change) on the computed recharge (vertical axes). Horizontal axes cross at estimated recharge values (base run). Parameters considered for sensitivity analysis were: P_o; α_h; K_{vv}; α_p; θ_{ceme}; b_s; Φ_s; θ_{wp}; θ_{fc}; curve number; K_{vs}; $\theta(t_i)$; V_h. Only key parameters and initial conditions are plotted. Perturbation ranges are shown in brackets

 DOI 10.1007/s10040-010-0658-1

Table 6 Summary of the relative sensitivity analysis performed for the selected boundary conditions

Boundary condition		Recharge					
		Annual row crops (lettuce and melon)		Perennial vegetables (artichoke)		Fruit trees (citrus)	
Name	*CP* (%)	*AS* (%)	*AS/CP*	*AS* (%)	*AS/CP*	*AS* (%)	*AS/CP*
Precipitation, *P*	+10	5.36	0.53	7.39	0.74	11.65	1.16
	–10	6	0.60	8.18	0.82	11.51	1.15
Reference evapotranspiration, ET_0	+10	9.04	0.90	10.03	1.00	5.57	0.56
	–10	10.79	1.08	14.36	1.44	9.22	0.92
Irrigation, Ir	+10	15.08	1.50	16.42	1.64	8.47	0.41
	–10	13.45	1.34	12.54	1.25	5.47	0.57
Height of crop, *Z*	+30	4.01	0.13	15.37	0.51	–	–
	–30	4.03	0.13	16.17	0.54	–	–

CP relative change (%) of a given variable or parameter; *AS* relative change (%) in the output value; *AS/CP* relative sensitivity

the plastic cover on summer crops had a major impact on the annual row crops recharge.

Sensitivity analyses

Figure 9 shows the effect on the estimated recharge values for some parameters (set 1) and initial conditions (set 2). A series of simulations were performed in which individual parameters and initial condition values were perturbed into a range (shown in brackets, see Fig. 9), while all other parameters and initial conditions were held at their baseline values (that is, the values used in the recharge calculations). The effect of perturbations on the estimated recharge (base run) was then evaluated.

Set 1 of sensitivity analysis involved evaluating a total of 11 parameters. The perturbation ranges of these parameters were sufficiently large and consistent with the scientific literature. Results of these calculations showed that recharge was most sensitive to five parameters in particular: field capacity θ_{fc}, wilting point θ_{wp}, hydric deficit limit value (θ_{ceme}, between θ_{fc} and θ_{wp}), curve number, and hypodermic flux depletion coefficient α_h (see Fig. 9). For θ_{fc}, θ_{wp}, θ_{ceme} and α_h the three crop types (annual row crops, perennial vegetables, fruit trees) present the same trend of recharge change with respect to the perturbations. However, with respect to the curve number, such perturbations are only affecting changes in the recharge for annual row crops and perennial vegetables. Set 2 of sensitivity analysis involved the evaluation of the initial conditions: initial water content in soil $\theta(t_i)$ and initial water volume in vadose zone V_h. Recharge was only sensitive to $\theta(t_i)$, with a similar trend for all three crops.

With regard to the sensitivity analysis for selected boundary conditions, effects due to temperature, number of daylight hours, wind velocity, air relative moisture or albedo appear to be included in ET_0. K_c causes a similar effect to ET_p according to Eq. 17, and it is not included in this analysis. The greatest change in the recharge is not always due to perturbations in the irrigation (Ir), but also to variations in the precipitation *P* in the case of fruit trees (citrus) (Table 6).

Conclusions

The daily water balance from water-table fluctuations (WTF) used in this study is presented as a suitable method for estimating groundwater recharge from farmland. It requires relatively low data density, generally available (meteorological and water level data), which can be estimated with reasonable accuracy, or obtained from literature with relative ease. On the other hand, it requires specific hydrodynamic conditions of the unconfined aquifer such as short lag span between the water application and the water arriving at the water table; also groundwater level increase should be only due to water arriving. The uncertainties associated with the large number of parameters that are employed and the particular features of the semi-arid climate are difficulties associated with this type of method and environment.

The irrigation return flow accounts for a substantial portion of recharge, as occurs on the Campo de Cartagena plain. Good agreements were found between observed and simulated water level measures, except in the case of perennial vegetables (artichoke), for which water-level fluctuations must be related to nearby pumping. The mean annual recharge values computed (from irrigation plus precipitation) during the study period (October 1999–September 2008) were 397 mm for annual row crops (lettuce and melon), 201 mm for perennial vegetables (artichoke) and 194 mm for fruit trees (citrus); these figures represented 31.4, 20.7 and 20.5% of the total applied water, respectively. The present study updates the water balance and recharge estimation carried out by the Spanish Geological Survey (IGME 1994). The results indicate that there is a greater amount of irrigation return flow than that estimated previously in the region, in spite of the current high irrigation efficiencies. A high recharge rate due to intensive precipitation events can be recognized. Improved irrigation scheduling based on soil-moisture status, weather conditions and crop water requirements could significantly reduce irrigation return flow. However, this is not an easy task, because rainfall is unevenly distributed into a few intensive events such as those that occur between September and December, with a meaningful contribution to recharge, as a consequence of

 DOI 10.1007/s10040-010-0658-1

constant high water content in the soil and the potentially preferential flow contribution.

More accurate results could be obtained by improving the quality of available data. Perhaps the most difficult aspect is specifying representative irrigation practices for the farmers, which may or may not be uniform across the region. To achieve greater reliability of model predictions, parameter uncertainty and correlation structure should be quantified to establish the confidence intervals.

Acknowledgements This study was part of the CGL-2004-05963-C04-01 and CGL2007-66861-C04-03 research projects funded by the Spanish Ministry of Science and Innovation's National Research Development and Innovation Plan (Spain). It is also included in the framework of the 08225/PI/08 research project financed by "Programa de Generación del Conocimiento Científico de Excelencia" of Fundación Seneca, Región de Murcia (II PCTRM 2007-10).

References

Allen RG, Pereira LS, Raes D, Smith M (1998) Crop evapotranspiration: guidelines for computing crop water requirements. Irrigation and drainage. Paper No. 56, FAO, Rome

Brunner P, Bauer P, Eugster M, Kinzelbach W (2004) Using remote sensing to regionalize local precipitation recharge rates obtained from the chloride method. J Hydrol 294(4):241–250

Candela L, von Igel W, Elorza FJ, Aronica G (2009) Impact assessment of combined climate and management scenarios on groundwater resources and associated wetland (Majorca, Spain). J Hydrol 376:510–527

CARM (2007) El Agua y la Agricultura en la Región de Murcia. Un Modelo de Eficiencia [Water and agriculture in Region de Murcia: an efficient model]. Secretary of Agriculture and Water, Region de Murcia, Murcia, Spain, 111pp

CARM (2008) Agrarian statistics data (in Spanish). Secretary of Agriculture and Water, Region de Murcia. http://siam.imida.es. Cited 1 September 2009

Carrica JC, Lexow C (2004) Evaluación de la recarga natural al acuífero de la cuenca superior del arroyo Napostá Grande, Provincia de Buenos Aires [Natural recharge estimation to the aquifer in the upper basin of the Napostá Grande beck]. Rev Asoc Geol Argentina 39(2):281–290

Castañeda C, García-Vera MA (2008) Water balance in the playa-lakes of an arid environment, Monegros, NE Spain. Hydrogeol J 16:87–102

Castel JR (2001) Consumo de agua para plantaciones de cítricos en Valencia [Water requirements for citrus crop in Valencia]. Fruticultura Profesional 123:27–32

Castel JR, Bautista I, Ramos C, Cruz G (1987) Evapotranspiration and irrigation efficiency of mature orange orchards in Valencia (Spain). Irrig Drain Syst 3:205–217

CSIRO (2008) TOPOG software. CSIRO Land and Water and the Cooperative Research Centre for Catchment Hydrology, Clayton, Australia. http://www.per.clw.csiro.au/topog/. Cited 15 December 2009

Dawes WR, Zhang L, Hatton TJ, Reece PH, Beale G, Packer I (1997) Evaluation of a distributed parameter ecohydrological model (TOPOG_IRM) on a small cropping rotation catchment. J Hydrol 191:64–86

de Vries JJ, Simmers I (2002) Groundwater recharge: an overview of processes and challenges. Hydrogeol J 10:5–17

Droogers P (2000) Estimating actual evapotranspiration using a detailed agro-hydrological model. J Hydrol 229:50–58

Garatuza-Payán J, Shuttleworth WJ, Encinas D, McNeil DD, Stewart JB, DeBruin H, Watts C (1998) Measurement and modelling evaporation for irrigated crops in northwest Mexico. Hydrol Process 12:1397–1418

Ghulam ZH, Bhutta MN (1996) A water balance model to estimate groundwater recharge in Rechna Doab, Pakistan. Irrig Drain Syst 10:297–317

Gracía-Santos G, Mazol V, Morales D, Gómez LA, Pisani B, Samper J (2005) Groundwater recharge in a mountain cloud laurel forest at Garajonay National Park (Spain). Geophys Res Abstr 7:00942

Hanson BR, Schwankl LJ, Schulbach KF, Pettygrove GS (1997) A comparison of furrow, surface drip irrigation on lettuce yield and applied water. Agric Water Manage 33:139–157

Haque A (2003) Estimating actual areal evapotranspiration from potential evapotranspiration using physical models based on complementary relationships and meteorological data. Bull Eng Geol Env 62:57–63

Healy RW, Cook PG (2002) Using groundwater levels to estimate recharge. Hydrogeol J 10:91–109

Horton RE (1919) Rainfall interception. Mon Weather Rev 47:603–623

IGME (1994) Las aguas subterráneas del Campo de Cartagena (Murcia) [Groundwater in the Campo de Cartagena (Murcia)]. Spanish Geological Survey, Madrid, Spain, 62 pp

ILRI (2005) SAHYSMOD version 1.7. Spatial agro-hydro-salinity model: description of principles, user manual, and case studies. International Institute for Land Reclamation and Improvement, Wageningen, The Netherlands

Jiménez J, García G, Queralt I, Aragón R, García-Arostegui JL, Solano F, Candela L (2007) Vadose zone characterization in an experimental plot under intensive agriculture. Preliminary results. In: Candela et al. (eds) International conference WAter POllution in natural POrous media at different scales (WAPO2). IGME Book series: Hidrogeología y Aguas Subterráneas 22, IGME, Madrid, pp 143–148

Jiménez-Martínez J, Skaggs TH, van Genuchten MTh, Candela L (2009) A root zone modelling approach to estimating groundwater recharge from irrigated areas. J Hydrol 367(1–2):138–149

Kendy E, Gérard-Marchant P, Walter MT, Zhang Y, Liu C, Steenhuis TS (2003) A soil-water-balance approach to quantify groundwater recharge from irrigated cropland in the North China Plain. Hydrol Process 17:2011–2031

Kroes JG, Van Damm JC (2003) Reference manual SWAP: Version 3.0.3. Report no. 773. Alterra Green World Res., Wageningen, The Netherlands

Lascano RJ, van Bavel CHM (2007) Explicit and recursive calculation of potential and actual evapotranspiration. Agron J 99:585–590

Lerner DN, Issar AS, Simmers I (1990) Groundwater recharge: a guide to understanding and estimating natural recharge. Report no. 8, International Association of Hydrogeologists, Kenilworth, UK, 345 pp

Lidón A, Ramos C, Rodrigo A (1999) Comparison of drainage estimation methods in irrigated citrus orchards. Irrig Sci 19:25–36

López-Rodríguez JJ, Giráldez-Cervera JV (1997) Evaluación de la modificación de la recarga por cambios en la cobertura vegetal [Aquifer recharge variations by ground cover changes]. In: Custodio E, Llamas R, Samper J (eds) La evaluación de la recarga a los acuíferos en la Planificación Hidrológica. AIH-GE, Barcelona, pp 209–227

Pachepsky YA, Smettem KRJ, Vanderborght J, Herbst M, Vereecken H, Wosten JHM (2004) Reality and fiction of models and data in soil hydrology. In: Feddes RA et al (eds) Unsaturated-zone modeling. Kluwer, Dordrecht, The Netherlands

Poulavassilis A, Anadanistakis M, Liakatas A, Alexandris S, Kerkides P (2001) Semi-empirical approach for estimating actual evapotranspiration in Greece. Agric Water Manage 51:143–152

Press WH, Flannery BP, Teukolsky SA, Vetterling WT (1989) Numerical recipes in Pascal: the art of scientific computing. Cambridge University Press, Cambridge, UK, 709 pp

Ramírez I, Vicente M, García J, Vaquero A (1999) Mapa digital de suelos de la Región de Murcia [Digital soil map of Region de

Murcia]. Consejería de Agricultura, Agua y Medio Ambiente. Handbook and CD-ROM (in Spanish), 78 pp
Samper J, García-Vera MA, Pisani B, Varela A, Losada JA, Alvares D, Espinha Marques J (2007) Using hydrological models and geographic information systems for water resources evaluation: GIS-VISUAL-BALAN and its application to Atlantic basins in Spain (Valiñas) and Portugal (Serra da Estrela). In: Lobo Ferreira JP, Vieira JMP (eds) Water in Celtic countries: quantity, quality and climate variability. IAHS Publ. no. 310, IAHS, Wallingford, UK, pp 259–266
Samper J, Huguet Ll, Ares J, García-Vera MA (2005) User's guide VisualBALAN v.2.0: código interactivo para la realización de balances hidrológicos y la estimación de la recarga [VisualBALAN v.2.0: interactive code to establish water balance and aquifer recharge]. Civil Engineering School of A Coruña, A Coruña, Spain, 150 pp
Sánchez MI, López F, Del Amor F, Torrecillas A (1989) La evaporación y evapotranspiración en el Campo de Cartagena y Vega Media del Segura. Primeros resultados [Evaporation and evapotranspiration in the Campo de Cartagena and Vega Media del Segura]. Anal Edafol Agrobiol. 47(9–10):239–1251
Scanlon BR, Healy RW, Cook PG (2002) Choosing appropriate techniques for quantifying groundwater recharge. Hydrogeol J 10:18–39
Sena C, Molinero J (2009) Water resources assessment and hydrogeological modelling as tool for the feasibility study of a closure plan for an open pit mine (La Respina Mine, Spain). Mine Water Environ 28:94–101
Sharma ML (1989) Groundwater recharge. Balkema, Rotterdam, The Netherlands, 323 pp
Simmers I (1988) Estimation of natural groundwater recharge. Reidel, Boston, MA, 510 pp
Soil Conservation Service (1975) Engineering field manual conservation practices. US Department of Agriculture, Washington, DC
Thornthwaite CW (1948) An approach toward a rational classification of climate. Geogr Rev 38:55–94
USGS (2008) Documentation of computer program INFIL3.0: a distributed-parameter watershed model to estimate net infiltration below the root zone: US Geol Surv Sci Invest Re 2008–5006, 98 pp
Wang B, Jin M, Nimmo JR, Yang L, Wang W (2008) Estimating groundwater recharge in Hebei Plain, China under varying land use practices using tritium and bromide tracers. J Hydrol 356:209–222
Zhang L, Dawes WR, Hatton TJ, Reece PH, Beale GT, Packer I (1999) Estimation of soil moisture and groundwater recharge using the TOPOG_IRM model. Water Resour Res 35:149–161

Water Air Soil Pollut (2011) 215:311–327
DOI 10.1007/s11270-010-0480-3

The Role of Leaky Boreholes in the Contamination of a Regional Confined Aquifer. A Case Study: The Campo de Cartagena Region, Spain

J. Jiménez-Martínez · R. Aravena · L. Candela

Received: 10 December 2009 / Accepted: 14 May 2010 / Published online: 4 June 2010

Abstract Poorly constructed wells (leaky or without a gravel pack) and abandoned wells can behave as conduits for the interconnection of aquifers at different depths and facilitate the transfer of contaminants between these aquifers. This is the case with Campo de Cartagena (SE Spain) where the primary land use is intensive irrigated agriculture, along with a high density of wells. The unconfined aquifer is heavily impacted by a high concentration of nitrate associated with agricultural activities. The present work provides a methodological approach to evaluate the impact of the unconfined aquifer on the water quality of the confined aquifer caused by leaky wells in high-density areas of production wells. The research approach included the use of geochemical and isotopic tools; specifically, nitrate was used as a tracer for evaluating the impact, and the code MIX_PROGRAM was used for mixing calculations. Results show an increase of the impact of the unconfined aquifer on the confined aquifer along the groundwater flow direction toward the coast, although this general pattern is controlled by local factors (pumping, intensity of agricultural practices, density of wells, and groundwater residence time).

Keywords Aquifer interconnection · Leaky borehole · Mixing rate · Campo de Cartagena

J. Jiménez-Martínez (✉) · L. Candela
Department of Geotechnical Engineering and Geosciences,
Technical University of Catalonia-UPC,
Gran Capitan sn,
08034 Barcelona, Spain
e-mail: joaquin.jimenez@upc.edu

J. Jiménez-Martínez · R. Aravena
Department of Earth and Environmental Sciences,
University of Waterloo,
Waterloo, ON, Canada

1 Introduction

Abandoned, leaky, and poorly constructed wells (leaky or without a gravel pack) may act as conduits transferring contaminants to underlying aquifers and are common features at many polluted groundwater sites. This fact has been observed in a number of studies under different geological scenarios and exploitation frameworks (e.g., Lacombe et al. 1995; Pulido-Bosch et al. 2000; Salama 2005; Carter et al. 2007). In a multilayer aquifer, abandoned or poorly constructed wells penetrate through geological strata otherwise considered impermeable (aquitard) that supposes open conduits for pollutant migration. Even if wells are properly designed and constructed with a long life expectancy, they can deteriorate with time and be abandoned or become damaged due to land planning. Also, they can be drilled illegally. Under such circumstances, any information of wells may be lost.

Aquifer interconnection may also occur via flow through aquitards in areas of reduced aquitard thickness which could be enhanced by water pumping in

the underlying confined aquifer (Hantush and Jacob 1955; Hantush 1960; Boulton 1963; Neuman and Witherspoon 1969). For the case of a possible flow rate through an open well (inside the well), Lacombe et al. (1995) demonstrated that flow is more dependent on the borehole radius than the existing vertical hydraulic gradient. In hydrology, mixing calculations are often viewed as a preliminary step in the process of building a conceptual model to identify where water comes from. Mixing models based on chemical and isotope data are commonly used to quantify hydraulic aquifer connection between aquifers (Adar and Nativ 2000; Banner et al. 1989; Larsen et al. 2003). The principal problem in mixing calculations is the uncertainty in the end members (properties, origin of mixing water) due to the spatial and temporal variability of water composition.

The present study was carried out in a semiarid region, Campo de Cartagena (SE Spain), where the land is intensively irrigated for agriculture (CARM 2008) and groundwater pollution from agriculture exists. The agricultural activities are practiced over an unconfined aquifer, which constitutes a source for contamination by agrochemicals and is separated from the lower confined aquifer by a thick aquitard. The objective is to evaluate the significance that abandoned and poorly constructed wells have on cross-formational groundwater flow and contaminant transport between the shallow unconfined and deep confined aquifers. The work provides a methodological approach based on the application of geochemical and isotopic tools and water mixing calculations from a numerical model. The state of saturation of groundwater samples (saturation index, *I*) for relevant minerals and ionic speciation were calculated using the PHREEQC code (Parkhurst and Appelo 1999). Water mixing calculations were estimated using the numerical code MIX_PROGRAM (Carrera et al. 2004), which provides theoretical estimates of the end-member concentrations, thereby reducing the uncertainty due to spatiotemporal variability and thus improving the quality of the output mixing calculations.

2 Study Site

The Campo de Cartagena basin is a 1,440-km^2 plain located in the Southeastern part of Mediterranean Spain (Fig. 1a). It is bordered to the east by the Mediterranean Sea and Mar Menor (hypersaline coastal lagoon) and to the north, south and west by small mountain ranges. The region is characterized by a semiarid Mediterranean climate, with an average temperature of 18°C and 300 mm of annual rainfall, which is unevenly distributed into a few intense events that are highly variable in space and time. Rainfall occurs mainly during spring and autumn. No permanent watercourse exists, and the area is drained by several ephemeral streams. Agriculture is the primary land use (Fig. 2). Drip irrigation is widely applied in the region due to the scarcity of water resources and the need for water conservation. The population's water supply relies on surface water imported from *Canales del Taibilla*. Water for agricultural irrigation is pumped from deep confined aquifers and a surface *water transfer* system from the *Tajo-Segura Aqueduct* (MIMAN 2000). This system which transfers water from the *Tajo basin* (central part of Spain) to the study region was initiated in 1980. Since 2005 and due to the high water demand for irrigation, desalination of brackish groundwater has been promoted by the farming community to increase available water resources.

2.1 Hydrogeological Setting

The study area is contained by a Neogene and Quaternary sedimentary basin located in the Eastern part of the Betic Cordillera. The sedimentary rocks unconformably overlie metamorphic basement rocks (Fig. 1a, b). A number of published and unpublished geologic and hydrogeologic studies of the area have been conducted (IGME 1994; Jiménez-Martínez et al. 2010); only a synthesis is presented here.

The Neogene sedimentary infill is mainly composed of low-permeability sediments (marls) with interlayered high-permeability material (limestones, sands, and conglomerates) deposited during the Tortonian stage through to the Quaternary period. Sands and conglomerates of Tortonian age, organic limestones of Messinian age, and sandstones of Pliocene age constitute the aquifer materials of the deep confined aquifers. Finally, overlying the Neogene sedimentary rocks and covering a great part of the Campo de Cartagena, the Quaternary sediments (conglomerates, sands, and silts) form the upper unconfined aquifer (IGME 1994; Fig. 1b).

Due to the load of agrochemicals applied in agricultural management (ammonium nitrate NH_4NO_3;

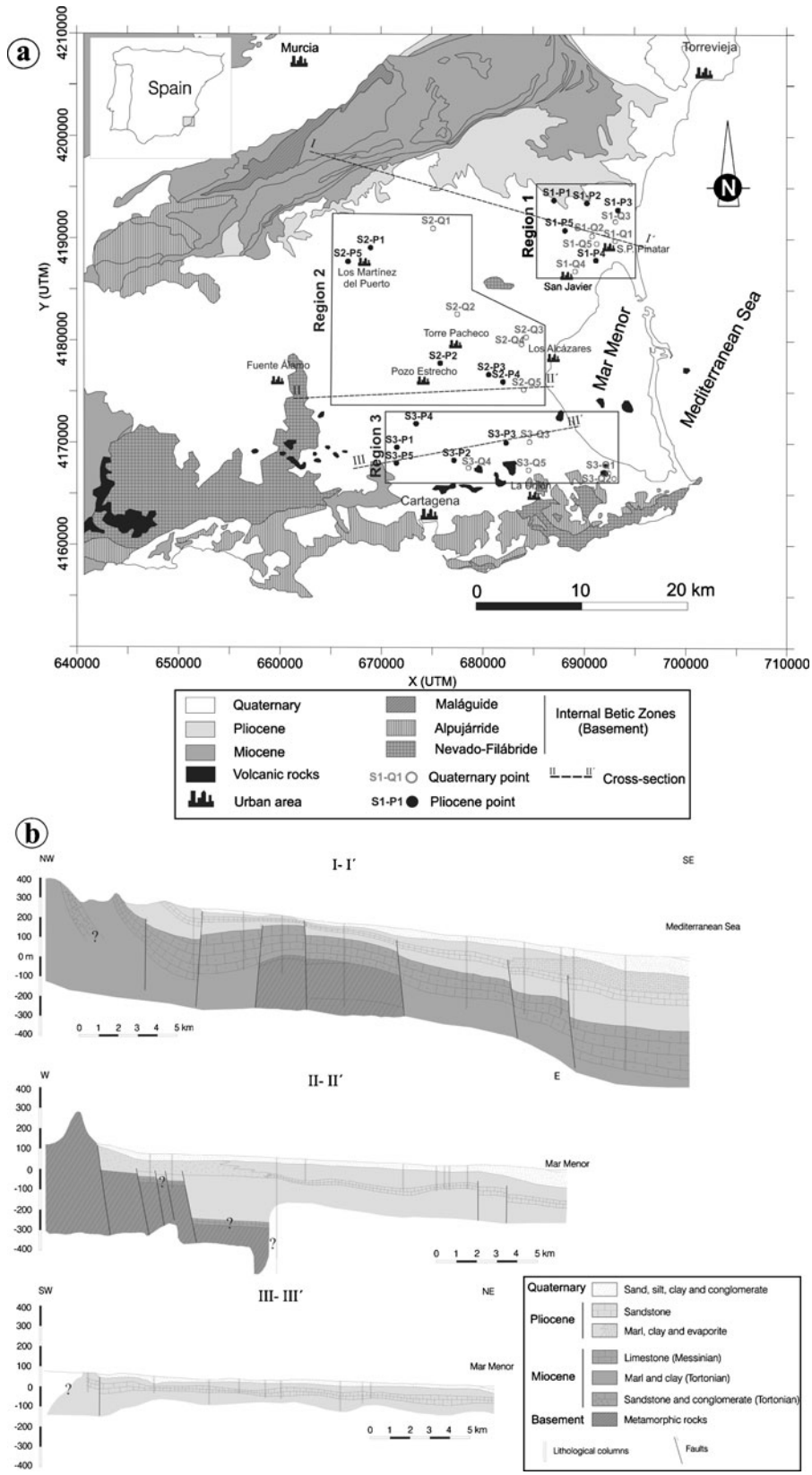

Fig. 1 **a** Study area and geological sketch. Location of the defined regions and sample points (S1 to S3 region; *P* Pliocene aquifer, *Q* Quaternary aquifer; 1 to *n* sample point). **b** Geological cross section

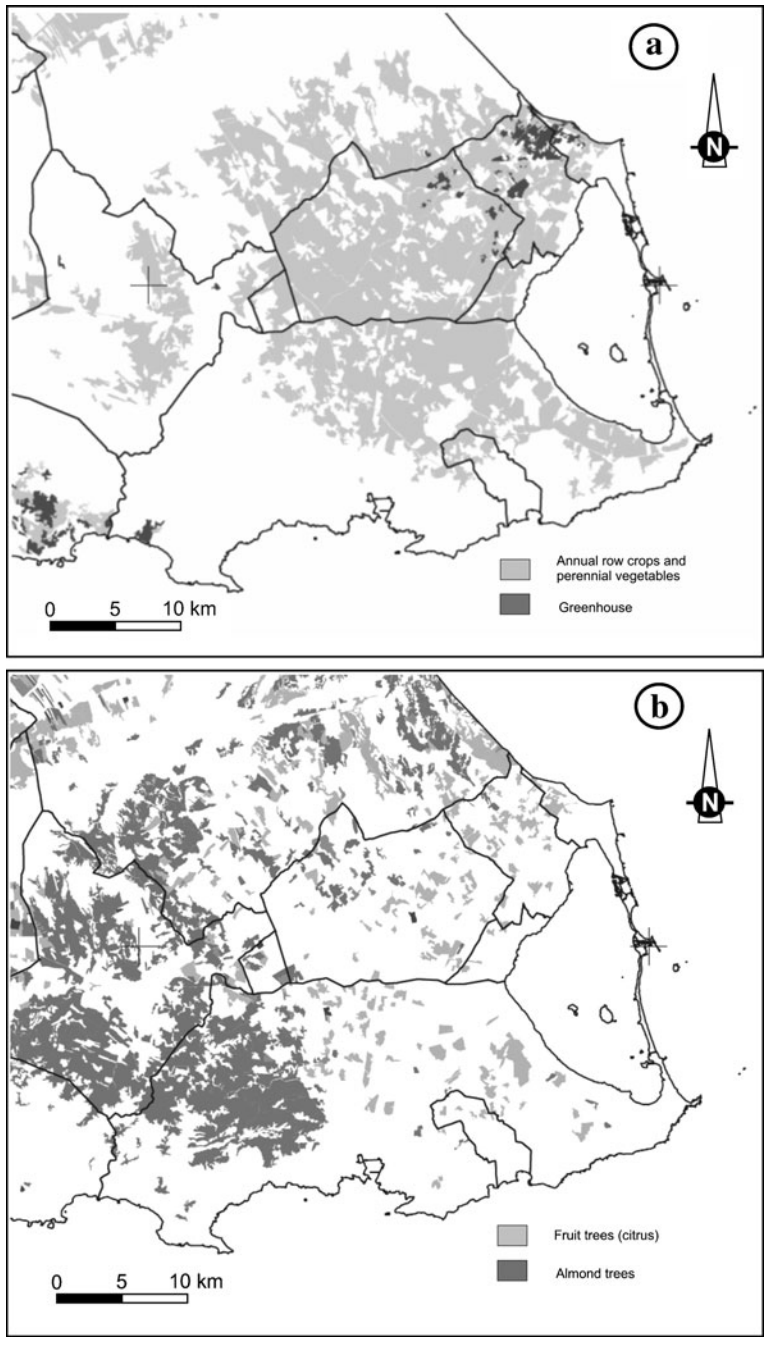

Fig. 2 Land covered by the principal crops (CARM 2008). **a** Vegetables and **b** fruit trees

phosphoric acid H_3PO_4; potassium nitrate KNO_3; calcium nitrate $Ca(NO_3)_2$; ammonium phosphate $(NH_4)_3PO_4$; and magnesium nitrate $Mg(NO_3)_2{\cdot}6H_2O$), the upper aquifer has been highly polluted by infiltration of irrigation return flows. Moreover, elevated pumping rates in wells as a consequence of water resources demand, along with the aquifers' interconnection through abandoned and poorly constructed wells, primarily impact on the quality and quantity of groundwater resources in the region. Further, groundwater discharge to the Mar Menor (a hypersaline lagoon) also causes an environmental impact on the flora and fauna in the lagoon area (Rodríguez Estrella 2000; García-Pintado et al. 2007). Mitigating

these risks depends on a full understanding of groundwater flow mechanisms and on the adequate construction of the network design of production wells (Frind et al. 2002).

2.2 Introduction to the Problem

The assessment of interconnection focuses on the Pliocene lower confined aquifer comprising sandstone and extending over an area of 817 km^2, and the Quaternary upper unconfined aquifer (conglomerates, sands, and silts), which outcrops over a surface of 1,135 km^2. The aquifers are separated by an aquitard comprising marls and evaporites (see cross sections Fig. 1b). The main groundwater flow direction in both aquifers is from northwest to southeast toward the coast, although local disturbances of the flow system occurs in the Northern part of the Pliocene aquifer due to the high density of wells and water extraction (Fig. 3a). During the 1960s and 1970s, the aquifers were intensively exploited. Since 1980, when the *Tajo-Segura water transfer system* was initiated, the total irrigated area has increased due to the new available water resources. In response, an increase of induced recharge by irrigation return flow has been produced. As a result, two mechanisms have led to a water-level rise in aquifers: irrigation return flows and decreased pumping from wells (Fig. 3b). Also, intensive mineral fertilizer application (0.9–1.6 tha^{-1}year^{-1}), which frequently exceeds crop needs, forms part of the agriculture management. This leads to the fact that, in old traditional agriculture practices, nitrogen losses to

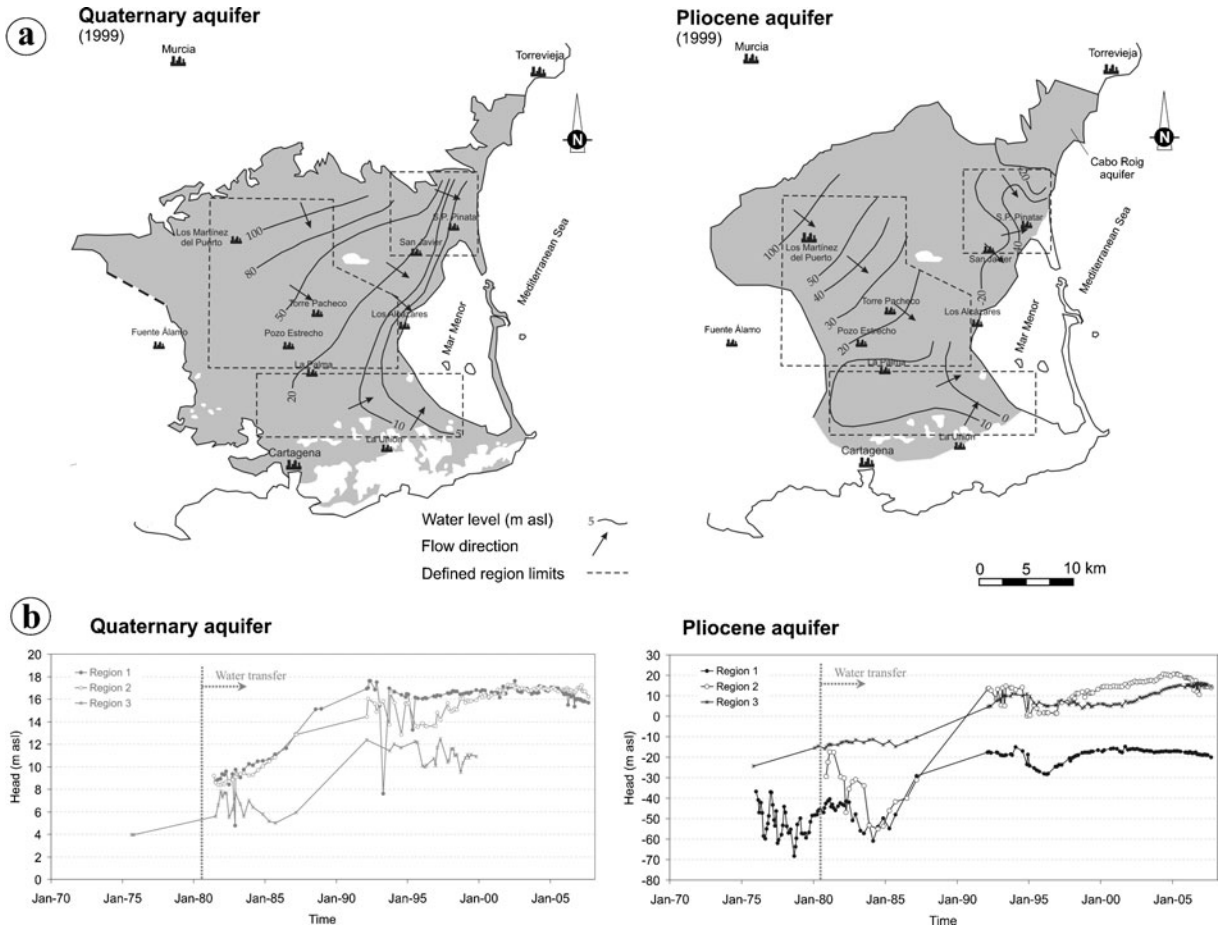

Fig. 3 **a** Hydraulic head and regional flow direction for the Quaternary (upper unconfined) and Pliocene aquifer (lower confined) recorded in 1999. **b** Hydraulic head evolution for each aquifer in the defined regions. *Dashed line* represents the arrival of *Tajo-Segura water transfer system* (source: Groundwater Level Monitoring Network of CHS-IGME)

the aquifer may vary by 50–90% of the application dose (Candela 2000).

A total of 966 registered wells exist (IGME data base); those wells exploit the Pliocene aquifer and deeper hydrostratigraphic units (Fig. 4), although estimation of the number of nonregistered wells (illegal) indicates that the total could be double the registered number or even greater. The mean density of wells per square kilometer is 1.18, with increasing density toward the coast. This great density of wells implies a high risk of interconnection between the two aquifers, although downward flow through the aquitard, which is composed of marls and evaporite lenses, should not be discarded. Pumping from the Pliocene aquifer may increase the difference of head potential between both aquifers and the downward gradient.

3 Methodology

Due to the broad extension of the study area, three regions were defined based on land use and regional geology (Fig. 1a). For region 1, where the highest density of wells occurs, the regional groundwater flow direction for both aquifers is toward the southeast, although local perturbations are observed in the lower confined aquifer (Pliocene). In region 2, groundwater flow direction changes from southeast to east in both aquifers. Finally, the groundwater flow component in both aquifers for region 3 is from southwest to northeast (Fig. 3a); it is the region with lowest density of wells and least land area covered by crops (see Figs. 2 and 4). The aquitard between the two aquifers is composed of marls in regions 2 and 3, while in region 1 it is mainly composed of evaporites (see Fig. 1b).

Groundwater records for the 1974–2008 monitoring surveys were provided by the Groundwater Quality Monitoring Network from the Water Authority (Confederación Hidrográfica del Segura-CHS and IGME). A field survey under the project framework was also carried out in 2008. The chemical data set includes physicochemical parameters (pH, temperature, and electrical conductivity), major ion content (Na^+, K^+, Ca^{2+}, Mg^{2+}, Cl^-, HCO_3^-, SO_4^{2-}, and NO_3^-), and CO_3^{2-}, NO_2^-, NH_4^+, and SiO_2. Some specific surveys in situ analysed dissolved oxygen measurements, heavy metals and environmental isotopes (^2H, ^{18}O, and ^{16}O). A subset of five water

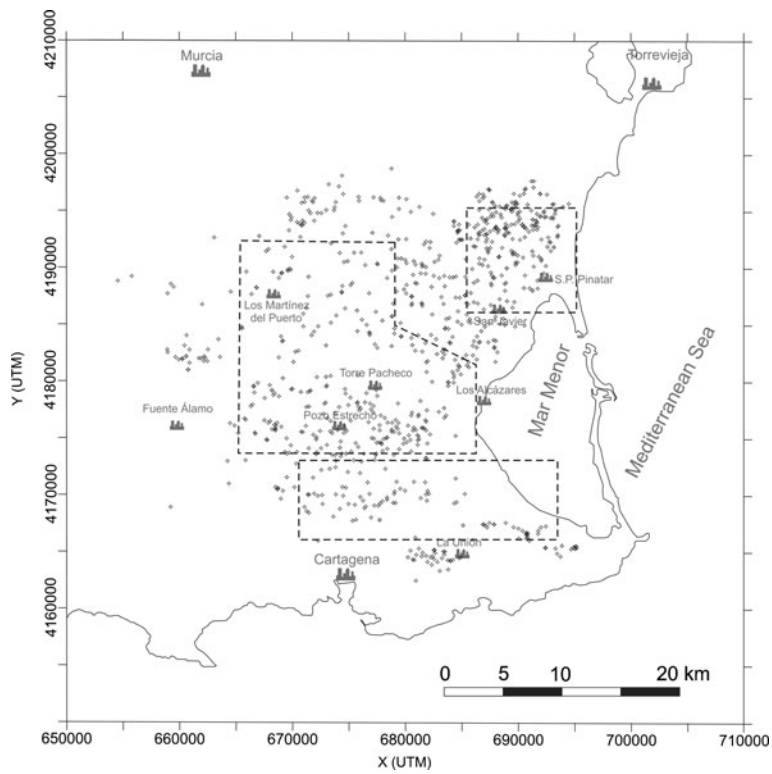

Fig. 4 Spatial distribution of wells reaching the Pliocene aquifer and/or deeper units (966 registered wells from the IGME database). The *dashed line* shows the three defined regions

sample points within the surveyed period for each aquifer and defined region was selected for this study. Selection was based on the geographic location, aquifer sampled, and length of available records.

Nitrate content in groundwater was the parameter selected as an indicator of cross-contamination due to its high concentration (460 mg l^{-1}) and broad spatial extent. Estimation of the shallow aquifer's impact on the deep aquifer was obtained through a water mixing approach based on chemical data. Finally, obtained results from nitrate content and mixing calculations were assessed through the study of environmental isotopes in groundwater samples.

3.1 Nitrate as an Indicator of Interconnected Aquifers

Nitrate is the most common contaminant in areas characterized by intensive agricultural activities. However, a content of up to 20 mg l^{-1} of nitrate (NO_3^-) in groundwater generated by the processes of nitrification of soil nitrogen (Frisch 1987) can be considered as the natural background concentration.

In regional groundwater flow systems, which are shaped by the geology, the attenuation processes regulate nitrate transport and control its distribution in aquifers. Nitrate attenuation may occur by dilution or denitrification. Dilution occurs through mixing of groundwater in the aquifer (Altman and Parizek 1995). Denitrification in reducing environments is the only geochemical process that permanently removes nitrate from aquifers. Nitrate reduction can be mediated by oxidation of organic matter (1), pyrite (2), and iron (3) under anaerobic conditions (Korom 1992; Starr and Gillhma 1993; Roberston and Schiff 2008):

$$5CH_2O + 4NO_3^- \rightarrow 2N_2 + 4HCO_3 + CO_2 + 3H_2O \quad (1)$$

$$5FeS_2 + 14NO_3^- + 4H^+ \rightarrow 7N_2 + 5Fe^{2+} + 10SO_4^{2-} + 2H_20 \quad (2)$$

$$10Fe^{2+} + 2NO_3^- + 14H_2O \rightarrow 10FeOOH + N_2 + 18H^+ \quad (3)$$

For the three defined regions, nitrate constitutes a good indicator for assessing the Quaternary and Pliocene interconnection. Homogeneity in the spatial distribution of land covered by crops (source of nitrate), along with the long-term records of nitrate concentration and dissolved oxygen values (oxidation reduction potential), supports this assumption.

3.2 Geochemical and Mixing Models

To calculate ionic speciation and state of saturation (saturation index) for relevant minerals, a well-known computer code for aqueous geochemical calculations, PHREEQC (Parkhurst and Appelo 1999), was applied. This preliminary step is necessary to evaluate the potential geochemical reactions occurring in the aquifer, since deviations from mixing lines could be attributed to chemical reactions (Pitkänen et al. 1999). Speciation and equilibrium calculations were carried out for the most complete groundwater record surveys from 1995, 2001, and 2005 (CHS-IGME database) and a project sampling survey was carried out in 2008.

When mixing calculations with real data from complex natural systems, uncertainties are always involved in the evaluation of the end-member concentrations, which are not derived primarily from analytical errors, but from its spatial and temporal variability as well as errors in the conceptual model of the flow system. If end members are properly identified, their mixing ratios can be accurately calculated. Therefore, the first task is to define the end members.

Concentrations of mixed samples (mainly affected by analytical errors) are likely to be more accurate than end members. This fact can be used to impose constraints on valid end-member concentration since taking mixing constraints into account may significantly reduce uncertainty in end-member concentration by imposing consistency. Consistency is dealt with in two ways: first, end members should fall on the mixing line, and second, mixed waters should fall within the interval defined by end members. The code MIX_PROGRAM (Carrera et al. 2004) permits the mixing ratios in mixed samples (Fig. 5a, for two end members) to be derived, allows for redefinition of mixing lines and can also be applied to more than two end members. The second condition does not constrain end member 2 but rather reduces the uncertainty of end member 1 (Fig. 5b). For an enhanced explanation of MIX_PROGRAM's methodological approach, the reader is referred to Carrera et al. (2004).

Two sources or end members and two chemical species, considered as conservative tracers, were defined. The two end members are the Quaternary (upper

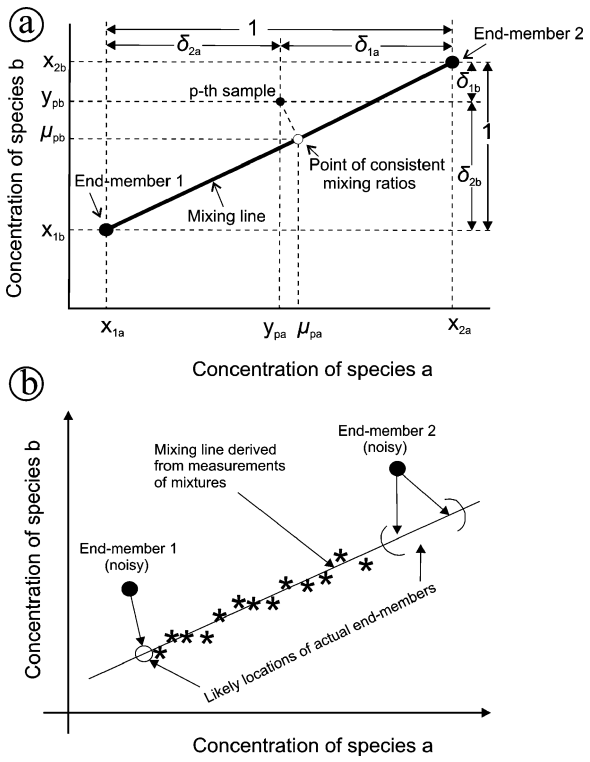

Fig. 5 **a** Illustration of mixing calculation approach. **b** Mixing line derived from measured samples by imposing consistency. y_{nl}, concentration of chemical species (a and b) in the mixed sample p. x_{nl}, concentration of the chemical species in the end members. δ_{pn}, mixing ratios of the end members in the sample p. μ_{pl}, concentration of the chemical species for the sample p in the point of consistent mixing ratio (modified from Carrera et al. 2004)

unconfined) and Pliocene (lower confined) aquifer water samples, and the two chemical species selected were chloride (Cl^-) and sulfate (SO_4^{2-}). Cl^- is a conservative compound but SO_4^{2-} can be affected by several processes. Sulfate reduction and pyrite oxidation within the aquifer control the SO_4^{2-} concentration in groundwater. Pursuant to reaction 4, ongoing SO_4^{2-} reduction can be recognized by the HCO_3^- increase. Pyrite oxidation (Eq. 5) and nitrate, instead of oxygen, as the electron acceptor (Eq. 6) can act as sulfate sources (Massmann et al. 2003):

$$2CH_2O + SO_4^{2-} \rightarrow 2HCO_3^- + H_2S \quad (4)$$

$$FeS_2 + 15/4O_2 + 7H_2O \rightarrow Fe(OH)_3 + 2SO_4^{2-} + 4H^+ \quad (5)$$

$$14NO_3^- + 5FeS_2 + 4H^+ \rightarrow 7N_2 + 10SO_4^{2-} + Fe^{2+} + 2H_2O \quad (6)$$

Table 1 Measured end-member concentrations for the three defined regions. Computed end-member concentrations from the MIX_PROGRAM (Carrera et al. 2004) are also shown

Aquifer	Species	Region 1				Region 2				Region 3			
		Number of samples (period)	m (mg l^{-1})	σ (mg l^{-1})	Computed end member	Number of samples (period)	m (mg l^{-1})	σ (mg l^{-1})	Computed end member	Number of samples (period)	m (mg l^{-1})	σ (mg l^{-1})	Computed end member
Quaternary	Cl^-	129 (1980–2008)	1,372.4	374.8	1,214.7	91 (1980–2008)	1,794.2	651.3	2,559.2	37 (1980–2008)	1,305.3	395.5	1,418.4
	SO_4^{-2}		624.9	201.7	1,082.2		1,270.4	437.1	1,871.3		766.2	430.4	1,122.6
Pliocene	Cl^-	3 (1970s)	493.7	17.6	457.4	4 (1970s)	1,121.3	141.9	974.9	3 (1970s)	1,053.0	20.8	1,041.1
	SO_4^{-2}		238.7	143.6	62.4		949.8	225.5	946.3		679.0	84.9	273.1

m mean, σ standard deviation

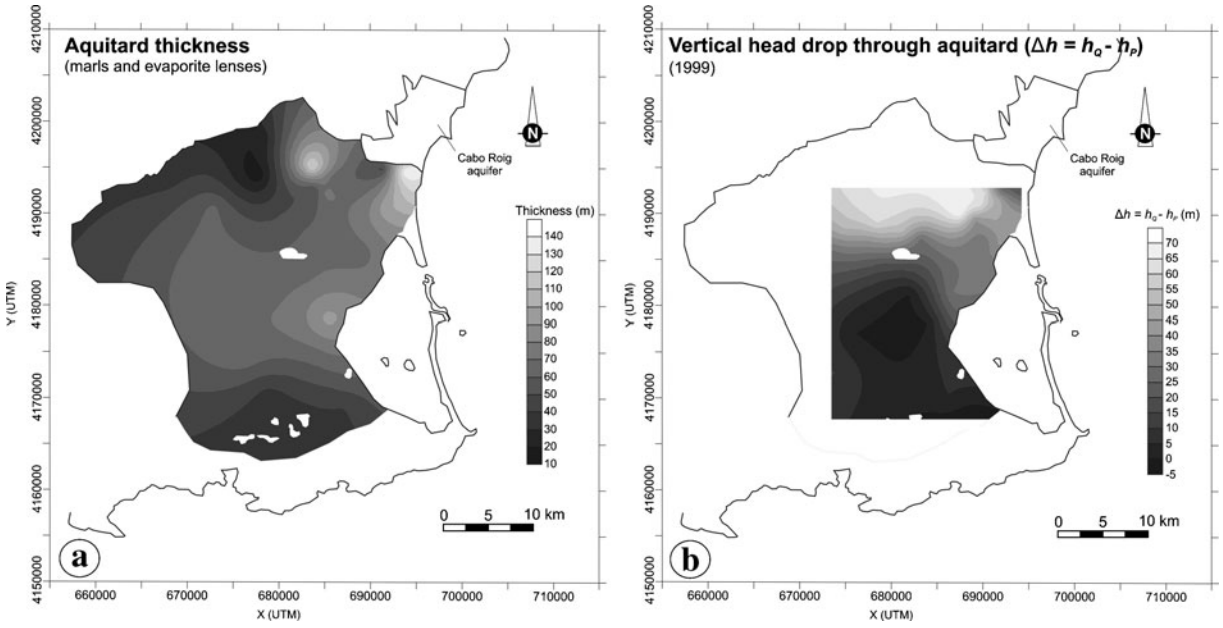

Fig. 6 **a** Thickness of the aquitard. **b** Vertical head drop (Δh) through the aquitard (h_Q: potential head (masl) of the unconfined Quaternary aquifer; h_P: potential head (masl) of the confined Pliocene aquifer)

For mixing calculations, data on Cl^- and SO_4^{2-} concentrations from 1980 (beginning of the *water transfer* and intensive agriculture) to the present time were selected as the Quaternary end member. For the Pliocene end-member natural background concentration in groundwater (1970s), a data set of the same chemical species was selected in each of the defined regions (Table 1). This data set is not affected by agricultural pollution.

3.3 Complementary Tools

To evaluate flow contribution through the aquitard (marls and evaporite lenses) to the lower confined aquifer, the following hydraulic variables were considered: thickness of the aquitard (Fig. 6a); vertical head difference through the aquitard (Fig. 6b), $\Delta h = h_Q - h_P$, with h_Q and h_P being the potential head (meter above sea level, masl) of the

Table 2 Nitrate concentration for each aquifer and defined regions

Region	Aquifer	Nitrate ion concentration[a]				
		Number of samples (period)	m (mg l^{-1})	σ (mg l^{-1})	Max (mg l^{-1})	Min (mg l^{-1})
Region 1	Quaternary	121 (1980–2008)	157.4	89.4	460	4
	Pliocene	58 (1976–2008)	40.7	60.6	221.6	0.04
Region 2	Quaternary	92 (1978–2008)	92.2	67.6	379.2	2
	Pliocene	76 (1980–2008)	54.9	54.5	250.0	0.8
Region 3	Quaternary	36 (1989–2008)	87.3	86.7	369.8	2.9
	Pliocene	71 (1976–2008)	70.6	67.6	317	3

[a] Source: Groundwater Quality Monitoring Network (CHS-IGME) and 2008 survey

m mean, σ standard deviation, *Max* maximum value, *Min* minimum value

unconfined Quaternary and confined Pliocene aquifer, respectively.

The Cl/Br ratio, used as an indicator of seawater intrusion or evaporite dissolution, was calculated in all available water samples in order to assess the importance of a third member for mixing calculations (Custodio and Herrera 2000). Finally, 15 environmental isotope analyses ($\delta^{18}O$ and $\delta^{2}H$) were used to confirm the existing connection between aquifers (Lu et al. 2008). Isotope analyses were carried out at the AGH Faculty of Physics and Applied Computer Science (Krakow, Poland). For both complementary indicators, only data from the 2008 project sampling survey were used.

4 Results and Discussion

4.1 Flow Through the Aquitard

Hydraulic conductivity of the aquitard ranges over several orders of magnitude, marls (10^{-5}–10^{-6}m day^{-1})

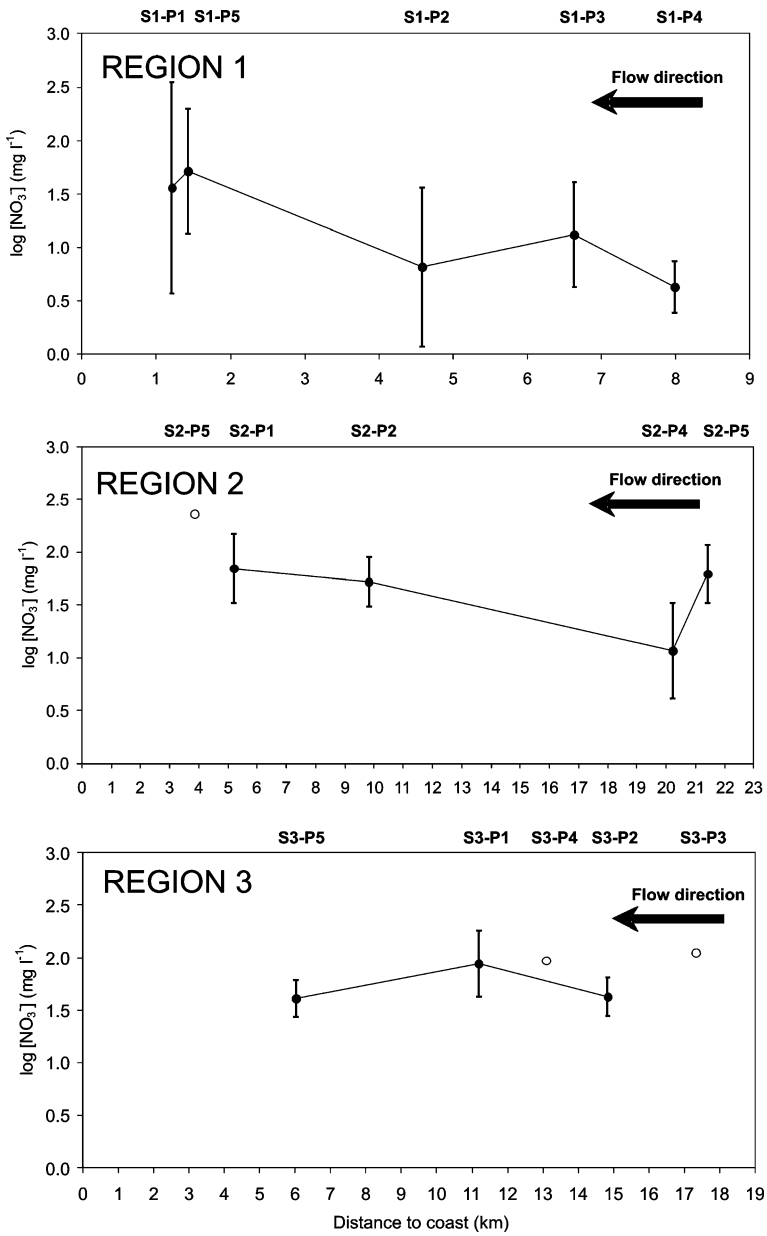

Fig. 7 Average nitrate concentration of Pliocene aquifer for selected sample points (*filled circles*) versus distance to coast for each region. *Vertical bars*: standard deviation. *Empty circles*: only one data available. *Arrows*: groundwater flow direction

and evaporites (10^{-10}m day^{-1}). Considering the highest hydraulic conductivity value of the aquitard, flow rate q ranges between 0 and $1.25{\cdot}10^{-5}$m day^{-1} for year 1999. The q values obtained can be considered representative for the study period, since the Δh has remained constant, as shown in Fig. 3b. Flow through the aquitard was excluded as a major contribution to the pollution process.

4.2 Nitrate as an Indicator

The Quaternary aquifer (upper unconfined) presents the highest nitrate concentration in groundwater with values ranging from 2.9 to 460 mg l^{-1} spatially distributed over the three regions, although lower values are detected in region 3 due to a low crop density. In the Pliocene confined aquifer, values between 0.04 and 317 mg l^{-1} of NO_3^- are observed (Table 2). Average concentration in wells located toward the coast show a generally increasing trend (Fig. 7), except for region 3, where nitrate average concentration is approximately constant, being controlled by the low hydraulic gradient of the Pliocene aquifer in this region. Nitrate presence in the unconfined aquifer clearly originates from the intensive agricultural practices (Table 2); however, in regards to the confined aquifer, much lower concentrations, even nil, should be expected since no agricultural development or anthropogenic activities take place in the recharge area (Northwestern part of the basin, see Fig. 1a, b). Moreover, the thick aquitard separating both aquifers should act as an impervious barrier, contributing to the attenuation of nitrate (Robertson et al. 1996) and related species (NO_2^- and NH_4^+) concentration if cross-formational flow occurs. Dissolved oxygen content in both aquifers ranges between 1 and 9.8 mg l^{-1}; therefore, nitrate attenuation in both aquifers, mediated by denitrification processes, is unlikely.

Figure 8 depicts the temporal evolution of nitrate concentration in both aquifers and regions for the longest data set record of sampling points. As shown in the graph, a generalized yearly increasing trend exists; however, region 2 presents the highest slope with 8.1 and 10.2 mg l^{-1}year^{-1} for the Quaternary (S2-Q4) and the Pliocene (S2-P3) aquifer, respectively.

The high variability in nitrate content observed in the lower confined aquifer (Pliocene) reflects the presence of pumping wells in the vicinity of a sampled point. Groundwater stratification due to water chemical composition (Ronen and Margaritz 1985; Guimerà 1998) may also exist.

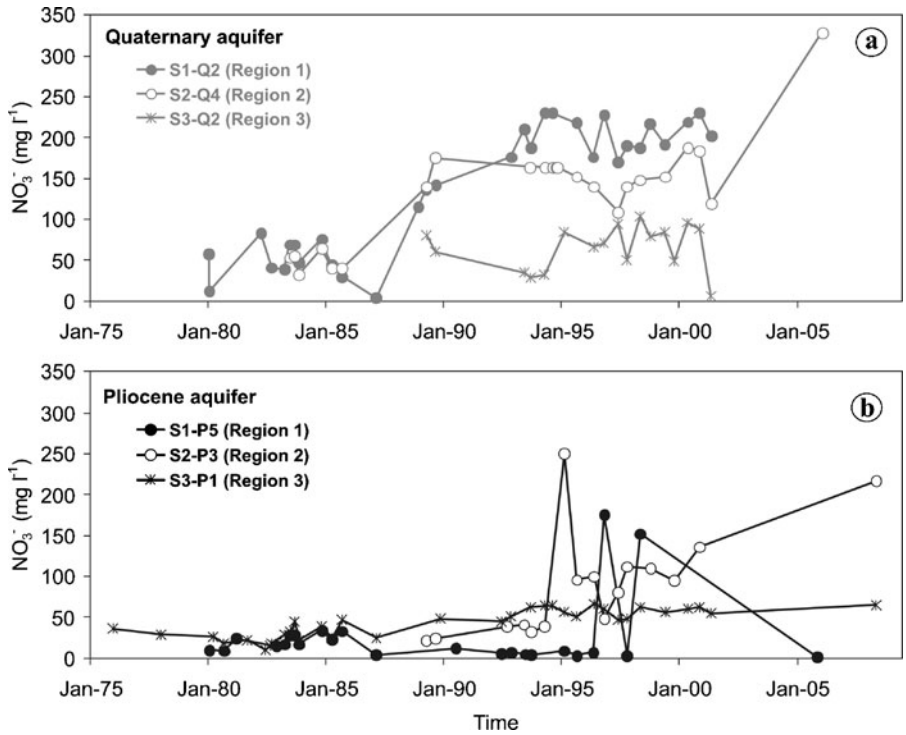

Fig. 8 Evolution of nitrate concentration for the three defined regions in both aquifers over time (only longest data set record are shown), **a** Quaternary and **b** Pliocene (source: Groundwater Quality Monitoring Network of CHS-IGME and 2008 survey)

4.3 Geochemical and Mixing Models

The saturation indices for calcite (I_{cal}), dolomite (I_{dol}), and gypsum (I_{gyp}), expressed in logarithmic form, are reported in Table 3. Based on obtained calculations, groundwater appears to be near saturation with respect to calcite, oversaturated with respect to dolomite, and undersaturated with respect to gypsum. The high positive values estimated for I_{dol} potentially may drive dolomite precipitation; this fact is not supported by experimental observations, since clogging by calcite or dolomite has not been detected either in wells or in aquifers. The occurrence of high Mg concentrations in water and the predicted dolomite saturation index can be explained by the intensive fertilizer dose applied (0.9–1.6 $tha^{-1}year^{-1}$) and

Table 3 Saturation index for dolomite (I_{dol}), calcite (I_{cal}), and gypsum (I_{gyp}) for specific sample points

Region	Aquifer	Sample point	Saturation index (I)											
		Mineral	I_{cal}				I_{dol}				I_{gyp}			
		Survey	1995	2001	2005	2008	1995	2001	2005	2008	1995	2001	2005	2008
Region 1	Quaternary	S1-Q1	0.66	0.29	0.14	0.80	1.55	0.84	0.34	1.75	−0.72	−0.79	−0.86	−0.87
		S1-Q2	0.87	1.29	–	–	2.20	3.17	–	–	−1.23	−1.45	–	–
		S1-Q3	0.77	1.07	–	1.15	1.78	2.28	–	2.48	−0.98	−0.63	–	−0.98
		S1-Q4	0.46	0.86	–	1.01	1.30	2.01	–	2.27	−1.54	−0.93	–	−0.81
		S1-Q5	0.70	–	–	0.78	1.59	–	–	2.15	−0.85	–	–	−1.27
	Pliocene	S1-P1	0.49	–	–	0.59	1.14	–	–	2.06	−1.66	–	–	−2.27
		S1-P2	0.56	–	–	1.05	1.34	–	–	2.16	−1.17	–	–	−1.33
		S1-P3	0.52	–	–	–	1.30	–	–	–	−1.19	–	–	–
		S1-P4	0.38	–	–	1.03	0.86	–	–	2.18	−0.63	–	–	−0.68
		S1-P5	0.67	–	0.10	–	1.54	–	0.49	–	−0.64	–	−0.66	–
Region 2	Quaternary	S2-Q1	0.56	1.01	–	–	1.37	2.17	–	–	−0.54	−0.43	–	–
		S2-Q2	0.31	0.71	–	–	1.08	1.72	–	–	−0.53	−0.85	–	–
		S2-Q3	0.55	0.69	–	0.97	1.50	1.63	–	2.27	−0.43	−0.41	–	−0.47
		S2-Q4	0.42	0.94	0.43	–	1.31	2.21	1.07	–	−0.53	−0.53	−0.39	–
		S2-Q5	–	–	0.72	–	–	–	1.67	–	–	–	−0.35	–
	Pliocene	S2-P1	0.50	0.25	0.18	1.00	1.22	0.68	0.55	2.21	−0.60	−0.39	−0.44	−0.55
		S2-P2	0.35	0.80	0.14	1.06	0.94	1.83	0.52	2.40	−1.10	−0.36	−0.39	−0.41
		S2-P3	0.91	0.83	–	1.09	2.16	1.91	–	2.26	−0.43	−0.36	–	−0.21
		S2-P4	–	–	0.27	–	–	–	0.71	–	–	–	−0.28	–
		S2-P5	–	–	–	–	–	–	–	–	–	–	–	–
Region 3	Quaternary	S3-Q1	0.63	1.14	–	–	1.67	2.29	–	–	−1.38	−0.87	–	–
		S3-Q2	0.37	0.75	–	–	1.04	1.76	–	–	−0.74	−0.86	–	–
		S3-Q3	–	–	0.28	–	–	–	0.67	–	–	–	−0.18	–
		S3-Q4	–	–	0.49	–	–	–	1.33	–	–	–	−1.10	–
		S3-Q5	–	–	−1.59	–	–	–	−2.85	–	–	–	−0.39	–
	Pliocene	S3-P1	0.45	0.68	–	1.08	1.18	1.56	–	2.17	−0.79	−0.78	–	−0.07
		S3-P2	0.76	1.07	0.16	1.06	1.80	2.31	0.62	2.17	−0.80	−0.74	−0.95	−0.75
		S3-P3	0.69	–	–		1.57	–	–	–	−1.06	–	–	–
		S3-P4	–	–	–	1.04	–	–	–	2.28	–	–	–	−0.49
		S3-P5	–	–	–	0.90	–	–	–	2.10	–	–	–	−0.75

Saturation index is presented in log form

mineral composition (e.g., kieserite $MgSO_4 \cdot H_2O$; magnesium nitrate $Mg(NO_3)_2 \cdot 6H_2O$, and other fertilizers enriched with ~4% Mg).

The spatial and temporal variability of the end-member' concentrations, in particular for the unconfined aquifer, constitute key information for the application of mixing models to evaluate the interconnection of aquifers and also to estimate mixing ratios. Moreover, the decision for SO_4^{2-} selection as one of the species for end-member definition and subsequently mixing ratios was due to several reasons: (1) presence of oxic conditions, similar HCO_3^- concentration, and nonexistent H_2S in both aquifers (reaction 4); (2) lack of pyrite in this geologic context (very low concentration of iron in groundwater; reaction 5); and (3) higher NO_3^- concentrations in the unconfined than in the confined aquifer, indicating that reaction 6 (nitrate as electron acceptor) is not possible

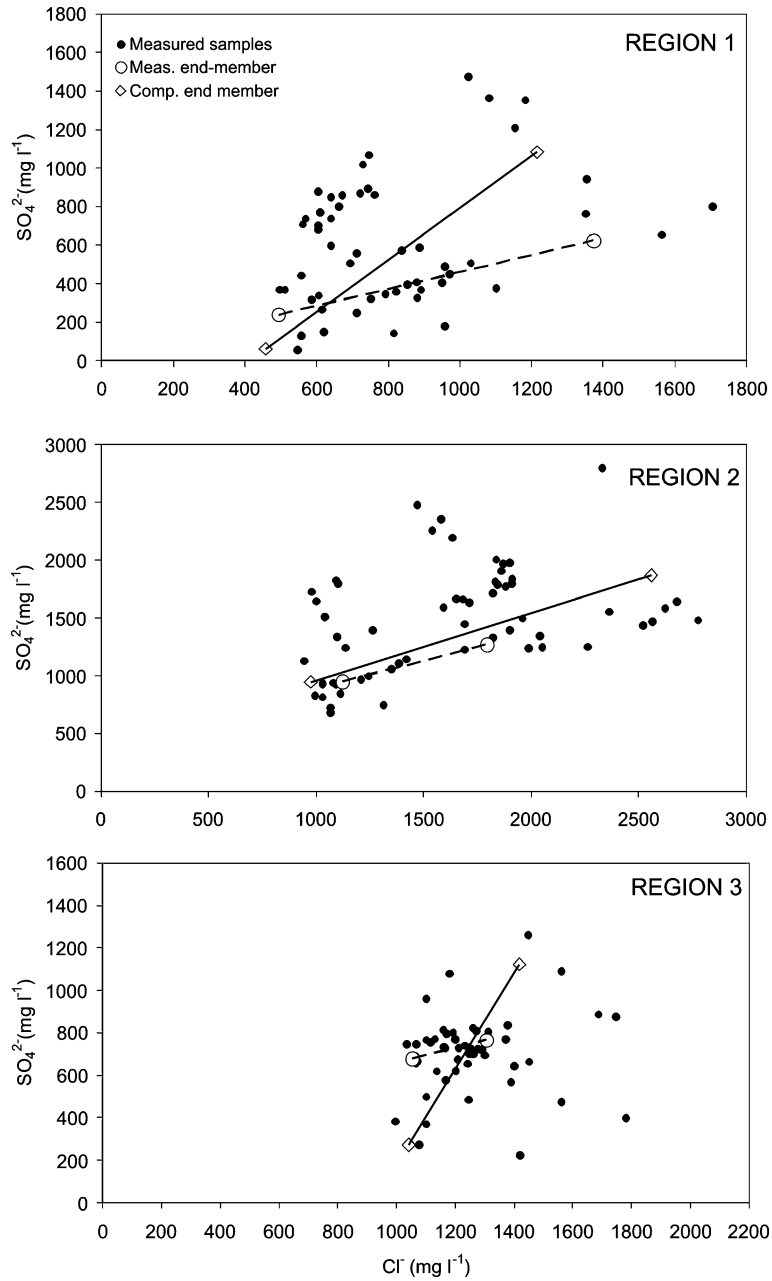

Fig. 9 Measured and computed end-member concentrations and mixing lines (*dashed* and *solid line*, respectively) for each defined region. Measured mixed samples are presented as *filled circles*

in the confined aquifer. Computed end members with the MIX_PROGRAM code (Table 1) as well as the computed mixing lines for each of the regions are shown in Fig. 9. The model runs not only allowed for obtaining more reliable mixing lines than those obtained through measured end members, it also allowed for assessment of the important existing differences between measured and computed end members, mainly for the Quaternary aquifer and for the three defined regions.

In the Pliocene aquifer, computed end members and mixing lines provide new consistent mixing ratios for the measured mixed samples. If the computed water mixing ratio Quaternary/Pliocene aquifers (mass fraction, *MFQIP*) is plotted versus distance to coast and flow direction (Fig. 10), an increasing trend of *MFQIP* average value and its variability toward the coast is observed, although local factors surrounding each sample point can disturb it. This result agrees with

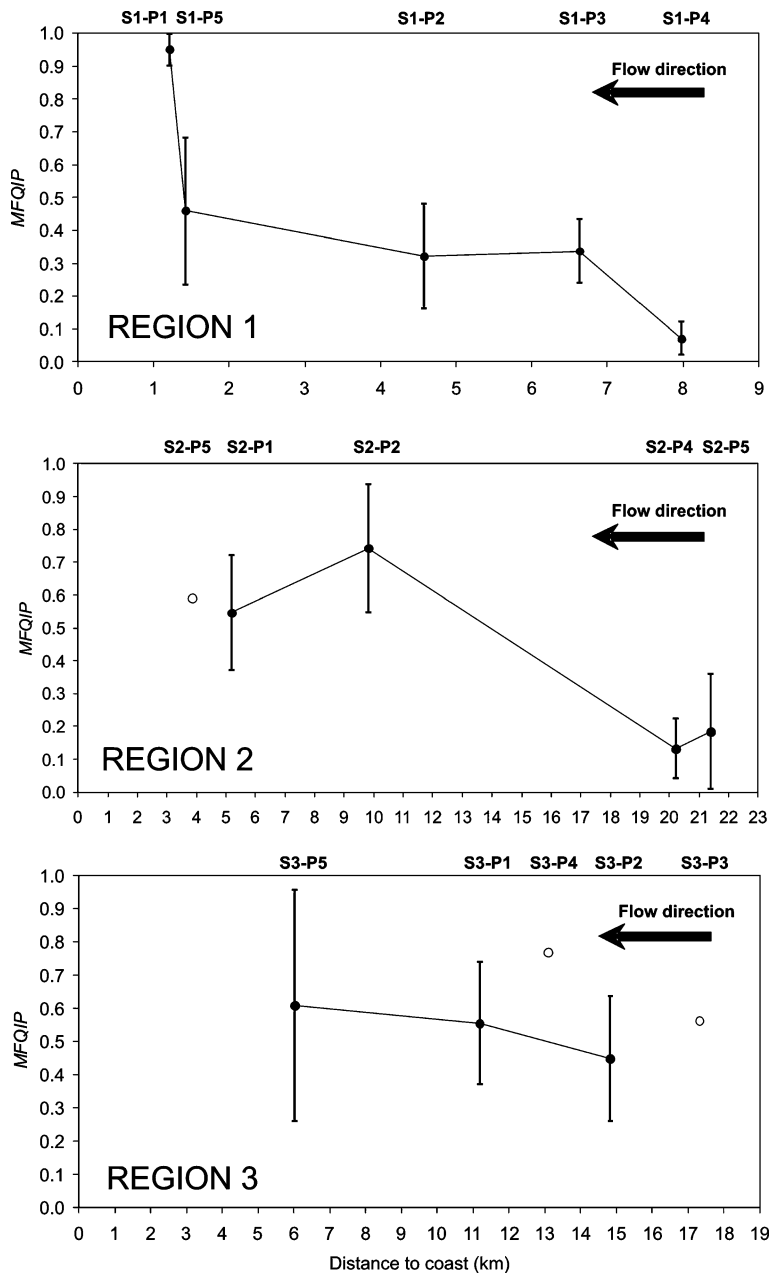

Fig. 10 Quaternary aquifer water mass fraction (computed mixing ratios *MFQIP*) introduced into the Pliocene aquifer versus distance to coast. *Filled circles*: average computed mixing ratios. *Vertical bars*: standard deviation. *Empty circles*: only one data available. *Arrows*: groundwater flow direction

the important number of wells reaching the Pliocene aquifer according to the groundwater flow direction. For region 1, even presenting the greatest density of wells, computed *MFQIP* values are the lowest (between 0.07 and 0.46) due to the short travel distance between recharge (upland) and discharge areas (toward the coast). In region 2, high *MFQIP* values, reaching up to 0.74, are observed due to high concentrations of Cl^- and SO_4^{2-} species in the Quaternary end member along with the longer groundwater travel distance across the Pliocene aquifer. Finally, for region 3, the sample points present similar average values of *MFQIP* (~0.53), although agricultural activity and the density of wells is lower than the other regions, this pattern appears to be controlled by the low hydraulic gradient of the Pliocene aquifer in this region.

Obtained values of the R=rCl/rBr ratio for both aquifers in sample points located in the vicinity of the coast are much lower than the sea water ratio ($R = 655 \pm 4$), indicating the absence of saline intrusion. For the Quaternary aquifer, R values are similar to those obtained for the irrigation water ($R = 213 \pm 62$), indicating their similar origin. Regarding the possible effect of the dilution of the middle aquitard evaporitic rocks (gypsum and halite), R values should be in the range of 1,200–5,400; therefore, this option must be dismissed (Fig. 11).

4.4 Hydrogen and Oxygen Environmental Isotopes

Results from the $\delta^{18}O$ and δ^2H isotopic composition survey presented in Fig. 12 show that groundwater

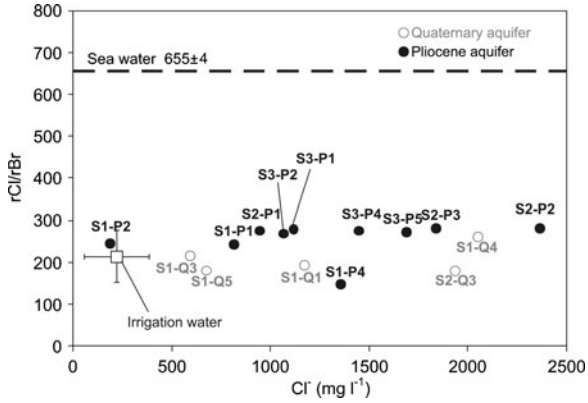

Fig. 11 Chloride concentration versus R=rCl/rBr for some sample points from both aquifers, irrigation water (*bars* represent standard deviations) and seawater

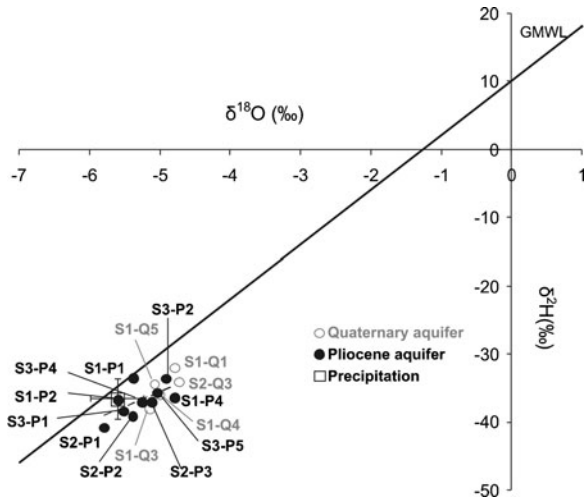

Fig. 12 Plot of $\delta^{18}O$ vs. δ^2H for precipitation (*bars* represent standard deviations) and available sample points of both aquifers. Precipitation data, GNIP/IAEA database (*GMWL* Global Meteoric Water Line; *dashed line* Pliocene meteoric water line)

samples of both aquifers fall below the average local precipitation (source GNIP/IAEA database) and also below the Global Meteoric Water Line, indicating secondary fractionation by evaporation. Imported water from the *Tajo-Segura Aqueduct* and groundwater used for irrigation are currently stored in small open air reservoirs, and due to evaporation processes, water becomes generally enriched in heavy stable isotopes (more positive values of $\delta^{18}O$) in comparison with water from precipitation less affected by evaporation processes (Jiménez-Martínez and Custodio 2008). For the Pliocene aquifer, a progressive enrichment of $\delta^{18}O$ content similar to the observed nitrate and *MFQIP* increase from inland to the coast is clearly observed.

5 Conclusion

A methodological approach to assess aquifer interconnection primarily based on the presence of nitrate in groundwater and numerical mixing calculations has been applied to the Campo de Cartagena area. Results from hydrogen and oxygen environmental isotope analyses in the same area also supported the findings.

The observed nitrate patterns in the Campo de Cartagena surface and deep aquifer provide information to assess the interconnection between the unconfined

contaminated aquifer and the deep confined aquifer. The study shows that the upper unconfined aquifer (Quaternary), which is contaminated by nitrate due to intensive agricultural activities, also constitutes the source of pollution of the lower confined aquifer (Pliocene). The induced leakage allowed the downward flow of contaminated water from the upper aquifer into the unpolluted lower confined aquifer.

Water mixing fractions were estimated using the numerical code MIX_PROGRAM (Carrera et al. 2004), which provides not only more accurate estimates of the end-member concentrations but also of the output mixing ratios. The mixing ratios approach showed that the Quaternary aquifer average mass fraction leaking into the Pliocene aquifer ranges between 0.07 and 0.74 and tends to increase toward the coast according to an increase in well density.

Results proved the validity of the applied methodology to assess aquifer interconnection in areas highly impacted by agricultural activities. Future works are needed for reducing the uncertainties associated to the spatiotemporal variability and quantifying the volume of exchanged water between the unconfined aquifer and the confined aquifer in the study area.

Acknowledgements This work has been developed under the framework of the CGL-2004-05963-C04-01 and CGL2007-66861-C04-03 research projects, financed by Ministry of Science and Innovation (Spain). It also is included within the 08225/PI/08 research project financed by "Programa de Generación del Conocimiento Científico de Excelencia" of Fundación Seneca, Región de Murcia (II PCTRM 2007-10). Gratitude is expressed to the Geological Survey of Spain (IGME) and to K. J. Wallis for her assistance in the revision of the text.

References

Adar, E. M., & Nativ, R. (2000). Use of hydrochemistry and isotopes in a mixing-cell to quantify the relative contribution of multiple-source contaminants to seepage from fractured chalk aquitard. *IAHS Publ, 262*, 315–320.

Altman, S. J., & Parizek, R. R. (1995). Dilution of nonpoint-source nitrate in groundwater. *Journal of Environmental Quality, 24*, 707–718.

Banner, J. L., Wasserburg, G. J., Dobson, P. F., Carpenter, A. B., & Moore, C. H. (1989). Isotopic and trace element constraints on the origin and evolution of saline groundwaters from central Missouri. *Geochimica et Cosmochimica Acta, 53*, 383–398.

Boulton, N. S. (1963). Analysis of data from non-equilibrium pumping tests allowing for delayed yield from storage. In: *Proceedings of Institution of Civil Engineers, 26*(6693), 469–482.

CARM. (2008). *Consejería de Agricultura y Agua de la Región de Murcia*. Agrarian Statistics Data. http://www.carm.es.

Carrera, J., Vazquez-Suñé, E., Catillo, O., & Sánchez-Vila, X. (2004). A methodology to compute mixing ratios with uncertain end-members. *Water Resources Research, 40*, W12101. doi:10.1029/2003WR002263.

Carter, J. T., Gotkowitz, M., Anderson, M. P. (2007). Vertical Hydraulic connection between a perched carbonate aquifer and an underlying regional aquifer. In: *Proceedings of 2007 GSA Denver Annual Meeting*.

Candela, L. (2000). Groundwater pollution from mineral fertilizers and pesticides in Spain. *Hydrogeologie, 3*, 85–91.

Custodio, E., & Herrera, C. (2000). Use of the ratio Cl/Br as a hydrogeochemical tracer in groundwater hydrology (in Spanish). *Boletín Geologico y Minero, 111*(4), 49–68.

Frind, E. O., Muhammad, D. S., & Molson, J. W. (2002). Delineation of three dimensional well capture zones for complex multi-aquifer systems. *Ground Water, 40*(6), 586–598.

Frisch, J. (1987). Pollution des eaux souterranines par les nitrates: l´impact sur l´agriculture moderne Europäische Konferenz. Einflüesse der Landwirtschaft auf die Wassenrressourcen. Folgen und zukünftige Entwincklugen, Berlin, pp. 103–123.

García-Pintado, J., Martínez-Mena, M., Barberá, G. G., Albaladejo, J., & Castillo, V. (2007). Anthropogenic nutrient sources and loads from a Mediterranean catchment into a coastal lagoon: Mar Menor Spain. *Science of the Total Environment, 373*, 220–239.

Guimerà, J. (1998). Anomalously high nitrate concentrations in ground water. *Ground Water, 36*(2), 275–282.

Hantush, M. S. (1960). Modification of the theory of leaky aquifers. *Journal of Geophysical Research, 65*(11), 3713–3725.

Hantush, M. S., & Jacob, C. E. (1955). Non-steady radial flow in an infinite leaky aquifer. *American Geophysical Union Transactions, 6*, 95–100.

IGME. (1994). *Las aguas subterráneas del Campo de Cartagena* (*Murcia*). IGME, 62 pp.

Jiménez-Martínez, J., & Custodio, E. (2008). Deuterium excess in rain and in recharge to aquifers in Circum-Mediterranean area and Spanish Mediterranean coast (in Spanish). *Boletín Geologico y Minero, 119*(1), 21–32.

Jiménez-Martínez, J., García-Aróstegui, J. L., Aragón, R., Candela, L. (2010). A quasi 3D geological model of the Campo de Cartagena, SE Spain: Hydrogeological implications. *Geologica Acta* (in press)

Korom, S. F. (1992). Natural denitrification in the saturated zone: A review. *Water Resources Research, 28*(6), 1657–1668.

Lacombe, S., Sudicky, E. A., Frape, S. K., & Unger, A. J. A. (1995). Influence of a leaky boreholes on cross-formational groundwater flow and contaminant transport. *Water Resources Research, 31*(8), 1871–1882.

Larsen, D., Gentry, R. W., & Solomon, D. K. (2003). The geochemistry and mixing of leakage in a semi-confined aquifer at a municipal well field, Memphis, Tennessee, USA. *Applied Geochemistry, 18*, 1043–1063.

Lu, H. Y., Liu, T. K., Chen, W. F., Peng, T. R., Wang, C. H., Tsai, M. H., et al. (2008). Use of geochemical modeling to

evaluate the hydraulic connection of aquifers: A case study from Chianan Plain, Taiwan. *Hydrogeology Journal, 16*, 139–154.

Massmann, G., Tichomirowa, M., Merz, C., & Pekdeger, A. (2003). Sulfide oxidation and sulfate reduction in a shallow groundwater system (Oderbruch Aquifer, Germany). *Journal of Hydrology, 278*, 231–243.

MIMAN. (2000). *Libro Blanco del Agua en España*. Spanish Ministry for the Environment.

Neuman, S. P., & Witherspoon, P. A. (1969). Theory of flow in a confined two aquifer system. *Water Resources Research, 5*(4), 803–816.

Parkhurst, D. L., & Appelo, C. J. L. (1999). *User's guide to PHREEQC (version 2)-A computer program for speciation, batch reaction, one-dimensional transport, and inverse geochemical calculations*. U. S. Geological Service. Water Resources Investigation Report 99-4259, Denver.

Pitkänen, P., Löffman, J., Koskinen, L., Leino-Forsman, H., & Snellman, M. (1999). Application of mass-balance and flow simulation calculations to interpretation of mixing at Äspö, Sweden. *Applied Geochemistry, 14*, 893–905.

Pulido-Bosch, A., Bensi, S., Molina, L., Vallejos, A., Calaforra, J. M., & Pulido-Leboeuf, P. (2000). Nitrates as indicators of aquifer interconnection. Application to the Campo de Dalias (SE-Spain). *Environmental Geology, 39*(7), 791–799.

Roberston, W. D., & Schiff, S. L. (2008). Persistent elevated nitrate in riparian zone aquifer. *Journal of Environmental Quality, 37*, 669–679.

Robertson, W. D., Russell, B. M., & Cherry, J. A. (1996). Attenuation of nitrate in aquitard sediments of Southern Ontario. *Journal of Hydrology, 180*(1–4), 267–281.

Rodríguez Estrella, T. (2000). Physical, chemical and biological changes induced by waters from the Tage-Segura canal in the hydrogeological unit of the Campo de Carthagena and in Mar Menor laguna (Murcia Province, Spain). *Hydrogéologie, 3*, 23–37.

Ronen, D., & Margaritz, M. (1985). High concentrations of solutes at upper part of the saturated zone (water table) of a deep aquifer under sewage-irrigated land. *Journal of Hydrology, 80*, 311–323.

Salama, R. B. (2005). Interconnectivity between the superficial aquifer and the deep confined aquifers of the Gnangara Mound, Western Australia. *Water, Air, and Soil Pollution, 5*, 27–44.

Starr, R. C., & Gillhma, R. W. (1993). Denitrification and organic carbon availability in two aquifers. *Ground Water, 31*(6), 934–947.

H31A-0757

TI: Tritium tracer test to estimate aquifer recharge under irrigated conditions

AU: Jimenez-Martinez, J
EM: joaquin.jimenez@upc.edu
AF: Department of Geotechnical Engineering and Geosciences, Technical University of Catalonia, Barcelona, Spain
AU: Tamoh, K
EM: karim.tamoh@upc.edu
AF: Department of Geotechnical Engineering and Geosciences, Technical University of Catalonia, Barcelona, Spain
AU: Candela, L
EM: lucila.candela@upc.edu
AF: Department of Geotechnical Engineering and Geosciences, Technical University of Catalonia, Barcelona, Spain

AB: Environmental tracers, as tritium, have been generally used to estimate aquifer recharge under natural conditions. A tritium tracer test to estimate recharge under semi-arid and irrigated conditions is presented. The test was carried out in an experimental plot under drip irrigation, located in SE Spain, with annual row crops (rotation lettuce and melon), following common agricultural practices in open air. Tritiated water was applied as an irrigation pulse, soil cores were taken at different depths and a liquid scintillation analyzer was used to measure the concentration of tritium in soil samples. Transport of tritium was simulated with SOLVEG code, a one-dimensional numerical model for simulating transport of heat, water and tritiated water in liquid and gas phase, which has been modified and adapted for this experience, including ground cover, root growth and root water uptake. One crop has been used to calibrate the modeling approach and other three crops to validate it. Results of flow and transport modelling show a good agreement between observed and estimated tritium concentration profile. For the period October 2007-September 2008, total drainage obtained value was 441 mm.

Jiménez-Martínez, J., Tamoh, K., Candela, L. (2009), Tritium tracer test to estimate aquifer recharge under irrigated conditions, *Eos Trans. AGU, 90*(52), Fall Meet. Suppl., Abstract H31A-0757

COMUNICACIONES A CONGRESOS

MINISTERIO
DE EDUCACIÓN
Y CIENCIA

INSTITUTO
GEOLÓGICO
Y MINERO DE ESPAÑA

Geophysical Research Abstracts,
Vol. 11, EGU2009-11131, 2009
EGU General Assembly 2009

Drainage estimation to aquifer and water use irrigation efficiency in semi-arid zone for a long period of time

J Jiménez-Martínez (1), J Molinero-Huguet (1,2), and L Candela (1)

(1) Department of Geotechnical Engineering and Geosciences, Technical University of Catalonia, UPC, Barcelona, Spain (joaquin.jimenez@upc.edu), (2) Amphos XXI Consulting S.L., Valldoreix, Barcelona, Spain

Water requirements for different crop types according to soil type and climate conditions play not only an important role in agricultural efficiency production, though also for water resources management and control of pollutants in drainage water. The key issue to attain these objectives is the irrigation efficiency. Application of computer codes for irrigation simulation constitutes a fast and inexpensive approach to study optimal agricultural management practices. To simulate daily water balance in the soil, vadose zone and aquifer the VisualBALAN V. 2.0 code was applied to an experimental area under irrigation characterized by its aridity. The test was carried out in three experimental plots for annual row crops (lettuce and melon), perennial vegetables (artichoke), and fruit trees (citrus) under common agricultural practices in open air for October 1999-September 2008. Drip irrigation was applied to crops production due to the scarcity of water resources and the need for water conservation. Water level change was monitored in the top unconfined aquifer for each experimental plot. Results of water balance modelling show a good agreement between observed and estimated water level values. For the study period, mean drainage obtained values were 343 mm, 261 mm and 205 mm for lettuce and melon, artichoke and citrus respectively. Assessment of water use efficiency was based on the IE indicator proposed by the ASCE Task Committee. For the modelled period, water use efficiency was estimated as 73, 71 and 78 % of the applied dose (irrigation + precipitation) for lettuce and melon, artichoke and citrus, respectively.

abstract id: **222**

topic: **6**
General hydrogeological problems

6.3
Groundwater contamination — monitoring, risk assessment and restoration

title: **Contamination of a regional confined aquifer by leaky boreholes. Campo de Cartagena case study (SE Spain)**

author(s): **Joaquín Jiménez-Martínez**
Department of Geotechnical Engineering and Geosciences, UPC, Spain,
joaquin.jimenez@upc.edu

Ramón Aravena
Department of Earth and Environmental Sciences, University of Waterloo, Canada,
roaraven@sciborg.uwaterloo.ca

Lucila Candela
Department of Geotechnical Engineering and Geosciences, UPC, Spain,
lucila.candela@upc.edu

keywords: aquifer interconnection, leaky borehole, nitrate, mixing rate, Campo de Cartagena

ABSTRACT

The present work provides a methodological approach to evaluate the impact of poorly constructed (leaky or without a gravel pack) and abandoned wells for facilitating the transfer of contaminants between aquifers at different depths. The approach was based on the use of nitrate as a tracer and the MIX_PROGRAM code for mixing calculations. Proposed methodology was applied to the Campo de Cartagena (SE Spain), where intensive irrigated agriculture takes place. The hydrogeologic unit consists of a multi-layer system constituted by an upper unconfined aquifer and a deep confined aquifer with a high density of wells exploitation (1.18 wells/km^2). Results show the increase of the unconfined aquifer impact on the confined aquifer along the groundwater flow direction toward the coast, although this general pattern is controlled by local factors (pumping, intensity of agricultural practices, density of wells and groundwater residence time).

INTRODUCTION

Abandoned, leaky and poorly constructed wells (leaky or without a gravel pack) may act as conduits transferring contaminants to underlying aquifers and are common features at many polluted groundwater sites. In a multi-layer aquifer, abandoned or poorly constructed wells penetrate through geological strata otherwise considered impermeable (aquitard) that supposes open conduits for pollutant migration. Aquifer interconnection may also occur via flow through aquitards in areas of reduced aquitard thickness which could be enhanced by water pumping in the underlying confined aquifer.

The present study was carried out in the Campo de Cartagena (SE Spain) (Fig. 1a), where the land is intensively irrigated for agriculture and groundwater pollution exists. The agricultural activities are practised over the unconfined aquifer, with an intensive mineral fertiliser application (0.9-1.6 t ha^{-1} yr^{-1}) which constitutes a source of contamination and is separated from the lower confined aquifer by a thick aquitard (Fig. 1b). The objective of the research is to evaluate the significance that abandoned and poorly constructed wells have on cross-formational groundwater flow and contaminant transport between the shallow unconfined and deep confined aquifers. The work provides a methodological approach based on the geochemical tools application and water mixing calculations from a numerical model. The state of saturation of groundwater samples for relevant minerals, and ionic speciation were calculated using the PHREEQC code (Parkhurst, Appelo, 1999). Water mixing calculations were carried out using the MIX_PROGRAM numerical code (Carrera et al., 2004), which provides theoretical estimates of the end-member concentrations, thereby reducing the uncertainty due to spatio-temporal variability and thus improving the reliability of the output mixing calculations.

METHODOLOGY

The regional groundwater flow direction for both aquifers is toward the coastal, from northwest to southeast. The aquitard between the two aquifers is composed of marls in regions 2 and 3, and mainly of evaporites in region 1 (Fig. 1b). Groundwater records for the 1974–2008 monitoring surveys were provided by the Quality Network of Water Authority (CHS-IGME). The chemical data set includes physico-chemical parameters (pH, temperature and electrical conductivity); major ion content (Na^+, K^+, Ca^{2+}, Mg^{2+}, Cl^-, HCO_3^-, SO_4^{2-}, and NO_3^-); and CO_3^{2-}, NO_2^-, NH_4^+, and SiO_2. Some specific surveys in situ analysed dissolved oxygen (DO) and heavy metals.

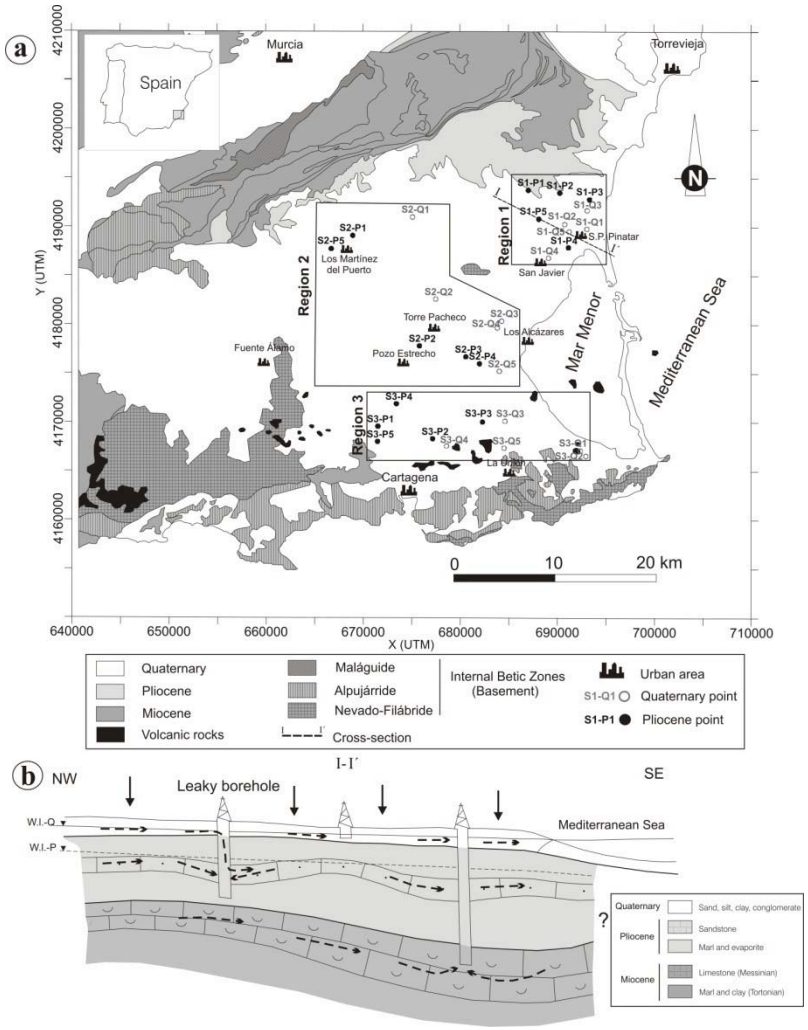

Figure 1. a) Study area and geological sketch. Location of the defined regions and sample points (S1 to S3 region; P: Pliocene aquifer; Q: Quaternary aquifer; 1 to n sample point). b) Geological cross section and conceptual model.

Due to the broad extension of the study area, three regions were defined based on land use and regional geology (Fig. 1a). A subset of five water sample points within the surveyed period for each aquifer and defined region was selected. Selection was based on the geographic location, aquifer sampled and length of available records.

Nitrate as an indicator of interconnected aquifers

In regional groundwater flow systems, which are shaped by the geology, the attenuation processes regulate nitrate transport and control its distribution in aquifers. Nitrate attenuation may occur by dilution, through mixing of groundwater in the aquifer (Altman, Parizek, 1995), or by denitrification. In reducing environments it is the only geochemical process that permanent-

ly removes nitrate from aquifers. Nitrate reduction can be mediated by oxidation of organic matter, pyrite and iron under anaerobic conditions (Korom, 1992).

For the three defined regions, nitrate constitutes a good indicator for assessing the Quaternary and Pliocene interconnection. Homogeneity in the spatial distribution of land covered by crops (source of nitrate), along with the long term records of nitrate concentration and dissolved oxygen values (oxidation-reduction potential), support this assumption.

Geochemical and mixing models

To calculate ionic speciation and state of saturation (saturation-index) for relevant minerals, PHREEQC was applied. This preliminary step is necessary to evaluate the potential geochemical reactions occurring in the aquifer, since deviations from mixing lines could be attributed to chemical reactions.

Concentrations of mixed samples, mainly affected by analytical errors, are likely to be more accurate than end-members, commonly with high spatial and temporal variability. This fact can be used to impose constraints on valid end-member concentration since taking mixing constraints into account may significantly reduce uncertainty in end-member concentration by imposing consistency. Consistency is dealt with in two ways: first, end-members should fall on the mixing line and second, mixed waters should fall within the interval defined by end-members. The MIX_PROGRAM code permits the mixing ratios in mixed samples to be derived, allows for redefinition of mixing lines.

The Cl/Br ratio (R), used as an indicator of seawater intrusion (R = 655±4) or evaporite dissolution (R = 1200–5400), was calculated in all available water samples in order to assess the importance of a third member for mixing calculations (Custodio, Herrera, 2000).

RESULTS AND DISCUSSION

Hydraulic conductivity of the aquitard ranges over several orders of magnitude, marls (10^{-5}–10^{-6} m d^{-1}) and evaporites (10^{-10} m d^{-1}). Considering the highest hydraulic conductivity value and vertical head difference through the aquitard, flow rate q ranges between 0–10^{-5} m d^{-1}. Flow through the aquitard was excluded as a major contribution to the pollution process.

Nitrate as an indicator

Average concentration in wells located toward the coast show a generally increasing trend (Fig. 2a), except for region 3, where nitrate average concentration is approximately constant, being controlled by the low hydraulic gradient of the Pliocene aquifer in this region. Nitrate presence in the unconfined aquifer clearly originates from the intensive agricultural practices; however, with regard to the confined aquifer much lower concentrations, even nil, should be expected since no agricultural development or anthropogenic activities take place in the recharge area (NW part of the basin, Fig. 1a and b). Moreover, the thick aquitard separating both aquifers should act as an impervious barrier, contributing to the attenuation of nitrate (Roberston et al., 1996) and related species (NO_2^- and NH_4^+) concentration if cross-formational flow occurs. DO content in both aquifers ranges between 1 and 9.8 mg l^{-1}; therefore, nitrate attenuation in both aquifers mediated by denitrification processes is unlikely.

The high variability of nitrate content observed in the lower confined aquifer (Pliocene) reflects the presence of pumping wells in the vicinity of a sampled point. Groundwater stratification due to water chemical composition (Guimerà, 1998) may also exist.

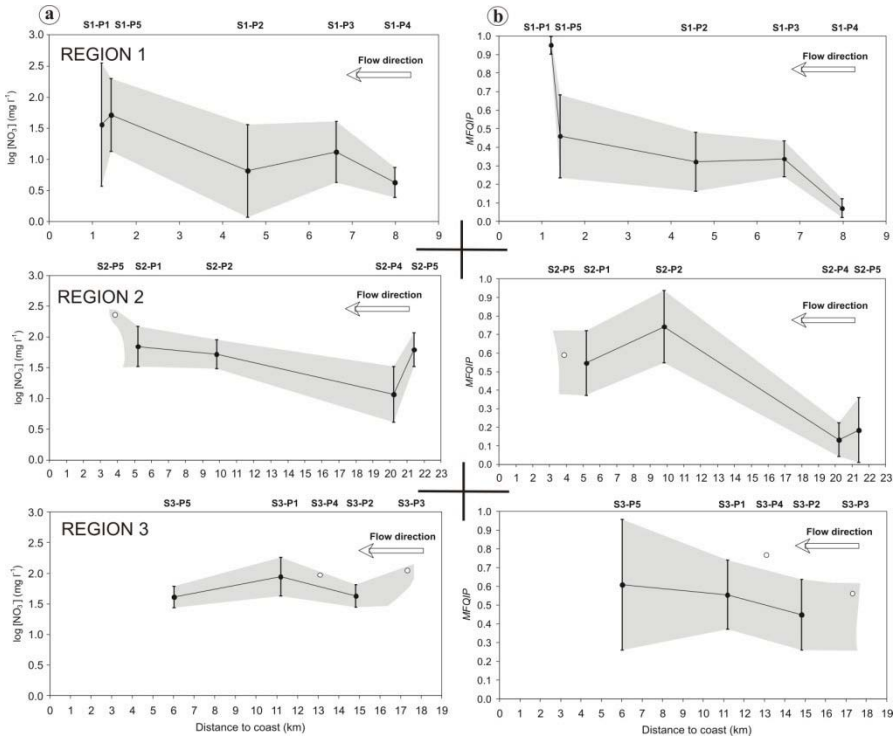

Figure 2. a) Average nitrate concentration of Pliocene aquifer for selected sample points versus distance to coast for each region. b) Quaternary aquifer water mass fraction (computed mixing ratios-MFQIP) introduced into the Pliocene aquifer versus distance to coast. Solid dots: average computed mixing ratios. Vertical bars: standard deviation. Empty circles: only one data available. Arrows: groundwater flow direction.

MIXING MODELS

The two end-members are the Quaternary (from 1980 to the present time) and Pliocene (natural background concentration 1970's, data set non-affected by agricultural pollution) aquifer water samples, and the two chemical species selected were chloride (Cl^-) and sulphate (SO_4^{2-}) (Table 1). Cl^- is a conservative compound but SO_4^{2-} can be affected by several processes. Sulphate reduction, pyrite oxidation and nitrate, instead of oxygen as the electron acceptor, control the SO_4^{2-} concentration in groundwater (Massmann et al., 2003). The decision for SO_4^{2-} selection was due to several reasons: (i) presence of oxic conditions, similar HCO_3^- concentration and non-existent H_2S in both aquifers; (ii) lack of pyrite in this geologic context (very low concentration of iron in groundwater); and (iii) higher NO_3^- concentrations in the unconfined aquifer than in the confined aquifer, indicating that NO_3^- as electron acceptor is not possible in the confined aquifer. Obtained values of the R = rCl/rBr ratio for both aquifers indicating the absence of saline intrusion and dilution of the middle aquitard evaporitic rocks (gypsum and halite). End-member data computed using the MIX_PROGRAM code for each of the regions are shown in

Tab. 1. The model runs not only allowed for obtaining more reliable mixing lines than those obtained through measured end- members, it also allowed for assessment of important existing differences between measured and computed end-members, mainly for the Quaternary aquifer and for the three regions.

Table 1. Measured end-member concentrations for the three defined regions (*m*: mean; *σ*: standard deviation). Computed end-member (e-m) concentrations from the MIX_PROGRAM (Carrera et al., 2004) are also shown.

Aquifer	Species	Region 1				Region 2				Region 3			
		Number samples (period)	*m* (mg l^{-1})	*σ* (mg l^{-1})	Computed e-m	Number samples (period)	*m* (mg l^{-1})	*σ* (mg l^{-1})	Computed e-m	Number samples (period)	*m* (mg l^{-1})	*σ* (mg l^{-1})	Computed e-m
Quaternary	Cl^-	129 (1980-2008)	1372.4	374.8	1214.7	91 (1980-2008)	1794.2	651.3	2559.2	37 (1980-2008)	1305.3	395.5	1418.4
	SO_4^{-2}		624.9	201.7	1082.2		1270.4	437.1	1871.3		766.2	430.4	1122.6
Pliocene	Cl^-	3 (1970´s)	493.7	17.6	457.4	4 (1970´s)	1121.3	141.9	974.9	3 (70´s)	1053.0	20.8	1041.1
	SO_4^{-2}		238.7	143.6	62.4		949.8	225.5	946.3		679.0	84.9	273.1

If the computed water mixing ratio Quaternary/Pliocene aquifers (mass fraction-*MFQIP*) is plotted versus distance to coast and flow direction (Fig. 2b), an increasing trend of the *MFQIP* average value and its variability toward the coast is observed, although local factors surrounding each sample point can disturb it. This result agrees with the important number of wells reaching the Pliocene aquifer according to the groundwater flow direction. For region 1, which presents the greatest density of wells, computed *MFQIP* values are the lowest (between 0.07 and 0.46) due to the short travel distance between recharge (upland) and discharge area (toward the coast). In region 2, high *MFQIP* values reaching 0.74 are observed due to high concentrations of Cl^- and SO_4^{2-} species in the Quaternary end-member along with the longer groundwater travel distance across the Pliocene aquifer. Finally, for region 3, sample points present similar average values of *MFQIP* (~0.53), although agricultural activity and the density of wells is lower than the other regions; this pattern appears to be controlled by the low hydraulic gradient of the Pliocene aquifer in this region.

CONCLUSIONS

Results proved the validity of the applied methodology to assess aquifer interconnection, primarily based on the presence of nitrate in groundwater and numerical mixing calculations, in areas highly impacted by agricultural activities as the Campo de Cartagena area.

The study shows that the upper unconfined aquifer (Quaternary), which is polluted by nitrate due to intensive agricultural activities, also constitutes the source of pollution of the lower confined aquifer (Pliocene). Contamination was caused by leaky wells in areas with high density of production wells and the induced leakage allowed for the downward flow of contaminated water from the upper aquifer into the unpolluted lower confined aquifer.

Water mixing fractions were estimated using the numerical code, which provides more accurate estimates of not only the end-member concentrations but also of the output mixing ratios. The mixing ratios approach showed that the Quaternary aquifer average mass fraction leaking into

the Pliocene aquifer ranges between 0.07 and 0.74 and tends to increase toward the coast following the increase of well density.

ACKNOWLEDGEMENTS

CGL-2004-05963-C04-01 and CGL-2007-66861-C04-03 research projects, Ministry of Science and Innovation (Spain). 08225/PI/08 research project, "Programa de Generación del Conocimiento Científico de Excelencia" of Fundación Seneca, Región de Murcia (II PCTRM 2007-10).

REFERENCES

Altman S.J., Parizek R.R., 1995: *Dilution of nonpoint-source nitrate in groundwater.* J. Environmental Qual., 24, pp. 707–718.

Carrera J., et al., 2004: *A methodology to compute mixing ratios with uncertain end-members.* Water Resour. Res., 40:W12101. doi:10.1029/2003WR002263.

Custodio E., Herrera C., 2000: *Use of the ratio Cl/Br as a hydrogeochemical tracer in groundwater hydrology (in Spanish).* Boletín Geológico y Minero, 111(4), pp. 49–68.

Guimerà J., 1998: *Anomalously High Nitrate Concentrations in Ground Water.* Ground Water, 36(2), pp. 275–282.

Korom S.F., 1992: *Natural Denitrification in the Saturated Zone: A Review, Water Resour.* Res., 28(6), pp. 1657–1668.

Massmann G., et al., 2003: *Sulfide oxidation and sulfate reduction in a shallow groundwater system (Oderbruch Aquifer, Germany).* J. Hydrol., 278, pp. 231–243.

Parkhurst D.L., Appelo C.J.L., 1999: *User's guide to PHREEQC (version 2) — A computer program for speciation, batch reaction, one-dimensional transport, and inverse geochemical calculations.* U.S. Geological Service. Water Resources Investigation Report 99–4259, Denver.

Robertson W.D., et al., 1996: *Attenuation of Nitrate in Aquitard Sediments of Southern Ontario.* J. Hydrol., 180 (1-4), pp. 267–281.

MULTIPHASE TRANSPORT OF TRITIUM IN UNSATURATED POROUS MEDIA. BARE AND VEGETATED SOILS

J. Jiménez-Martínez, K. Tamoh and L. Candela

Department of Geotechnical Engineering and Geosciences, Technical University of Catalonia, UPC, Barcelona, Spain. joaquin.jimenez@upc.edu

Abstract. *Tritium, a low radioactive isotope, released to the atmosphere and hydrosphere by nuclear activities (nuclear power stations, radioactive waste disposal), can be placed in soil surface like tritiated rain or present in contaminated groundwater. Under both circumstances it can be re-emitted to the atmosphere throughout the vadose zone. Beyond, tritium is of particular value in hydrology studies as a tracer for soil moisture and groundwater movement. In the ground surface tritium concentration varies sharply and is very sensitive to many interrelated factors like rainfall amount, evapotranspiration rate, root depth and water table position rendering modeling a rather complex task. One modeling approach is based on SOLVEG, a one-dimensional numerical model to simulate gaseous and liquid-phase tritium transport through soils. Processes include tritium diffusion in both, gas and liquid phase, advection and dispersion of liquid tritium in non-tritiated water, radioactive decay and equilibrium partitioning between gas and liquid phase. This work describes the modeling approach and results of a tritiated rain ($7.3 \cdot 10^{8}$ Bq m^{-3}) on an unconfined aquifer (non-contaminated) with cultivated soil. In the soil decontamination process, simulations show that main roles are played by the vegetation and re-emission, this last due to tritium concentration gradient between soil and atmosphere air humidity. Re-emission is generally produced during night-time, since during day-time it is coupled to the evaporation process. After a period of fifteen months tritium background concentration in soil is attained. The code has been updated and adapted in order to include ground cover, root growth and root water uptake, which allows its further application in bare or vegetated (perennial vegetation or cultivated area) soil surface and shallow or deep water table level (contaminated or non-contaminated aquifer).*

1. INTRODUCTION

Tritium (^{3}H, half-life 12.33 yr), being chemically identical to hydrogen and thus interacting directly with water and organic substances, differs considerably in its behavior from other radionuclides in the environment (Raskob, 1995). Tritiated water (HTO_l) has a volatile character, gas phase (HTO_g). Tritiated water can easily diffuse in ordinary water and move with it, either in liquid phase or in vapor phase (Figure 1). In a soil cover with vegetation, an important sink of the HTO_l stored in the soil is the root water uptake and subsequent loss of HTO_l by vapor exchange with the atmosphere through stomata (Kline and Stewart, 1974).

Tritium, a near ideal tracer, integrates all of the processes that jointly affect water flow in the vadose zone. Thus, tracer behavior represents a very robust indicator of water movement in soil and has been used in obtaining quantitative estimates of water fluxes. In (semi-)arid regions, it has been suggested that solute diffusion in aqueous phase and in aqueous plus gas phase for a volatile solute (e.g. tritium) may be the principal mode of solute transport in the unsaturated zone (Barnes et al., 1994; Joshi et al., 1997; Scanlon, 1992).

Modeling the alternate upward and downward transport of tritium close to the ground surface generally requires rather complex models and detailed input because tritium concentration varies sharply and is very sensitive to many interrelated factors including rainfall amount, evapotranspiration rate or root depth. Many numerical models exist to predict tritium migration throughout the unsaturated zone. Such models, which have been generally developed by atomic energy agencies, can be used to predict the

effect of tritiated rain or the reemission of tritium from polluted groundwater to the atmosphere throughout the vadose zone (Täschner, et al., 1995; Garcia et al., 2009).

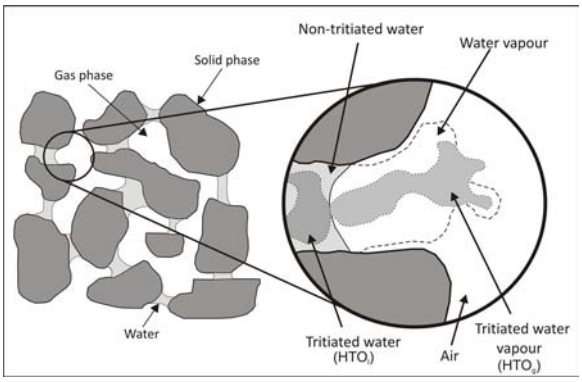

Figure 1. Tritiated and non-tritiated water conceptual behaviour in liquid and gas phase within an unsaturated porous media.

A numerical modeling approach to simulate multiphase transport of tritium in unsaturated porous media is described. For validation, a field test on a vegetated soil surface has been carried out. The modeling approach utilized was SOLVEG (Yamazawa and Nagai, 1997; Yamazawa, 2001), a one-dimensional numerical model for simulating transport of heat, water and tritiated water in liquid and gas phase through a bare soil. The code has been modified and adapted for vegetated soils; which includes presence of ground cover, root growth and root water uptake. The main objectives of this work are: in first place, to establish a water balance as result of an accurate tritium mass balance from a relatively sampling low density; secondly, to evaluate the main processes that affect both, liquid and gas phase, as well as the soil decontamination velocity.

2. MODELING APPROACH DESCRIPTION

The modeling approach is based on SOLVEG (Yamazawa and Nagai, 1997; Yamazawa, 2001), a one-dimensional numerical finite-difference model for simulating transport through unsaturated bare soil of heat, water in liquid and gas phase, tritiated water in liquid (HTO_l) and gas (HTO_g) phase and also their soil-atmosphere exchange. Radioactive decay is considered as well. In SOLVEG advection and diffusion terms are resolved with an explicit and semi-implicit scheme, respectively. To adapt the code to the experimental conditions, it was modified in order to include ground cover, root growth and root water uptake processes, and the boundary conditions were also modified. Hourly data values to solve the above mentioned items are used.

Although isotopically different, the HTO_l and H_2O molecules present similar behavior, e.g. no exiting fractionation processes are produced as a result of evaporation and transpiration, however, differences exist between re-emission and evaporation processes. Re-emission is a mechanism that generally acts during night-time and is depending on the HTO_l content in the uppermost soil layer and the concentration of HTO_g in the air adjacent to the soil surface. During day-time, the re-emission is coupled to the evaporation process (Täschner et al., 1997).

2.1 Water flow and vapor

The model simulates water content θ and the specific humidity of soil air W_a along soil profile. The equation for the liquid water movement is of classical Richards' type with additional terms concerning transpiration E_t (via root water uptake) and evaporation-condensation E_e, sinks/sources of water:

$$\frac{\partial \theta}{\partial t} = -\frac{1}{\rho_w}\left[\frac{\partial q}{\partial z} + (E_e + E_t)\right] \tag{1}$$

being ρ_w water density.

The vertical flow of water is expressed as:

$$q = -\rho_w\left[D(\theta)\frac{\partial \theta}{\partial z} + K(\theta)\right] \tag{2}$$

where hydraulic conductivity $K(\theta)$ and water retention $h(\theta)$ curves were estimated using the power law equations of Campbell (1974):

$$K(\theta) = K_s\left(\frac{\theta}{\theta_s}\right)^{2b+3} \tag{3}$$

$$h(\theta) = h_s\left(\frac{\theta}{\theta_s}\right)^{-b} \tag{4}$$

being b the so-called pore size distribution index and $2b+3$ pore disconnectedness index. h_s and K_s are saturated pressure head and saturated hydraulic conductivity, respectively. Whilst soil water diffusivity $D(\theta)$ is expressed by:

$$D(\theta) = K(\theta)\frac{\partial h}{\partial \theta} \tag{5}$$

The equation for water vapor contains a diffusion term and an evaporation-condensation term:

$$\frac{\partial(\theta_s - \theta)W_a}{\partial t} = \frac{\partial}{\partial z}\left[D_{wa}\tau_a(\theta)\frac{\partial W_a}{\partial z}\right] + \frac{E_e}{\rho_a} \tag{6}$$

The model does not consider advection of soil air, which might be caused by air pressure variations at the ground surface or the infiltration of water. D_{wa} is the water vapor diffusion coefficient in air. $\tau_a(\theta)$ is the tortuosity for soil air at θ. Analogous to Jackson et al., (1974), the model uses $\tau_a(\theta) = (\theta_s - \theta)/1.5$.

The evaporation-condensation of water in soil is expressed as:

$$E_e = \frac{\rho_a}{r_e(\theta)}\left[W_{sat}(T_s) - W_a\right] \qquad \text{when} \qquad W_{sat}(T_s) > W_a \tag{7}$$

The evaporation-condensation is based on the concept that soil evaporation-condensation driving force is the difference of specific humidity between the evaporation site (surface of soil water, W_{sat}) and the pore air W_a. Moreover, evaporation is regulated by the density of moist air ρ_a, as function of temperature, and the evaporation resistance r_e, this last one experimentally determined for the some soil types as function of θ (Kondo and Saigusa, 1994; Kondo and Xu, 1997). It is assumed that water condensation occurs in a

very short time to keep the specific humidity of soil air lower than or equal to the saturation specific humidity at the soil temperature (T_s).

The upper boundary condition of Eq. (1) is determined by the continuity of liquid water flux at the ground surface. When soil water exceeds the saturated soil water content (θ_{s0}), the model assumes that excess water is stored at the ground surface, therefore runoff is equal to zero. The lower boundary condition corresponds to free drainage or constant head for deep or shallow water table, respectively.

The boundary condition for the specific humidity (W_a) Eq. (6) can be determined by the following equation:

$$E_0 = -\rho_a D_{wa} \tau_a(\theta) \left. \frac{\partial W_a}{\partial z} \right|_{z=0} + E_{e0} \tag{8}$$

where

$$E_{e0} = \int_{-\delta z_0}^{0} E_e dz \tag{9}$$

and

$$E_0 = \rho_a c_E \left| u_r \right| (W_{a0} - W_r) f(t) \tag{10}$$

This boundary condition assumes that water vapor flux from the ground surface to the atmosphere is composed by the sum of diffused water vapor flux from inside of the uppermost soil layer and direct evaporation from surface (δ_{z0}-thick) in contact with the atmosphere. c_E is the bulk transfer coefficient, a thermodynamic coefficient dependent among others meteorological variables of the wind velocity u_r (Matsushima and Kondo, 1995) which permits to estimate the evaporation efficiency from a bare soil. To represent the ground cover in the model, a sigmoid curve $f(t)$ has been used. For perennial vegetation, a constant value between 1 and 0, which represents the surface fraction exposed, is considered. In cultivated areas, natural crop growth typically follows an S-shaped pattern (e.g. Overman and Scholtz, 2002). When a crop is first planted, ground cover is non-existent, potential evaporation is maximal, and thus $f(t) = 1$. Conversely, when the crop reaches the mid-season growth stage, ground cover is complete, evaporation is effectively zero, and thereafter $f(t) = 0$. All that remains is specifying the transition from $f(t) = 1$ at planting to $f(t) = 0$ at the beginning of the mid-season growth stage.

2.2 Tritiated water (HTO_l) flow and vapor (HTO_g)

The equations for transport of tritium, in liquid (HTO_l) and gas (HTO_g) phase are:

$$\frac{\partial \theta C_w}{\partial t} = -\frac{1}{\rho_w} \frac{\partial q C_w}{\partial z} + \frac{\partial}{\partial z} \left[D_T \frac{\partial C_w}{\partial z} \right] - (e_e + e_t) \tag{11}$$

$$\frac{\partial (\theta_s - \theta) C_a}{\partial t} = \frac{\partial}{\partial z} \left[D_{Ta} \tau_a(\theta) \frac{\partial C_a}{\partial z} \right] + e_e \tag{12}$$

where C_w and C_a are HTO_l and HTO_g concentration, respectively. Both equations are linked by the evaporation-condensation term inside the soil, e_e:

$$e_e = \frac{\rho_a}{r_e(\theta)} \left[\frac{W_{sat}(T_s) C_w}{\rho_w} - \frac{C_a}{\rho_a} \right] \tag{13}$$

As for the non-tritiated water, this term is controlled by the evaporation resistance r_e. The mass of tritium extracted by root water uptake corresponds to the product between root water uptake and HTO_l concentration at each depth.

The gas phase equation (Eq.12) only includes a diffusion term, being D_{Ta} the molecular HTO_g diffusion coefficient in air. In the case of the liquid phase (Eq. 11), it includes the advection and hydrodynamic dispersion (effective diffusion-dispersion, D_T) term, the latter including molecular diffusion and mechanical dispersion, which is a function of the velocity of water flow in soil:

$$D_T = \tau_w(\theta) D_{Tw} + \frac{\lambda q}{\rho_w} \tag{14}$$

The surface boundary condition for the liquid phase (HTO_l) equation (Eq. 11) is specified by an additional term only for the top layer (ground surface) expressing a gain of HTO_l due to precipitation plus irrigation. Mass dilution due to precipitation plus irrigation is indirectly accounted by the increase of θ on the left hand side of the Eq. 11. The HTO_l evaporation from ground surface to the atmosphere is expressed in a similar manner as that of non-tritiated water, but independently:

$$e_0 = -D_{Ta}\tau_a(\theta)\left.\frac{\partial C_a}{\partial z}\right|_{z=0} + e_{e0} \tag{15}$$

where

$$e_{e0} = \int_{-\delta z_0}^{0} e_e dz \tag{16}$$

and

$$e_0 = c_E \left|u_r\right| (C_{a0} - C_r) f(t) \tag{17}$$

2.3 Heat conduction and thermal characteristics

The heat conductivity of soil is obtained according to McCumber and Pielke (1981) formulation, which states that the relationship between soil thermal conductivity $\lambda_t(\theta)$ and soil water potential h is nearly independent from soil type. This relation comes from fitting the Al Nakshabandi and Kohnke's (1965) data. Soil temperature, T_s, is expressed as heat conduction equation, which includes three terms: conduction, latent heat exchange (sink/source of heat) for soil water evaporation-condensation, and advection (convection) heat transport due to liquid water movement. The heat conduction through plant root is assumed to be negligible. The upper boundary condition for soil temperature is a ground surface heat budget equation. Constant soil temperature is assumed as lower boundary condition.

2.4 Root water uptake and root growth

Root water uptake due to transpiration is considered as a water and HTO_l sink term. A reference evapotranspiration ET_0, at hourly time steps and obtained through Penman-Monteith method, was used to estimate transpiration. The potential evaportranspiration ET_p was calculated using crop specific coefficient (K_c), which characterizes plant water uptake and evaporation relative to the reference vegetation (Allen et al., 1998). K_c can be considered constant to perennial vegetation, whereas in cultivated areas it changes in terms of growth stages. Once obtained potential transpiration (T_p) (e.g.

Kroes and Van Dam, 2003; Pachepsky et al., 2004; Jiménez-Martínez et al., 2009), defined as water removed from soil due to plant water uptake, it is equally distributed over the root zone. This sink term was computed by a method introduced by Campbell and Norman (1998) based on soil water status. Actual transpiration, E_t, is calculated according to Feddes et al. (1978):

$$E_t(\theta) = \alpha(\theta)\frac{T_p}{z_{root}} \tag{18}$$

being $\alpha(\theta)$ the dimensionless water stress response function ($0 \le \alpha \le 1$) describing water uptake reduction due to drought stress. For $\alpha(\theta)$, a modified functional form introduced by Feddes et al. (1978) was applied:

$$\alpha(\theta) = \begin{cases} 1, & \theta_3 \le \theta < \theta_s \\ \dfrac{h(\theta) - h_4}{h_3 - h_4}, & \theta_4 \le \theta < \theta_3 \\ 0, & \theta \le \theta_4 \text{ or } \theta = \theta_s \end{cases} \tag{19}$$

where h_3 and h_4 are threshold parameters such that uptake is at the potential rate when the water content is between θ_3 and θ_s, it drops off when $\theta < \theta_3$, and becomes zero for $\theta < \theta_4$ or $\theta = \theta_s$.

To simulate the change in rooting depth with time for crops, a growth model is required. The model assumes the classical Verhulst-Pearl logistic growth function, achieving a maximum depth at the end of the crop development stage.

3. FIELD TEST FOR MODEL VALIDATION

3.1 Experimental setup

In order to validate the above presented modeling approach, a test was conducted at the Tomas Ferro Agricultural Science Center, a research facility operated by the Technical University of Cartagena, located in the Campo de Cartagena (SE Spain). It took place from 17 May 2007 to 21 August 2008, comprising day of year (DOY) 137-599 (DOY 1 = 1st January 2007).

An experimental plot measuring 7×2 m was established for crop cultivation. The soil is a *silty loam* soil (USDA classification system), and the groundwater level in the field site was at a depth of 14 m below the surface. The plot was managed according to agricultural practices and soil tillage that are common in the region, including crop rotation system and drip irrigation. The plot sides were also cultivated with the same crops and agricultural management conditions were undertaken to avoid boundary effects. An important aspect of the agricultural practices in this area is the application of a plastic cover during summer crop to reduce the direct evaporation from ground surface.

3.2 Tracer input and monitoring system

On 19 June 2007 (DOY 170), a solution of tritiated water (12 L), with a concentration $7.3 \cdot 10^8$ Bq m^{-3}, was sprinkled (simulated rainfall) over the plot. Subsequently, 250.2 L of tracer-free water was applied to the soil surface in order to push down the labeled water and also to reduce tracer losses due to evaporation. Solution was prepared in the study site before application.

Soil profile monitoring for tritium transport was performed by destructive sampling. Soil cores were obtained by means of hand drilling and the maximum depth was 180 cm. Soil samples from cores were taken at regular depth intervals (being representative for a depth interval of 10 cm) and given times, and sampled length was determined from the expected tracer concentration profile. To prevent possible contamination, from overlying layers, soil samples were taken from the inner part of the core, and immediately stored in leak proof bottles and transported in iceboxes to avoid tritium loss by evaporation. The most intensive data collection for model calibration took place from 17 May to 10 September 2007 (DOY 137-253). The following sampling period from 11 September 2007 to 21 August 2008 (DOY 254-599), less intensive, was used for model prediction.

Meteorological data (hourly) for the site were available from a weather station (SIAM, 2008) located 235 m from the experimental plot. The measurement of tritium in precipitation was obtained from a station that belongs to the Global Network Isotopes in Precipitation (GNIP/IAEA, 2009) located 15 km to NE of the experimental plot.

The samples were analyzed at the CEDEX-Isotopic Techniques Lab. (Spanish Government) using a liquid scintillation alpha-beta spectrometer (Tri-Carb 2560 TR/XL, Packard Instruments).

4. RESULTS AND DISCUSSION

4.1 Field data

For the initial part of the experiment (DOY 170-253), for model calibration, soil profile HTO_l concentration in the four sampling surveys undertaken is shown in figure 2. At the end of this first period, HTO_l migration attained a maximum depth of 60 cm after 73 days. In figure 3, HTO_l profiles for prediction period (DOY 254-599) are shown. Background HTO_l concentration in soil profile was 925 Bq m^{-3} and the movement of the tracer' peak centre of mass through the soil profile is clearly observed in the sampling campaigns. In general, the relative standard deviation (%) from laboratory sample analyses was lower for high HTO_l concentration values. The HTO_l concentration decreased exponentially due to plant transpiration, evaporation and "night-reemission", this last one was a result of the high soil and atmosphere tritium concentration gradient during the first days of the experiment. After 429 days, total duration of the field test, the background HTO_l concentration in soil was practically recovered.

4.2 Model calibration and prediction

The period DOY 170-253 was used for model calibration. The initial input parameters for modeling (Table 1) resulted in simulations that were in poor agreement with field data. A manual calibration process was used. Several parameterizations were considered by varying the number and type of parameters, following the principle of parsimony (i.e. fewer fitted parameters) only variations of two parameters were undertaken, saturated hydraulic conductivity of the soil, K_s, and dispersivity, λ. θ_s and ρ_s were obtained in laboratory, some parameters of table 1 were considered fixed (ρ_w; D_{wa}; D_{Ta}; D_{Tw}; M_w; M_{solid}) and the rest were taken from literature according to a given soil (h_s; b) and plant type (θ_3; θ_4).

To assess goodness-of-fit between data and simulated values several statistics, *RMSE*, *MAE* and *MRE*, were used (Table 2). Final fitted parameters (Table 1) were obtained by minimizing the objective function (*MRE*) and by visual inspection of the model fit to the data.

Table 1. Summary of prescribed values when not fitted parameters and final fitted parameter estimates.

Parameter			Prescribed	Fitted	Unit
Soil physical properties					
	Textural fractions	Sand	15.79		%
		Silt	79.32		%
		Clay	4.89		%
	Bulk density	ρ_s	1560±120		kg m^{-3}
Soil hydraulic properties					
	Saturated water content	θ_s	0.372		m^3 m^{-3}
	Saturated pressure head	h_s	-0.759 [a b]		m
	Saturated hydraulic conductivity	K_s	0.281 10^{-5} [a b]	0.868 10^{-5}	m s^{-1}
	Pore size distribution index	b	5.33 [a b]		-
Flow and transport (liquid and gas phase)	Water density	ρ_w	1000		kg m^{-3}
	Water vapor diffusion coeff. in air	D_{wa}	2.60 10^{-5} [c]		m^2 s^{-1}
	Molecular HTO_g diffusion coeff. in air	D_{Ta}	2.47 10^{-5} [d]		m^2 s^{-1}
	Molecular HTO_l diffusion coeff. in water	D_{Tw}	2.24 10^{-9} [e]		m^2 s^{-1}
	Dispersivity of HTO_l	λ	0.05 [f]	0.10	m
Thermal properties					
	Specific heat of solids	M_{solid}	733 [g]		J kg^{-1} K^{-1}
	Specific heat of water	M_w	4186 [g]		J kg^{-1} K^{-1}
Vegetation (Root water uptake reduction parameters for Eq.19)	From h_3 [h] and Eq.4	θ_3	0.259-0.270		m^3 m^{-3}
	From h_4 [h] and Eq.4	θ_4	0.154		m^3 m^{-3}

[a]Clapp and Hornberger (1978); [b]Cosby et al. (1984); [c]Cussler (1997); [d]Mayers et al. (2005); [e]Mills (1973); [f]Yamazawa (2001); [g]Farouki (1986); [h]Wesseling (1991) and Taylor and Ashcroft (1972)

In figure 2 measured and calibrated HTO_l concentration soil profiles (C_w/C_{w0}) are shown. The most prominent feature of the calibration period (DOY 170-253) is the strong decrease of HTO_l concentration in soil. Although experimental data are relatively sparse and the maximum concentration decreases by three orders of magnitude after seventy days, predicted pattern of HTO_l concentration is generally in good agreement with the data. Table 2 gives goodness-of-fit results for the calibrated data.

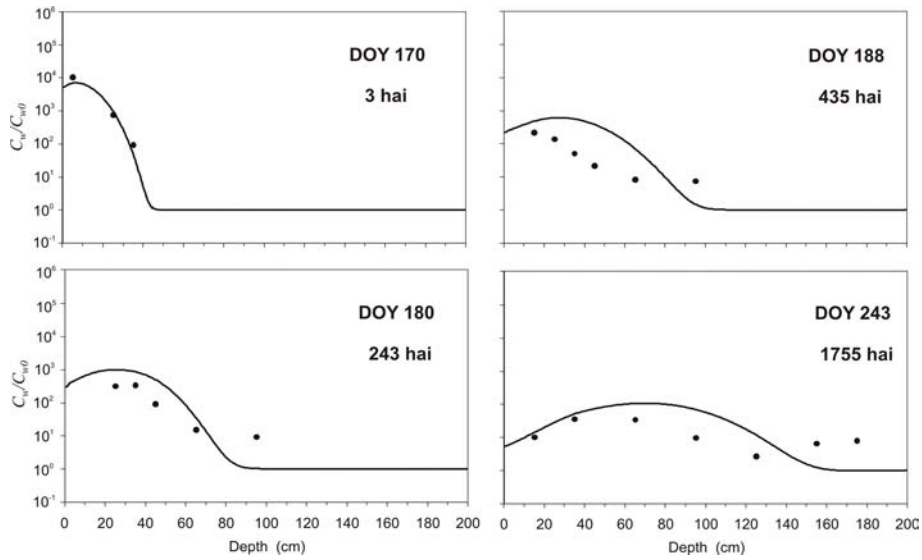

Figure 2. Comparison of field data (points) and model predictions (solid lines) for the calibration period (DOY 170-253). hai: hours after injection.

After calibration, the model was used to predict the tritium (HTO_l and HTO_g) transport during the period DOY 254-599; the results are presented in figure 3. The agreement between field observations and simulations appears to be better than statistical results (*MRE*), probably due to the gradual decrease of HTO_l in soil and lower influence of soil-atmosphere processes. Goodness-of-fit results are given in Table 2.

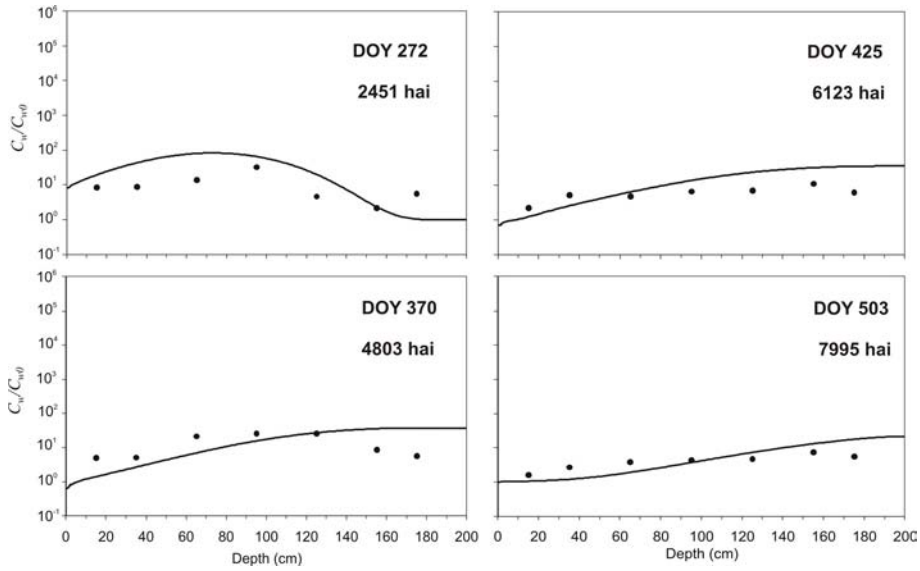

Figure 3. Comparison of field data (points) and model predictions (solid lines) for the prediction period (DOY 254-599). hai: hours after injection.

Table2. Goodness-of- fit for simulated and experimental values. *RMSE* = Root Mean Square Error; *MAE* = Mean Absolute Error; *MRE* = Mean Relative Error.

Simulation	*RMSE*[a]	*MAE*[b]	*MRE*[c]
Calibration period (DOY 170-253)	785158.1	326002.7	0.580
Prediction period (DOY 254-599)	17817.2	11370	0.681

Presence of HTO_l in sampled profiles at higher depths than simulated can be explained by preferential flow generation through roots and cracks within the first centimeters of the soil profile (tilled soil). Also, only one averaged water retention $h(\theta)$ and hydraulic conductivity $K(\theta)$ curves were considered for the total soil profile, which could also account for the difference.

4.3 Water and tritium. Flux and mass balance

The sing convention in the numerical simulations of liquid and vapor mass flux, for both water and tritium, was negative fluxes-upward and positive fluxes-downward. Liquid and vapor mass fluxes for water and tritium were plotted (figure 4) for a water pulse on the experimental plot, which took place in summer (11-19 July 2007, DOY192-200). Results for the upper 2 m, root zone and unsaturated zone, shown the depth of soil most affected by diurnal variations in temperature, evaporation and root water uptake.

In figure 4a, data for the plotted period showed a large downward water flux (q_w) during the first day (DOY 192) in the top 30 cm, when water pulse was applied, whereas q_w for the rest of the days were upward due to evaporation and root water uptake. The reached depth by the roots in this moment is clearly recognized. Vapor flux (q_v) was upward up to a certain depth, which was increasing each day due to the drying process of the top soil. Under this "evaporation front" there was a thickness of soil where q_v was downward, although of lower magnitude than upward flux. A similar trend was found between liquid (q_{Tw}) and vapor (q_{Tv}) tritium mass fluxes, these were downward up to 25-30 cm depth, and on the contrary, between 30 and 90 cm depth both fluxes were upward. Total (or net) mass fluxes ($\boldsymbol{q}$), estimated for the simulation period are shown in figure 4b. Net vapor flux ($\boldsymbol{q}_v$) was one order of magnitude less than net water flux ($\boldsymbol{q}_w$). The greatest difference between net liquid ($\boldsymbol{q}_{Tw}$) and vapor ($\boldsymbol{q}_{Tv}$) tritium mass flux occurs in the top 1 m, being it larger in the first one than in the second one.

For hourly data, not shown here, predicted q_v was downward between 3 and 30 cm depth during the day and upward from 30 to 0 cm depth at night. The large downward q_v during the day correspond to steep temperature gradients during this time. Downward q_v in winter are much lower than in summer because soil temperatures in winter are lower. The amplitude of diurnal variations in q_v decreases with depth.

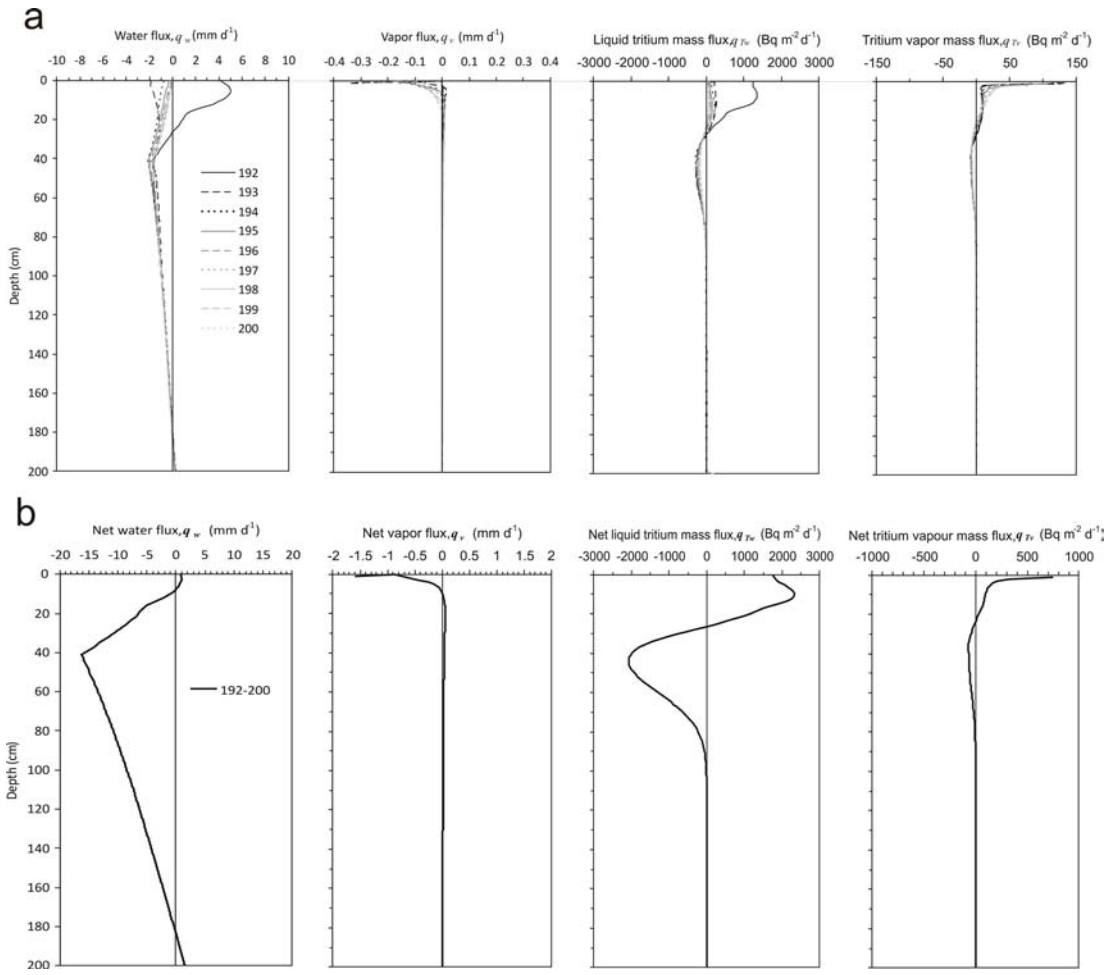

Figure 4. a. Computed water (q_w) and vapor (q_v) flux expressed as water column (1mm d^{-1} = 1 kg m^{-2}d^{-1}); and computed liquid (q_{Tw}) and vapor (q_{Tv}) tritium mass flux (Bq m^{-2} d^{-1}) for a water pulse along 8 days (11-19 July 2007, DOY192-200). **b.** Total (or net) mass fluxes ($\boldsymbol{q}$) calculated for the mentioned simulation period.

One of the objectives of the modeling experiment was to establish an accurate soil water balance. As for the water balance components, water addition due to irrigation and precipitation, losses by transpiration, evaporation and drainage, and changes in soil water storage were considered. The figure 5a shows cumulative computed values of the mentioned water balance components. On the other hand, the second objective was to establish an accurate tritium mass balance. The tritium mass included in each water balance components and states have been considered (Figure 5b): tritium mass in liquid and gas phase; evaporated and transpirated tritium mass; deep drainage of tritium mass; and radioactive decay. The tritium mass decay after 83 days (1992 hours), between the day of tracer injection and the harvest of the first crop (melon), was 95%.

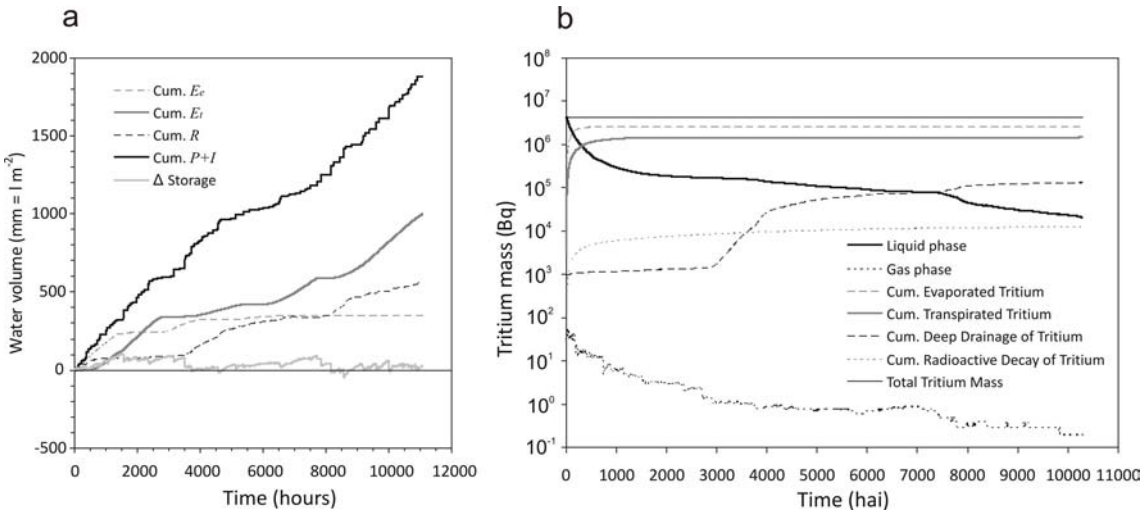

Figure 5. a. Computed water balance components as cumulative values, include: evaporation E_e, transpiration E_t, drainage R, water input $P+I$. Current water storage (ΔStorage) is also ploted. **b.** Tritium mass included in each water balance components and states, it involves: tritium mass in liquid and gas phase, evaporated and transpirated tritium mass, deep drainage of tritium mass, and radioactive decay.

4.4 Molecular diffusion in liquid and gas phase

Hydrodynamic dispersion (D_T) is defined as the sum of effective molecular diffusion (D_p) and mechanical dispersion (D_d) (Eq. 14). D_p, also called *pore diffusion*, is a function of molecular diffusion coefficient in free solution (D_{Tw}) and the tortuosity of the medium as function of water content (τ_w), $D_p = \tau_w(\theta) D_{Tw}$. D_{Tw} was taken directly from the literature (Mills, 1973) and was used to determine the range of possible values of D_p. Previous researches on different clay soils (bentonite, kaolinite, montmorillonite) reported a value of D_p for tritium in the range of 4.5-17·10^{-4} mm^2 s^{-1} (Phillips and Brown, 1968; Gillham et al., 1984). Young and Ball (1998) found a D_p in the range 3.8-5.9·10^{-4} mm^2 s^{-1} for a soil with 35% clay, 38% silt, and 27% sand. Toupiol et al. (2002) reported a value of D_p ranges between 4 and 8·10^{-4} mm^2 s^{-1} for a compacted soil with 30%, clay, 33% silt, and 37% sand. D_p for this study (silty loam) was estimated to range between 2.4·10^{-4} mm^2 s^{-1} and 4.7·10^{-4} mm^2 s^{-1} (10^{-10} m^2 s^{-1}). On the other hand, mechanical dispersion is equal to the product of the seepage velocity v_s ($v_s = q/\theta$) and the dispersivity λ ($D_d = \theta\, v_s\, \lambda$), as shown in Eq. 12. While advection controls the transport of HTO_l in all soil

profile, mechanical dispersion (D_d) decrease with depth and effective molecular diffusion (D_p) stay more or less constant along the profile.

The transport of HTO_g only includes the diffusion term, effective molecular diffusion or *pore diffusion* (Eq. 12). The model was run including in the Eq. 14 the advection term for HTO_g that supposes the diffusion of non-tritiated vapor in air (Eq. 6). The obtained results with the included change were the same that those obtained considering only effective molecular diffusion, which shows that this last one was the main transport process of HTO_g.

5. CONCLUSION

Net vapor flux was one order of magnitude less than water flux. On the other hand, field data and obtained simulations indicate that tritium movement primarily occurs in liquid phase, although during drying conditions tritium movement mainly occurs in gas phase. The difference between net tritium mass fluxes (liquid and vapor phase) occurs in the top soil, whereas for the net water mass fluxes (liquid and vapor phase) it is in all soil thickness. The different behavior between titiated and non-tritiaded water and vapor is due to molecular diffusion in the first one. Molecular diffusion was found to be the most important transport mechanism of tritium in vapor phase, whereas advection-dispersion was for the liquid phase. The effective molecular diffusion between $2.4 \cdot 10^{-4}$ mm^2 s^{-1} and $4.7 \cdot 10^{-4}$ mm^2 s^{-1} was found for liquid tritium in a silty loam soil (16% sand, 79% silt, 5% clay).

The sink terms, tritium evaporation, transpiration, deep drainage and radioactive decay contributed with 61.51%, 34.65%, 3.13% and 0.29% of tritium loss, respectively. The error in the tritium mass balance was 0.5%. After 83 days tritium mass decay was 95%. The tritium background concentration in soil is practically recovered after 429 days.

Acknowledgements
CGL-2004-05963-C04-01 and CGL2007-66861-C04-03 research projects, Spanish Ministry of Science and Innovation. 08225/PI/08 research project, “Programa de Generación del Conocimiento Científico de Excelencia” of the Fundación Seneca, Región de Murcia (II PCTRM 2007-10). We are grateful for the support provided by the Technical University of Cartagena.

REFERENCES

Allen, R.G. et al., 1998. Crop evapotranspiration. Guidelines for computing crop water requirements. Irrigation and Drainage. Paper No. 56, FAO, Rome, Italy.

Al Nakshabandi, G., Kohnke, H., 1965. Thermal conductivity and diffusivity of soils as related to moisture tension and other physical properties. Agri. Meteo. 2, 271–279.

Barnes, C.J. et al., 1994. The distributed recharge mechanism in the Australian arid zone. Soil Sci. Soc. Am. J. 58(1), 31-40.

Campbell, G.S., 1974. A simple method for determining unsaturated conductivity from moisture retention data. Soil Sci. 117, 311-314.

Campbell, G.S, Norman, J.M., 1998. An Introduction to Environmental Biophysics. 2nd ed. Springer-Verlag, New York.

Clapp, R., Hornberger, G., 1978. Empirical equations for some soil hydraulic properties. Water Resour. Res., 20, 601-604.

Cosby, B. J. et al., 1984. A Statistical Exploration of the Relationships of Soil Moisture Characteristics to the Physical Properties of Soils. Water Resour. Res., 20(6), 682-690.

Cussler, E.L., 1997. Diffusion: Mass transfer in fluid systems. Cambridge Univ. Press, New York.

Farouki, O.T., 1986. Thermal properties of soils. Series on Rock and Soil Mechanics 11 (Trans Tech, 136 pp.).

Feddes, R. A. et al., 1978. Simulation of Field Water Use and Crop Yield. John Wiley and Sons, NY.

Gillham, R.W. et al., 1984. Diffusion of non-reactive and reactive solutes through fine-grained barrier materials. Can Geotech. J. 21,541-550.
Garcia, C.A. et al., 2009. Transport of tritium contamination to the atmosphere in an arid environment. Vadose Zone J. 8, 450-461.
GNIP/IAEA, 2009. International Atomic Energy Agency. Isotopes Hydrology Information System. The ISOHIS Database, http://isohis.iaea.org/.
Jackson, D.R. et al., 1974. Diurnal soil water evaporation. Comparison of measured and calculated soil water fluxes. Soil Sci. Soc. Amer. J., 38, 861-866.
Jiménez-Martínez, J. et al., 2009. A root zone modelling approach to estimating groundwater recharge from irrigated areas. J. Hydrol. 367 (1-2), 138-149.
Joshi, B. et al., 1997. Subsurface hydrologic regime and estimation of diffuse soil water flux in a semi arid region. Electronic J. of Geotechnical Engineering. http:/geotech.cive.okstate.edu/ejge/ppr9702/index.htm.
Kline, J.R.,Stewart, M.L., 1974. Tritium uptake and loss in grass vegetation which has been exposed to an atmospheric source of tritiated water. Health Physics 26, 567-573.
Kondo, J., Saigusa, N., 1994. Modeling the evaporation from bare soil with a formula for vaporization in the soil pores. J. Meteorological Society of Japan 72(3), 413-421.
Kondo, J., Xu, J., 1997. Seasonal variations in the heat and water balance for nonvegetated surfaces. J.Applied Meteorology 36(12), 1676-1695.
Kroes, J.G., Van Damm, J.C., 2003. Reference manual SWAP: Version 3.0.3. Rep. 773. Alterra Green World Res., Wageningen, the Netherlands.
Matsushima, D., Kondo, J., 1995. An estimation of the bulk transfer coefficients for a bare soil surface using a linear model. J. Applied Meteorology 34(4), 927-940.
Mayers, C.J. et al., 2005. Modeling tritium transport through a deep unsaturated zone in arid environment. VZJ 4, 967-976.
McCumber, M.C., Pielke, R.A., 1981. Simulations of the effects of surface fluxes of heat and moisture in a mesoscale numerical model 1 soil layer. Journal of Geophysical Research 86 (C10), 9929-9938.
Mills, R., 1973. Self-diffusion in normal and heavy water in the range 1-45º. J. Phys. Chem. 77, 685-688.
Overman, A.R., Scholtz, R.V., 2002. Mathematical Models of Crop Growth and Yield. Marcel Dekker, Inc. New York.
Pachepsky, Y.A. et al.., 2004. Reality and fiction of models and data in soil hydrology. In: Feddes R.A. et al. (Eds.), Unsaturated-zone modeling. Kluwer Academic Publishers, Dordrecht, the Netherlands.
Phillips, R.R., Brown, D.A., 1968. Self diffduion of tritiated water in montmorillonite and kaolinite Clay. Soil Sci. Soc. Am. J. 32, 302-306.
Pruess, K.A., Oldenburg C., Moridis, G., 1999. THOUGH2 user's guide. Version 2.0. LBNL-43134. Lawrence Berkeley Natl. Lab., Berkeley, CA.
Scanlon, B.R., 1992. Evaluation of Liquid and Vapor Water Flow in Desert Soils Based on Chlorine 36 and Tritium Tracers and Nonisothermal Flow Simulations. Water Resour. Res., 28(1), 285-297.
SIAM, 2008. Servicio de Información Agraria de Murcia. Climatology Data. Available from: <http://siam.imida.es>.
Täschner, M. et al., 1995. Investigations and modelling of tritium re-emissions from soil. Fusion Technology, 28, 976-981.
Täschner, M. et al., 1997. Measurements and modeling of tritium reemission rates after HTO depositions at sunrise and at sunset. J. Environ. Radioactivity 36, 219-235.
Toupiol, C. et al., 2002. Long-term tritium transport through field-scale compacted soil liner. J. Geotech. Geoenviron. Eng. 128(8), 640-650.
Yamazawa, H., 2001. A one-dimensional dynamical soil atmosphere tritiated water transport model. Environmental Modelling and Software 16, 739-751.
Yamazawa, H., Nagai, H., 1997. Development of one-dimensional atmosphere-bare soil model. JAERI-Data/Code 97-401.
Young, D.F., Ball, W.P., 1998. Estimating diffusion coefficients in low permeability porous media using a macropore column. Environ. Sci. Technol. 32, 2587-2584.

Use of TDR to estimate aquifer recharge in intensively irrigated areas

J. Jiménez-Martínez[1], A. Jiménez[2] and L. Candela[1]

[1]*Department of Geotechnical Engineering and Geosciences, Technical University of Catalonia, Campus Nord-Gran Capitán s.n. , 08034 Barcelona, Spain. joaquin.jimenez@upc.edu / www.h2ogeo.upc.es*

[2]*Department of Agricultural Science and Technology, Technical University of Cartagena, Paseo Alfonso XIII 52, 30203 Cartagena, Murcia, Spain*

ABSTRACT

A variety of methods, each with varying degrees of accuracy, are available for estimating deep percolation to aquifers. We present a procedure for estimating percolation in irrigated semi-arid regions, where its accurate knowledge is important for the sustainable management of the scarce water resources. An experimental site, located in the Campo de Cartagena (SE, Spain) and operating under field conditions, was equipped with access tubes for monitoring soil water content (θ) using TDR and tensiometers for pressure head (h) up to the depth of 120 cm, to establish the $\theta(h)$ and $K(h)$ functions. Linear correction was sufficient to locally calibrate the TDR measurements by means of the direct comparison with soil moisture laboratory data. Data on θ and h variation with time and depth were collected during the May 2007-September 2008 period. Irrigation return flow was estimated using a modeling approach in which evapotranspiration and soil moisture dynamics for annual row crops (lettuce and melon) were simulated with the HYDRUS-1D code. Computed evapotranspiration and percolation during the hydrological year 2007-2008, where the applied water was 1284 mm, were 697 and 561 mm, respectively. A good agreement was obtained between calibrated (h and θ) and predicted (θ) simulations with field observations, $RMSE$~0.026 for θ in the predicted period. TDR results combined with data on land use and cropping patterns, allow estimating successfully the amount of percolation associated with irrigated agriculture.

1. INTRODUCTION

In (semi-)arid regions accurate knowledge of water infiltration, evaporation, and transpiration is of great importance for the sustainable management of scarce water resources (Garatuza-Payán, et al., 1998). This fact is crucial in areas where intensive irrigated agriculture is practiced.

Measurements of water infiltration rate through the vadose zone, usually estimated by means of analytical or numerical solutions with varying degrees of success, constitute an important input for groundwater recharge assessment. The best method for a particular situation depends on the spatial and temporal scales being considered and on the intended application of the recharge estimate (Scanlon et al., 2002). One difficulty in unsaturated sediments is related to the nonlinear dependence between hydraulic conductivity and water content, because temporal variations in water content are followed by large temporal variations in the hydraulic conductivity values, continuous measurements of water content must be obtained for a reasonable estimation of the temporal variations in hydraulic conductivity. Obviously, to avoid unreliable measurements, they should be performed with the minimal disturbance of the sediment column (Rimon et al., 2007). Time Domain Reflectrometry (TDR) is a soil science technique widely used to monitor soil water content, and several studies have used TDR measurements for groundwater recharge estimations (e.g. Alaoui and Eugster, 2004; Ladekarl et al., 2005; Rimon et al., 2007).

The aim of this study was to assess water infiltration under annual row crops (rotation lettuce and melon) during one hydrological year in the Campo de Cartagena, SE of Spain, semi-arid region where irrigated agriculture is prevalent. To achieve this objective, an experimental plot was instrumented with tensiometers and TDR to monitor soil water dynamics. The code used to model was the well known HYDRUS-1D (Šimůnek et al., 2005). Moisture dynamics are simulated with the Richards equation and root water uptake due to transpiration is calculated according to Feddes et al. (1978).

2. MATERIALS AND METHODS

2.1 Study site

The Campo de Cartagena plain comprises an area of 1440 km^2 in the Region de Murcia, southeast Spain (Fig. 1). The climate is Mediterranean with an average annual rainfall of 300 mm unevenly distributed into a few intensive events, usually between September and December, and a mean annual temperature of 18ºC. Estimates of annual potential evapotranspiration (ET_p) range from 800 to 1200 mm y^{-1}, depending on the estimation method applied (Sánchez et al., 1989). The dominant industry and land use is agriculture, both irrigated and rainfed. Irrigated farmland comprises an area of approximately 299 km^2, with 128.1 km^2 of annual row crops (principally lettuce and melon), 34.1 km^2 of perennial vegetables (principally artichoke), and 136.8 km^2 of fruit trees (principally

citrus). Drip irrigation is widely used in their production due to the scarcity of water resources and need for water conservation.

The top unconfined aquifer (Fig. 1), of Quaternary age and detritic origin, extends over a plain of 1135 km^2 with an average thickness of 50 m. The average hydraulic gradient in this aquifer is 0.001-0.005 m m^{-1}, as well and the hypodermic flow in the vadose zone is non-existent. Piezometric level measured in the inner part of the study area is 14 m below the surface. The unconfined aquifer, under intensive agricultural practices, receives return flow from irrigation and precipitation.

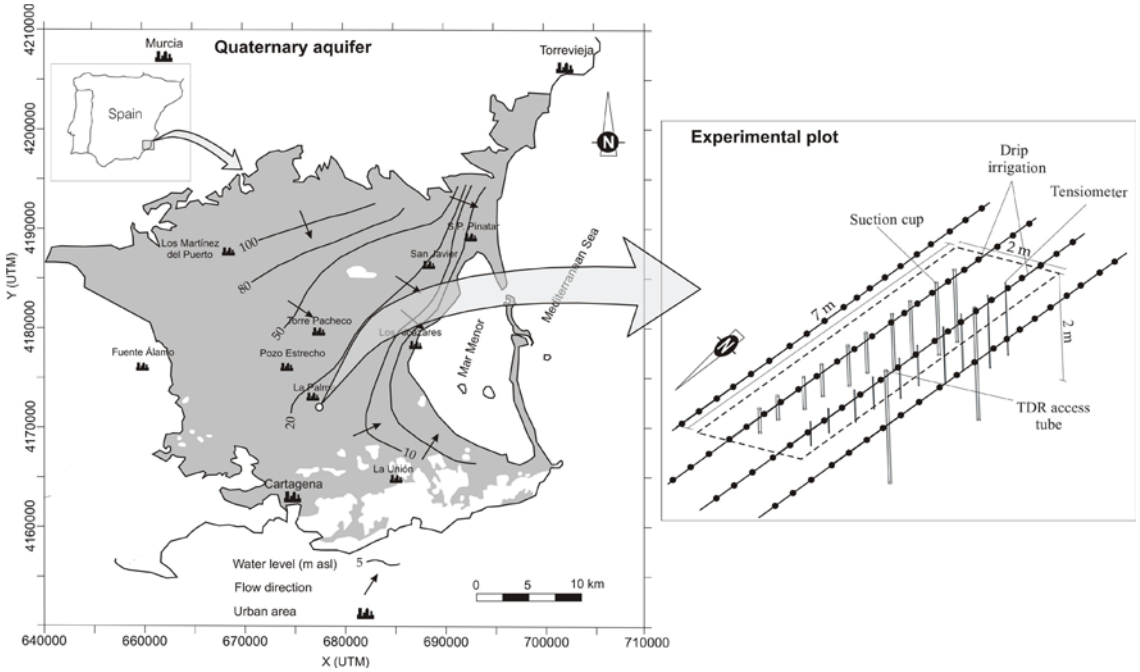

Figure 1. The Campo de Cartagena area (SE Spain) and Quaternary aquifer outcrop. Experimental plot location and instrumentation set-up.

2.2 Field experiment

The test was conducted on an experimental plot at the Tomas Ferro Agricultural Science Center (Technical University of Cartagena). An experimental plot measuring 7×2 m was established on a *silty loam*, soil relatively uniform across the Campo de Cartagena region (Ramírez et al., 1999). The site was managed following agricultural practices that are common in the region, including crop rotation (melon and lettuce) and drip irrigation. The drip irrigation system consisted of 16 mm inside diameter tubing, 4 L h^{-1} emitters 30 cm spacing. It needs to be mentioned an important aspect of the agricultural practices in this region is the use of a plastic cover during summer crop (melon) to reduce the direct evaporation from the ground surface. The surroundings of the experimental plot

were cultivated with same crops under the same conditions to avoid contour effects. Meteorological data for the site were available from the Servicio de Información Agraria de Murcia (SIAM, 2008).

To characterize the soil physical properties, two soil cores were extracted from the plot to a depth of 2 m. Soil bulk density (Grossman and Reinsch, 2002) and particle-size distribution (Gee and Or, 2002) were determined in the laboratory (Table 1).

The plot was instrumented with a duplicate set of tensiometers for pressure head measurements (h) (Soilmoisture Equipment Corp, Goleta, CA, USA), vertically installed at 30, 45, 60, 90 and 120 cm depth (10 tensiometers total), and two 44 mm diameter, 2 m deep access tubes (fibreglass) for soil moisture measurements with a TRIME-FM3 TDR probe (Imko GmbH, Ettlingen, Germany). The TDR probe is one of the techniques producing minimum disturbance of the soil column. Moreover, it permits continuous real time water content (θ) measurements. According to Laurent et al., (2005), to evaluate the performance of the TRIME-tube soil water content profiling under field conditions, the TRIME measurements were directly compared with their respective reference soil water content values determined gravimetrically (Topp and Ferré, 2002) and volumetrically recalculated from bulk density (Grossman and Reinsch, 2002). A simple linear relationship was sufficient to accurately calibrate the TRIME-tube system. θ and h data were collected weekly and each two days, respectively.

3. NUMERICAL MODELLING

3.1 Water flow

To simulate the infiltration process the HYDRUS-1D code (Šimůnek et al., 2005) was applied. The governing equation for water flow is the 1D Richard's equation including a sink term. This last one is specified in terms of a potential root water uptake rate and a stress factor that prescribes the reduction in uptake that occurs due to drought stress (Feddes et al., 1978).

The soil hydraulic properties were modeled using the van Genuchten-Mualem constitutive relationships (van Genuchten, 1980):

$$\theta(h) = \begin{cases} \theta_r + \dfrac{\theta_s - \theta_r}{\left[1 + |\alpha h|^n\right]^{1-1/n}} & h < 0 \\ \theta_s & h \geq 0 \end{cases} \quad [1]$$

$$K(h) = K_s S_e^{\,l} \left\{1 - \left[1 - S_e^{\,n/(n-1)}\right]^{1-1/n}\right\}^2 \quad [2]$$

being S_e is effective saturation:

$$S_e = \frac{\theta(h) - \theta_r}{\theta_s - \theta_r} \quad [3]$$

where θ_s = saturated water content; θ_r = residual water content; K_s = saturated hydraulic conductivity; α = air entry parameter; n = pore size distribution parameter; and l = pore connectivity parameter. The parameters α, n, and l are empirical coefficients that determine the shape of the hydraulic functions.

Running the model required specifying the hydraulic parameters θ_r, θ_s, α, n, K_s, and l. These parameters were estimated using Rosetta (Schaap et al., 2001), a pedotransfer function model that predicts hydraulic parameters from soil texture and related data. The hydraulic parameters were predicted using data for bulk density and percentages of sand, silt, and clay. Estimated parameters are given in Table 1. Refinements to these parameter estimates were made subsequently based on model fitting to a subset of the measured θ and h data (details given below). To reduce the number of free parameters, was assumed l = 0.5, which is a common assumption.

Table 1. Measured soil textural fractions and bulk density data. Estimated hydraulic parameters by Rosetta and fitted hydraulic parameter values with 95% confidence intervals*.

Depth (cm)	Textural fractions (%)			Bulk Density (g cm^{-3})	θ_r (cm cm^{-3})	θ_s (cm cm^{-3})	α (cm^{-1})		n (-)		$\text{Log}_{10}(K_s)$ (cm d^{-1})
	Sand	Silt	Clay				Rosetta $\text{Log}_{10}(\alpha)$	Fitted	Rosetta $\text{Log}_{10}(n)$	Fitted	
0-30	18.7	76.0	3.5	1.45	0.04 ±0.02	0.38 ±0.06	-2.18 ±0.51	0.078 ±0.010	0.21 ±0.09	1.16 ±0.01	1.67 ±0.49
30-60	13.8	80.2	6.0	1.52	0.05 ±0.03	0.38 ±0.06	-2.16 ±0.51	0.046 ±0.005	0.21 ±0.09	1.23 ±0.02	1.48 ±0.52
60-90	19.5	77.2	3.3	1.58	0.04 ±0.03	0.35 ±0.07	-2.01 ±0.66	0.014 ±0.004	0.19 ±0.11	1.27 ±0.07	1.48 ±0.67
90-150	10.8	82.0	6.6	1.70	0.04 ±0.03	0.38 ±0.08	-2.03 ±0.76	0.020 ±0.002	0.18 ±0.11	1.46 ±0.05	1.12 ±0.80

*Confidence intervals are two standard deviations (95%).

An atmospheric boundary condition (presented in section 4.2) was implemented at the soil surface while a free drainage condition was used at the bottom, the latter condition being appropriate due to fact that the water table was far below the root zone, 12 m (Šimůnek et al., 2005).

4.2 Potential evapotranspiration and root growth

Implementing the atmospheric boundary condition required specifying daily irrigation and precipitation rates, as well as the potential evaporation and transpiration rates. To determine evaporation and transpiration, we calculated a reference evapotranspiration $ET_0(t)$ using the Penman-Monteith method. The crop potential evapotranspiration $ET_p(t)$ was then given by (Allen et al., 1998):

$$ET_p(t) = K_c(t) \cdot ET_0(t) \quad [4]$$

where $ET_0(t)$ was discretized in daily time steps and $K_c(t)$ is a crop-specific coefficient that characterizes plant water uptake and evaporation relative to the reference crop. Allen et al. (1998) method and data (length of the growth stages and K_c values) were used to specify for each crop the value of K_c during each growth stage.

With ET_p given by Eq. [4], crop potential evaporation $E_p(t)$ can be calculated according to:

$$E_p(t) = ET_p(t) \cdot \exp^{-\beta \cdot LAI(t)} \quad [5]$$

where β (≈ 0.4) is the radiation extinction coefficient and $LAI(t)$ is the leaf area index. However, as $LAI(t)$ data were not available, it was calculated:

$$E_p(t) = ET_p f(t) \quad [6]$$

where the function $f(t)$ was specified based on the following reasoning. When a crop is first planted, ground cover is nonexistent, potential evaporation is maximal, transpiration is zero, and thus $f(t) = 1$. Conversely, when the crop reaches the mid-season growth stage, ground cover is complete, evaporation is effectively zero, and thereafter $f(t) = 0$. All that remains is specifying the transition from $f(t) = 1$ at planting to $f(t) = 0$ at the beginning of the mid-season growth stage, we modeled this transition using a sigmoid curve.

With the HYDRUS atmospheric boundary condition, water evaporates from the soil surface at the potential rate E_p (a flux boundary condition) as long as the pressure head at the surface remains above a threshold value, h_{crit}.

With ET_p and E_p given by Eqs. [4] and [5], the potential transpiration $T_p(t)$ was specified by:

$$T_p(t) = ET_p(t) - E_p(t) \quad [7]$$

The modelled rooting depth was assumed to increase with time according to a logistic growth function (Šimůnek et al., 2005), achieving a maximum depth at the end of the crop development stage. Values for the maximum rooting depth for particular crops were derived from Allen et al. (1998).

4. RESULTS AND DISCUSSION

4.1 Model calibration and prediction

During the first crop cultivation (melon, A) from 17 May to 10 September, 2007, comprising day of year (DOY) 137-253 (DOY 1 = 1st January 2007), θ (weekly) and h data (each two days) were collected. Using the initial hydraulic parameter estimates by Rosetta, resulted in simulations that were in poor agreement with the experimental observed data. Data set from the first crop (melon, A) and the parameter optimization routines of HYDRUS-1D were used for soil hydraulic parameters calibration. Several parameterizations were considered which differed

according to the number of soil layer (from 1 to 4) and the number and type of hydraulic parameters that were fitted for each layer. The best overall parameterization was determined based on diagnostic information provided by the HYDRUS-1D routines, visual inspection of the model fit to the data, and the principle of parsimony. The best parameterization was found to involve four soil layers with two adjustable parameters, α and n, for each layer (Table 1). This first crop allowed the most accurate $\theta(h)$ and $K(h)$ functions establishment for our soil.

With the fitted $\theta(h)$ and $K(h)$ functions, the model was used then to predict the soil moisture dynamics during the growing periods of three more crops. The first one (lettuce, B) between 25 September and 24 December 2007 (DOY 268-358), the second (lettuce, C) between 3 January and 2 April 2008 (DOY 368-458) and finally, the third (melon with plastic cover, D) from 3 April to 21 August 2008 (DOY 459-599). Figure 2 compares water content (θ) predictions with TRIME-tube measurements at different depths, showing a good agreement between them. Measures of goodness-of-fit for calibration and prediction period are given in Table 2.

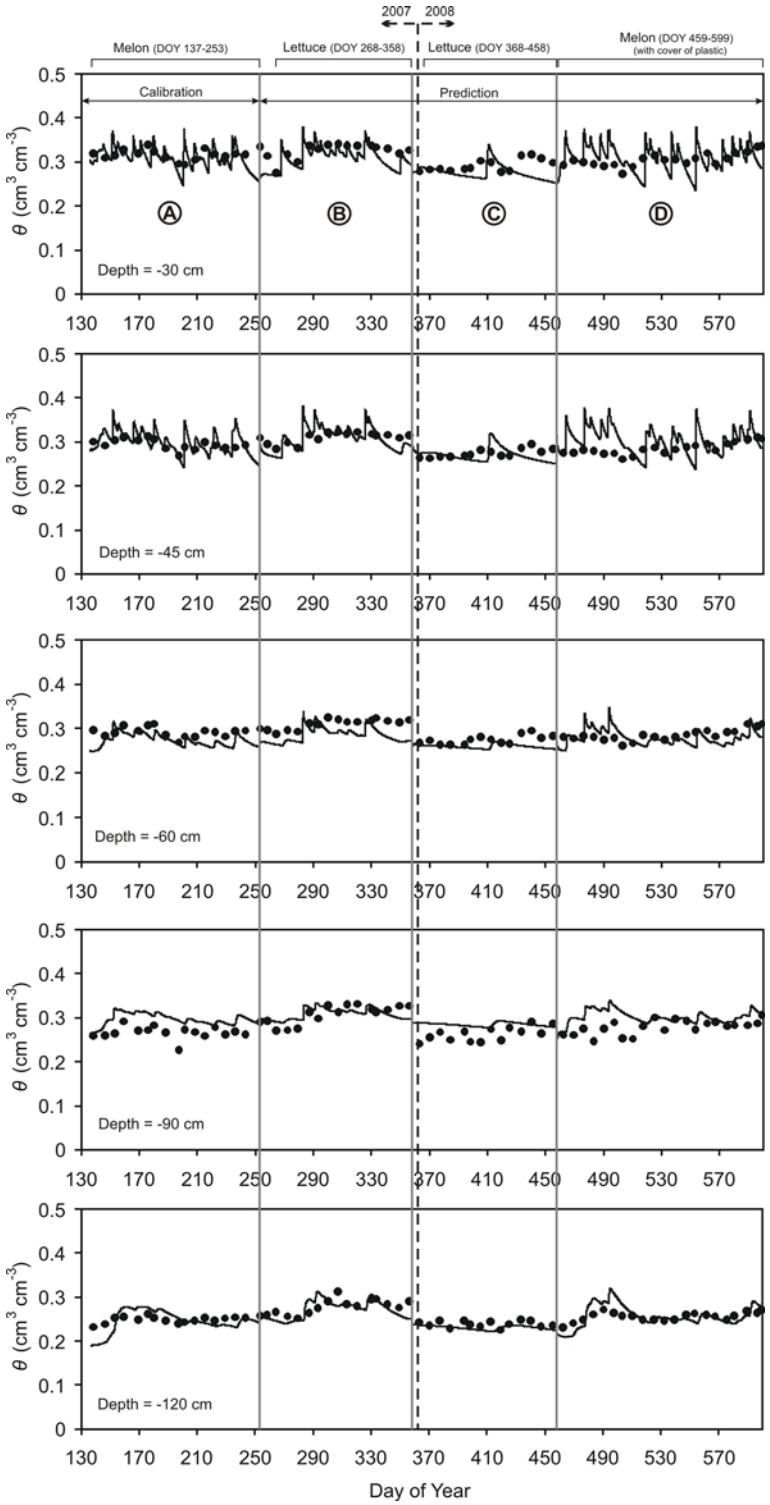

Figure 2. Comparison of field measured (TRIME-FM3 TDR) and HYDRUS simulated soil water content (points and solid lines, respectively) at the selected depths, for calibration (DOY 137-253) and prediction (DOY 254-599) period. The grey vertical lines indicate simulated intervals (crop periods).

Table 2. Goodness-of-fit measures for simulations and experimental data.

Simulation	Data Set	*RMSE*†	*MAE*‡
A Melon (DOY 137-253) (calibration)	Water content (θ)	0.029	0.024
	Pressure head (h)	33.776	27.971
B Lettuce (DOY 268-358) (prediction)	Water content (θ)	0.023	0.019
C Lettuce (DOY 368-458) (prediction)	Water content (θ)	0.022	0.018
D Melon, with plastic cover (DOY 459-599) (prediction)	Water content (θ)	0.027	0.021
Total prediction period (DOY 254-599)	Water content (θ)	0.026	0.021

† Root mean square error, $RMSE = \sqrt{\frac{1}{n}\sum_{i=1}^{n}(x_i - y_i)^2}$; ‡ Mean absolute error, $MAE = \frac{1}{n}\sum_{i=1}^{n}|x_i - y_i|$

DOY: day of year. For DOY1 = 1st January 2007.

4.2 Recharge estimation

The simulations were used to evaluate soil water balance and calculate the recharge rate generated by each crop at different time of the year. Drainage from the bottom of the soil profile (at 150 cm depth) was considered return flow, equal to the groundwater recharge rate as hypodermic flow is non-existent (14 m vadose zone thickness). The percentages of computed recharge with respect to applied water ($P + I$) for the cropping periods are shown in Table 3. The important percolation percentage (68.2%) during the first lettuce crop (B) was due to higher precipitation and lower transpiration between September and December (DOY 254-358). The difference in the percentage of recharge between the first (A) and second melon (D) crop is the consequence of the plastic cover application during the second one, since direct evaporation from ground surface is null. On the other hand, technical problems in the irrigation system led to a large water volume (77 mm) application on the experimental plot during the second melon crop (D). For 2007-2008 hydrological year total recharge was 561 mm that accounts for 43% of the total applied water ($P + I$).

Table 3. Water input (P+I) and computed actual evaporation (E_a), actual transpiration (T_a) and bottom drainage for each crop.

Crop period	I (mm)	P (mm)	I+P (mm)	E_a (mm)	T_a (mm)	Deep percolation (mm)	Deep percolation (%)
A Melon (DOY 137-253) (calibration)	557	32	589	72	375	128	21.7
B Lettuce (DOY 268-358) (prediction)	206	197	403	58	62	275	68.2
C Lettuce (DOY 368-458) (prediction)	123	61	184	46	134	48	26
D Melon (DOY 459-599) (prediction) (with plastic cover)	617	80	697	10	376	238	34.1
Total prediction period (DOY 254-599)	946	338	1284	114	572	561	43

5. CONCLUSIONS

For the experimental exercise, good agreement was achieved between field measurements and numerical simulations. The accuracy after local calibration with linear correction and the frequency of weekly field TDR measurements of water content (θ) allowed a good assessment of percolation in irrigated horticulture.

For the October 2007-September 2008 period the mean deep infiltration (recharge) was of 561 mm for annual row crops (set lettuce and melon). Although the agricultural practices from farmers are sound, the rainfall is unevenly distributed into a few intensive events, like between September and December, thus it contributes meaningfully to deep percolation due to preferential flow of water since soil water content is consistently high. Calculations indicate a high level of recharge late in the year (October-December) when potential evapotranspiration was lower, and in summer time due to crops plastic cover. Improved irrigation scheduling based on soil moisture status (for lettuce crop Sept-Dec) and crop water requirements (for melon crop with plastic cover Apr-Aug) could significantly reduce return flows.

Acknowledgements

This work has been developed within CGL-2004-05963-C04-01 and CGL2007-66861-C04-03 research projects, Plan Nacional I+D+i Ministry of Science and Innovation (Spain). It also is included in the framework of the 08225/PI/08 research project financed by "Programa de Generación del Conocimiento Científico de Excelencia" of Fundación Seneca, Región de Murcia (II PCTRM 2007-10).

REFERENCES

Alaoui, A., Eugter, W., 2004. Dual-porosity modeling of groundwater recharge: testing a quick calibration using in situ moisture measurements, Areuse River Delta, Switzerland. Hydrolgeol. J. 12, 464-475.

Allen, R.G., Pereira, L.S., Raes, D., Smith, M., 1998. Crop evapotranspiration. Guidelines for computing crop water requirements. Irrigation and Drainage. Paper No. 56, FAO, Rome, Italy.

Feddes, R. A., Kowalik, P.J., Zaradny, H., 1978. Simulation of Field Water Use and Crop Yield. John Wiley and Sons, NY.

Garatuza-Payán, J., Shuttleworth, W.J., Encinas, D., McNeil, D.D., Stewart, J.B., DeBruin, H., Watts, C., 1998. Measurement and Modelling evaporation for irrigated crops in Northwest Mexico. Hydrol. Process. 12, 1397-1418.

Gee, G.W., Or, D., 2002. Particle Size Analysis. In: Dane, J., Topp, C. (Eds.), Methods of soil analysis, Part 4, SSSA Book Series: 5, Am. Soc. Agron., Madison, WI. pp. 255–294.

Grossman, R.B., Reinsch, T.G., 2002. Bulk Density and Linear Extensibility. In: Dane, J., Topp, C. (Eds.), Methods of soil analysis, Part 4, SSSA Book Series: 5, Am. Soc. Agron., Madison, WI. pp. 201–228.

Ladekarl, U.L., Rasmussen, K.R., Christensen, S., Jensen, K.H., Hansen, B., 2005. Groundwater recharge and evapotranspiration for two natural ecosystems covered with oak and heather. J. Hydrol. 300, 76-99.

Laurent, J.P., Ruelle, P., Delage, L., Zaïri, A., Ben Nouna, B., Adjmi, T., 2005. Monitoring Soil Water Content Profiles with a Commercial TDR System: Comparative Field Tests and Laboratory Calibration. Vadose Zone J. 4, 1030–1036.

Ramírez, I., Vicente, M., García, J., Vaquero, A., 1999. Mapa digital de suelos de la Región de Murcia. Consejería de Agricultura, Agua y Medio Ambiente. Handbook and CD-ROM. pp. 78.

Rimon, Y., Dahan, O., Nativ, R., Geyer, S., 2007. Water percolation through the deep vadose zone and groundwater recharge: Preliminary results based on a new vadose zone monitoring system, Water Resour. Res., 43, W05402, doi:10.1029/2006WR004855.

Sánchez, M.I., López, F., Del Amor, F., Torrecillas, A., 1989. La evaporación y evapotranspiración en el Campo de Cartagena y Vega Media del Segura. Primeros resultados. Anales de Edafología y Agrobiología, 1239-1251.

Scanlon, B.R., Healy, R.W., Cook, P.G., 2002. Choosing appropriate techniques for quantifying groundwater recharge. Hydrogeol. J. 10, 18-39.

Schaap, M.G., Leij, F.J., van Genuchten, M.Th., 2001. ROSETTA: a computer program for estimating soil hydraulic parameters with hierarchical pedotransfer functions. J. Hydrol. 251, 163-176.

SIAM, 2008. Servicio de Información Agraria de Murcia. Climatology Data. Available from: <http://siam.imida.es>.

Šimůnek, J., van Genuchten, M.Th., Šejna, M., 2005. The HYDRUS-1D Software Package for Simulating the Movement of Water, Heat, and Multiple Solutes in Variability Saturated Media, Version 3.0. Department of Environmetal Sciences University of California Riverside, Riverside, California, USA. 270 pp.

Topp, G.C., Ferré, P.A., 2002. Thermogravimetric Method Using Convective Oven-Drying. In: Dane, J., Topp, C. (Eds.), Methods of soil analysis, Part 4, SSSA Book Series: 5, Am. Soc. Agron., Madison, WI. pp. 422-424.

van Genuchten, M. Th., 1980. A closed-form equation for predicting the hydraulic conductivity of unsaturated soils. Soil Sci. Soc. Am. J. 44, 892-898.

ESTIMACIÓN DE LA RECARGA POR RETORNO DE RIEGO A TRAVÉS DE LA ZNS EN ÁREAS DE AGRICULTURA INTENSIVA BAJO CLIMA SEMI-ÁRIDO. ANÁLISIS DE SENSIBILIDAD

J. Jiménez-Martínez[1]*, J. Molinero[1,2] y L. Candela[1]

1: Dpto. Ingeniería del Terreno, Cartografía y Geofísica
Universidad Politécnica de Cataluña
Campus Nord-Gran Capitán s/n, 08034 Barcelona, España.
e-mail: joaquin.jimenez@upc.edu/lucila.candela@upc.edu, web: http://www.h2ogeo.upc.es

2: Amphos XXI Consulting S.L.
Passeig de Rubí 31, 08197 Valdorreix, Barcelona, España.
e-mail: jorge.molinero@amphos21.com, web: http://www.amphos21.com

Palabras clave: semi-árido, cultivos, balance, recarga, evapotranspiración

RESUMEN. *Para la evaluación de la recarga al acuífero en el Campo de Cartagena (SE España) correspondiente al periodo 1999-2008 se aplicó el código VisualBALAN v. 2.0. El estudio se realizó en cultivos de regadío clasificados en tres grandes grupos: anuales (lechuga y melón), perennes (alcachofa) y árboles frutales (cítricos). La metodología desarrollada ha permitido estimar la recarga producida por precipitación y riego, siendo los valores medios anuales obtenidos de 394, 201 y 194 mm para cultivos anuales, perennes y árboles frutales, respectivamente en el periodo estudiado. Los resultados muestran el papel preponderante de las lluvias (torrenciales) frente al riego (alta eficiencia) sobre la recarga total, el constante alto contenido de agua en el suelo facilita el proceso de infiltración de las mismas. El análisis de sensibilidad realizado, muestra que los parámetros que tienen una mayor incidencia sobre la recarga son la capacidad de campo, punto de marchitez, coeficiente agotamiento del flujo hipodérmico, CEME y número de curva; para las condiciones iniciales y de contorno son contenido inicial de agua en suelo y riego, respectivamente.*

ABSTRACT. *To evaluate water recharge to the aquifer (1999-2008) in the Campo de Cartagena area (SE Spain) the VisualBALAN v. 2.0 code was applied. The study was carried out for three different groups of crops: annual row crops (lettuce and melon), perennial vegetables (artichoke) and fruit trees (citrus). The annual mean recharge values obtained from the applied methodology and studied period were 394, 201 and 194 mm for annual row crops, perennial vegetables and fruit trees, respectively. The assessment of rainfall events in the final recharge is clearly observed, due to the continuous high water content in soil that facilitates the infiltration process of it. The sensitivity analysis shows that the most important parameters affecting recharge are field capacity, wilting point, hypodermic flow depletion coefficient, CEME parameter and curve number; initial water content in soil and irrigation are the most important to initial and boundary conditions, respectively.*

1. INTRODUCCIÓN

La correcta estimación de la recarga a los acuíferos es un aspecto indispensable para el conocimiento de los recursos hídricos disponibles en una unidad acuífera así como para evaluar su vulnerabilidad a la contaminación. En las regiones áridas y semi-áridas la ausencia de cursos superficiales, los aspectos climáticos relacionados con la distribución espacial y temporal de la precipitación y evapotranspiración, y la existencia de procesos de flujo predominantemente de tipo preferencial (Scanlon et al. 2002), constituyen aspectos añadidos que aumentan la complejidad de su estimación. Por otro lado, dado que las condiciones climáticas favorecen la implantación de agricultura intensiva, en determinadas cuencas la estimación de la recarga resulta un ejercicio complejo debido a la presencia de regadío. Para la gestión sostenible de los generalmente escasos recursos hídricos que caracterizan a estas zonas climáticas la correcta cuantificación de la recarga, evaporación y transpiración es de gran

importancia para una obtención fiable de los recursos disponibles (Garatuza-Payan et al. 1998).

El Campo de Cartagena (SE España), región climáticamente caracterizada como semi-árida, la horticultura constituye la principal actividad económica. El objetivo principal de este trabajo se centra en la estimación de la recarga por retorno de riego para diferentes cultivos y de la evapotranspiración *real* para un largo periodo de tiempo (9 años) mediante la aplicación de VisualBALAN v. 2.0 (Samper et al. 2005), un código de balance hídrico distribuido. VisualBALAN ha sido aplicado en numerosos casos de estudio, destacar entre otros muchos trabajos: Carrica y Lexow (2004), García-Santos et al. (2005) y Samper et al. (2007).

2. ÁREA DE ESTUDIO

El Campo de Cartagena comprende un área de 1440 km^2 situada al sureste de España (Murcia). El clima es mediterráneo con una temperatura media anual de 18 ºC y una precipitación media anual de 300 mm, distribuida en pocos eventos intensos producidos en primavera y otoño. La evapotranspiración potencial anual (ET_p) oscila entre 800 y 1200 mm $año^{-1}$, en función del método empleado en su estimación (Sánchez et al. 1989). El uso principal del suelo es para agricultura de secano o regadío, la superficie de regadío cultivada comprende un área aproximada de 299 km^2, distribuidos en 128.1 km^2 de cultivos hortícolas de tipo anual (principalmente lechuga y melón) y 34.1 km^2 de tipo perenne (principalmente alcachofa), y 136.8 km^2 de árboles frutales (principalmente cítricos) (CARM, 2008). Debido a la escasez de recursos hídricos se aplica riego localizado mayoritariamente.

Para la realización del estudio de recarga se seleccionó una zona experimental con agricultura intensiva desarrollada sobre el acuífero libre superior, constituido por materiales detríticos (principalmente limos) de edad cuaternaria. El acuífero tiene una extensión de 1135 km^2, un espesor medio de 50 m y presenta un gradiente hidráulico entre 0.001 y 0.005 m/m. La intensa actividad agrícola que se desarrolla sobre la superficie del acuífero derivó en su transformación en un sumidero de agroquímicos y condujo a un descenso continuado del nivel freático. La puesta en funcionamiento del *Trasvase Tajo-Segura* en 1980 tuvo como consecuencia el cese de los bombeos y la recuperación de niveles.

Un estudio preliminar llevado a cabo por el Instituto Geológico y Minero de España (IGME, 1994) estimó en 69 hm^3 la recarga anual al acuífero libre superior, de ellos 46 hm^3 por recarga natural y 23 hm^3 debidos al retorno de riego. El cálculo de la recarga por retorno de riego realizado por el IGME fue basado solo en el agua de riego aplicada y no considera el agua añadida por precipitación. La recarga producida por precipitación en áreas cultivadas fue implícitamente incluida en la estimación de la recarga natural, la cual fue un valor único calculado para toda la región. En nuestro trabajo es calculada la recarga producida conjuntamente por riego y precipitación para diferentes cultivos.

3. METODOLOGÍA

El estudio se realizó en tres parcelas experimentales donde se desarrollaron diversos cultivos: *L y M*, cultivo hortícola anual (rotación de lechuga y melón); *A*, cultivo hortícola perenne (alcachofa) y *C*, árboles frutales (cítricos). La superficie de las tres parcelas experimentales es de 1 ha (10000 m^2). Alrededor de las parcelas experimentales se llevaron a cabo idénticas prácticas agrícolas y cultivos para evitar efectos de contorno.

La selección de las parcelas experimentales se basó en los siguientes criterios: permanencia de los tipos de cultivo seleccionados a lo largo del periodo estudiado (1999-2008), existencia de un piezómetro para control del acuífero (CHS, 2008) y la presencia de una estación meteorológica en las proximidades de la zona de estudio (SIAM, 2008). En las parcelas experimentales (*L y M*; *A*; *C*) se aplicaron prácticas agrícolas habituales en el Campo de Cartagena (Tabla 1), incluyendo rotación en el caso de cultivos hortícolas anuales, riego localizado y necesidades hídricas. Se debe mencionar que los cultivos hortícolas estivales (melón) se realizan bajo plástico para incrementar la eficiencia de riego.

Los suelos son de tipo limo-arenosos según la clasificación textural de suelos USDA, y presentan gran homogeneidad en todo el Campo de Cartagena (Ramírez et al. 1999).

Tabla 1. Principales características de las parcelas experimentales (fuentes: **Allen et al. 1998 y ** CARM, 2007)

Parcela experimental	Cultivo	Altura media cultivo*	Máxima profundidad raíces*	Espaciado márgenes	Riego localizado			Necesidades hídricas**
					Diámetro interior	Espaciado emisores	Caudal	
		(cm)	(cm)	(m)	(mm)	(cm)	(l h^{-1})	(m^3 ha^{-1} $año^{-1}$)
L-M	lechuga / melón	30 / 30	30-50 / 80-150	1	16	30	4	3288 / 6169
A	alcachofa	70	60-90	1.7	16	40	4	6623
C	cítricos	400	80-150	6	16	25-125	4	6407

4. ESTIMACIÓN DE LA RECARGA MEDIANTE UN MODELO DE BALANCE

4.1. Modelo de balance hídrico

Para la obtención del balance hídrico se utilizó VisualBALAN v. 2.0 (Samper et al. 2005), un modelo computacional que permite establecer el balance hídrico en el suelo, zona no saturada y acuífero. Para la realización de la estimación el modelo asume propiedades homogéneas en cada una de estas tres zonas.

Para la obtención del balance hídrico en el suelo, uno de los aspectos importantes es la apropiada estimación de la evapotranspiración *ET*. Para el cálculo de la evapotranspiración de referencia $ET_0(t)$ se aplicó el método FAO Penman-Monteith y la evapotranspiración potencial $ET_p(t)$ se obtuvo a partir de Allen et al. (1998):

$$ET_p(t) = K_c(t) \cdot ET_0(t) \tag{1}$$

siendo $K_c(t)$ el coeficiente de cultivo especifico, que caracteriza la absorción de agua por la planta y la evaporación relativa al cultivo de referencia para cada estadío de crecimiento. Para cultivos hortícolas perennes se aplicó $K_c = 0.95$ como valor medio anual (Allen et al. 1998), y para árboles frutales se utilizó un valor medio mensual (Castel, 2001), aunque el valor medio anual es $K_c = 0.68$ para una superficie de suelo sombreada ≥ 64 %. La evaporación potencial $E_p(t)$ se calculó a partir de:

$$E_p(t) = ET_p(t) \cdot \exp^{-\beta \cdot LAI(t)} \tag{2}$$

donde β (≈ 0.4) es el coeficiente de extinción de la radiación y $LAI(t)$ es el índice foliar calculado mediante:

$$E_p(t) = ET_p f(t) \tag{3}$$

La función $f(t)$ varía entre $f(t) = 1$ para un suelo sin cubierta vegetal donde la evaporación es máxima y la transpiración es cero y $f(t) = 0$ cuando el cultivo alcanza su estadio medio de crecimiento y la evaporación es cero. La transición entre $f(t) = 1$ y $f(t) = 0$ se modela mediante una curva sigmoidal (Jiménez-Martínez et al. 2009).

Finalmente, la transpiración potencial $T_p(t)$ queda definida como:

$$T_p(t) = ET_p(t) - E_p(t) \tag{4}$$

De acuerdo con las prácticas agrícolas en la zona, el cálculo de la $ET_p(t)$ para cultivos de invierno (lechuga) se estimó mediante la Ec. (1). Para el cultivo estival (melón) dado que $E_p(t)$ es cero al realizarse el cultivo bajo plástico, la $T_p(t)$ se obtiene a partir de la Ec. (4). Para cultivos hortícolas perennes y árboles frutales se asumió su total desarrollo por lo que la $ET_p(t)$ se calcula a partir de la Ec. (1).

Los valores de precipitación, *P,* y riego, *Ir*, se distribuyen entre intercepción *In*, escorrentía E_s e infiltración *I*. La fracción de *P* que es interceptada por la vegetación supone una pérdida de agua por evaporación y la

reducción de la escorrentía. Parte del agua infiltrada por *P* y *Ir* se pierde por evapotranspiración, *ET*, y otra es almacenada en el suelo, $\Delta\theta$. En este trabajo *In* se calculó por el Método de Horton (López, 1997) y E_s mediante el método de Número de Curva (Soil Conservation Service, 1975). Existen varios métodos que permiten relacionar la evapotranspiración real $ET_a(t)$ y la evapotranspiración potencial $ET_p(t)$, para su obtención en este trabajo se utilizó el Método Exponencial (Samper et al. 2005).

Se asumió que el suelo es homogéneo e isótropo, la fase gaseosa no afecta al flujo de agua, el flujo de agua debido a gradientes térmicos es despreciable, y se consideró una recarga difusa para calcular la recarga potencial hacia la zona no saturada, P_e. VisualBALAN ofrece varias opciones para resolver este aspecto, en este caso se ha usado el Método Convencional (Samper et al. 2005). En la zona no saturada, P_e puede subdividirse en flujo hipodérmico, Q_h , y flujo vertical o percolación, Q_p. Ambos son función del volumen de agua almacenado por unidad de superficie, V_h, de la permeabilidad horizontal, K_{hv}, y vertical ,K_{vv} ,y de un coeficiente de agotamiento para el flujo hipodérmico,α_h, y flujo vertical, α_p. El balance de agua en la zona no saturada se resolvió mediante un esquema explicito.

Para calcular el nivel de agua en el acuífero, el código VisualBALAN establece el balance de agua para cada Δt. Para su cálculo las parcelas experimentales fueron consideradas como una sola celda. El volumen de agua V_a y la altura del nivel *h* están referidas a un nivel de referencia (nivel base) h_0, al cual corresponde un volumen V_{a0}. El volumen de agua almacenado respecto al valor de referencia $\Delta V_a = (V_a - V_{a0})$, se relaciona con la variación de nivel $\Delta h = (h - h_0)$, a través de la porosidad efectiva, m_e, mediante $\Delta V_a = m_e \Delta h$. El balance de agua en el acuífero se realiza considerando un flujo de entrada vertical o percolación, Q_p, y la descarga subterránea, Q_s., la cual depende de un coeficiente de agotamiento α_s, y este a su vez es función del coeficiente de almacenamiento del acuífero *S*.

4.2. Análisis de sensibilidad

En la utilización de los modelos se presentan diversas fuentes potenciales de incertidumbre, que además pueden afectar a la precisión y fiabilidad de las predicciones finales por lo que es necesario un análisis de sensibilidad e incertidumbre. Por un lado se pueden distinguir incertidumbres derivadas de los parámetros y condiciones iniciales del modelo y por otro, las asociadas a las condiciones de contorno. Cuantificar el efecto de la incertidumbre sobre los cálculos de recarga requiere el conocimiento de su variabilidad estadística y correlación estructural. Sin embargo, el análisis de sensibilidad puede aportar información sobre la incertidumbre del modelo dada su estrecha relación.

Para el análisis de la incertidumbre sobre los parámetros y las condiciones iniciales del modelo, el análisis de sensibilidad se realizó a partir de la opción incluida en VisualBALAN. En el segundo caso, incertidumbre asociada a las condiciones de contorno, se realizó un análisis de sensibilidad relativa definida como *AS*/*CP*. Para ello se realizó un cambio relativo en las variables de entrada (input) *CP* definido como $|P_s\text{-}P_b|/P_b$ 100, y en los datos de salida (output) *AS* definido como $|C_s\text{-}C_b|/C_b$ 100, donde P_s y P_b son valores de la variable usados para el análisis de sensibilidad y modelo base calibrado, respectivamente, y C_s y C_b son datos de salida calculados en el análisis de sensibilidad y modelo base calibrado, respectivamente.

5. RESULTADOS Y DISCUSIÓN

5.1. Resultado modelación

El periodo para el que se desarrolló el experimento fue de nueve años hidrológicos comprendidos entre Octubre de 1999 y Septiembre de 2008. La calibración y validación se efectuó para cultivos hortícolas anuales (lechuga y melón), para cultivos hortícolas perennes (alcachofa) y árboles frutales (cítricos), aunque en el presente trabajo solo son presentados los resultados de las calibraciones (Figura 1).

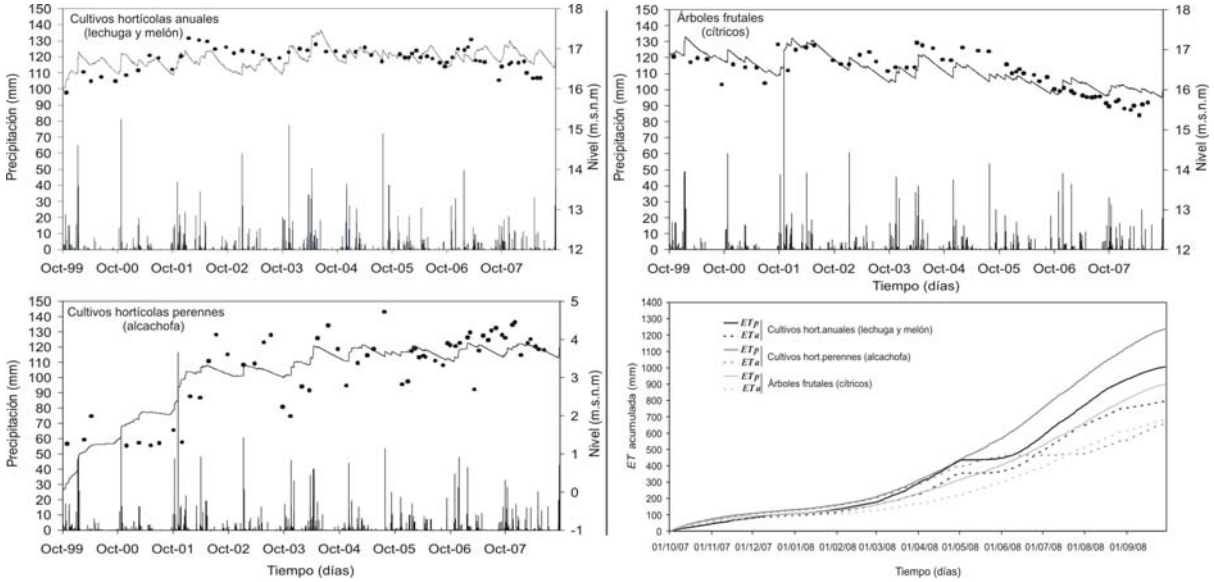

Figura 1. Evolución piezométrica para el modelo calibrado, niveles medidos y precipitaciones en cada tipo de cultivo. ET_p y ET_a acumuladas en el último año hidrológico (Oct 2007-Sept 2008) para cada tipo de cultivo.

Tabla 2. Valores iniciales de los parámetros y valores estimados para los ajustados en cada tipo de cultivo para el periodo completo estudiado (Oct 1999-Sept 2008). Medidas de bondad de ajuste entre nivel medido y simulado.

Parámetros	Cultivos hortícolas ANUALES		Cultivos hortícolas PERENNES		Árboles frutales	
	Valor inicial	Valor ajustado	Valor inicial	Valor ajustado	Valor inicial	Valor ajustado
Calibrados						
Lluvia mínima para aguacero (mm)	2	2	2	2	2	2
Coef. agotamiento flujo hipodérmico, α_h (día^{-1})	0.01	0.01	0.01	0.01	0.01	0.01
Coef. Agotamiento descarga subterránea, α_s (día^{-1})	0.0173	0.0050050	0.0173	0.0009812	0.0173	0.0009812
Coeficiente de almacenamiento, S	0.2	0.2098	0.2	0.2065	0.2	0.2
Nivel de descarga del acuífero, h_0 (m)	15.80	15.78	1.50	1.50	13.55	13.57
Permeabilidad vertical zona no saturada, K_{vv} (mm día^{-1})	432	432	432	432	432	432
Coef. agotamiento flujo vertical , α_p (día^{-1})	0.6931	0.6931	0.6931	0.6931	0.6931	0.6931
CEME (mm) [valor límite de déficit hídrico, entre *FC* y *WP*]	20	1.549	20	0.965	20	1.006
*Fijados**						
Espesor suelo, b_s (cm)	50		100		150	
Porosidad total suelo, Φ_s (cm^3 cm^{-3})	0.4		0.4		0.4	
Punto de Marchitez, *WP* (cm^3 cm^{-3})	0.1		0.1		0.1	
Capacidad de Campo, *FC* (cm^3 cm^{-3})	0.2		0.2		0.2	
Número de Curva**	58		58		25	
Permeabilidad vertical suelo, K_{vs} (cm s^{-1})	0.0004		0.0004		0.0004	
Bondad del ajuste						
Error cuadrático medio, *RMSE*	0.309		0.590		0.348	
Error medio absoluto, *MAE*	0.256		0.480		0.294	

*Parámetros fijados, tomados de Jiménez et al. (2007) y Jiménez-Martínez et al. (2009). ** Soil Conservation Service, 1975.

La simulación con los parámetros iniciales del modelo condujo a resultados que presentaban un pobre ajuste respecto a los datos medidos. Por ello, se realizaron numerosos intentos de calibración de parámetros en las tres zonas (suelo, zona no saturada, acuífero) mediante las rutinas de optimización de parámetros incorporadas en VisualBALAN y datos medidos (niveles). Entre las diversas parametrizaciones consideradas, se seleccionó aquella considerada óptima a partir del diagnóstico de la información proporcionada por las rutinas de VisualBALAN (entre otras el error cuadrático medio, *RMSE*), inspección visual y principio de parsimonia. La mejor parametrización está constituida por ocho parámetros seleccionados entre un total de catorce (Tabla 2). Los valores finales de los parámetros ajustados resultaron muy similares para las tres parcelas experimentales,

hecho que confirma la hipótesis inicial sobre la homogeneidad del tipo de suelos (Ramírez et al. 1999) y del relleno Cuaternario.

5.2. Balance hídrico y estimación de la recarga

El balance hídrico y la recarga para cada tipo de cultivo se calculó a partir del los modelos calibrados (periodo completo Oct 1999-Sept 2008). La Figura 2 muestra la evolución de la recarga anual para cada cultivo. Si se tiene en cuenta que la dosis de riego anual es prácticamente invariable a lo largo del tiempo, la variación en la recarga anual se explica a partir de la cantidad de precipitación producida. La recarga media para cultivos hortícolas es de 397 ± 70 mm [media ± desviación estándar] en anuales, de 201 ± 64 mm para perennes y 194 ± 75 mm para árboles frutales durante el periodo estudiado. Los valores de drenaje son muy similares a los resultados obtenidos por otros autores para este tipo de cultivos (Castel et al. 1987; Hanson et al. 1997; Lidón et al. 1999). Debido a la alta dosis y muy alta frecuencia de riego, el incremento de la recarga se produce durante los intensos episodios de lluvia, coincidiendo con importantes ascensos en los niveles (Figura 1). El rápido ascenso del nivel es debido al escaso espesor de zona no saturada en las parcelas experimentales, siendo 3, 11 y 8 m para *L y M*, *A* y *C*, respectivamente. Por otro lado el constante alto contenido de agua en el suelo, facilita el proceso de infiltración durante la lluvia. En los diagramas circulares se han representado valores medios correspondientes a los componentes del balance hídrico en cada cultivo y periodo estudiado (Oct 1999-Sept 2008). Se observa un valor alto de *In* en los cultivos hortícolas perennes y árboles frutales (debido a sus importantes valores de *LAI*). Destacar que Q_h y E_s son muy bajos en los tres casos, como era de esperar por observaciones de campo.

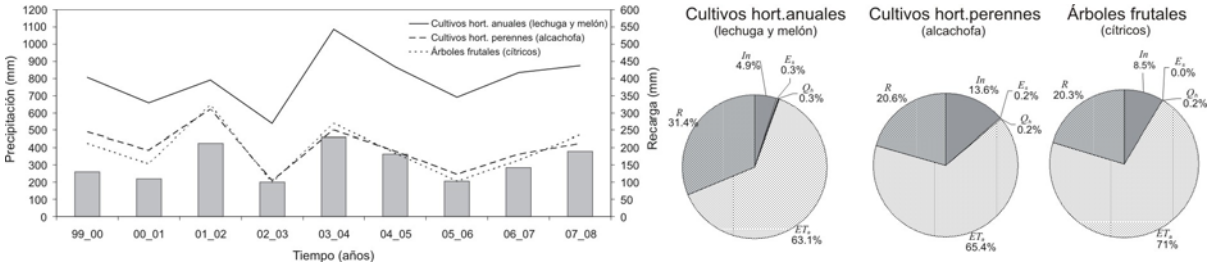

Figura 2. Evolución anual de la recarga para cada cultivo. Cantidad total de precipitación en cada año hidrológico (barras grises). Diagramas circulares con los valores medios de los diferentes componentes del balance hídrico para cada tipo de cultivo.

La Figura 1 muestra los valores acumulados de ET_p y ET_a para el último año hidrológico en los tres cultivos. El valor de ET_a fue generalmente más bajo que ET_p dada la imposibilidad del suelo en determinados momentos de mantener los valores de la T_p. Este hecho se presenta principalmente en cultivos hortícolas perennes, donde no existe riego en los meses de Julio y Agosto.

5.3. Análisis de sensibilidad

La perturbación de cada uno de los parámetros fue llevada a cabo considerando fijos el resto, valores obtenidos en el modelo calibrado (Tabla 2). El resultado del análisis muestra que de todos los parámetros incluidos en el modelo, la recarga es especialmente sensible a cinco de ellos: capacidad de campo *FC*, punto de marchitez *WP*, *CEME* (valor límite de déficit hídrico, entre *FC* y *WP*), Número de Curva y coeficiente de agotamiento del flujo hipodérmico α_h (ver Figura 3). Dado que el presente modelo considera cada parcela experimental como una sola celda, la recarga es solo sensible a los parámetros del suelo. La recarga sufre cambios de igual magnitud en los tres tipos de cultivo para perturbaciones en los parámetros *FC*, *WP*, *CEME* y α_h. El Número de Curva supone cambios en la recarga para cultivos hortícolas anuales y perennes, pero no en los árboles frutales.

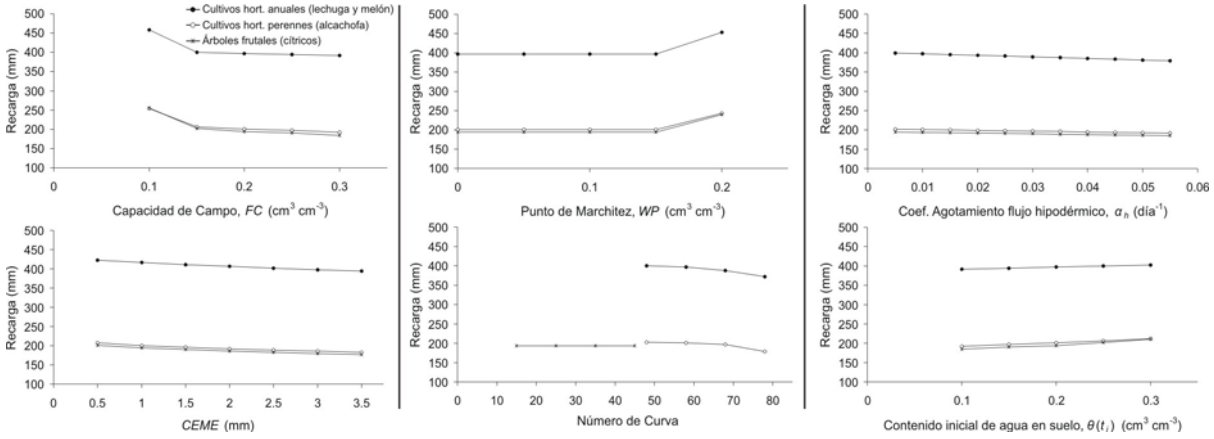

Figura 3. Sensibilidad de la recarga a la perturbación de varios parámetros (p) y condiciones iniciales (c. i.) para cada tipo de cultivo (solo mostrados los p y c. i. a los que es sensible la recarga)

El segundo paso del análisis de sensibilidad consiste en la perturbación de las condiciones iniciales (contenido inicial de agua en suelo $\theta(t_i)$, nivel inicial del acuífero h, volumen de agua almacenado por unidad de superficie en la zona no saturada V_h, nivel de referencia del acuífero h_0). En este caso la recarga fue sensible solo a $\theta(t_i)$, con un patrón de cambio similar para los tres cultivos.

Tabla 3. Resumen del análisis de sensibilidad relativa para las condiciones de contorno en cada tipo de cultivo

Condiciones contorno		Recarga					
		Cultivos hortícolas ANUALES		Cultivos hortícolas PERENNES		Árboles frutales	
Nombre	Cambio relativo (%) CP	Cambio relativo (%) AS	Sensibilidad relativa AS/CP	Cambio relativo (%) AS	Sensibilidad relativa AS/CP	Cambio relativo (%) AS	Sensibilidad relativa AS/CP
Precipitación, P	10	5.36	0.53	7.39	0.74	11.65	1.16
Evapotranspiración referencia, ET_0	10	9.04	0.90	10.03	1.00	5.57	0.56
Riego, Ir	10	15.08	1.50	16.42	1.64	8.47	0.41
Altura del cultivo	30	4.03	0.13	15.37	0.51	-	-

Para las condiciones de contorno fue desarrollado un análisis de sensibilidad relativo (Tabla 3). En este análisis se incluyeron: P, ET_0, Ir y altura de la planta. Efectos debidos a temperatura, número de horas de sol, velocidad del viento, humedad relativa ambiental o albedo quedan incluidos en ET_0. K_c causa efectos similares a los de ET_0, de acuerdo con la Ec. (1) dada la relación existente entre estos parámetros. Al contrario de lo que cabría esperar, el cambio más importante no siempre lo produce Ir, como es en el caso de los árboles frutales donde lo fue P.

6. CONCLUSIONES

El retorno de riego supone una parte sustancial de la recarga a los acuíferos en zonas semi-áridas con agricultura intensiva, como ocurre en el Campo de Cartagena y cuya precipitación anual es del orden de 300 mm. Sin embargo, las intensas lluvias que de forma episódica se producen en estas zonas juegan un papel fundamental. Los valores medios de recarga a partir del agua aplicada (precipitación + riego) para el periodo estudiado (Oct 1999-Sept 2008) fueron de 397, 201 y 194 mm para cultivos hortícolas anuales, cultivos hortícolas perennes y árboles frutales respectivamente, superiores a las estimaciones previas existentes. La aplicación del regadío en función del estado de humedad del suelo, condiciones climáticas y necesidades hídricas de los cultivos, podría reducir significativamente la recarga por retorno de riego.

En comparación con otras técnicas habituales, la aplicación del modelo en esta zona ha demostrado ser una herramienta de gran utilidad y sencilla aplicación para la estimación de la recarga en condiciones de regadío.

Agradecimientos. Este trabajo ha sido desarrollado dentro de los proyectos CGL-2004-05963-C04-01 y CGL2007-66861-C04-03, plan nacional I+D+I del Ministerio de Ciencia e Innovación. También queda incluido en el marco del proyecto 08225/PI/08 "Programa de Generación del Conocimiento Científico de Excelencia" Fundación Seneca, Región de Murcia (II PCTRM 2007-10).

REFERENCIAS

Allen, R.G., Pereira, L.S., Raes, D., Smith, M., 1998. *Crop evapotranspiration. Guidelines for computing crop water requirements.* Irrigation and Drainage. Paper No. 56, FAO, Rome, Italy.

CARM, 2007. *El Agua y la Agricultura en la Región de Murcia. Un Modelo de Eficiencia*. Consejería de Agricultura y Agua de la Región de Murcia. pp. 111.

CARM, 2008. Consejería de Agricultura y Agua de la Región de Murcia. Datos estadísticos agrarios. Disponible: <http://www.carm.es>.

Carrica, J. C. y Lexow, C., 2004. Evaluación de la recarga natural al acuífero de la cuenca superior del arroyo Napostá Grande, Provincia de Buenos Aires. *Revista de la Asociación Geológica Argentina, 39 (2)*, 281-290.

Castel, J.R., 2001. Consumo de agua para plantaciones de cítricos en Valencia. *Fruticultura profesional, 123*, 27-32.

Castel, J.R., Bautista, I., Ramos, C., Cruz, G., 1987. Evapotranspiration and irrigation efficiency of mature orange ochards in Valencia (Spain). *Irrig. Drain. Syst. 3*, 205-217.

CHS, 2008. Confederación Hidrografica del Segura. Datos piezométricos. Disponible: <http://www.chsegura.es>.

Gracía-Santos, G., Mazol, V., Morales, D., Gómez, L. A., Pisani, B, Samper, J., 2005. Groundwater recharge in a mountain cloud laurel forest at Garajonay National Park (Spain). *Geophysical Research Abstract, Vol. 7*, 00942.

Garatuza-Payán, J., Shuttleworth, W.J., Encinas, D., McNeil, D.D., Stewart, J.B., DeBruin, H., Watts, C., 1998. Measurement and Modelling evaporation for irrigated crops in Northwest Mexico. *Hydrol. Process. 12*, 1397-1418.

Hanson, B.R., Schwankl, L.J., Schulbach, K.F., Pettygrove, G. S., 1997. A comparison of furrow, surface drip irrigation on lettuce yield and applied water. *Agric. Water Manage. 33*, 139-157.

IGME, 1994. *Las aguas subterráneas del Campo de Cartagena (Murcia)*. IGME, Madrid, España, 62 pp.

Jiménez, J., García, G., Queralt, I., Aragón, R., García-Arostegui, J. L., Solano, F., Candela, L., 2007. Vadose zone characterization in an experimental plot under intensive agriculture. Preliminary results. International conference WAter POllution in natural POrous media at different scales (WAPO2). Publicaciones del Instituto Geológico y Minero de España. Serie: Hidrogeología y Aguas Subterráneas. Nº 22. 143-148.

Jiménez-Martínez, J., Skaggs, T.H., van Genuchten, M.Th., Candela, L., 2009. A root zone modelling approach to estimating groundwater recharge from irrigated areas. *J. Hydrol. 367 (1-2)*, 138-149.

Lidón, A., Ramos, C., Rodrigo, A., 1999. Comparison of drainage estimation methods in irrigated citrus ochards. *Irrig. Sci. 19*,25-36.

López, J., 1997. Evaluación de la recarga por cambios en la cobertura vegetal. En: Custodio, E., Llamas, R., Samper, J. (Eds.), La evaluación de la recarga a los acuíferos en la Planificación Hidrológica. Series ITGE, Madrid, España. pp. 455.

Ramírez, I., Vicente, M., García, J., Vaquero, A., 1999. *Mapa digital de suelos de la Región de Murcia*. Consejería de Agricultura, Agua y Medio Ambiente. Guía y CD-ROM. pp. 78.

Samper, J., García Vera, M. A., Pisani, B., Varela, A., Losada, J. A., Alvares, D., Espinha Marques, J., 2007. Using hydrological models and Geographic Information Systems for water resources evaluation: GIS-VISUAL-BALAN and its application to Atlantic basins in Spain (Valiñas) and Portugal (Serra da Estrela). En: Lobo Ferreira, J. P., Vieira, J. M. P. (Eds.), Water in Celtic Countries: Quantity, Quality and Climate Variability. *IAHS 310*, 259-266.

Samper, J., Huguet, Ll., Ares, J., García Vera, M.A., 2005. Manual Usuario. VisualBALAN v.2.0: Código interactivo para la realización de balances hidrológicos y la estimación de la recarga. pp 150.

Sánchez, M.I., López, F., Del Amor, F., Torrecillas, A., 1989. La evaporación y evapotranspiración en el Campo de Cartagena y Vega Media del Segura. Primeros resultados. *Anales de Edafología y Agrobiología*, 1239-1251.

Scanlon, B.R., Healy, R.W., Cook, P.G., 2002. Choosing appropriate techniques for quantifying groundwater recharge. *Hydrogeol. J. 10*, 18-39.

SIAM, 2008. Servicio de Información Agraria de Murcia. Datos climáticos. Disponible: <http://siam.imida.es>.

Soil Conservation Service, 1975. Engineering field manual conservation practices. U. S. Department of Agriculture.

A 3D geological model of the Campo de Cartagena, SE Spain: Hydrogeological implications

J. Jiménez-Martínez[1*]; L. Candela[1], J.L. García-Aróstegui[2] and R. Aragón[2]

[1]Department of Geotechnical Engineering and Geosciences, Technical University of Catalonia, UPC, Jordi Girona 1-3, 08094 Barcelona, Spain. * Corresponding author: E-mail: joaquin.jimenez@upc.edu

[2]Geological Survey of Spain, IGME, Murcia Office. Avda. Miguel de Cervantes, 45, 30009, Murcia, Spain

ABSTRACT. Knowledge and understanding of geologic basins for hydrogeologic purposes requires an accurate 3D geological architecture representation. For model building, surface and subsurface data integration with the interpretation of geophysical survey and lithologic logs is needed. A methodology to reconstruct geometric architecture of the sedimentary basin and relationships among stratigraphic formations, as well as to define hydrostratigraphic units has been applied to the Campo de Cartagena Neogene formations. Data analysis included seismic reflection profiles and gravimetric data from oil exploration, electric resistivity surveys and 491 lithologic logs. The 3D model obtained from a close integration of stratigraphic and geophysical data was generated through a computer-based tool. It presents a common framework and a good starting point for hydrogeologic applications.

KEYWORDS: stratigraphy, hydrostratigraphy, 3D visualization, Campo de Cartagena

1. INTRODUCTION

In arid and semi-arid regions, water requirements for human and ecosystem needs are usually covered by existing aquifer resources. This fact implies an adequate management of the groundwater system, which first of all relies on a geologic formation

and requires an accurate knowledge (Frind et al., 2002). A thorough understanding of the geological structure is essential for groundwater flow system characterisation and to draw up appropriate strategies to expand the scope of water protection, and to achieve good ecological and chemical status (Directives 2000/60/EC and 2006/118/EC). Geological conceptual model assumptions greatly condition groundwater flow models and as a result may lead to incorrect outcomes (Robins et al., 2005). Also, presence of heterogeneities in geological records, usually associated with facies changes, conditions groundwater hydrodynamic (Cabello et al., 2007). Therefore, accurate knowledge of the geological formations, geometrical aspects, spatial relationship among them, and presence of tectonic features that deform them are essential (Gámez, 2007). Although for hydrogeologic numerical models the analysis and representation of geological architecture are often made on a 2D basis, a 3D analysis is necessary to gain a better understanding of complex geological systems.

The subsurface geophysical survey techniques constitute a powerful tool to determine the geometry of lithological formations, reducing the geologic uncertainty among wells and improving the 3D subsurface knowledge (Martelet et al., 2004). A close integration of stratigraphic and geophysical data helps to determine presence of confining layers as well as the subsurface aquifers and aquitards. However, this is not an easy task, due to the heterogeneity of the data, and applications still represent a significant challenge to be overcome (Ross et al., 2005).

The aim of this research is to establish the 3D subsurface geometry and hydraulic relationship of the different aquifer units that form the Campo de Cartagena, by combining information provided by stratigraphic logs, geophysical data and surface geology. The Campo de Cartagena plain (SE of Spain), located in a semi-arid region where the primary land use is intensive irrigated agriculture (CARM, 2008), is

characterised by an intensive groundwater exploitation and man-made pollution. The established 3D geological model will provide a common initial framework for hydrogeologic applications.

2. CAMPO DE CARTAGENA

2.1 Study area

The Campo de Cartagena basin is a 1440 km^2 plain with elevations ranging between sea level and 1065 m.a.s.l. located in the Southeastern part of Mediterranean Spain (Fig. 1). To the South and East the area is limited by the Mediterranean Sea, and by low mountain ranges to the North and West. The region is characterised by a semi-arid Mediterranean climate, with an average temperature of 18 ºC and 300 mm of annual rainfall which is unevenly distributed into a few intense events that are highly variable in space and time. Rainfall is mainly produced during spring and autumn. Agriculture is the primary land use, with drip irrigation widely used in the region due to a scarcity of water resources and the need for water conservation. No permanent watercourse exists and the area is drained by several ephemeral streams. The population's water supply mainly relies on groundwater resources and the *Tajo-Segura water transfer*, which transfer water from the *Tajo basin* (central part of Spain) to the study region and was initiated in 1980. Water resources from private (owned by farmers) desalination plants of brackish groundwater have greatly increased since 2005.

2.2 Geological setting

The area constitutes a Neogene and Quaternary sedimentary basin located in the Eastern part of the Betic Cordillera. The detrital sedimentary rocks are unconformably laid over three metamorphic complexes that conform the Internal Zones of the

77 cordillera. The metamorphic complexes are from bottom to top: Nevado-Filábride,
78 Alpujárride and Maláguide (Fig. 1). The Nevado-Filábride Complex is mainly
79 composed by marbles and mica-schists of Palaeozoic, Permian and Triassic age; it
80 outcrops in the Cartagena-La Unión and Los Victorias mountain ranges to the South and
81 West of the study area respectively (Ovejero et al., 1976; Manteca and Ovejero, 1992;
82 Manteca et al., 2004). The Alpujárride Complex, outcropping in the Cartagena-La
83 Unión and Carrascoy mountain ranges (North), is composed by schists, marbles,
84 phyllites and quartzites of Permian and Triassic age (López-Garrido et al., 1997; Sanz
85 de Galdeano et al., 1997; García-Tortosa et al., 2000a, García-Tortosa et al., 2000b).
86 Finally, the Maláguide Complex is formed by Permian and Triassic sandstones,
87 quartzites, silts, conglomerates and limestones and outcrops in the northern part of the
88 area (García-Tortosa et al., 2000c).
89 The NE-SW to E-W normal faults rupturs the bedrock, developing several horst
90 and graben structures, as the Cabezo Gordo and Riquelme *horsts* or Torre Pacheco and
91 San Javier *grabens* (Rodríguez Estrella, 1986; Rodríguez Estrella and Lillo, 1992). The
92 block structure (*horst* and *graben*) is also observed in the Cartagena-La Unión mountain
93 range (Robles-Arenas et al., 2006). During the Tortonian, dacites and basalts flows,
94 result of the volcanic eruption favoured by fractures as a consequence of the tectonic
95 activity, were deposited in the Southern part of the basin (Duggen et al., 2005).
96 The Neogene sedimentary rocks, with a thickness of 2000 m, are lightly folded
97 by settlement. Overlying the Neogene sedimentary rocks, the Quaternary sediments
98 cover great part of the surface of Campo de Cartagena, which are affected by the recent
99 tectonic activity at local sites (Giménez, 1997). The sedimentary infill was divided in
100 stratigraphic units by several authors, based on oil companies, and summarized in
101 IGME (1994). To establish hydrostratigraphic units in the present work, the new

stratigraphic units redefined by IGME (2005) according to litostratigraphic and paleontologic criteria have been used (Table 1). The observed stratigraphic variability and structural complexity of the area has important implications for the conceptual hydrogeological model establishment.

2.3 Hydrogeological framework

The sedimentary infill of the basin is mainly composed by detrital, low-permeability sediments (marls) with interlayered high-permeability material (limestones, sands and conglomerates) deposited during the Tortonian through to the Quaternary period. Sands and conglomerates of Tortonian age, organic limestones of Messinian and sandstones deposited during the Pliocene constitute the potential aquifer materials. The Quaternary sediments are also detrital and form the upper unconfined aquifer (ITGE, 1994). Therefore, the hydrogeologic system is constituted by deep confined aquifers (Tortonian, Messinian and Pliocene age) and a Quaternary unconfined shallow aquifer (ITGE 1991; Rodríguez Estrella, 1995). The deep aquifers are an important source of water, which is processed by private desalination plants mainly in the case of one of them (Pliocene), while the unconfined aquifer is barely exploited due to contamination by agrochemicals from irrigation return flows. High pumping rates from desalination plants, pollution by agrochemicals, along with aquifers connected through poorly constructed wells (Jiménez-Martínez et al., 2010), constitute the main hydrogeological problems in the area.

3. METHODOLOGY AND DATA GATHERING

The initial step was to carry out an intensive search of available literature, current investigations taking place in the area and other sources of information. Many

surveys conducted by public agencies and oil exploration companies were not research-oriented. Useful information include a great number of published and unpublished reports, which are confidential to a greater or lesser extent, covering geologic mapping, geophysical data and geologic logs.

To build the 3D subsurface geological and hydrogeological model, a wide range of geophysical records based on measurement variations of the electrical properties of sub-soil materials (VES, ETR) and density, and lithological columns from well logs were compiled. The geologic information was standardised according to the stratigraphic units and criteria (lithology, fossil content, etc) defined by IGME (2005) and López-Bermúdez and Conesa-García (1990) (Table 1) to facilitate correlation between geologic boreholes and geophysical data. The applied stratigraphic criteria and descriptions agree with those of other similar basins on the Mediterranean coast (Friend and Dabrio, 1996).

3.1. Geologic boreholes and stratigraphic logs

A total of 491 geologic borehole logs were collected for further stratigraphic examination and sedimentary basin reconstruction. Boreholes were mainly carried out for groundwater exploration purposes under rotary, percussion and percussion-rotary drilling where continuous stratigraphic logs were rarely recorded. Borehole density increases from inland towards the coast as well as in agricultural areas. The drilled depth for groundwater exploration varies between a few meters up to 750 m. Two wells for oil exploration reaching more than 1000 m of depth (Ini-Coparex, 1967 and 1970) through which loggings were developed (self potential, resistivity, sonic log, gamma ray and neutron log), helped to improve the lithology characterisation and hydraulic

properties. Moreover, an additional borehole (982 m deep) for deep brine injection (Ramos and Sánchez, 2003) was also analysed.

3.2. Geophysical data

The following geophysical surveys were obtained and further analysed in order to understand the deep structure of the Campo de Cartagena basin: Seismic reflection profiles, Vertical Electrical Soundings-VES, Electrical Tomography Resistivity-ETR (Loke and Barker, 1996; Loke, 2000), residual and Bouguer gravimetric maps, and Thermal Remote Tomography-TRT (Rolandi et al., 2008).

Seismic reflection profiles

Sepesa (1968) and Chevron Oil (1982, 1984, 1985 and 1986) carried out a large number of seismic refection studies in the area. Only three of them (S-84-58; MM-1 and S-85-82) are shown in Fig. 2. Lengths of profiles are generally greater than 10 km and no spatial surface pattern is observed. The maximum exploration was of 3000 m, where the MM survey (Sepesa, 1968) is less accurate than the S survey (Chevron, 1982, 1984, 1985 and 1986).

The processing and interpretation of reflection profiles based on the analysis of the seismic signal against travel time, considering models of velocity [double time (milliseconds) vs. depth] obtained from deep oil exploration boreholes, provides estimates of the thickness, layering, depth and facies changes of geologic materials besides basin boundary delineation.

For the identification of the different deeply buried geophysical units and basin structural and stratigraphic information, data analysis followed the classical seismic procedure (i.e. reflection endings, erosional truncation, onlap, downlap and configurations).

176 ***Electrical resistivity profiles***

177 The IGME (1983) electrical resistivity measurements here analysed, a
178 continuation of a previous one developed in 1976 by IGME, consists of 150 VES
179 grouped into 5 profiles in a linear transect. Besides, in November 2007, an ETR survey
180 to assess the lateral extent of geologic formations at the Southern limit of the basin was
181 carried out (Jiménez-Martínez et al., 2008). A total of 6 profiles of apparent resistivity
182 with a maximum length of 470 m and a maximum exploration depth of 96 m were
183 obtained.

184 ***Gravimetric data***

185 The Bouguer anomaly reveals the presence of masses with densities differing
186 from earth average by large and local variations. A regional anomaly is due only to
187 large-scale changes such as crustal thickening or thinning, while a residual anomaly
188 expresses the presence of local rock bodies without the influence of changes in the
189 crustal properties. The residual gravimetric anomalies constitute a useful tool to
190 determine the geometry of geological formations (Duque et al., 2008). Residual and
191 Bouguer anomaly maps were developed by Chevron Oil Company Spain during 1984-
192 1986. Density variations between sediments and basement allowed the measurements
193 interpretation in terms of shape, size and position of subsurface structures (ITGE, 1989).

194

195 **4. APPROACH**

196 The three-dimensional architecture of the basin was generated through a
197 graphical interface (AutoCad®). The first step was the identification and definition of
198 hydrostratigraphic units and the establishment of geologic correlations among them,
199 based on the Neogene stratigraphic units previously defined by IGME (2005) and the
200 Quaternary (López-Bermúdez and Conesa-García, 1990) (Table 1). Recorded

information from the existing borehole data base was not very useful due to the low quality (or absence) of geologic descriptions. This fact also made the establishment of correlation between them a complex task (Fig. 3).

Subsurface lithological changes and sediment thickness estimation was further performed by a joint analysis of gravimetric and seismic profiles and lithological logs from well characterised boreholes (Fig. 2). Results from VES and ETR also allowed a decrease in the subsurface uncertainties (geometry and lithology) between wells, by providing geophysical records to assess stratigraphic correlation. It needs to be mentioned that in some VES, the high salinity of water-bearing sediments, the presence of paleo-groundwater, and man-made pollution, all contributed to compromising the final interpretation. The presence of saline water overpowers the signal given by a lithology.

Finally, 16 geo-referenced geological cross-sections integrating all reliable data, surface and subsurface information (geological boreholes, seismic profiles, gravimetric data, VES and ETR), were used to build a 3D model. Figure 4 shows the constructed diagram; only lower boundaries of the stratigraphic units are presented.

5. GEOLOGICAL MODEL AND HYDROGEOLOGICAL IMPLICATIONS

5.1 Geological model

The unconsolidated Quaternary sediments cover the greater part of the Campo de Cartagena surface. Neogene rocks outcrop in the Northern part of the study area and are slightly dipping under the Quaternary. They are unconformly deposited over the basement materials and present several open folds as a result of bedrock settlement (Fig. 5). Neogene materials are also highly deformed by faults and joints, in some cases also affecting the Quaternary.

The geologic structure of the area is rather complex. Two principal grabens, Torre-Pacheco and San Javier, and horsts, Cabezo Gordo (that crops out) and Riquelme, are the most important structural features of the bedrock. The Torre-Pacheco sub-basin is characterised by the presence of two depocentres reaching a thickness of 2000 m, located to the NW of Los Martínez village and a third depocentre with a thickness of 2300 m located to the SW of Los Alcazares. The San Javier sub-basin has only one depocentre of 2000 m thick located 5 km to the NW of San Javier (Fig. 6).

The relationship between sedimentary infill of Quaternary and Neogene age at the basin boundaries is principally controlled by faults and basal unconformities. The *"Cartagena-La Unión fault"* (Manteca and García, 2001) and other existing structural features, together with the metamorphic rocks of the Cartagena-La Unión mountain range (Jiménez-Martínez et al., 2008), characterise the sedimentary basin Southern limit. A similar structural relationship with Los Victorias mountain range can be identified in the Western part (see section M Fig. 5). Presence of faults in the surroundings of Mar Menor (a hyposaline coastal lagoon) has been indicated by published works (Rodríguez Estrella, 1983, 1986 and 2004; Rodríguez Estrella and Lillo, 1992, Rolandi et al., 2008), whilst further North at the basin contact with the Mediterranean Sea, they have not been observed. Regrettably, for the present model the presence of faults cannot be confirmed due to the lack of seashore geologic and geophysical information.

5.2 Hydrostratigraphic units

From the data set analysis of the Neogene and Quaternary sedimentary package and stratigraphic units, eight hydrostratigraphic aquifer units (*Qt*; *LT*; *VLV*; U_{TCL}; *Co*; *PC*, *CG* and *ER*) and six aquitard units (U_{LT}; *EE*; L_{VLV}; *TLC*; *LGC* and *At*) were defined.

The hydroestratigraphic units, mainly of detrital origin, range from middle Miocene to the Quaternary. A summary of the associated stratigraphic formation; lithology and hydraulic characteristics are presented in Table 1. Aquifer unit areal extensions have been plotted in Fig. 7; Table 2 presents the principal geometric characteristics derived from this work and hydraulic properties obtained from previous works (IGME, 1994) and pumping test analyses (Rodríguez-Estrella et al. 2004; unpublished data) for each defined unit. It needs to be mentioned that due to the remarkable spatial variability of the geologic media, those values must be considered in many cases as punctual estimates.

In the I-III stratigraphic unit, four aquifer units are distinguished from bottom to top: *ER*, conglomerate and sandstone; *CG*, conglomerate; *PC*, sandy limestone and conglomerate; *Co*, sandstone. The areal extent of the *ER*, *CG*, *PC* and *Co* aquifer units below the Campo de Cartagena coastal plain is not known accurately as they also show lateral facies changes among them. Their presence appears to be limited to some lithological columns and small reflections detected in the seismic profiles (Fig. 7). For the aquifer units *PC* and *Co*, respectively, lateral facies changes are observed to the centre of the basin, as illustrated in the H and C cross-sections (Fig. 5). All aquifer units pinch out towards the SE of the area.

Within the stratigraphic unit IV, a local aquifer unit of approximately 40 m thickness, U_{TLC}, composed of oolitic limestone, has been also identified.

The stratigraphic unit V presents a single aquifer unit, *VLV*, constituted by sandstone which is only present in the mid-North of Campo de Cartagena. The *VLV* unit presents two different lower aquitards depending of the sub-basin: the L_{VLV} unit in the San Javier sub-basin, and the *TLC* unit in the Torre-Pacheco sub-basin. The Cabezo Gordo horst outcrops in the Southern part of the *VLV* aquifer unit surface extension,

276 formed by marbles and limestone of the basement. The hydraulic connection between
277 the aquifers and the basement materials is unknown. To the East, the unit is deeping
278 under the Mediterranean Sea, but neither geologic, structural nor stratigraphic
279 information exists. The *VLV* aquifer unit has not being observed in the mid-South of the
280 study area (Fig. 7). This fact supports the structural control by a fault hypothesis stated
281 in previous works (ITGE 1989, 1991 and 1994); the movement along the fault would
282 move down the VLV aquifer unit to the mid-South of the Campo de Cartagena. As the
283 fault has not been detected neither in the S-84-58 seismic profile (Chevron, 1984) (Fig.
284 3) nor in G cross-section (Fig. 5), and given the lack of information supporting the
285 tectonic feature, the authors consider a lateral facies change to be the best explanation.
286 The stratigraphic unit VI presents a single aquifer unit, *LT*, constituted by
287 sandstone. The *LT* aquifer unit practically covers the entire area of the Campo de
288 Cartagena (Fig. 7), except in the surroundings of the Los Victorias mountain range
289 (Western area, see cross-section M in Fig. 5), where sandstone changes to silt, clay and
290 conglomerate (Mora et al., 1988). The hydraulic relation with Cabezo Gordo horst and
291 Los Victorias mountain range (partially formed by marbles and limestone) is unknown.
292 At the Northeastern part, the *LT* aquifer unit is hydraulically disconnected from the rest
293 of the unit and it is named Cabo Roig aquifer (Fig. 7). The Mar Menor boundary is
294 conformed by faults which may act as hydraulic barriers avoiding seawater intrusion in
295 the aquifer (Rodríguez Estrella, 1983, 1986, 2004; Rodríguez Estrella and Lillo, 1992;
296 Rolandi et al., 2008). Further to the North, in contact with the Mediterranean Sea,
297 presence of faults has not been detected.
298 Finally, the stratigraphic unit Q, *Qt* aquifer unit, outcrops over almost the entire
299 Campo de Cartagena area. It constitutes the upper unconfined aquifer (Fig. 7), receiving
300 natural recharge from precipitation and by irrigation return flow. To the Southern

301 border, geometric relationships between the *Qt* aquifer unit and the Cartagena-La Unión
302 mountain range (derelicted mining area) present structural features similar to Neogene
303 materials (faults and basal unconformities). However, the hydraulic connection still
304 remains unknown, a potential risk of pollution by heavy metals and sulphurs may exist
305 (García, 2004; Robles-Arenas, 2006).
306
307 **6. CONCLUSIONS**
308 Representation and analysis of geological architecture for specific applied
309 research, for example groundwater modelling, are often simplistic approximations of
310 real aquifer geometry. Generally, numerical model restrictions condense or simplify
311 details. However, a detailed 3D basin study analysis integrating more interrelated
312 concepts from different disciplines is necessary to gain a better understanding of
313 geological systems. To build the stratigraphic architecture of the basins, to identify the
314 potential aquifer formations and to discuss the relationship between aquifer formations
315 and the bedrock, both geophysical and geological information and well-log data are the
316 basic tools. Integration of applied geophysical techniques with stratigraphic data allows
317 more accurate prediction of changes in subsurface geology.
318 For the Campo de Cartagena basin, the integration of a large dataset of
319 geophysical surveys and lithological logs has allowed a detailed geometric definition of
320 aquifer and aquitard units. Data analysis has provided new insights for reducing the
321 uncertainty associated with basin geometry characterisation and geologic
322 heterogeneities, previously defined in other studies as tectonic features and more
323 recently in this work many of them as lateral facies changes. The implication is obvious.
324 For a more precise geologic interpretation and in consequence a more accurate
325 hydrogeological model, lateral facies changes are the basis for the system

326 understanding. Results also allowed establishing the principal differences between the
327 San Javier and Torre-Pacheco sub-basins.

328 In the Campo de Cartagena basin there are multiple aspects that still require a
329 more detailed study. Offshore data, for the *VLV* and *LT* aquifer units continental and
330 marine data correlation, are needed for assessing aquifer-sea connection and
331 vulnerability to seawater intrusion due to natural or pumping conditions along the entire
332 shoreline. As observations are incomplete, a deeper investigation of the Cartagena-La
333 Unión Southern boundary mechanisms, that may increase the aquifer potential risk to
334 heavy metals and sulphurs contamination from the abandoned mining area, is necessary.
335 Finally, relationships between the Neogene sedimentary package aquifer units and the
336 basement, and the areal extension of aquifer units beneath the Campo de Cartagena
337 plain, require a thorough investigation.

338 The obtained results on aquifer geometry and hydraulic parameters constitute a
339 good starting point to all kind of future hydrogeologic studies raised in the Campo de
340 Cartagena basin: to redesign the groundwater level and quality monitoring network;
341 numerical flow and agrochemical contaminants transport model. The applied approach
342 and the sedimentological aspects shown in this paper may be transferred to similar
343 Neogene basins existing in the circum-Mediterranean area.

344

345 **ACKNOWLEDGEMENTS**

346 This work has been developed under the framework of the CGL-2004-05963-C04-01
347 and CGL2007-66861-C04-03 research projects, financed by Ministry of Science and
348 Innovation (Spain). It also is included within of the 08225/PI/08 research project
349 financed by “Programa de Generación del Conocimiento Científico de Excelencia” of
350 Fundación Seneca, Región de Murcia (II PCTRM 2007-10). Gratitude is expressed to

A. Pedrera (Geological Survey of Spain) and D. Collins (Kansas Geological Survey), as well as the reviewers E.O. Frind (University of Waterloo) and C. Duque (University of Copenaghen) for helpful comments on the paper.

REFERENCES

Cabello, P., Cuevas, J.L., Ramos, E., 2007. 3D modelling of grain size distribution in Quaternary deltaic deposits (Llobregat Delta, NE Spain). Geologica Acta, 5(3), 231-244.

CARM, 2008. Consejería de Agricultura y Agua de la Región de Murcia. Agrarian Statistics Data. Available from: <http://www.carm.es>.

CHEVRON, 1982. S-82 Seismic Survey. Fondo Documental del Archivo de Hidrocarburos del Ministerio de Industria, Turismo y Comercio.

CHEVRON, 1984. S-84 Seismic Survey. Fondo Documental del Archivo de Hidrocarburos del Ministerio de Industria, Turismo y Comercio.

CHEVRON, 1985. S-85 Seismic Survey. Fondo Documental del Archivo de Hidrocarburos del Ministerio de Industria, Turismo y Comercio.

CHEVRON, 1986. Seismic Survey S-86. Fondo Documental del Archivo de Hidrocarburos del Ministerio de Industria, Turismo y Comercio.

376 Duggen, S., Hoernle, K., van den Bogaard, P., Garbe-Schönberg, D., 2005. Post-
377 Collisional Transition from Subduction to Intraplate-type Magmatism in the
378 Westernmost Mediterranean: Evidence for Continental-Edge Delamination of
379 Subcontinental Lithosphere. Journal of Petrology, 46(6), 1155-1201.
380
381 Duque C., Calvache M. L., Pedrera A., Martín Rosales W., López-Chicano M., 2008.
382 Combined time domain electromagnetic soundings and gravimetry to determine marine
383 intrusion in a detrital coastal aquifer (Southern Spain). Journal of Hydrology, 349, 536-
384 547.
385
386 European Community, 2000. The Water Framework Directive 2000/60/EC of the
387 European Parliament and of the Council of Establishing a Framework for Community
388 Action in the Field of Water Policy, European Community, Brussels.
389
390 European Community, 2006. Directive 2006/118/EC of the European Parliament and of
391 the Council on the protection of groundwater against pollution and deterioration,
392 European Community, Brussels.
393
394 Friend, P. J., Dabrio, D. J., 1996. Tertiary basins of Spain: the stratigraphic record of
395 crustal kinematics. Cambridge University Press, 400 pp.
396
397 Frind, E.O., Muhammad, D.S., Molson, J.W., 2002. Delineation of three dimensional
398 well capture zones for complex multi-aquifer systems. Ground Water, 40(6), 586–598.
399

Gámez, D., 2007. Sequence stratigraphy as a tool for water resources management in alluvial coastal aquifers: application to the Llobregat delta (Barcelona, Spain). Doctoral Thesis. Technical University of Catalonia, 177 pp.

García, C., 2004. Impacto y riesgo ambiental de los residuos minero-metalúrgicos de la Sierra de Cartagena-La Unión (Murcia-España). Doctoral Thesis. Polytechnical University of Cartagena, 424 pp.

García-Tortosa, F.J., López-Garrido, A., Sanz de Galdeano, C., 2000a. Las unidades de Cabo Tiñoso y Peñas Blancas: Revisión y caracterización estratigráfica de las unidades alpujárrides del sector entre Mazarrón y Cartagena (Murcia, España). Estudios Geológicos, 56, 31-40.

García-Tortosa, F.J., López-Garrido, A., Sanz de Galdeano, C., 2000b. Las unidades alpujárrides y maláguides entre Cabo Cope y Cabo de Palos (Murcia, España). Geogaceta, 28, 67-70.

García-Tortosa, F.J., López-Garrido, A., Sanz de Galdeano, C., 2000c. Présence du complexe tectonique Malaguide à l'est de Carthagène (zone interne Bétique, Espagne). C.R. Acad. Sci. Paris, Sciences de la Terre et des Planètes. Earth and Planetary Sciences, 330, 139-146.

Giménez, J., 1997. Quantificació de les deformacions verticals recents a l'Est de la Península Ibèrica a partir d'anivellaments topogràfics de precisió. Doctoral Thesis. University of Barcelona, 364 pp.

IGME, 1983. Campaña de prospección geofísica en el Campo de Cartagena (Murcia). Sondeos Eléctricos Verticales. Technical report (unpublished).

IGME, 2005. Estudio de la información geológica y geofísica del subsuelo (sísmica de reflexión y sondeos) en el sector SE de la Provincia de Murcia. Consejería de Industria y Medio Ambiente de la Región de Murcia. 37 pp. Annex 1-37. Technical report (unpublished).

INI-COPAREX, 1967. San Miguel de Salinas 1 Borehole. Fondo Documental del Archivo de Hidrocarburos del Ministerio de Industria, Turismo y Comercio.

INI-COPAREX, 1970. San Miguel de Salinas 2 Borehole. Fondo Documental del Archivo de Hidrocarburos del Ministerio de Industria, Turismo y Comercio.

ITGE, 1989. Geometría de los acuíferos del Campo de Cartagena (Murcia) Volume 1/3 Memory. Volume 2/3 Maps. Volume 3/3 Annex: inventario de puntos de agua. Technical report (unpublished).

ITGE, 1991. Estudio Hidrogeológico del Campo de Cartagena (2ª Fase). Volume 1/2 Memory. Volume 2/2 Annex 1, 2, 3 and 4. Technical report (unpublished).

ITGE, 1994. Las aguas subterráneas del Campo de Cartagena (Murcia). ITGE, 62 pp.

449 Jiménez-Martínez, J., Aravena, R., Candela, L., 2010. The role of leaky boreholes on
450 the contamination of a regional confined aquifer: A case study in the Campo de
451 Cartagena region, Spain. Water, Air & Soil Pollution. doi: 10.1007/s11270-010-0480-3.
452
453 Jiménez-Martínez, J., Himi, M., Robles-Arenas, V.M., Díaz, Y., Casas, A., Candela, L.,
454 2008. Identificación mediante tomografía eléctrica del límite geológico entre el Campo
455 de Cartagena y la Sierra de Cartagena-La Unión. In: Pérez Torrado, F. and Cabrera
456 Santana M.C. (eds.) VII Congreso Geológico de España, Las Palmas de Gran Canaria.
457 Geotemas, 10, 295-298.
458
459 Lambán, J.L., Aragón, R., 2003. Estado de la intrusión marina en el Campo de
460 Cartagena: evaluación preliminar a partir de la composición química del agua
461 subterránea. In: Proceedings of Coastal Aquifers Intrusion Technology: Mediterranean
462 Countries (TIAC'03). IGME Book series, Madrid, 345-355.
463
464 Loke, M.H., Barker R.D., 1996. Rapid least-squares inversion of apparent resistivity
465 pseudosections by a quasi-Newton method. Geophysical Prospecting, 44(1), 131-152.
466
467 Loke, M.H., 2002. RES2DINV. Rapid 2D Resistivity & IP Inversion. Geoelectrical
468 Imaging 2D & 3D. Geotomo Software.
469
470 López-Bermúdez, F., Conesa-García, C., 1990. Características granulométricas de los
471 depósitos aluviales en el Campo de Cartagena. Cuadernos de Investigación Geográfica,
472 16, 31-54.
473

López-Garrido, A. C., Pérez López, A., Sanz de Galdeano, C., 1997. Présence de Facies Muschelkalk dans des unités Alpujarrides de la région de Murcie (Cordillere Bétique, SE de I'Espagne) et implications paléogéographiques. C. R. Acad. Sc. Paris. Sér. l1a., 324, 647-654.

Manteca, J.I., García, C., 2001. La falla de Cartagena-La Unión. Aportación visual de su existencia gracias a una obra pública. In: F. Guillen and A. Del Ramo (eds.). Patrimonio Geológico, Cultura y Medio Ambiente. University of Murcia, 239-246.

Manteca, J.I., Ovejero, G., 1992. Los yacimientos Zn, Pb, Ag-Fe del distrito minero de La Unión-Cartagena, Bética Oriental (Zn, Pb, Ag-Fe ore deposits of La Unión-Cartagena mining district, eastern Betic Cordillera). In: J. García and J. Martínez (eds.). Recursos Minerales de España, CSIC, 1085-1101.

Manteca Martínez, J.I., Rodríguez Martínez-Conde, J.A., Puga, E., Díaz de Federico, A., 2004. Deducción de la existencia de un relieve Nevado-Filábride durante el Mioceno Medio-Superior, actualmente bajo el mar, al sur de las sierras costeras alpujárrides de El Roldán y La Muela (oeste de Cartagena, Cordillera Bética Oriental). Rev. Soc. Geol. España, 17(1-2), 27-37.

Martelet, G., Calcagno, P., Gumiaux, C., Truffert, C., Bitri, A., Gapais, D., Brun, J.P., 2004. Integrated 3D geophysical and geological modelling of the Hercynian Suture Zone in the Champtoceaux area (south Brittany, France). Tectonophysics, 382, 117-128.

Mora Cuenca, V., Rodríguez Estrella, T., Aragón Rueda, R., 1988. Intrusión marina fósil en el Campo de Cartagena (Murcia). In: Proceedings of Coastal Aquifers Intrusion Technology: Mediterranean Countries (TIAC'88). IGME Book series, Madrid, 221-236.

Ovejero, G., Jacquin, J.P., Servajean, G., 1976. Les minéralisations et leur contexte géologique dans la Sierra de Cartagena (Sud-Est de L'Espagne) (Mineralizations and their geologic context in the Sierra de Cartagena (SE Spain)). Bulletin Société Géologique de France (7), XVIII (3), 613-633.

Ramos, G., Sánchez, J., 2003. Estructura geológica profunda "Murcia Sur-I". Definición geológica, geométrica y confinamiento. In: Proceedings of Coastal Aquifers Intrusion Technology: Mediterranean Countries (TIAC'03). IGME Book series, Madrid, 691-700.

Robins, N.S., Rutter, H.K., Dumpleton, S., Peach, D.W., 2005. The role of 3D visualisation as an analytical tool preparatory to numerical modelling. Journal of Hydrology, 301, 287–295.

Robles-Arenas, V.M., Rodríguez, R., García, C., Manteca, J.I., Candela, L., 2006. Sulphide-mining impacts in the physical environment: Sierra de Cartagena-La Unión (SE Spain) case study. Environmental Geology, 51, 47-64.

Rodríguez Estrella, T., 1983. Criterios hidrogeológicos aplicables al estudio de la neotectónica en el Sureste Español. Mediterránea Ser. Geol., 2, 53-66.

Rodríguez Estrella, T., 1986. La Neotectónica en la Región de Murcia y su incidencia en la ordenación del territorio. In: Proceedings 1ª Jornadas de estudio del fenómeno sísmico y su incidencia en la ordenación del territorio. Murcia, 281-303.

Rodríguez Estrella, T., 1995. Funcionamiento hidrogeológico del Campo de Cartagena. Hidrogeología, 11, 21-38.

Rodriguez Estrella, T., 2004. Decisive influence of neotectonics on the water connection between the Mediterranean Sea, Mar Menor and the Campo de Cartagena aquifers. (South-East of Spain): Consequences on extracting sea water by means of borings for desalination. In: L. Araguás, E. Custodio and M. Manzano (eds.). Proceedings 18th SWIM Groundwater and Saline Intrusion. IGME Book series, Madrid, 745-758.

Rodríguez Estrella, T., Jiménez-Martínez, J., López Chicano, M., 2004. Ensayo de correlación entre transmisividades y espesores de los acuíferos del Plioceno y Messiniense del Campo de Cartagena (Murcia y Alicante). In: Proceedings VIII Simposio de Hidrogeología. Zaragoza, Spain. Vol. XXVI, 239-249.

Rodríguez Estrella, T., Lillo, M., 1992. Geomorfología del Mar Menor y sectores litorales contiguos (Murcia-Alicante). Estudios de geomorfología en España. In: Proceedings II Reunión Nacional de Geomorfología, 787-807.

Rolandi Sánchez-Solís, M., Yugin, V., Herrero Pacheco, J. L. 2008. Aportación al conocimiento de la caracterización y el funcionamiento hidrogeológico de la U.H. del

Campo de Cartagena (Cuenca del Segura), mediante utilización de técnicas de Tomografía Remota Térmica. In: Proceedings IX Simposio de Hidrogeología. Elche, Spain. Vol. XXVIII, 691-700.

Ross, M., Parent, M., Lefebvre, R., 2005. 3D geologic framework models for regional and land-use management: a case study from a Quaternary basin of southwestern Québec, Canada. Hydrogeology Journal, 13, 690–707.

Sanz de Galdeano, C., López-Garrido, A. C., García-Tortosa, F.J., Delgado, F., 1997. Nuevas observaciones en el Alpujárride del sector centro-occidental de la Sierra de Carrascoy (Murcia). Consecuencias paleogeográficas. Estudios Geológicos, 53, 229-236.

SEPESA, 1968. MM Seismic Survey. Fondo Documental del Archivo de Hidrocarburos del Ministerio de Industria, Turismo y Comercio.

Figures and Tables

FIGURE 1. Study area and geological sketch. Map location of seismic profiles, lithologic columns and cross-section locations. m.r.: mountain range. (Modified from IGME, 2005).

FIGURE 2. Seismic reflection profiles: S-84-58 (Chevron, 1984); MM-1 (Sepesa, 1968); S-85-82 (Chevron, 1985) and geographic location. Modified from IGME (2005). (AQT.-BUR.: Aquitanian-Burdigalian. LANG.: Langhian, SERRV.: Serravalian).

572

573 FIGURE 3. Stratigraphic correlation between SMS·1 (Ini-Coparex, 1967) and SMS·2
574 (Ini-Coparex, 1970) lithological columns. See location in Fig. 1.

575

576 FIGURE 4. Imported cross-sections are set as lines. The lines represent the lower
577 boundary of the stratigraphic units defined in Table 1 (white colour). In grey colour is
578 shown the shoreline.

579

580 FIGURE 5. Fence diagram of the stratigraphic and hydrostratigraphic units of the
581 Campo de Cartagena basin. (see Table1).

582

583 FIGURE 6. Campo de Cartagena basin, isobaths of the Mesozoic basement. The two
584 sub-basins (Torre-Pacheco and San Javier) with the existing depocentres are clearly
585 observed (Modified from IGME, 2005).

586

587 FIGURE 7. Surface spatial extension for the *Qt*, *LT*, *VLV* and jointly *ER*, *CG*, *PC* and
588 *Co* aquifer units has been mapped. The dashed line represents either unknown unit
589 border or lateral facies change, in the *Qt* aquifer unit it constitutes the groundwater
590 boundary.

591

592 TABLE 1. Campo de Cartagena geologic basin. Summary of stratigraphic and
593 hydrostratigraphic units, formations, lithology and hydraulic properties of the Neogene
594 and Quaternary sedimentary package. Modified from López-Bermúdez and Conesa-
595 García (1990) and IGME (2005).

596

597 TABLE 2. Information required for numerical modelling of the Campo de Cartagena
598 hydrostratigraphic units. S_s: Storage coefficient/formation thickness (ITGE, 1994;
599 Rodríguez Estrella et al., 2004; unpublished data).

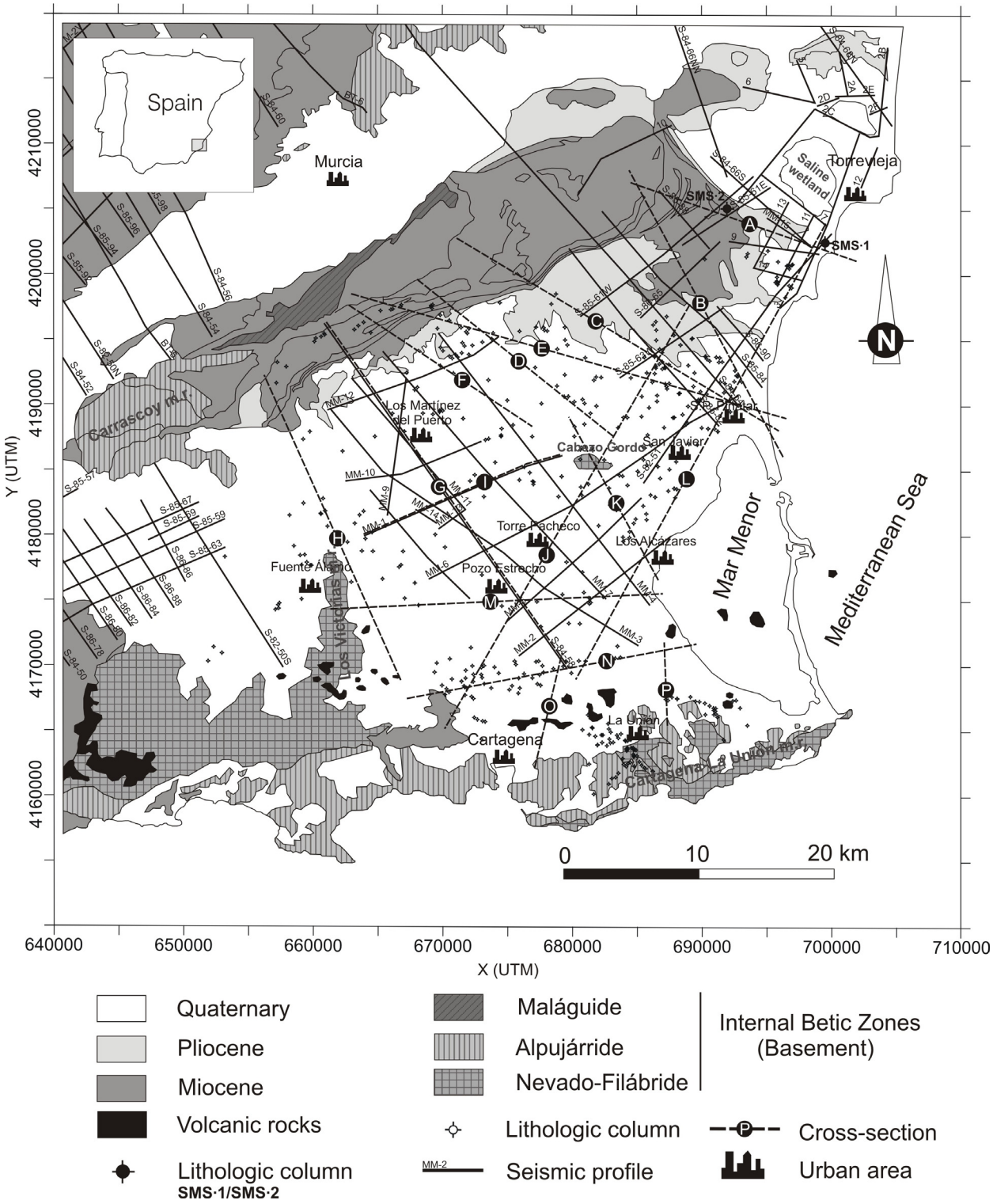
Spain
Murcia
Torrevieja
Saline wetland
SMS·2
SMS·1
Carrascoy m.t.
Los Martínez del Puerto
Cabezo Gordo
San Javier
Torre Pacheco
Los Alcázares
Fuente Álamo
Pozo Estrecho
Los Victorias
Mar Menor
Mediterranean Sea
Cartagena
La Unión
Sierra de La Unión-El Algarrobo
0
10
20 km
Y (UTM)
X (UTM)
4210000
4200000
4190000
4180000
4170000
4160000
640000
650000
660000
670000
680000
690000
700000
710000
Quaternary
Pliocene
Miocene
Volcanic rocks
Lithologic column
SMS·1/SMS·2
Maláguide
Alpujárride
Nevado-Filábride
Internal Betic Zones (Basement)
Lithologic column
Seismic profile
Cross-section
Urban area

FIGURE 1.

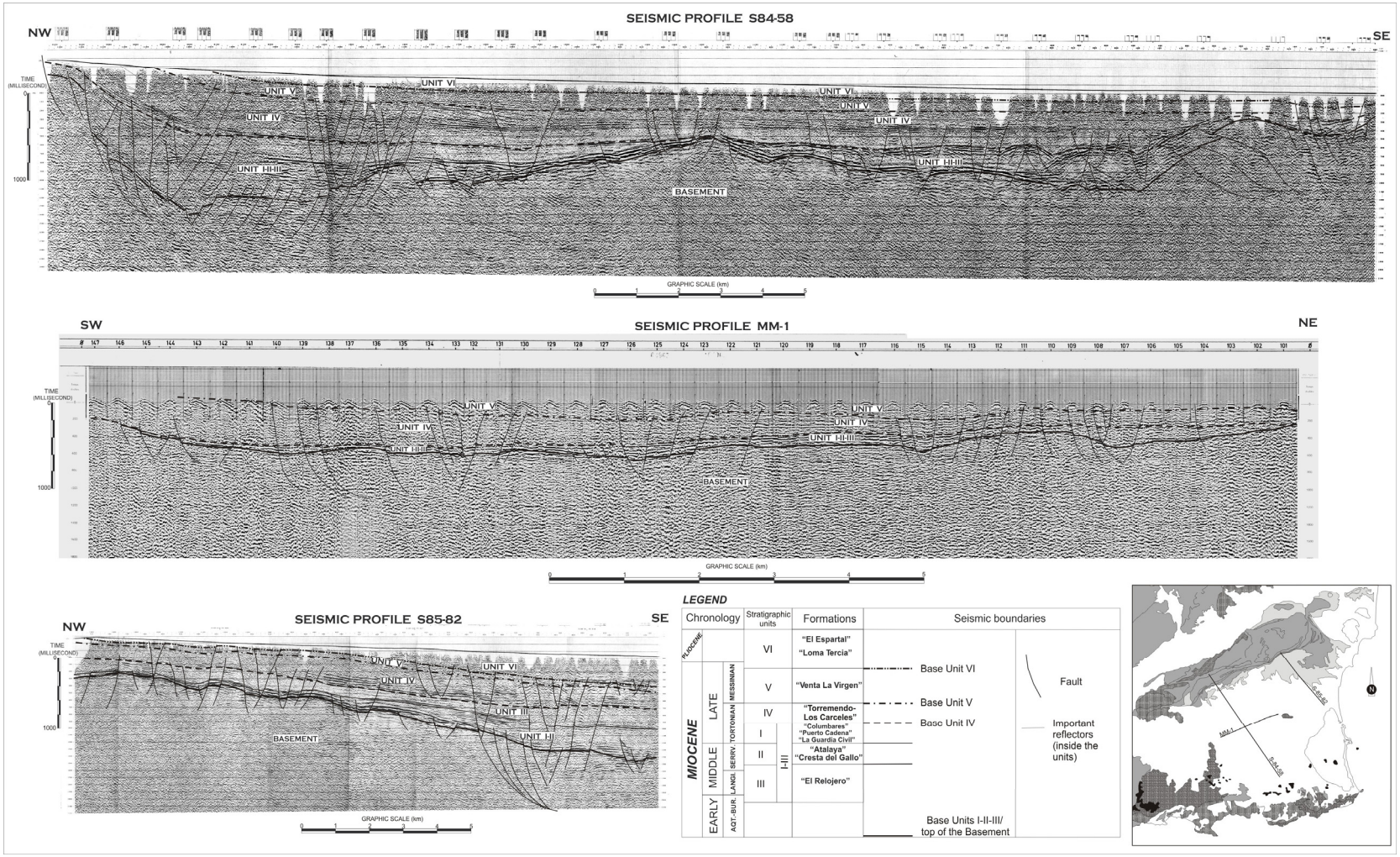
SEISMIC PROFILE S84-58
NW
SE
TIME (MILLISECOND)
1000
UNIT V
UNIT VI
UNIT IV
UNIT HHIII
BASEMENT
GRAPHIC SCALE (km)
SW
SEISMIC PROFILE MM-1
NE
SEISMIC PROFILE S85-82
LEGEND
Chronology
Stratigraphic units
Formations
Seismic boundaries
PLIOCENE
MIOCENE
LATE
MIDDLE
EARLY
MESSINIAN
TORTONIAN
SERRAV.
LANGI.
AQT.-BUR.
VI
V
IV
I
II
III
I-III
"El Espartal"
"Loma Tercia"
"Venta La Virgen"
"Torremendo-Los Carceles"
"Columbares"
"Puerto Cadena"
"La Guardia Civil"
"Atalaya"
"Cresta del Gallo"
"El Relojero"
Base Unit VI
Base Unit V
Base Unit IV
Base Units I-II-III/ top of the Basement
Fault
Important reflectors (inside the units)
MM-1
S84-58
S85-82
N

FIGURE 2.

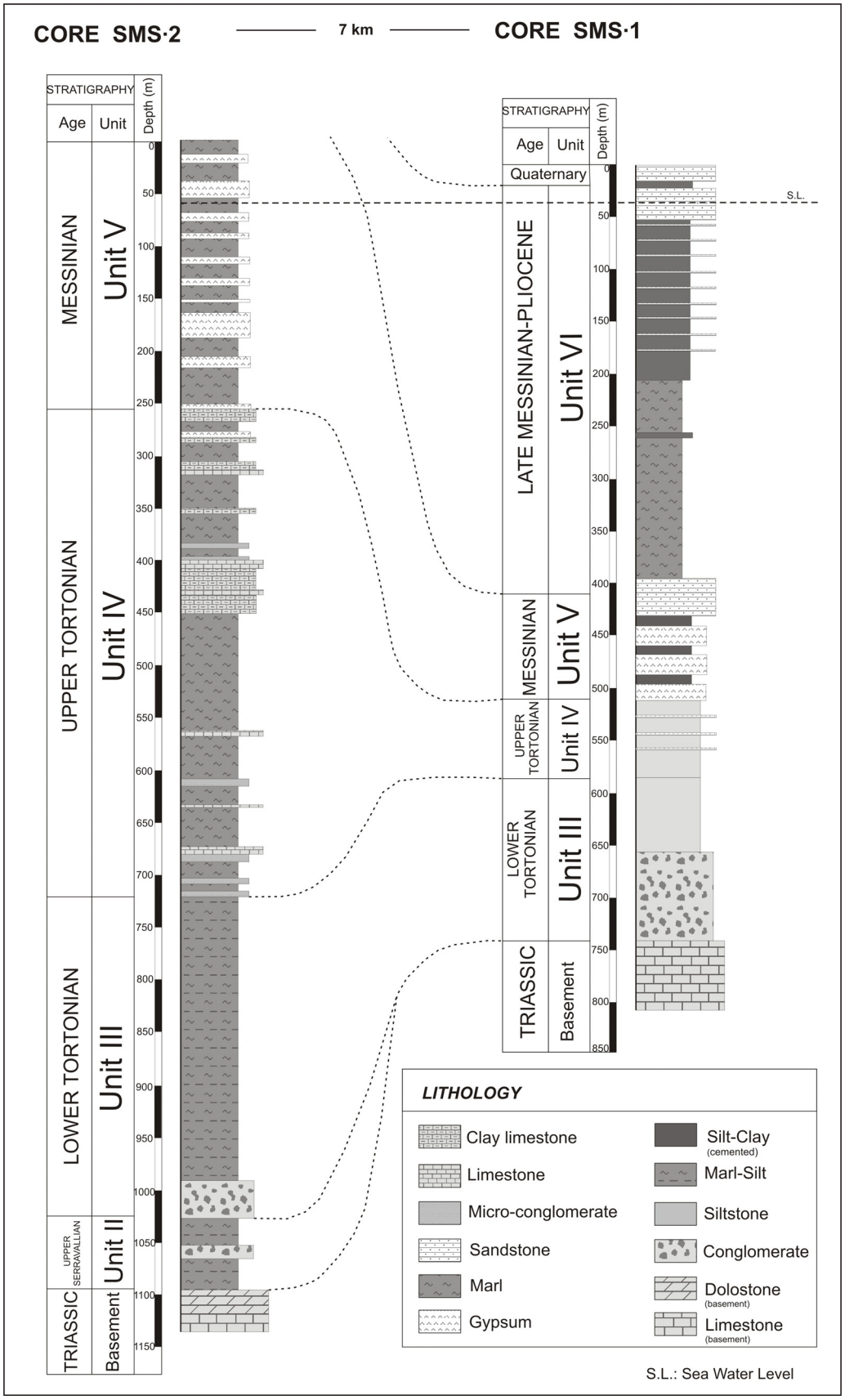
CORE SMS·2
7 km
CORE SMS·1
STRATIGRAPHY
Age
Unit
Depth (m)
MESSINIAN
Unit V
UPPER TORTONIAN
Unit IV
LOWER TORTONIAN
Unit III
UPPER SERRAVALLIAN
Unit II
TRIASSIC
Basement
Quaternary
LATE MESSINIAN-PLIOCENE
Unit VI
S.L.
LITHOLOGY
Clay limestone
Limestone
Micro-conglomerate
Sandstone
Marl
Gypsum
Silt-Clay (cemented)
Marl-Silt
Siltstone
Conglomerate
Dolostone (basement)
Limestone (basement)
S.L.: Sea Water Level

FIGURE 3.

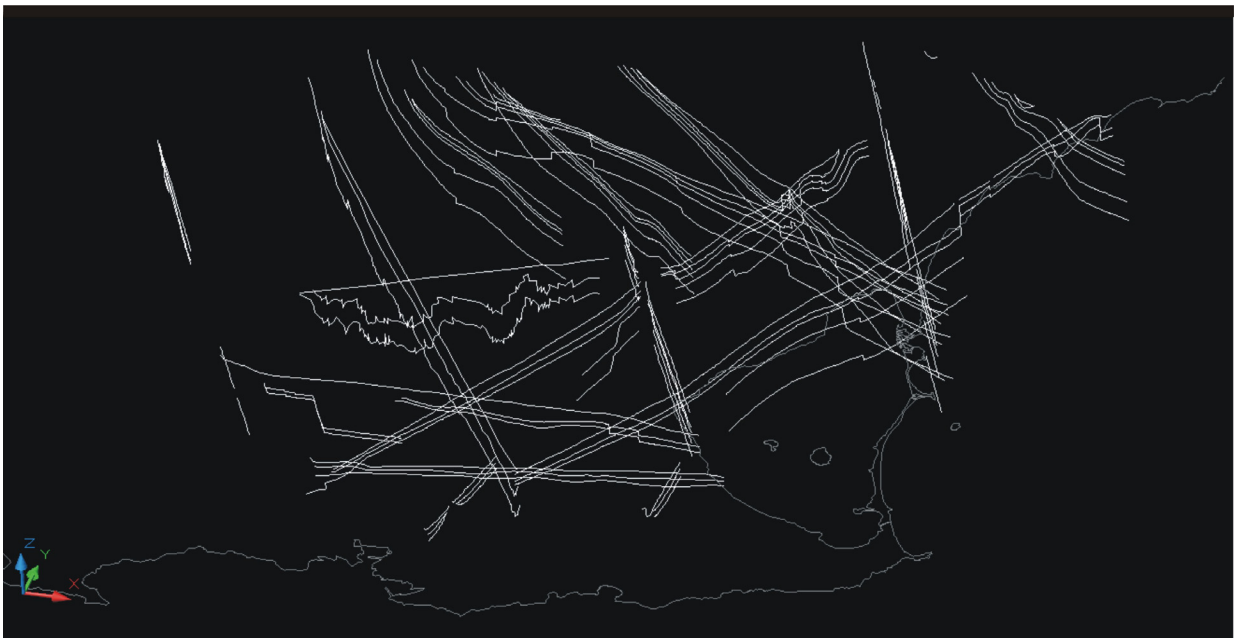

FIGURE 4.

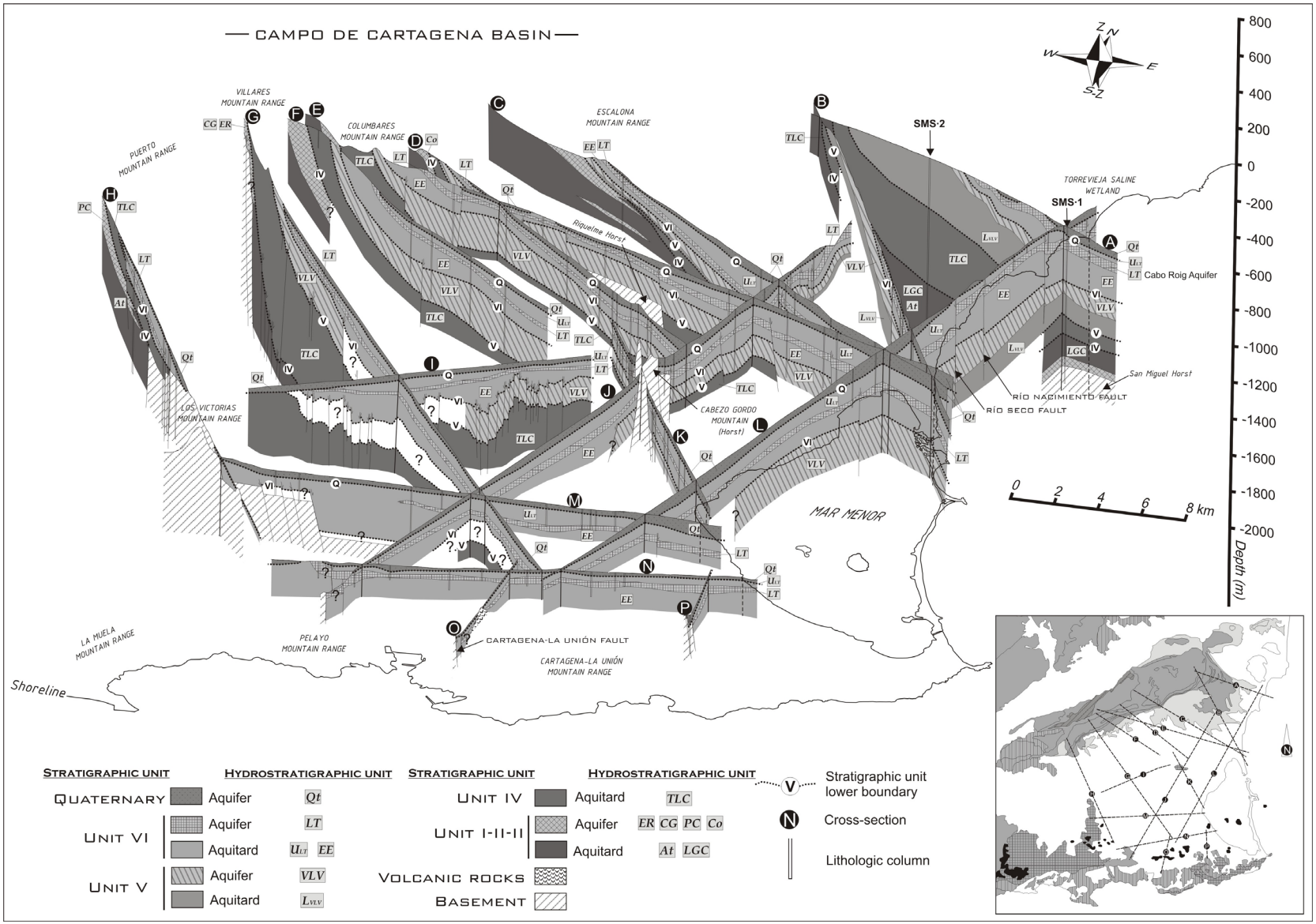
CAMPO DE CARTAGENA BASIN
VILLARES MOUNTAIN RANGE
COLUMBARES MOUNTAIN RANGE
ESCALONA MOUNTAIN RANGE
PUERTO MOUNTAIN RANGE
LOS VICTORIAS MOUNTAIN RANGE
LA MUELA MOUNTAIN RANGE
PELAYO MOUNTAIN RANGE
CARTAGENA-LA UNIÓN MOUNTAIN RANGE
Riquelme Horst
CABEZO GORDO MOUNTAIN (Horst)
TORREVIEJA SALINE WETLAND
SMS-1
SMS-2
San Miguel Horst
RÍO NACIMIENTO FAULT
RÍO SECO FAULT
CARTAGENA-LA UNIÓN FAULT
MAR MENOR
Cabo Roig Aquifer
Shoreline
0 2 4 6 8 km
Depth (m)
800 600 400 200 0 -200 -400 -600 -800 -1000 -1200 -1400 -1600 -1800 -2000
STRATIGRAPHIC UNIT
HYDROSTRATIGRAPHIC UNIT
QUATERNARY Aquifer Qt
UNIT VI Aquifer LT
Aquitard ULT EE
UNIT V Aquifer VLV
Aquitard LVLV
UNIT IV Aquitard TLC
UNIT I-II-II Aquifer ER CG PC Co
Aquitard At LGC
VOLCANIC ROCKS
BASEMENT
Stratigraphic unit lower boundary
Cross-section
Lithologic column

FIGURE 5.

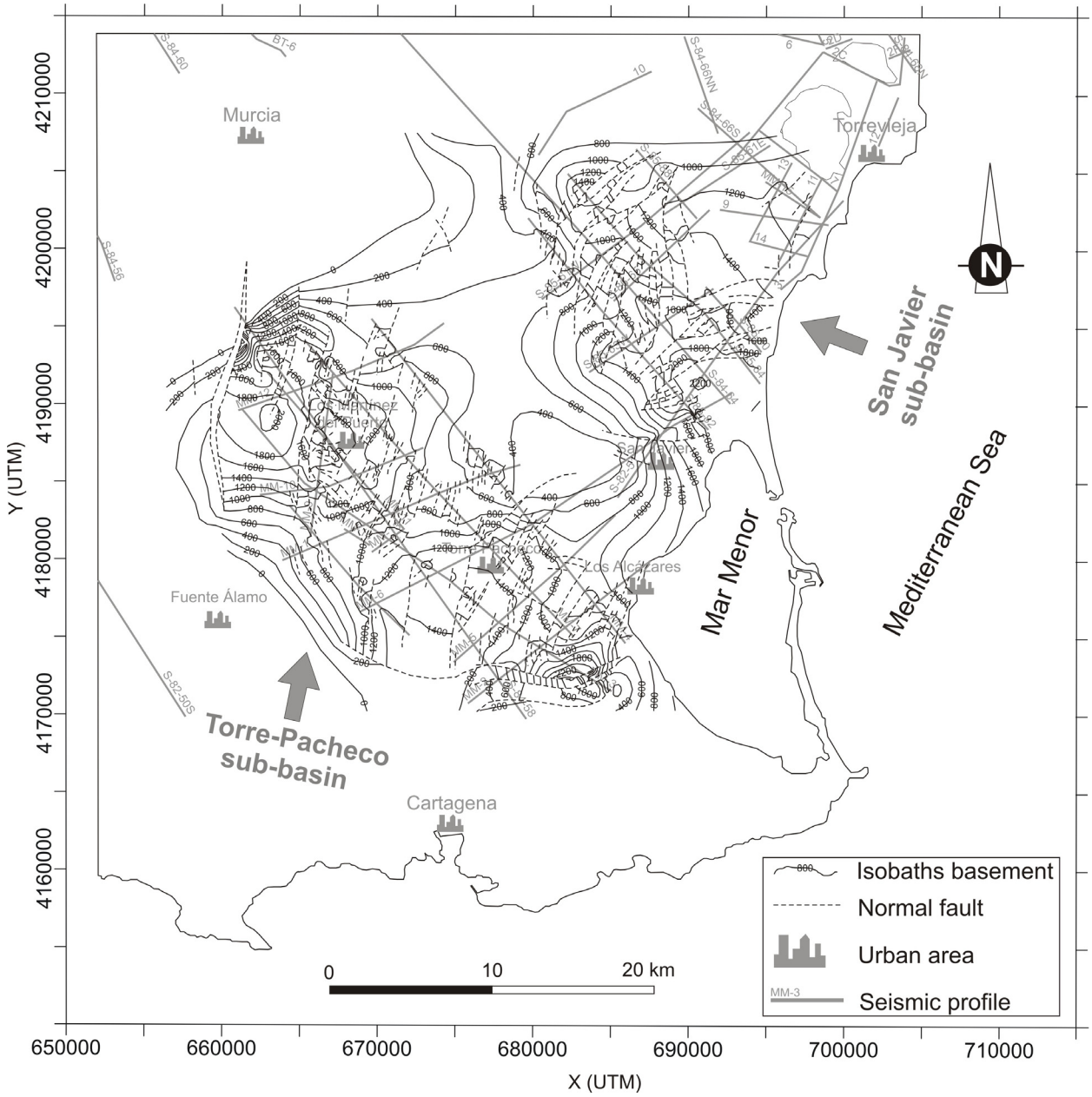
Murcia
Torrevieja
San Javier
sub-basin
Mediterranean Sea
Mar Menor
Los Alcázares
Fuente Álamo
Torre-Pacheco
sub-basin
Cartagena
N
Isobaths basement
Normal fault
Urban area
Seismic profile
0
10
20 km
Y (UTM)
X (UTM)
650000
660000
670000
680000
690000
700000
710000
4160000
4170000
4180000
4190000
4200000
4210000

FIGURE 6.

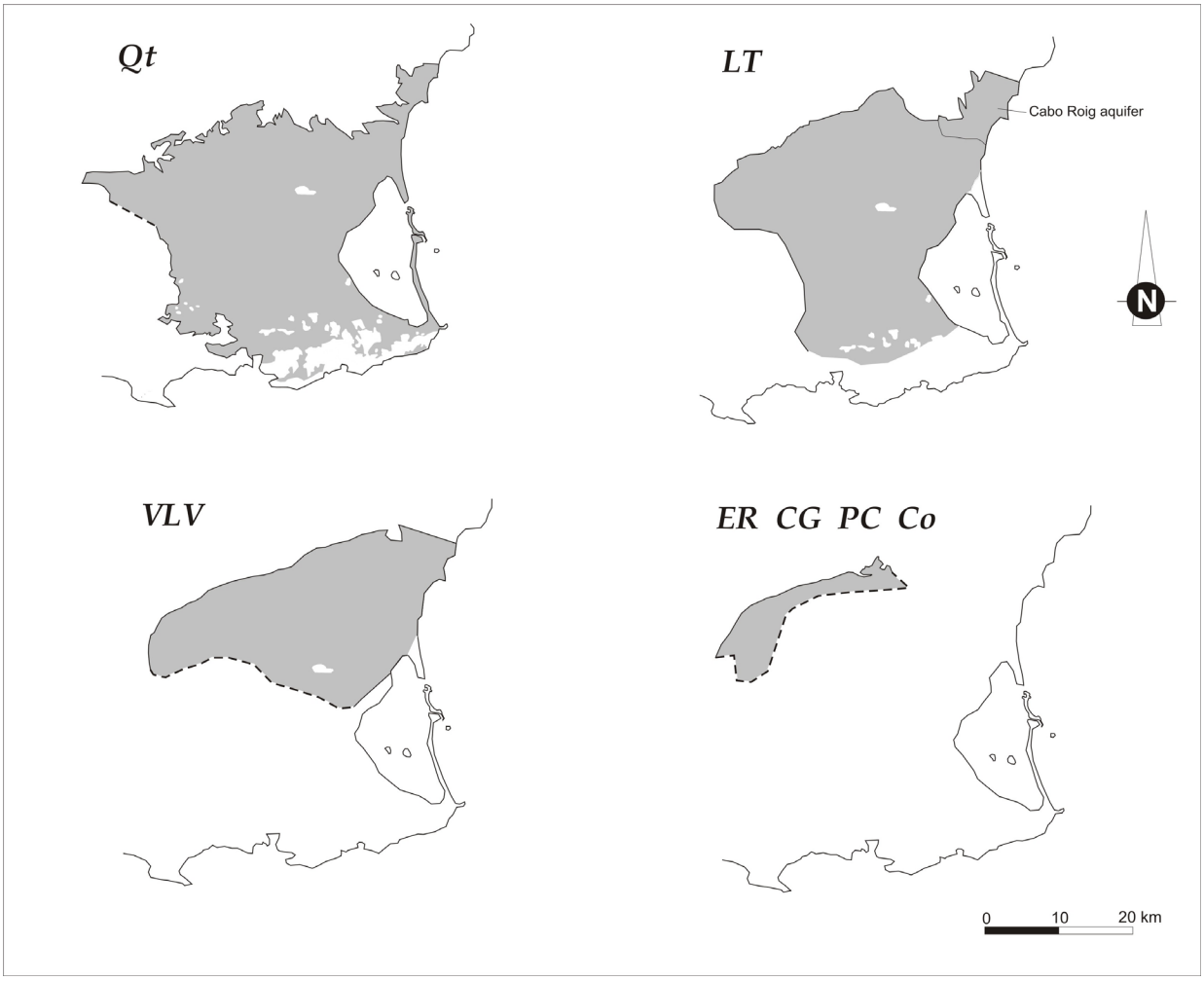

FIGURE 7.

TABLE 1.

Chronology			Stratigraphic units		Formations	Lithology	Observations	Hydraulic properties	Hydrostratigraphic units
Quaternary			Q			Sand, silt, clay, conglomerate, caliche and sandstone		Aquifer	$Q\,t$
PLIOCENE			V I			Marl and evaporite	Intra-Messinian erosive surface, unconformity with the unit V	Aquitard	U_{LT}
					"Loma Tercia"	Sandstone		Aquifer	$L\,T$
					"El Espartal"	Clay and sand		Aquitard	$E\,E$
MIOCENE	LATE	MESSINIAN	V		"Venta La Virgen"	Sandstone		Aquifer	$V\,L\,V$
						Evaporite and marl		Aquitard	L_{VLV}
		TORTONIAN	I V			Oolitic limestone	Very local (thickness 40m)	Aquifer	U_{TLC}
					"Torremendo-Los Carceles"	Marl and clay with intercalations of limestone and sand	Variable thickness	Aquitard	$T\,L\,C$
			III	I - III	"Columbares"	Sandstone	Abundant fragments of echinoderms,oysters, etc.	Aquifer	$C\,o$
					"La Guardía Civil"	Marl and clay with intercalations of sand		Aquitard	$L\,G\,C$
					"Puerto Cadena"	Sandy limestone and conglomerate		Aquifer	$P\,C$
	MIDDLE	SERRV.	II		"Atalaya"	Marl with intercalations of sand	Influencie of differential subsidence	Aquitard	$A\,t$
					"Cresta del Gallo"	Conglomerate		Aquifer	$C\,G$
		LANGI.	I		"El Relojero"	Conglomerate and sandstone with thin intercalations of marl	Internal structures of cross stratification	Aquifer	$E\,R$
	EARLY	AQT.-BUR.							
BASEMENT									

TABLE 2.

Stratigraphic Unit	Hydrostratigraphic Unit	Type	Out cropping surface (km^2)	Total surface (km^2) known (optimistic scenario)	Depth* (m) Top / Bottom	Thickness b (m) Average [max.]	Hydraulic conductivity K (m d^{-1}) Av. [max. / min.]	Specific storage S_s (m^{-1}) [max. / min.]	Specific yield S_y Av. [min. / max.]	Effective porosity m_e Av. [min. / max.]	Total porosity $Ø$ Av. [min. / max.]	Observations
Q	*Qt*	aquifer	1135	1135	0 / 50	55 [150]	0.5 [10^{+3} / 10^{-6}]	-	0.2 [0.1 / 0.4]	0.23 [0.1 / 0.4]	0.4 [0.15 / 0.6]	
VI	U_{LT}	aquitard	-	-	50 / 85	60 [110]	-	-	-	-	-	
	LT	aquifer	22	817	85 / 130	30 [110]	8 [10^{+1} / 10^{-4}]	[10^{-4} / 10^{-6}]	-	0.25 [0.1 / 0.4]	0.3 [0.035 / 0.38]	Fractured
	EE	aquitard	-	-	130 / 195	90 [180]	-	-	-	-	-	
V	*VLV*	aquifer	28	570	195 / 315	125 [240]	6.5 [10^{+1} / 10^{-5}]	[10^{-4} / 10^{-6}]	-	0.19 [0.01 / 0.4]	0.3 [0.05 / 0.5]	Fractured
	L_{VLV}	aquitard	-	-	-	-	-	-	-	-	-	
IV	U_{TLC}	aquifer	-	-	-	- [40]	-	-	-	-	-	Very local
	TLC	aquitard	-	-	315 / -	- [800]	-	-	-	-	-	
I-II-III	*Co*	aquifer	25**	43 (230)**	-	90 [200]**	-	-	-	0.24 [0.1 / 0.4]**	-	Lateral facies changes between aquifer units
	LGC	aquitard										
	PC	aquifer										
	At	aquitard				70						
	CG	aquifer										
	ER	aquifer										

*Central part of the basin.

**Average value for all aquifer hydrostratigraphic units.

Identification of freshwater/saltwater interface via Electrical resistivity tomography: Campo de Cartagena aquifer (SE Spain)

J. Rey[a,1], J. Martínez[b], G. G. Barberá[c], J. L. García-Aróstegui[d], J. García-Pintado [e]

[a] Dpto. de Geología, Escuela Politécnica Superior de Linares, Universidad de Jaén, 23700 Linares, Jaén, Spain. e-mail: jrey@jaen.es

[b] Dpto. Ingeniería Mecánica y Minera, Escuela Politécnica Superior de Linares, Universidad de Jaén, 23700 Linares, Jaén, Spain. e-mail: jmartine@ujaen.es

[c] Department of Soil and Water Conservation and Organic Waste Management, CEBAS-CSIC, 30100 Espinardo, Murcia, Spain. e-mail: gbarbera@cebas.csic.es

[d] Instituto Geológico y Minero de España, 30008 Murcia, Spain. e-mail: j.arostegui@igme.es

[e] Euromediterranean Water Institute, Campus de Espinardo, 30100 Espinardo, Murcia, Spain. e-mail: jgarcia@ija.csic.es

ABSTRACT

Coastal lagoons are ecosystems of great socioeconomic and environmental importance. Their ecological condition depends to a large extent upon their contact with the open sea and the influence exerted upon them by their surrounding terrestrial catchment area. Electrical resistivity tomography (ERT) provides very useful information about their geological structure and the saltwater/freshwater interface. Also, ETR supports the parameterization, calibration and validation of mathematical models, and enables us to understand the interaction between surface aquifers and the coastal lagoons. This interaction is a two-way process as overuse of the aquifers can result in marine sea water intrusion, and natural or artificial changes in the dynamics of the hydrological and hydrogeological system can alter the discharge of fresh or

[1] Author for correspondence. Tel.: +34 953 648512
E-mail address: jrey@ujaen.es

brackish water into the lagoons, which can have serious effects on its overall condition. We have used ERT to analyse the Quaternary aquifer in the Campo de Cartagena (Murcia, south-east Spain), which is in contact with the coastal lagoon Mar Menor and from which large amounts of water were pumped in the period 1960s and 80s. This is a very heterogeneous and anisotropic detrital aquifer, whose interface is geometrically very irregular. In spite of this, the freshwater–saltwater transition zone shows a marked change in electrical resistivity from relatively high resistivities in the shallow freshwater zone to considerably lower ones in the deeper sediments, which are saturated with salt water. We were able to identify two different zones of the aquifer; a lower one affected by the intrusion of saltwater; and a higher area, where the water is less salty due to an increase in fresh run-off water coming from irrigation. The technique also enabled us to distinguish between two different mechanisms by which water from the sea invades the land: wide area exploitation which mostly imposes a horizontal advance of the interface, and local intensive pumping which leads to vertical rise (upconing).

Keywords: electrical resistivity tomography; marine seawater intrusion; detrital coastal aquifer; salinity interface; Campo de Cartagena; Mar Menor lagoon.

1. Introduction

In coastal aquifers in direct contact with the sea, a state of equilibrium is created between the flow of saltwater and freshwater. When these natural conditions are altered, due to either an increase or a reduction in the flow of freshwater, the freshwater/saltwater balance shifts. Saltwater intrusion occurs when extractions of water from aquifers cause a depletion of freshwater, thus allowing saltwater to invade the land. Experience shows that once salinity increases, the process advances extremely quickly. However, after pumping cessation the aquifer may take a long time to reverse the process and return to the initial state of equilibrium. This may alter the clay matrix of the zone affected by the intrusion, leading to deterioration that is expensive to remedy. For this reason, the salinization of coastal aquifers is the greatest hydrogeological risk affecting

coastal regions, which are often densely populated and highly dependent upon groundwater resources (Naji et al., 1998; Nowroozi et al., 1999; Wilson et al., 2006; Morrow et al., 2010). In addition, coastal lagoons are peculiar ecosystems whose state depends fundamentally on the degree of confinement of their waters, i.e., their connection with the open sea. This means that changes in the level of discharge of water from the land (either run-off or groundwater) can affect the relationship between the coastal lagoon and the open sea.

In recent decades, one of the great challenges that hydrogeology is facing is how to determine the geometry of the freshwater/saltwater interface in coastal areas, and its evolution over time. By monitoring the interface we can define the sustainable level of exploitation of the aquifers. This information is essential given the likely future growth in water demand its role during periods of drought. At the same time, this will enable us to understand the relationship between the dynamics of the lagoon and its terrestrial environment.

The great difference between the resistivity of saltwater-saturated zones and freshwater-saturated zones has been used by a number of researchers to assess the levels of saltwater intrusion in coastal areas (Van Dam and Meulenkamp, 1967; Nowroozi et al., 1999; Wilson et al., 2006; Massey and Taylor, 2007; Nielsen et al., 2007; Kouzana et al., 2010; Morrow et al., 2010). Electrical tomography is an effective geophysical method in that it provides geological and structural information on the one hand, whilst on the other, a relatively precise image of the geometry of the freshwater/saltwater interface at any given time (Griffiths and Baker, 1993; de Franco et al., 2009; Martínez et al., 2009).

The aim of this work has been to assess the effectiveness of ERT to define the shape of the interface between fresh water and saltwater by applying it to the Neogene basin of the Campo de Cartagena (Murcia, Southern Spain; Fig. 1), in which the intensive use of coastal aquifers caused serious saltwater intrusion in the 1960s and 1980s (Mora et al., 1988; Rodríguez-Estrella, 2003). The Campo de Cartagena acts as the drainage basin for the Mar Menor coastal lagoon (Fig. 1), one of the largest such lagoons in the Mediterranean. This area is very

important in agricultural terms and also receives large numbers of tourists. Its water resources vary in origin (water conducted from the River Tajo to the River Segura, groundwater, desalinated water, and regenerated water). The rapid expansion of irrigated farming land in the 1950s caused very significant changes to the area's hydrological and hydrogeological systems, thus creating innumerable water-resource problems to which scientific research may hold the key.

Our research was focused on the contact between the Quaternary aquifer and the Mar Menor. We had two main objectives: firstly to assess the usefulness of electrical resistivity tomography for identifying the freshwater/saltwater interface, and secondly to evaluate possible changes in the interface caused by human activities.

2. Study area

2.1. Geological and hydrogeological context

From a geological point of view, the Campo de Cartagena is one of several post-tectonic inland basins in the Betic Cordillera. It is filled with Neogene rocks (Enadimsa, 1983; IGME, 1974; ITGE, 1994), most commonly lutite and marl facies, although there are also intercalations of conglomerates, calcarenites and sandstones. This infilling lies discordantly on rocks from the metamorphic basement that crop out to the south of the Campo de Cartagena (Fig. 1).

According to IGME (1974) and ITGE (1994), the sedimentary cover is made up on the whole of materials from the Miocene (mainly Tortonian-Messinian), Pliocene and Quaternary. The Tortonian is characterized by a 200 m-thick unit of polygenic conglomerates and sands, followed by marl facies. On top there is a member about 125 m thick composed of Messinian bioclastic limestones and calcarenites fining upwards to marls. The Pliocene is characterized by detrital levels, beginning with about 20 m of sands that fine upwards to marls and clays (about 90 m) and within which there are gypsum intercalations. Finally the Quaternary shows clay and silt facies and locally conglomerates and sands.

The Quaternary unit is normally around 40-60 m thick, although it can be over 100 m thick at certain points near the coast (IGME, 1974; ITGE, 1994; Jiménez-Martínez et al, 2009a, 2009b, 2010).

The formation and later evolution of the basin was due to Neogene distensive tectonics. The considerable differences in the thickness of the sedimentary cover (Fig. 2) are related to concomitant differences in subsidence that generated areas of troughs and swells. This structuring is linked to the activity of normal faults with strike orientations N 45W, NE-SW and W-E, which controlled deposition during the Messinian, Pliocene and even the Quaternary. The faulting system explains very significant differences in thickness at points quite close together: the Pliocene varies from between 10 m and 110 m thick, the Messinian from 80 and 210 m, and locally the Quaternary can be as thick as 150 m (ITGE, 1994).

From a hydrogeological point of view, the sector in question belongs to the hydrogeological unit of the Campo de Cartagena. At a general level, five overlying aquifers have been identified (Jiménez-Martínez et al., 2009a). These are associated with the Triassic of the basement (carbonates), Tortonian (conglomerates), Messinian (bioclastic limestones), Pliocene (sandstones) and Quaternary (gravel and sands). In terms of hydrogeological productivity, the main aquifer layers correspond to the Messinian and Pliocene aquifers, separated by an interval of marls. The top of the Pliocene aquifer is generally at a depth of 60 m to 135 m, while the bottom is between 75 m and 160 m, its average thickness ranging from 15 m to 20 m. In the central section, adjacent to the Mar Menor, the top of the aquifer lies 135 m below sea level and is covered with a 90 m interval of clays, marls and gypsums. The Quaternary aquifer layer, which is the subject of this research, lies above the Pliocene marl facies. In hydrogeological terms this superficial aquifer is of little consequence but it is very important in environmental terms (Alías and Ortiz, 1975; Ministerio de Medio Ambiente, 2006; García-Pintado et al., 2007).

A hydrochemical study of the Quaternary aquifer revealed the presence of chlorides and sulphates, with a predominance of the former. Sodium is the most

common of the cations, followed normally by magnesium (ITGE, 1994). The chloride content and electrical conductivity was very high even at some distance from the coast (782 mg/l and 4,522 µS/cm), although the highest values for these parameters were observed near the coast (from 1,910 to 2,307 mg/l and 8,672 to 9,822 µS/cm).

Several previous studies have analysed the overuse of the Pliocene and Quaternary aquifers and the concomitant seawater intrusion processes (Mora et al., 1988; Lambán y Aragón, 2003; Rodríguez-Estrella, 2003; Jiménez-Martínez et al., 2009a). Groundwater was the main source for water until the construction of the Tajo-Segura interbasin conduit in 1979. This system transports water from the basin of the river Tajo in central Spain to that of the river Segura in the Southeast. During the 1980s, the gradual increase in the quantities of water transferred along with an exceptionally high rainfall in 1989, led to a significant reduction in the pumping of groundwater and a rise in the piezometric levels that was especially significant in the Quaternary aquifer. From the beginning of the 1990s water levels remained stable at considerable height above sea-level and were influenced by the existence of drainage and the aquifer's relationship with the Mar Menor. Then, in recent years groundwater pumping has increased sharply due to a reduction in the volume of water being transferred. Depending upon specific needs arising in each hydrological year, the lower aquifers now provide between 30% and 90% of the total water resources. In the past, the Quaternary aquifer layer was in general scarcely exploited by the farmer because of its limited productivity (low pumping flow rates) and its relatively high salinity. However, the introduction of a number of sparse small private desalination plants in recent years has led them to change their point of view, subsequently increasing the pumping rates.

2.2. The Mar Menor lagoon

The Mar Menor is one of the largest coastal lagoons in the Mediterranean, with a surface area of 135 km^2, a perimeter of 74 km and a volume of 610 hm^3 (Arévalo, 1988). The lagoon has undergone severe changes over recent decades. Communication with the Mediterranean Sea has been increased by

dredging the main channels between them to make it easier for recreational vessels to pass through and this has led to a reduction in the natural salinity of the lagoon, which is higher than that of the open sea. The development of irrigation-based agriculture has had a varying effect on the hydrological and hydrogeological relationship between the lagoon and the land surrounding it. Some recent effects can be easily identified though, such as an increase in fresh water caused by the Tajo-Segura interbasin conduit has altered the vegetation in the wetlands that surround the lagoon, favouring the expansion of beds of *Phragmmites australis* reeds (Carreño et al., 2008). The increase in agriculture combined with an extensive tourism-related building development have produced very high levels of pollution (García-Pintado et al., 2007), which has led to the eutrophication of the lagoon with undesirable effects such as an explosion in jellyfish populations (Pérez-Ruzafa et al., 2002) and changes in waterbird communities (Robledano et al., in press).

The environmental and economic importance of the coastal lagoon and its surroundings, along with the deterioration of its environmental quality, has led to a number of studies regarding factors affecting the environmental system and its flow and hydrochemical dynamics (e.g., Perez-Ruzafa, 2005; Jiménez-Carceles and Álvarez-Rogel, 2008; García-Pintado et al., 2009). In the context of the existing coastal lagoon eutrophication problems, the Quaternary aquifer plays a fundamental role. García-Pintado et al. (2007) estimated that water exfiltrated from the Quaternary aquifer provide 10% (0.7 hm^3 yr^{-1}) of the surface discharge from the Rambla del Albujón (the main natural drainage system) into the Mar Menor. The remaining 90% can be attributed to a sum of agricultural and urban point-source discharges. On the other hand, they estimated that nitrogen loads into the lagoon using the Quaternary aquifer as pathway amount to 360 t yr^{-1} of dissolved inorganic nitrogen (DIN), from which 344 yr^{-1} are direct groundwater coastal discharge, and 16 t yr^{-1} exfiltrate into the *rambla* before entering into the lagoon.

3. Materials and Methods

We used electrical resistivity tomography, a non-destructive, geo-electrical technique that analyses the materials in the subsoil on the basis of their electrical behaviour and distinguishes between them by measuring their electrical resistivity (Telford et al., 1990). In recent years it has been used with increasing frequency in geological studies (Store et al., 2000; Suzuki et el., 2000; Caputo et al., 2003; Colella et al., 2004; Maillet et al., 2005) and particularly in hydrogeological research (Auken et al., 2003; Sumanovac, 2006). The method is based on positioning a number of electrodes along a series of profiles with a set distance between them. This distance depends upon the degree of resolution, the depth and the objectives being sought, in such a way that the closer the distance between the electrodes the greater the resolution, and the farther the distance the greater the depth at which readings can be taken (Sasaki, 1992). In this research we generally used a spacing of 5 m between the electrodes and a Wenner-Schlumberger array, so as to ensure that we could reach the depths required to study the Quaternary aquifer while maintaining sufficient resolution. The bottom of this aquifer layer is generally located at depths ranging 40 m and 100 m.

The electrodes are connected to a power source and current meters and a specific sequential programme for each objective is used to select which array of electrode should be operating at any given time and how they should be laid out. A resistivity reading is taken for each electrode array and attributed to a specific geometric point in the subsoil. The electrical tomography equipment used in this study was the RESECS model, manufactured by Deutsche Montan Technologie (DMT). This is a multi-electrode device with an integrated computer that can handle up to 960 electrodes. The power source is 250W and 2.5 A, which generates impulses of 880 Vp-p. The device has a built-in transmitter, receiver and power supply. Other interesting features include the automatic processor of apparent resistivity and chargeability, real-time resistivity control in 2D and 3D, control of the current and voltage injection curve, regulation of injection time, and built-in PC and integrated switching processor.

The interpretations of the electrical tomography profiles were based on the real resistivities obtained in the field, which were processed using specific

RES2DINV resistivity and induced polarization interpretation software (Griffiths and Barker, 1993). The inversion programme is based on the least-squares method with an enforced smoothness constraint, modified with the Quasi-Newton optimization technique. This inversion method constructs a model of the subsoil using rectangular prisms and determines the resistivity value for each of them, so minimizing the differences between the observed and the calculated apparent resistivity values (Loke and Barker, 1996; Loke and Dahlin, 2002).

In this study we undertook 12 electrical tomography profiles in different areas of the contact zone between the aquifer and the coast of the Mar Menor (Fig. 1). First, in the design of the tomography survey we arranged a set of profiles perpendicularly to the coastline, so as to be able to detect possible cases of marine intrusion. In addition, in order to obtain resistivity sections perpendicular to the drainage paths of the Quaternary aquifer, we deployed a number of profiles parallel to the coastline, interspersed with the aforementioned set. The length of the profiles ranged from 320 m to 784 m, which enabled us to reach investigation depths of between 60 m and 150 m. Table 1 shows the characteristics of each profile.

4. Results and Discussion

Figures 3, 4 and 5 show the resistivity values represented by a colour scale. In spite of the enormous variability in the resistivity values measured in the region, this colour scale is constant for all the profiles. The aim is for the colours to be associated with resistivity values in each of the profiles, so that electrical features and relationships among profiles are readily identifiable.

In general, three levels can be identified on the vertical axis of all the profiles (Fig. 3, 4 and 5). The level closest to the surface, about 10-m thick, shows low resistivity values in the range 4-80 Ω.m. At this level low resistivity values alternate with small intercalated tapering bodies that present somewhat higher values. This unit could be interpreted as being one of channel formations filled with conglomerates or sands, immersed in clay facies (Profiles 1, 4, 5, 6, 7, 8, 9, 10 and 11). Two different sectors can be identified in this first level: higher

values in the order of 50-80 Ω.m. appear towards the middle of the basin. These may be associated with fine sandy detrital facies that are either unsaturated (Profiles 1, 2, 6, 9, 10 and 12) or well-saturated in fresh or slightly brackish water, with resistivity values of around 10 Ω.m (Profiles 3, 4 and 11). Towards the coastline the values tend to fall to as low as 1 Ω.m, a fact that may be explained by the presence of brackish waters (Profile 1 and 3 in Fig. 3). The contact between these two sectors must be at the freshwater/saltwater interface.

Below the first level, most of the profiles register a fall in resistivity, which could correspond to the freshwater/saltwater interface. At deeper levels the zone saturated in brackish water appears, probably associated with the saline wedge, which can be identified by particularly low resistivity values of 0.5-2 Ω.m (Profiles 1, 3, 4, 5, 6, 7, 8, 9, 10, 11, 12). In the profiles furthest from the coast the fall in resistivity values appears either at greater depths (Profiles 6 and 12 Fig. 4 and Fig. 5) or cannot be detected at all (Profile 1, Fig. 3).

The third level appears at varying depths of between 20 m and 100 m, and is characterized by a sharp increase in resistivity, showing values of over 200 Ω.m. These facies may correspond to the basement or to detritical Pliocene intensely fractured (Profiles 1, 2, 4, 5, 7, 8, 9, 10, 12).

In short, the freshwater/saltwater interface is very complex. It could be put down firstly to lithological changes characterized by intercalated tapering porous levels (sand and gravel) on both the vertical and the horizontal axis (Profiles 3, 4, 5, 8, 10) that give way to very slightly permeable lutite facies. Secondly, this surface is influenced by the balance between the flow of freshwater and saltwater. In this way, we discovered that there was a residual saltwater intrusion at deeper levels: a reduction in pumping activity means that the quality of the water near the surface recovers more quickly, whilst at greater depths the intrusion remains. In other words, saltwater recedes seawards more readily from the levels closest to the surface (Profiles 1, 5, 8, 10, 11, 12: Fig. 3, Fig. 4 and Fig. 5). As might be expected, this latter phenomenon was most intense in river courses where the freshwater flow was greatest. As can be seen in Profile

11, which was aligned parallel to the coast, two lateral sectors can be distinguished within this first surface layer (Profile 11; Fig. 5): the highest values between 10-12 Ω.m. appear in the NE sector near the reed-beds, whereas towards the SW, away from the drainage network, the values tend to fall, reaching 1-4 Ω.m.

Thirdly, the morphology of the freshwater/saltwater interface is affected by the upconing of saltwater produced by boreholes, which even with low pumping levels are still functioning in the Quaternary aquifer. By way of illustration, in Profile 7, at about 185m from the origin of the profile and coinciding with a working borehole, we observed that low resistivities associated with brackish water facies reached the surface (Fig. 4). At about 260 m, 330 m and 410 m from the origin we also detected areas with very low resistivities at quite shallow depths. In these last four cases, however, the separation from the main mass of brackish water suggests that this effect is caused by a past marine intrusion that is now a fossil relict. In other words, the fact that these boreholes are hardly ever or never used cancels out the upconing effect. Very similar results can be seen in Profiles 3 and 4 (Fig. 3), Profile 5 (Fig. 4) and Profile 12 (Fig. 5).

On the whole, our results suggest a strong dynamic over recent years in the interaction between the Mar Menor lagoon and the Quaternary aquifer in the Campo de Cartagena brought about by human activities. The overuse of the aquifers prior to the construction of the Tajo-Segura interbasin conduit altered the hydraulic gradient thus causing a quite generalized marine intrusion. The arrival of external resources reversed the intrusion process and at the surface there is now a saturation of fresh and/or brackish water. This “freshening” process, related to anthropogenic events, has been observed for example in the Venetian Lagoon (Gattacceca et al., 2009). Natural processes, such as a period of particularly high rainfall, can also contribute to reversing the process of marine intrusion (Pulido-Leboeuf, 2004). This dynamic form of interaction between the Quaternary aquifer and the water from the sea may have had an influence on the changes observed in the lagoon since 1960, although scientists have yet to quantify the effects of this relationship. More detailed investigation into this question is very important because, in the light of the fact that these

systems are semi-confined, the dynamics of coastal lagoons are highly controlled by their terrestrial environment.

5. Conclusions

This electrical tomography study was conducted in the Campo de Cartagena (Murcia, SE Spain), in a Neogene basin filled with Tertiary and Quaternary materials of varying thickness. Our research focused on the surface Quaternary materials that make up a coastal aquifer of little consequence in hydrogeological terms, but with huge environmental importance. These materials are generally sands and gravels of alluvial origin immersed in clay facies. The aquifer was overused in the 1960s to 80s, which led to marine intrusion. Subsequently, the volume of water extracted from the aquifer fell, thus allowing saltwater to recede seaward, with concomitant gradual improvements in the chemical quality of the waters.

The 12 electrical tomography profiles were of varying lengths, which enabled us to reach different investigation depths ranging from 59 m to 148 m. The information provided by the real resistivity models indicates that in the first 10 m below the surface, low resistivity levels alternate with small intercalated bodies that present higher resistivity values. This unit could be interpreted as channel formations filled with conglomerates or sands, immersed in clay facies.

The highest resistivity levels (around 50-80 Ω.m) in the first level appear towards the middle of the basin. These are interpreted as unsaturated facies. The values fall as the facies become saturated in fresh water (around 10 Ω.m), dropping to as low as 1 Ω.m, which is associated with the freshwater/saltwater interface.

From depths of about 10m downwards, we noticed a spectacular drop in resistivity, with values of between 1-3 Ω.m being registered. This may correspond to the Quaternary aquifer saturated in brackish water from the Mar Menor. Occasionally, at depths of less than 10m, the brackish facies may almost reach the surface at certain points, a phenomenon that may be related

to the upconing effect caused by borehole wells. In many cases, this process appears to be separate from the main mass of brackish water, which suggests that these may be remains of some previous saltwater intrusion, which is no longer active due to the drop in water extraction from the aquifer. At the same time, the variations in resistivity on the vertical axis have enabled us to show that marine recession has been most effective near the surface, where brackish water can no longer be detected.

References

Alías,L.J., Ortiz R., 1975. Características fisiográficas y ambientales de interés edafogenético del Campo de Cartagena (Murcia). Anales de Instituto Botánico Cavanilles 32, 1021-1037.

Arévalo, L., 1988. El Mar Menor como sistema forzado por el Mediterráneo. Control hidráulico y agentes fuerza. Boletín del Instituto Español de Oceanografía 5, 63-96.

Auken, E., Jørgensen, F., Sørensen, K.I., 2003. Large-scale TEM investigation for groundwater. Exploration Geophysics 34,188–194.

Caputo, R., Piscitelli, S., Oliveto, A., Rizzo, E., Lapenna, V., 2003. High-resolution resistivity tomographies in active tectonic studies. Examples from the Tyrnavos Basin, Greece. Journal of Geodynamics 36, 19–35.

Carreño, M.F., Esteve, M.A., Martínez, J., Palazón, J.A., Pardo, M.T., 2008. Habitat changes in coastal wetlands associated to hydrological changes in the watershed. Estuarine, Coastal and Shelf Science 77, 475-483.

Colella, A., Lapenna, V., Rizzo, E., 2004. High-resolution imaging of the High Agri Valley Basin (Southern Italy) with electrical resistivity tomography. Tectonophysics 386, 29– 40.

de Franco, R., Biella, G., Tosi, L., Teatini, P., Lozej, A., Chiozzotto, B., Giada, M., Rizzetto, F., Claude, C., Mayer, A., Bassan, V., Gasparetto-Stori, G., 2009. Monitoring the saltwater intrusion by time lapse electrical resistivity tomography: The Chioggia test site (Venice Lagoon, Italy). Journal of Applied Geophysics 69, 117–130.

Enadimsa, 1983. Campaña de prospección geofísica en el Campo de Cartagena (Murcia). Sondeos eléctricos verticales (unpublished).

García-Pintado, J., Martínez-Mena, M., Barberá,G.G., Albaladejo, J., Castillo, V.M., 2007. Anthropogenic nutrient sources and loads from a Mediterranean catchment into a coastal lagoon: Mar Menor, Spain. Science of the Total Environment 373, 220–239.

García-Pintado, J., Barberá, G.G., Erena, M., Castillo, V.M., 2009. Calibration of structure in a Distributed Forecasting model for a semiarid flash Flood: dynamic surface storage and channel roughness. Journal of Hydrology 377, 165–184.

Gattacceca, J.C., Vallet-Coulomb, C., Mayer, A., Claude, C., Radakovitch, O., Conchetto, E., Hamelin, B., 2009. Isotopic and geochemical characterization of salinization in the shallow aquifers of a reclaimed subsiding zone: The southern Venice Lagoon coastland. Journal of Hydrology 378, 46-61.

Griffiths, D.H., Barker, R.D., 1993. Two-dimensional resistivity imaging and modelling in areas of complex geology. Journal of Applied Geophysics 29, 211-226.

IGME, 1974. Mapa Geológico y Memoria Explicativa de la Hoja 1:50.000 de Llano del Beal, 16 p.

ITGE, 1994. Las aguas subterráneas del campo de Cartagena (Murcia). MINER, 62 p.

Jiménez-Carceles, F.J., Álvarez-Rogel, J., 2008. Phosphorus fractionation and distribution in salt marsh soils affected by mine wastes and eutrophicated water: a case study in SE Spain. Geoderma 144, 299–309.

Jiménez-Martínez, J., Aragón, R., García-Aróstegui, J.L., 2009a. Hidrogeología y recursos hídricos subterráneos en el área Campo de Cartagena - Mar Menor. In: Mar Menor, Fundación IEA, 55-77.

Jiménez-Martínez, J., Skaggs, T.H., van Genuchten, M. Th., Candela, L., 2009b. A root zone modelling approach to estimating groundwater recharge from irrigated areas. Journal of Hydrology 367, 138–149.

Jiménez-Martínez, J., Aravena, R., Candela, J., 2010. The Role of Leaky Boreholes in the Contamination of a Regional Confined Aquifer. A Case

Study: The Campo de Cartagena Region, Spain Water. Air Soil Pollution (in press).

Kouzana, L., Benassi, R., Ben Mammou, A., Sfar Felfoul, M., 2010. Geophysical and hydrochemical study of the seawater intrusion in Mediterranean semi arid zones. Case of the Korba coastal aquifer (Cap-Bon, Tunisia). Journal of Africa Earth Sciences (in press).

Lambán, L.J., Aragón, R., 2003. Estado de la intrusión marina en el Campo de Cartagena: Evaluación preliminar a partir de la composición química del agua subterránea. In: Tecnología de la intrusión de aguas de mar en acuíferos costeros: Países mediterráneos. IGME, 345-355.

Loke, M.H., Barker, R.D., 1996. Rapid least-squares inversion of apparent resistivity pseudosections by a quasi-Newton method. Geophysical Prospecting 44, 131-152.

Loke, M.H., Dahlin, T., 2002. A comparison of the Gauss-Newton and quasi-Newton methods in resistivity imaging inversion. Journal of Applied Geophysics 49, 149-162.

Maillet, G.M., Rizzo, E., Revil, A., Vella, C., 2005. High resolution electrical resistivity tomography (ERT) in a transition zone environment: Application for detailed internal architecture and infilling processes study of a Rhône River paleo-channel. Marine Geophysical Researches 26, 317-328.

Martínez, J., Benavente, J., García-Aróstegui, J.L., Hidalgo, C.H., Rey, J., 2009. Contribution of electrical resistivity tomography to the study of detrital aquifers affected by seawater intrusion–extrusion effects: The river Vélez delta (Vélez-Málaga, southern Spain). Engineering Geology 108, 161–168.

Massey, A.C., Taylor, G.K., 2007. Coastal evolution in south-west England, United Kingdom: An enhanced reconstruction using geophysical surveys. Marine Geology 245, 123-140.

Ministerio de Medio Ambiente, 2006. Informe de sostenibilidad ambiental del Plan Especial de Actuación en situaciones de alerta y eventual sequía en la Cuenca Hidrográfica del Segura, 21 p.

Mora, V., Rodriguez-Estrella, T., Aragón, R., 1988. Intrusión marina fósil en el Campo de Cartagena (Murcia). TIAC´88: Tecnología de la Intrusión en Acuíferos Costeros, Almuñecar, 221-236.

Morrow, F.J., Ingham, M.R., McConchie, J.A., 2010. Monitoring of tidal influences on the saline interface using resistivity traversing and cross-borehole resistivity tomography. Journal of Hydrology 389, 69-77.

Naji, A., Ouazar, D., Cheng, H.D., 1998. Locating the saltwater-freshwater interface using nonlinear programming and h-adaptive BEM. Engineering Analysis with Boundary Elements 21, 253-259.

Nielsen, L., Jørgensen, N.O., Gelting, P., 2007. Mapping of the freshwater lens in a coastal aquifer on the Keta Barrier (Ghana) by transient electromagnetic soundings. Journal of Applied Geophysics 62, 1-15.

Nowroozi, A., Horrocks, S., Henderson, P. 1999. Saltwater intrusion into the freshwater aquifer in the eastern shore of Virginia: a reconnaissance electrical resistivity survey. Journal of Applied Geophysics 42, 1–22.

Pérez-Ruzafa, A., Fernández, A.I., Marcos, C., Gilabert, J., Quispe, J.I., García-Charton, J.A., 2005. Spatial and temporal variations of hydrological conditions, nutrients and α chlorophyll in a Mediterranean coastal lagoon (Mar Menor, Spain). Hydrobiologia 550, 11–17.

Pérez-Ruzafa, A., Gilabert, J., Gutiérrez, J.M., Fernández, A.I., Marcos, C., Sabah, S., 2002. Evidence of a planktonic food web response to changes in nutrient input dynamics in the Mar Menor coastal lagoon, Spain. Hydrobiologia 475, 359-369.

Pulido-Leboeuf, P., 2004. Seawater intrusion and associated processes on a small coastal complex aquifer (Castell de Ferro, Spain). Applied Geochemistry 19, 1517-1527.

Robledano, F., Martínez, J., Esteve, M.A., in press. Determinants of wintering waterbird changes in a Mediterranean coastal lagoon affected by eutrophication. Ecological Indicators.

Rodríguez Estrella, T., 2003. Situación de la intrusión marina en la Cuenca del Segura: evolución desde TIAC´88. In: Tecnología de la intrusión de aguas de mar en acuíferos costeros: Países mediterráneos. IGME, 499-507.

Sasaki, Y., 1992. Resolution of resistivity tomography inferred from numerical simulation. Geophysical Prospecting 40, 453–464.

Store, H., Storz, W., Jacobs, F., 2000. Electrical resistivity tomography to investigate geological structures of earth's upper crust. Geophysical Prospecting 48, 455-471.

Sumanovac, F., 2006. Mapping of thin sandy aquifers by using high resolution reflection seismics and 2-D electrical tomography. Journal of Applied Geophysics 59, 345-346.

Suzuki, K., Toda, S. Kusunoki,K., Fujimitsu, Y., Mogi, T., Jomori, A., 2000. Case studies of electrical and electromagnetic methods applied to mapping active faults beneath the thick quaternary. Engineering Geology 56, 29-45.

Telford, W.M., Geldart L.P., Sheriff, R.E., 1990. Applied Geophysics, Cambridge University Press, 770 p.

Van Dam, J.C., Meulenkamp, J.J., 1967. Some results of the geo-electrical resistivity method in groundwater investigations in The Netherlands. Geophysical Prospecting 15, 92–115.

Wilson, S.R., Ingham, M., McConchie, J.A. 2006. The applicability of earth resistivity methods for saline interface definition. Journal of Hydrology 316, 301-312.

FIGURE CAPTIONS

Figure 1. Location of the study area and geological sketch map of the Campo de Cartagena aquifer and the Mar Menor coastal lagoon (from IGME, 1974). Points 1-12 show the deployment of the electrical tomography profiles (Table 1 shows the characteristics of each profile). Line A-B marks a geological cross-section (see Fig. 2).

Figure 2. Geological cross sections at the North of the study area (from ITGE, 1994). Its location is shown in Figure 1.

Figure 3. Electrical resistivity tomography profiles 1-4. The position of each profile is shown in Figure 1. The vertical scale (depth) is slightly greater than the

horizontal one (m). Colour scale for resistivity (Ω.m) is common for all plots. Labels indicate interpretation, and labels with question marks show inferred/uncertain aquifer layers.

Figure 4. Electrical resistivity tomography profiles 5-8. The position of each profile is shown in Figure 1. Same as Fig. 3.

Figure 5. Electrical resistivity tomography profiles 9-12. The position of each profile is shown in Fig. 1. Same as Fig. 3.

Table 1. Characteristics of the 12 electrical resistivity tomography profiles undertaken. A Wenner-Schlumberger electrode array was used for all of them.

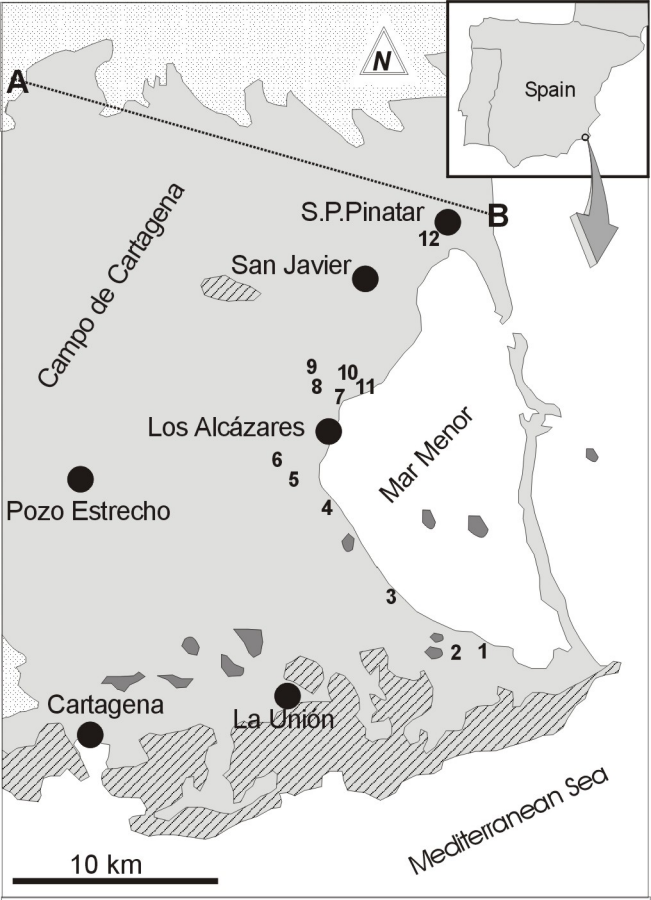
A
B
N
Spain
S.P.Pinatar
12
San Javier
Campo de Cartagena
9
8
10
7
11
Los Alcázares
Mar Menor
6
5
Pozo Estrecho
4
3
2
1
Cartagena
La Unión
Mediterranean Sea
10 km
Quaternary
Volcanic rocks
Miocene-Pliocene
Internal Betic Zones (basement)

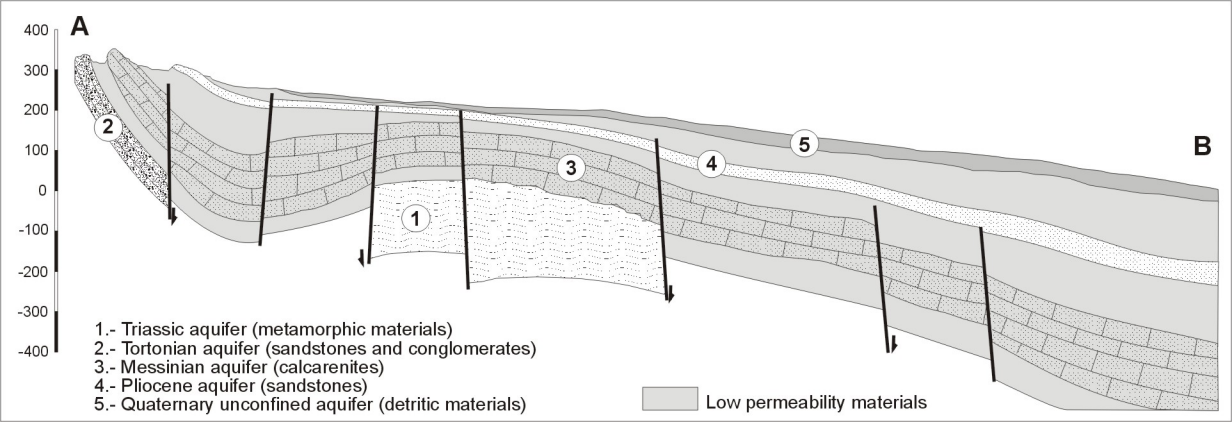
A
B
400
300
200
100
0
-100
-200
-300
-400
1
2
3
4
5
1.- Triassic aquifer (metamorphic materials)
2.- Tortonian aquifer (sandstones and conglomerates)
3.- Messinian aquifer (calcarenites)
4.- Pliocene aquifer (sandstones)
5.- Quaternary unconfined aquifer (detritic materials)
Low permeability materials

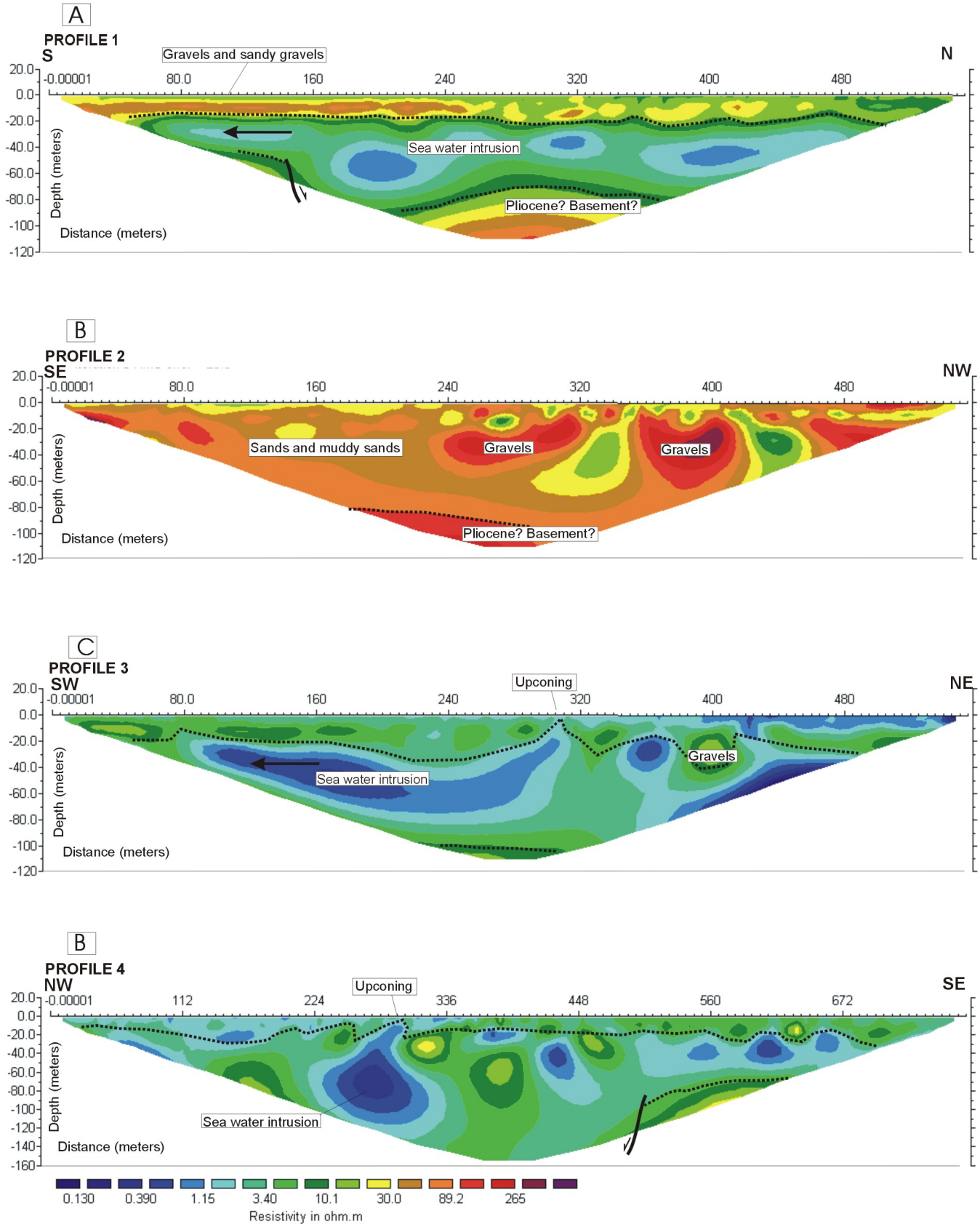
A
PROFILE 1
S
N
Gravels and sandy gravels
Sea water intrusion
Pliocene? Basement?
Depth (meters)
Distance (meters)
B
PROFILE 2
SE
NW
Sands and muddy sands
Gravels
Gravels
Pliocene? Basement?
Depth (meters)
Distance (meters)
C
PROFILE 3
SW
NE
Upconing
Gravels
Sea water intrusion
Depth (meters)
Distance (meters)
B
PROFILE 4
NW
SE
Upconing
Sea water intrusion
Depth (meters)
Distance (meters)
0.130
0.390
1.15
3.40
10.1
30.0
89.2
265
Resistivity in ohm.m

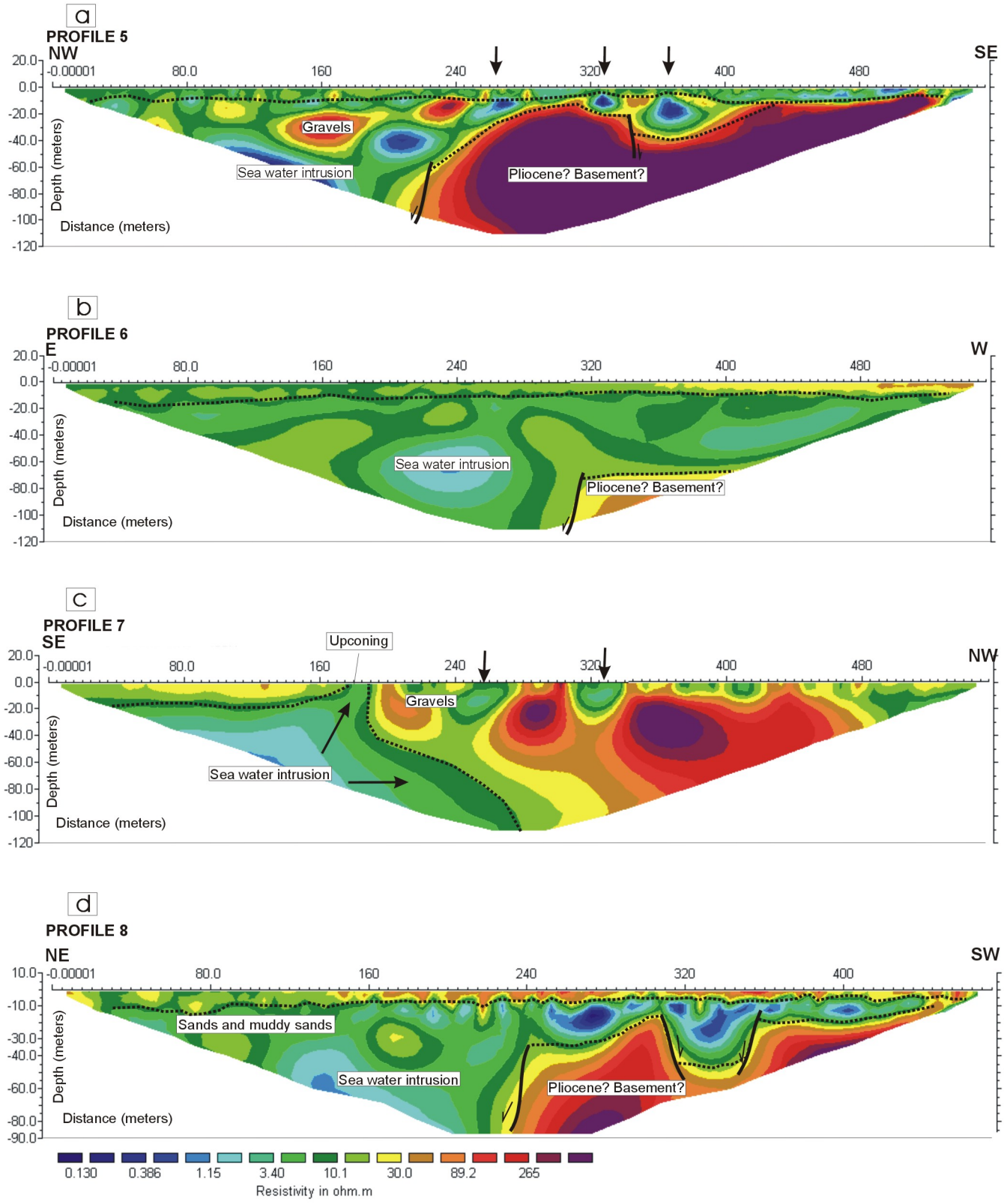
a
PROFILE 5
NW
SE
20.0
0.0
-20.0
-40.0
-60.0
-80.0
-100
-120
-0.00001
80.0
160
240
320
400
480
Depth (meters)
Distance (meters)
Gravels
Sea water intrusion
Pliocene? Basement?
b
PROFILE 6
E
W
Sea water intrusion
Pliocene? Basement?
c
PROFILE 7
SE
NW
Upconing
Gravels
Sea water intrusion
d
PROFILE 8
NE
SW
10.0
-10.0
-30.0
-40.0
-60.0
-80.0
-90.0
Sands and muddy sands
Sea water intrusion
Pliocene? Basement?
0.130
0.386
1.15
3.40
10.1
30.0
89.2
265
Resistivity in ohm.m

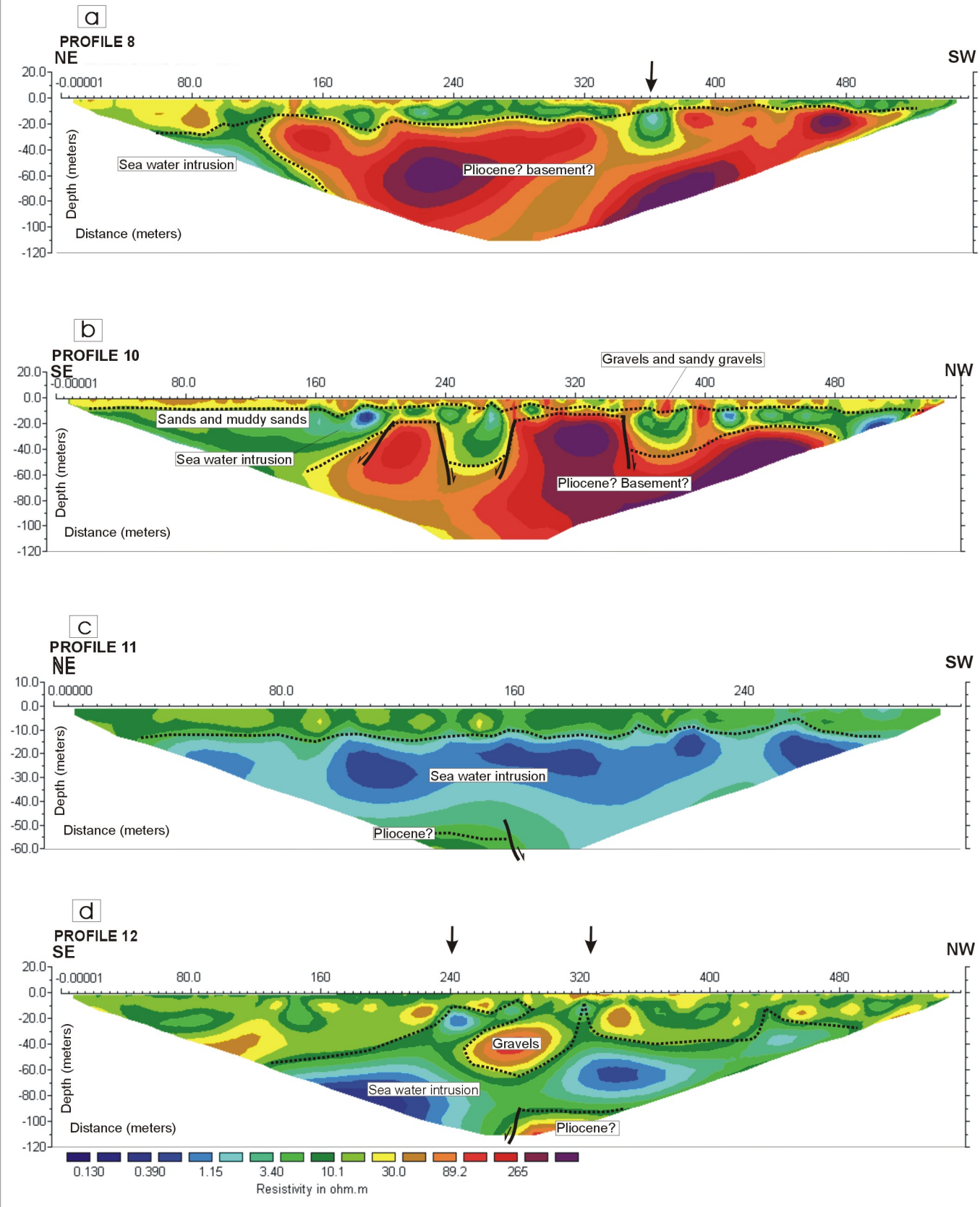
a
PROFILE 8
NE
SW
20.0
0.0
-20.0
-40.0
-60.0
-80.0
-100
-120
-0.00001
80.0
160
240
320
400
480
Depth (meters)
Sea water intrusion
Pliocene? basement?
Distance (meters)
b
PROFILE 10
SE
NW
Gravels and sandy gravels
Sands and muddy sands
Sea water intrusion
Pliocene? Basement?
Depth (meters)
Distance (meters)
c
PROFILE 11
NE
SW
10.0
0.0
-10.0
-20.0
-30.0
-40.0
-50.0
-60.0
0.00000
80.0
160
240
Depth (meters)
Sea water intrusion
Distance (meters)
Pliocene?
d
PROFILE 12
SE
NW
Gravels
Sea water intrusion
Pliocene?
Depth (meters)
Distance (meters)
0.130
0.390
1.15
3.40
10.1
30.0
89.2
265
Resistivity in ohm.m

Profile	Coastline orientation	Total length(m)	Direction	Electrodes space(m)	Electrodes required	Measurements	Maximum depth (m)	Signs of Intrusion (Quaternary aquifer)
1	Perpend	560	N180ºE	5	112	2809	105,7	No
2	Parallel	560	N120ºE	5	112	2809	105,7	Yes
3	Perpend	560	N30ºE	5	112	2808	105,7	Yes
4	Parallel	784	N125ºE	7	112	2809	148	Yes
5	Parallel	560	N170ºE	5	112	2809	105,7	Yes
6	Perpend	560	N90ºE	5	112	2787	105,7	Only lower part
7	Perpend	560	N120ºE	5	112	2809	105,7	Yes
8	Paralell	480	N20ºE	5	96	1903	89,5	Yes
9	Paralell	560	N20ºE	5	112	2809	105,7	Yes
10	Perpend	560	N135ºE	5	112	2722	103,8	Yes
11	Paralell	320	N20ºE	5	64	880	58,9	Yes
12	Perpend	560	N135ºE	5	112	2809	105,7	Only lower part